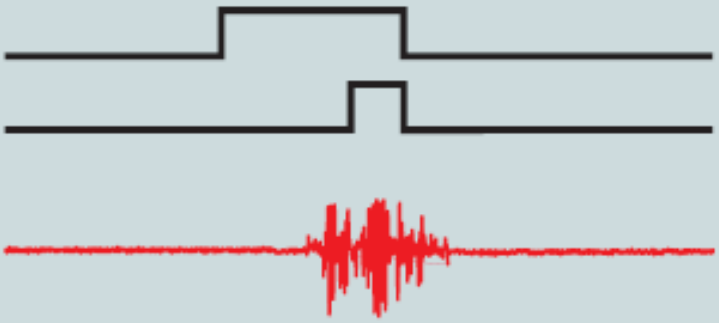

DOCTORAL THESIS

Functional properties of hippocampal circuitry

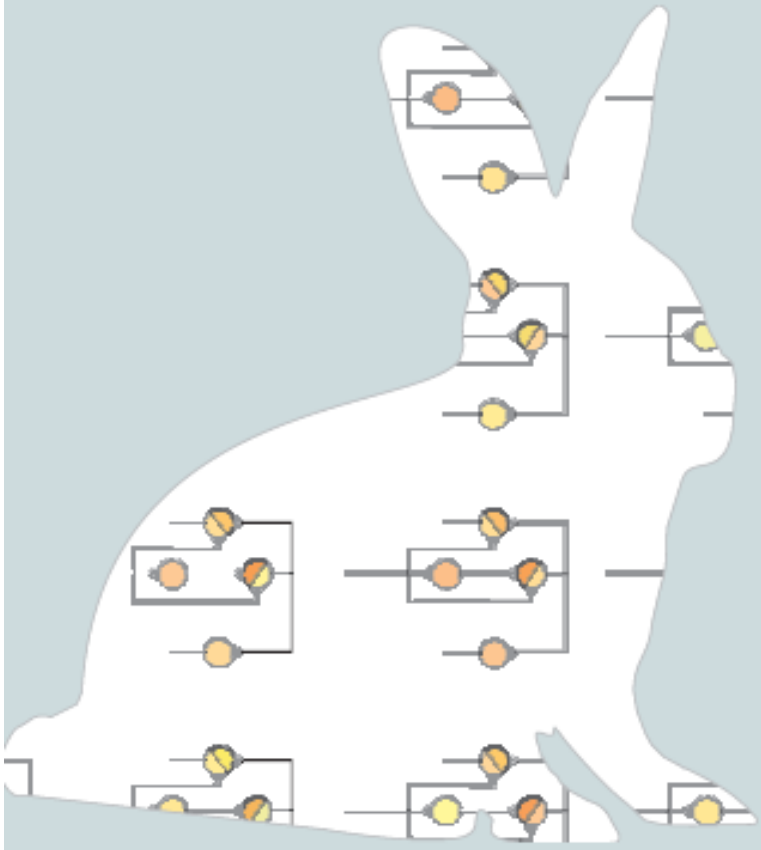

ALEJANDRO CARRETERO GUILLÉN

Director
Prof. Dr. Agnès Gruart i Massó
Department of Physiology, Anatomy and Cellular Biology

UNIVERSIDAD PABLO DE OLAVIDE SEVILLA

Agnès Gruart i Massó
División de Neurociencias
Universidad Pablo de Olavide
Carretera de Utrera Km. 1
41013 Seville (Spain)

Phone: + 34 954 349 511
E-mail: agrumas@upo.es
http://www.divisiondeneurociencias.es/

Doña Agnès Gruart i Massó, Catedrática de Fisiología en el Departamento de Fisiología, Anatomía y Biología Celular de la Facultad de Ciencias Experimentales de la Universidad Pablo de Olavide,

CERTIFICA

que el presente trabajo titulado "**Functional properties of hippocampal circuitry**" ha sido realizado bajo su dirección y supervisión por D. Alejandro Carretero Guillén, Licenciado en Ciencias Biológicas por la Universidad de Sevilla, y considera que reúne las condiciones y el rigor científico para ser presentado y defendido como Tesis Doctoral.

Sevilla, 7 de Octubre de 2015

Fdo.: Agnès Gruart i Massó

RESUMEN

El aprendizaje es el mecanismo mediante el cual el sistema nervioso se adapta a los cambios en las condiciones ambientales y sociales mediante la generación de nuevos comportamientos y/o actividades mentales. Estas habilidades motoras y cognitivas adquiridas se almacenan en diversas formas de memoria (declarativas, procedimentales, etc.) en función del tipo de aprendizaje adquirido. Los aprendizajes más frecuentemente abordados de forma experimental se suelen clasificar en no asociativos (como la habituación y la sensibilización) y asociativos (principalmente los condicionamientos clásico e instrumental). La participación de las estructuras nerviosas depende del tipo de aprendizaje y memoria que se considere. Uno de los modelos experimentales más utilizados en el estudio de los mecanismos neuronales que subyacen al aprendizaje asociativo es el condicionamiento clásico del reflejo corneal, el cual se ha estudiado en muy diversas especies de mamíferos, incluida la especie humana. El condicionamiento clásico del reflejo corneal se induce habitualmente mediante la presentación de un estímulo neutro (el estímulo incondicionado) incapaz de inducir per se una respuesta palpebral (por ejemplo, un tono de una determinada frecuencia) que se sigue de un soplo de aire aplicado a la córnea (el estímulo incondicionado) que sí es capaz de inducir una respuesta refleja palpebral. La presentación conjunta y repetida de ambos estímulos termina por producir la aparición de una respuesta condicionada cada vez que se presenta el estímulo condicionado (esto es, el tono). Existen dos paradigmas básicos de condicionamiento clásico o pavloviano: el paradigma de demora y el paradigma de traza. En el primer caso, el estímulo condicionado está presente hasta que se aplica el estímulo incondicionado y ambos terminan de forma simultánea. En el segundo caso, el estímulo condicionado termina antes de la presentación del estímulo incondicionado por lo que existe un intervalo de tiempo (la traza) separando ambos estímulos. Es tradicional asumir que ambos tipos de condicionamiento se generan en estructuras cerebrales diferentes, el de demora en el cerebelo y el de traza en el hipocampo. Sin embargo estudios previos de nuestro grupo han mostrado que ambas estructuras participan en ambos paradigmas de condicionamiento, así como otras muchas como las cortezas sensorial, motora y prefrontal, determinados núcleos talámicos y otras estructuras subcorticales como el complejo amigdalino y el núcleo rojo. En la presente Tesis Doctoral se han estudiado los cambios funcionales que ocurren en seis sinapsis diferentes del circuito intrínseco del hipocampo y de las vías aferentes al mismo durante el condicionamiento de traza en el conejo despierto. Los animales experimentales se sometieron a condicionamientos de demora y de traza, pero

también se estudiaron el efecto sobre dichas sinapsis hipocampales del contexto en el que se sitúa al animal durante la prueba de aprendizaje, así como los cambios que producen la presentación no emparejada de los estímulos condicionado e incondicionado (es decir, durante un pseudocondicionamiento). Los resultados obtenidos indican que tanto el contexto como el pseudocondicionamiento modifica la actividad de las sinapsis entre la vía perforante y los tres elementos neuronales que forman el circuito intrínseco del hipocampo, esto es, las células granulares del giro dentado y las células piramidales de las áreas CA3 y CA1. Por el contrario, el condicionamiento clásico del reflejo corneal con los paradigmas de traza y de demora modifica la actividad sináptica dentro del circuito intrínseco del hipocampo, principalmente en las sinapsis entre el giro dentado y CA3 y entre CA3 y CA1 tanto homo- como contralateralmente. En una segunda serie experimental se estudió el efecto sobre este tipo de aprendizaje asociativo de la desconexión funcional transitoria del giro dentado. Esta desconexión funcional transitoria se realizó mediante la inyección local controlada de un adenovirus portador del ADN necesario para la síntesis controlada del fragmento C de la toxina tetánica. La síntesis de esta neurotoxina se activó mediante la inyección de doxiciclina. La expresión del fragmento C de la toxina tetánica en las neuronas del giro dentado produjo su desconexión funcional de sus neuronas blanco, esto es, de las células piramidales de CA3. Con este modelo experimental se pudo demostrar que la expresión de respuestas palpebrales condicionadas en conejos disminuye significativamente o, incluso, desaparece durante el periodo en que existe una desconexión funcional entre el giro dentado y las neuronas piramidales de CA3. Sin embargo, se pudo demostrar así mismo que las memorias desaparecidas durante el periodo de desconexión funcional reaparecen en el momento en que terminó la expresión de la toxina tetánica en las neuronas del giro dentado. Estos resultados permiten sugerir que tal vez las memorias asociadas a este tipo de aprendizaje asociativo no se almacenan, como se ha supuesto hasta el momento presente, en la ultraestructura y composición molecular de los contactos sinápticos dentro del circuito intrínseco del hipocampo.

LIST OF ABBREVIATIONS

A:	Anterior
ANOVA:	Analysis of variance
AP:	Antero-posterior
CA1:	Area 1 of the cornu Ammonis
CA2:	Area 2 of the cornu Ammonis
CA3:	Area 3 of the cornu Ammonis
CAMKII:	CaM-dependent protein kinase II
cAMP:	cyclic Adenosine monophosphate
CS:	Conditioned stimulus
CS-US:	Conditioned and unconditioned stimuli
coll:	collaterals
D:	Depth / Dorsal
deg/s:	degrees per second
DG:	Dentate gyrus
Dox:	Doxycycline
DPX:	Distrene plasticizer xylene
EC:	Entorhinal cortex
EMG:	Electromyography
Extinc:	Extinction
fEPSP(s):	field Excitatory postsynaptic potential(s)
fMRI:	functional Magnetic resonance imaging
FN:	Facial nucleus
h:	hour
Hab:	Habituation
Hipp:	Hippocampus
hSYN:	human Synapsin 1
IgG:	Immunoglobulin G
Inj:	Injection
INSIST:	Inducible silencing of synaptic transmission
IP:	Interpositus (of cerebellum)
L:	Lateral
LFP:	Local field potential
Min:	minute
OO:	Orbicularis oculi
Para:	Parasubiculum
PB:	Phosphate buffer
PBS:	Phosphate-buffered saline
PP:	Perforant pathway
Pre:	Presubiculum
PSD95:	Postsynaptic density 95
P_{tet}bi:	Bidirectional tetanus promoter
rAAVs:	recombinant Adeno-associated viruses
Rec:	Recording
Retr:	Retrieval
RN:	Red nucleus
rtTA:	reverse tetracycline-controlled transactivator
s:	second
St:	Stimulus
Sub:	Subiculum
tdTOM:	tandem dimer Tomato
TeTxLC:	Tetanus toxin light chain

Thr:	Threshold
tTA:	tetracycline-controlled transactivator
US:	Unconditioned stimulus
V:	Ventral
VGLUT:	Vesicular glutamate transporter 1
VP16-CREB:	cyclic Adenosine monophosphate response element binding

CONTENTS

1. INTRODUCTION

1.1 GENERAL ASPECTS OF MOTOR AND COGNITIVE LEARNING

All motor and cognitive actions, both simple and complex, are originated by the activity of the brain. When organisms add new behaviors to their repertoire, a learning process has to be produced in the brain. In accordance, learning is the mechanism by which the nervous system adapts to environmental pressures and constraints by the generation of appropriate new behaviors. During actual learning, the neural information needs to be encoded, stored, and retrieved through memory processes. For this reason, neural principles underlying learning and memory should be studied under the best possible physiological conditions —namely, in alert behaving animals.

In a first approach to Cognitive Neurosciences, terms like “learning” and “memory” could be interchanged due to their conceptual proximity and to the fact that they are reciprocally dependent. However, learning refers to the process mentioned initially, where an organism incorporates new information in its biological system, while memory could be defined as the process that allows the storage of this information and the possibility for its future retrieval (Kandel et al., 2000).

Many different definitions have been used for memory up till the present day. It seemed clear from the beginning that memory could not be defined as a single process or as a unique skill, but as a certain number of processes, each one covering some different purposes and operating according to different principles. All of these processes together enable the emergence of a capability termed “memory” (Tulving, 1985; Schacter, 1987; Squire, 1987).

Memory storage is the process in which encoded information is preserved and kept intact. According to the Atkinson-Shiffrin theory (Atkinson and Shiffrin, 1968), memory storage occurs in three different systems: sensory memory, short-term memory, and long-term memory (**Figure 1**). This model of the different systems of memory storage is today widely accepted by neuroscientists.

Sensory memory is the shortest-term element of memory (**Figure 1**). It is the ability to retain impressions of sensory information after the original stimuli have already ended. It acts as a kind of buffer for stimuli received through the senses of sight, hearing, smell, taste, and touch, which are retained accurately, but very briefly. The sensory memory for visual stimuli is sometimes known as iconic memory; the memory for aural stimuli is known as echoic memory.

Short-term memory refers to a cognitive system that is used for holding sensory events, names, or other items for a brief period of time. Baddeley and Hitch (1974) developed some years ago an alternative model of short-term memory which they named working memory. The interchangeable use of short-term memory and working

memory (**Figure 1**), when dealing with simple-span tasks versus complex-span tasks, indicates that the differentiation between the two concepts is far from clear (Aben et al., 2012).

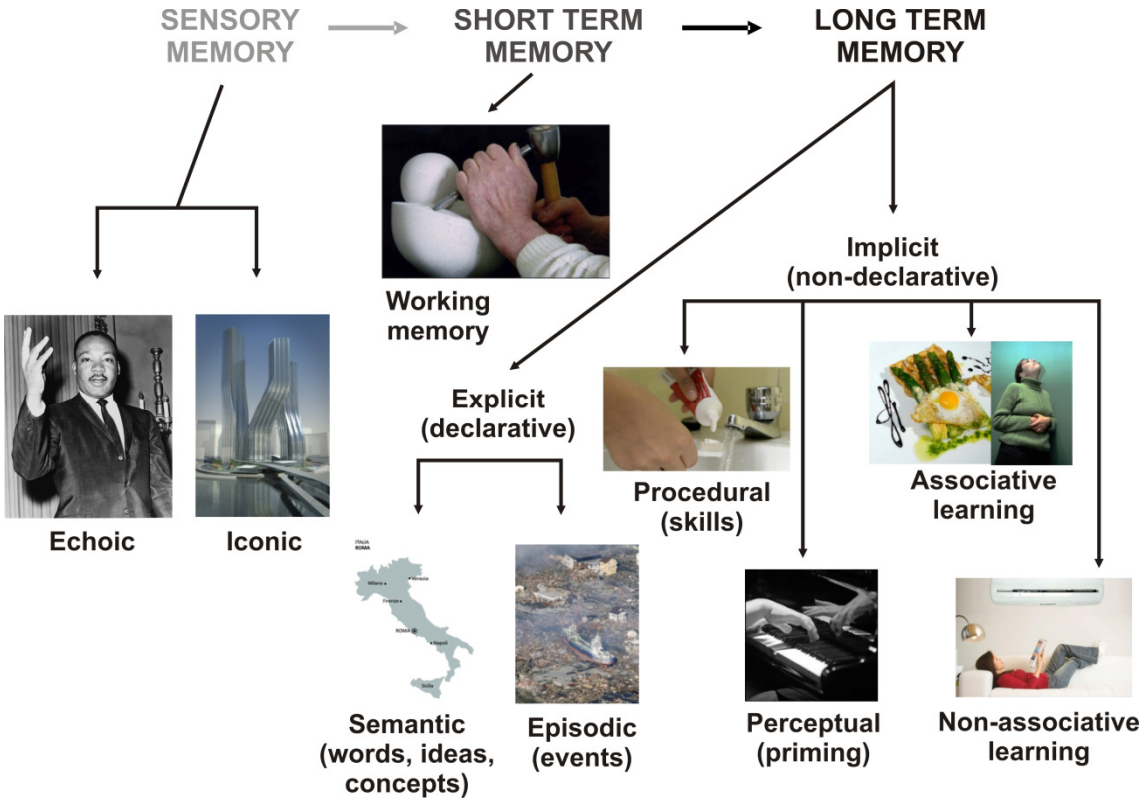

Figure 1. Diagram of the types of memory. Memory is not a single unitary process, usually. In fact, memory is usually subdivided in different types, which could be supported by different brain structures and circuits. The components of the main division are sensory memory (< 1 s), short-term memory (or working memory, < 1 min), and long-term memory (life-time). Long-term memory can be explicit (which implies consciousness of the information that is being retrieved) and implicit (comprising information in the form of skills, motor learning, etc. that can be observed) (modified from Atkinson and Shiffrin, 1968).

Long-term memory is often divided in two further main types (**Figure 1**): explicit (or declarative) memory and implicit (or procedural or non-declarative) memory (Cohen and Squire, 1980). Explicit or declarative memory ("knowing what") is a conscious recollection of recently (or not so recently) presented information (Graf et al., 1985). This is a complex kind of memory, since it enables the organisms to construct internal models of the world in their nervous systems (Craik, 1983) and to open a window for recalling the past through information previously collected. It is termed explicit memory as it consists of information that is explicitly stored and retrieved, although it is more properly a subset of declarative memory. Declarative memory can be further subdivided into episodic memory and semantic memory. Implicit or non-declarative

memory involves functions that are not under conscious control. It includes associative learning (such as classically conditioned eyeblink responses) and non-associative learning (habituation or sensitization), procedural memory or skill learning (such as riding a bike), and the effects or priming that facilitate the acquisition of information in the modality specific to the presentation of the information.

The division between short-term and long-term memory (and the subtypes explicit and implicit) is not so clear if we consider observations made by researchers in the nineteenth century. There were many studies of automatic writing where different investigators described the emergence of knowledge acquired by subjects during past episodes, a knowledge that they were unaware of possessing (Binet, 1890; Prince, 1914). According to Barkworth (Barkworth, 1891) it seems that "*nothing is ever forgotten though the bygone memories evoked by pencil, or crystal, may appear so new and strange that we fail to recognize them as ever having been included in our experience*", but although biological systems tend not to be enclosed within categories, some limits are needed in order to offer an explanation with the available data.

In the case of the automatic writing, it is remarkable that motor learning is influenced by the personal experience of the experimental subjects. It does not go unnoticed that the repetition of a task improves its performance, like the pianist training for re-playing a song, so there is a participation of the explicit and implicit memory systems in the motor learning, as is shown in some behavioral studies where—while these systems compete to control performance—learning within these networks can occur in parallel (Curran et al., 1993; Willingham et al., 2002; Song et al., 2007).

All of these different types of long-term memory are assumed to be stored in different regions of the brain and undergo quite different functional processes (Zola-Morgan and Squire, 1993). It is generally accepted by neuroscientists that declarative memories are encoded by the hippocampal, entorhinal, and perirhinal cortices (all within the medial temporal lobe of the brain), but are consolidated and stored in the temporal cortex and elsewhere. Procedural memories, on the other hand, could involve the hippocampus, but it seems that cerebellum, putamen, caudate nucleus, and the motor cortex, all of which are involved in motor control, could have a crucial role as well. Learned skills, such as riding a bike, are stored in the putamen; instinctive actions, such as grooming, are stored in the caudate nucleus; and the cerebellum seems to be involved with timing and coordination of body skills. Thus, without the medial temporal lobe (the structure that includes the hippocampus), a person is still able to form new procedural memories (such as playing the piano, for example), but cannot remember the events during which they happened or were learned. Although one could establish a phrenology of the memory, many data and experimental

approaches indicate that much more study is needed in order to correctly explain the mechanisms of the learning and memory processes (Delgado-García and Gruart, 2006).

1.1.1 Challenges to the study of the generation of learned responses

While intense experimental attention is being given to the search for molecular mechanisms underlying the acquisition and storage of acquired motor and cognitive abilities, less attention is being paid to the neural centers involved in the actual generation of the newly acquired (motor) abilities, and the network neural properties underlying cognitive processes. Indeed, in a review of the achievements of the past 40 years in the understanding of the biology of learning, no special mention is made of the generation of learned movements —that is, experimental attention has apparently been concentrated on the description of how learning is acquired and stored at the molecular level (Kandel, 2009). Furthermore, in the list of open-ended questions still unanswered with an experimental explanation, no mention at all is made of how new movements are generated and controlled and how their cognitive counterparts are built up. This void is conspicuous and can be extended to many other reviews of this exciting field of research (Citri and Malenka, 2008; Neves et al., 2008; Thompson and Steinmetz, 2009; Dragoi and Tonegawa, 2011).

A challenging approach could be to propose that learning and memory are functional states (as opposed to localized, transient processes) underlying the acquisition of new motor abilities across the learning process (Sánchez-Campusano et al., 2011). Those functional states would require the participation of numerous neural structures, as well as their proper and timed activation, and that the generation of motor responses is an important component of the learning process. It is also of interest to take into account that, apart from the classical structures closely related to the learning and memory processes, many other neural structures can be included in the functional state proposal, since the cognitive capabilities will change depending on the environmental (temperature, noise, researcher, etc.) and individual (motivation, attention, pain, etc.) constraints.

A second challenging perspective could be to demonstrate that, after all, long-term memories might not be stored in synapses. It has long been believed that memories were stored in the synapses of neurons. However, when those synapses are destroyed, the memories they hold must be lost as well. There is significant empirical support for the idea, proposed by Ramón y Cajal more than a century ago (Cajal, 1894), that long-term memories are expressed in the brain, in part by changes in synaptic connectivity and/or strength. A corollary of this idea, accepted by many, if not

most, modern neuroscientists, is that memories are maintained by persistent molecular and cellular alterations in synaptic structures themselves (Bailey and Kandel, 2008; Kandel et al., 2014). Although no conclusive results have been obtained until now in this regard. In contrast, some recent data support the contention that the persistence of memory does not require the stability of particular synaptic connections; for example, when using the marine mollusk *Aplysia californica* as an experimental model (Chen et al., 2014).

1.2 ASSOCIATIVE LEARNING

Associative learning requires long-term memory procedures and it belongs to the non-declarative (implicit) category (**Figure 1**). The concept of associative learning is based on the assumption that ideas and experiences reinforce one another and can be linked to enhance the learning process. Associative learning has been widely studied. Three main types could be differentiated:

- Classical conditioning: an association is established between the repeated presentation of two independent stimuli in such a way that one becomes predictive for the other.

- Operant conditioning: an association occurs between a given behavior and its consequences, a fact that reinforces this behavior. The relevant point is that this behavior is new for the individual, and when it is executed, a positive or negative reinforcement is obtained. In this way, a relationship can be established between the behavior and its consequences. Finally, the probability of expression of the behavior is modified by the individual according to its consequences.

- Vicarious conditioning: this type learning is acquired by observing the reactions of others to an environmental stimulus that is salient to both the observer and the demonstrator. The saliency of the stimulus is characterized by its relevance (e.g., fear) and ability to produce emotional arousal. Vicarious conditioning is a particularly important process in observational learning. One effect of vicarious conditioning may be increased imitation of the demonstrator by the observer, in that observers imitate successful models. The greater the positive reinforcement of the model's reaction, the more the observer tends to imitate those responses.

Classical conditioning was first demonstrated by Ivan Pavlov, who received the Nobel Prize in Physiology and Medicine in 1904 for his studies on the mechanisms

underlying the digestive system of dogs. Pavlov developed a procedure for surgically implanting a tube, called a fistula, into living animals (**Figure 2A**). This allowed him to collect and measure digestive secretions when he presented food to a dog. These secretions were similar to those released in the stomach or the mouth in a chronic preparation in living animals.

Developing his experiments, Pavlov realized that if he repeated the food (meat powder) presentations several times, the dog salivated to all of them. Moreover, if he repeatedly rang a tuning fork just before presenting the meat powder (the sound slightly preceded the presentation of the food), the animal came to associate the tuning fork with the presentation of the meat powder, and it would begin to salivate when the tuning fork started to ring. In fact, for a while the dog would even salivate if the tuning fork was rung but no food was presented (**Figure 2B**). In Pavlov's paradigm, the meat normally elicits salivation without experimenter intervention (it is a reflex response) and it is termed unconditioned stimulus. These reflex responses are termed unconditioned responses. The tuning fork comes to elicit salivation only if repeatedly paired with the meat, and it is termed the conditioned stimulus. The salivation evoked by the sound is termed the conditioned response (**Figure 2B**). Both unconditioned and conditioned responses are assumed to be similar but not identical, in terms of composition, duration, amount, etc.

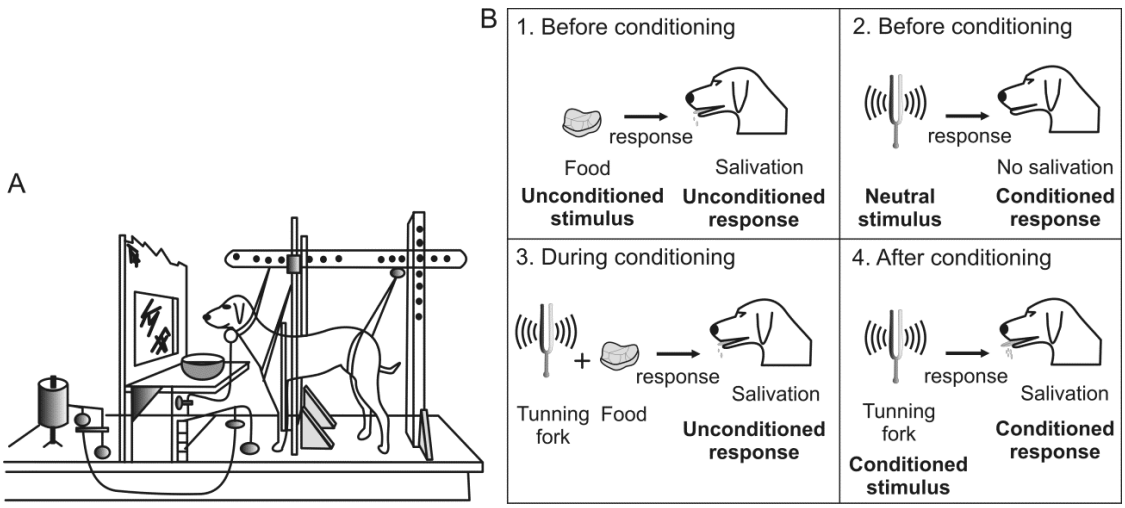

Figure 2. Representation of the experiments performed by Ivan Pavlov. A, Dogs were taken into a room for the training session and they were prepared for the extraction of the salivary fluids. **B,** The classical conditioning paradigm proposed by Pavlov had four steps, in which the dogs received i) a stimulus (unconditioned stimulus) that evoked a reflex (unconditioned) response. He used food that produced salivation; ii) a neutral stimulus for this response (tuning fork sound); iii) both stimuli closely paired and dogs salivated; and finally iv) only the tuning fork sound that now produced the salivation of the animals. This last step demonstrated that the tone had become a conditioned stimulus that produced salivation (now a conditioned response.

1.2.1 Classical eyeblink conditioning

Classical conditioning of eyelid responses is an associative motor learning paradigm which is acquired progressively. Although this paradigm has been well known since the 1930s, it was only used and studied in the early 1960s. The contribution of Isidore Gormezano and his collaborators in this field is noteworthy—they carried out all the necessary modifications of the Plexiglas restraining box and the stimuli delivery system to improve the recordings of classical conditioning in the albino rabbit model. In their experiments they measured eyeball retraction and nictitating membrane movement (Moore and Gormezano, 1961; Gormezano et al., 1962), and developed very accurate protocols for eyelid classical conditioning in albino rabbit (Schneiderman et al., 1962). Those studies have been extremely important for understanding all the subjacent processes in the acquisition of new motor skills. However, the passive character of nictitating membrane movements, in contrast to the active and complex response of the eyelid motor system, makes this latter more suitable for the study of the subjacent neural system that supports the generation of the conditioned responses. After Gormezano's experiments, some modifications have been introduced in the set-up for the classical conditioning of the corneal reflex in rabbits (**Figure 3**).

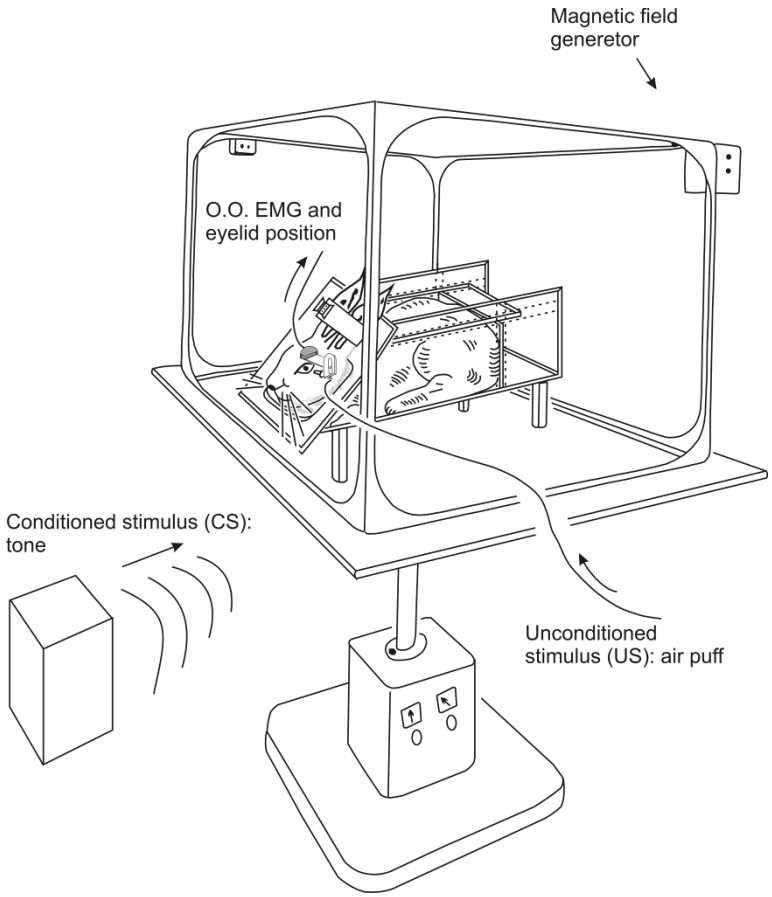

Figure 3. Diagram of the set-up used for training rabbits in the eyeblink classical conditioning using a magnetic field generator frame. Animals were restricted in their movements in a Plexiglas restraining box. A tone was presented to the animal preceding the air puff that elicited a reflex eyeblink response (unconditioned response). After a number of pairings, the animals started to respond to the tone with the closing of the eye (conditioned response). The tone (conditioned stimulus) was presented through a loudspeaker located in front of the rabbit, and the air puff (unconditioned stimulus) was directed at the cornea using a plastic tube.

In the eyeblink conditioning protocol, an unconditioned stimulus (usually an air puff directed at the cornea) which evokes a reflex response (in this case, the closure of the eyelid) is paired with a neutral stimulus (a tone) which does not produces this eyelid displacement. These two stimuli are paired in such a way that the tone precedes the air-puff presentation. After several paired trials, the subject starts to present conditioned responses, closing the eyelid just after the conditioned stimulus (tone) appears and before presentation of the unconditioned stimulus (air puff).

An exhaustive description of the kinetics and the frequency domain properties of spontaneous, reflex, and conditioned eyelid responses can be found elsewhere (Evinger et al., 1984; 1991; Gruart et al., 1995, 2000; Sánchez-Campusano et al., 2011), as well as the underlying neural mechanisms that maintain a basal oscillation allowing a fast, correct, and gradual response to sensory stimuli (Welsh, 1992; Domingo et al., 1997; Trigo et al., 1999a, 2003). These already available data and the docile nature of rabbits offer a good experimental system for the study of the neural basis of associative learning.

An additional point of complexity is the definition of the specific paradigm to be used among the many described for classical eyeblink conditioning. The nature of the stimuli and the way that they are combined at the moment of the presentation to the animal is crucial in order to obtain conditioned responses. Regarding the nature, and despite different sensory modalities being eligible for conditioned and unconditioned stimuli [a weak air puff (Gruart et al., 1997) or a flash of light (Welsh and Harvey, 1991) for conditioned stimulus, and a mechanical stimulation or an electrical stimulus in the trigeminal nerve (Woody et al., 1992) for unconditioned stimulus], the combination formed by a tone as conditioned and an air puff as unconditioned stimulus seems to be the one providing the best results. With respect to the way that stimuli are presented to the experimental animal, trace and delay paradigms are the most effective.

In the case of the delay paradigm, the conditioned stimulus is presented first, but before its end the unconditioned stimulus is presented too, so both coexist for a short period of time and co-terminate. A wide variety of temporal relationships can be found in the literature for this paradigm, but the optimal interval for the acquisition of conditioning is between 200 ms and 400 ms (Thompson, 1988). In contrast, the trace eyeblink paradigm has as a particularity that the conditioned and unconditioned stimuli are temporally separated by a gap that can be shorter or longer depending on the cognitive demands that the researcher wants to study; this gap is normally within an interval of 0.1-0.5 s. Longer intervals usually produce a failure in the proper acquisition of the conditioned response.

The eyelid/nictitating membrane motor system has been widely used as an experimental model for the study of associative learning, using different classical conditioning paradigms (Gormezano et al., 1983; Clark and Squire, 1998; Thompson and Krupa, 1994; Delgado-García and Gruart, 2006; Thompson and Steinmetz, 2009). In addition, and for appropriate quantification purposes, the use of the search coil in a magnetic field technique for the precise recording of both reflex and conditioned eyeblinks was introduced (Evinger, 1995; Gruart et al., 1995), thereby making possible a precise analysis of eyelid responses. Indeed, a detailed knowledge of eyelid kinematics seems to be necessary for the subsequent study of neural processes underlying these motor responses and the causal relationships between them (Domingo et al., 1997; Trigo et al., 1999a, 2003; Sánchez-Campusano et al., 2009).

Eyelid performance during associative learning depends upon motivational and emotional states, as well as on the attentive level, previous experiences, sensory receptor thresholds, and motor system training (Cardinal et al., 2002; Madroñal et al., 2010; Bongers et al., 2015). In this sense, it can be proposed that learning and memory processes are the result of underlying neural functional states (as opposed to discrete and localized phenomena) requiring the participation of numerous nervous structures as well as their correct participation and timing. Surprisingly, many researchers still argue that a learning process such as the one involving the classical conditioning of eyelid responses requires the participation only of the cerebellum, when using delay paradigms, or of the hippocampus when using trace paradigms (Thompson, 2005; Gerwig et al., 2007; Green and Arenos, 2007; Thompson and Steinmetz, 2009), the two structures appearing to be necessary and sufficient to accomplish this learning process. Nevertheless, in the last few years, several authors have approached the study of many other neuronal structures that could also be related with these learning paradigms (**Figure 4**), such as the inferior colliculus (Freeman et al., 2007), the thalamus (Halverson et al., 2010), the amygdala (Rorick-Kehn and Steinmetz, 2005), the striatum (Blázquez et al., 2002), and the prefrontal cortex (Leal-Campanario et al., 2007).

1.2.2 Neural substrates of classical conditioning

As indicated above, of all the possible neural structures involved in the generation of conditioned eyelid responses, the ones receiving the least attention have been those constituting the descending premotor and motor pathways for eyelid responses (**Figure 4**). Some authors have disputed the involvement of the motor cortex in the generation of learned eyeblinks. In some cases (in rabbits or ferrets) the whole cortex is removed as a routine step prior to conditioning sessions (Kelly et al., 1990; Svensson et al.,

2006). However, there is increasing evidence regarding the involvement of the somatosensory, acoustic, and prefrontal cortices in sensory processing of the conditioned stimulus during classical conditioning (Gruart et al., 2000; Zotova et al., 2000; Freeman et al., 2007; Leal-Campanario et al., 2006, 2007, 2013). while Woody and colleagues reported changes in the firing activities of motor cortical cells recorded intracellularly during the paired presentation of conditioned and unconditioned stimuli (Birt et al., 2003). In this regard, experiments carried out with humans during the classical conditioning of the corneal reflex have shown, using neuroimaging techniques, the activation of various cortical areas during the learning process (Knuttinen et al., 2002) or during attentional eyeblinks (Martens and Wyble, 2010). Taken together, the above experimental studies carried out during the learning process allow suggesting that to generate a conditioned eyelid response many sensory and motor structures, as well as functional circuits, need to be activated. Only in this way is it possible to obtain the required movement, with the appropriate kinematics as well as the appropriate timing. The inactivation of some of these neural structures might, on occasion, modify some movement properties (amplitude, velocity, profile) without evoking their complete disappearance (Jiménez-Díaz et al., 2004). This latter fact might be another source of misunderstanding regarding the generation of learned responses. Recently, the study of the neural substrates of classical conditioning has been extended to mice (Gruart et al., 2014; Yang et al., 2015).

The detailed study of eyelid kinematics has allowed concluding that the profile and biomechanical properties of learned eyelid responses are different from those presented by reflex responses (Evinger, 1995; Gruart et al., 1995; Domingo et al., 1997; Sánchez-Campusano et al., 2007, 2009, 2011), suggesting a different neural origin for the two types of movement. In this regard, it has been shown that reflex eyelid responses in the cat are characterized by a very fast (up to 2000 deg/s) downward displacement of the upper eyelid, whereas conditioned responses never reach 400 deg/s (Gruart et al., 1995). These results also suggest that the motor neural commands generating reflex responses are mainly concentrated in the somas of the orbicularis oculi motoneurons, whilst the conditioned eyelid responses are generated by afferent terminals impinging upon distal dendrites of those motor cells (Trigo et al., 1999a). This information is extremely important for the proper formulation of the state functions corresponding to a given set of neural structures and the actual movement evoked (Sánchez-Campusano et al., 2011).

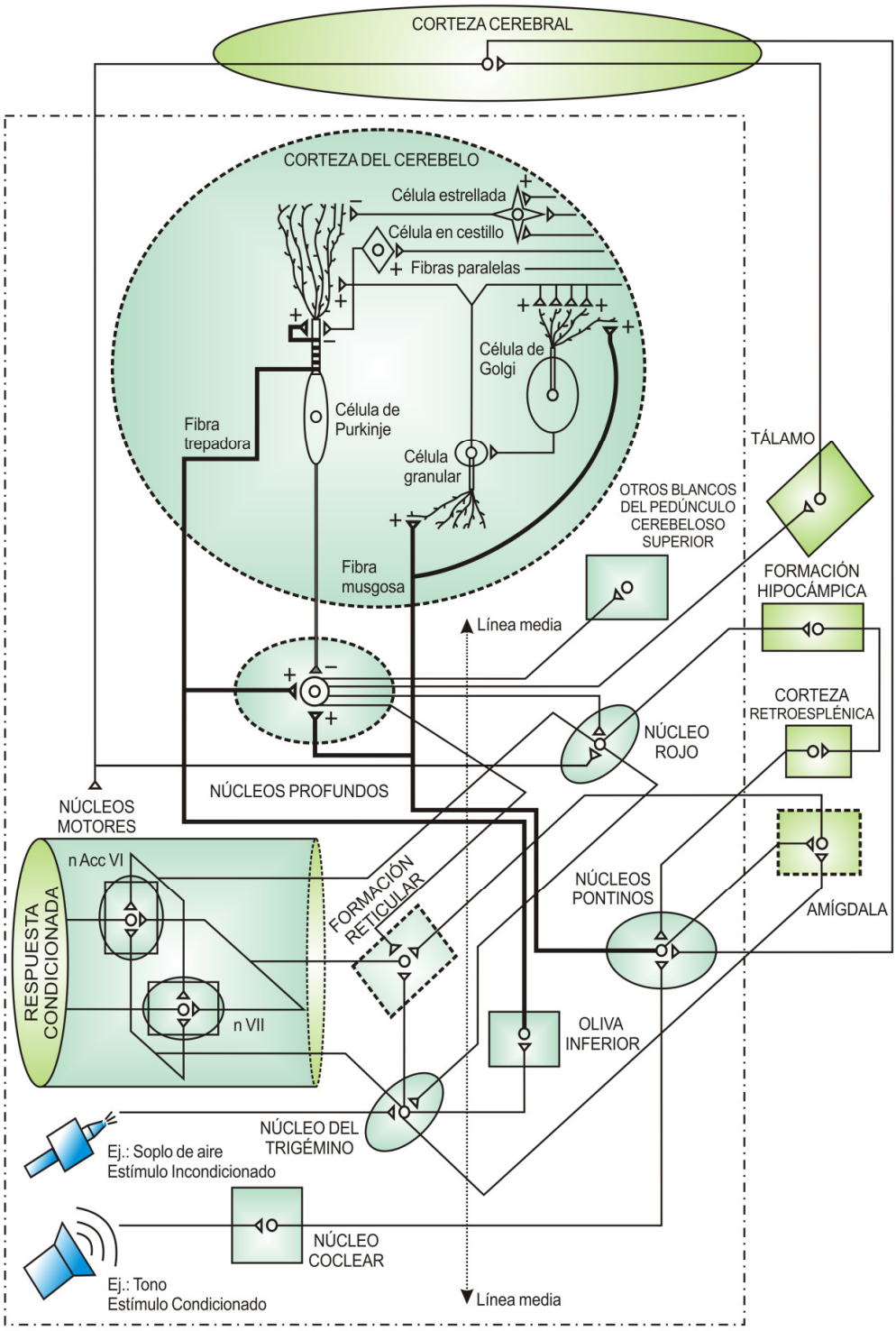

Figure 4. Diagrammatic representation of structures and circuits related with the eyeblink classical conditioning. This diagram gives an idea of the complexity in forming a relatively simple learned response, such as a conditioned eyelid movement. Many researchers have accepted the idea (not yet convincingly demonstrated) that delay conditioning depends on the cerebellum and that trace conditioning depends on the hippocampus (taken from Sánchez-Campusano, 2007).

It is widely accepted that trace conditioning protocols imply a higher difficulty and require the participation of different neural structures to accomplish a correct level of learning, whereas delay conditioning could be acquired involving the participation of a few or just one. The structures underlying these two types of associative learning are still a matter of discussion, and there are two main streams defending opposing theories regarding the neural sites responsible for the acquisition and consolidation of these eyelid responses.

Addressing the first theory, which locates the site for this specific learning in the cerebellum, requires special mention of John Eccles, whose studies of the cerebellum were ground-breaking. Although the first observations of the relationship of execution of movements and this structure was made at the beginning of the 20th century (Holmes, 1917), it was not until considerably later that Eccles hypothesized that the cerebellum would be involved in the development of learned movements (Eccles et al., 1967). Indeed, he described a possible circuit for cerebellar control of movements (Eccles, 1967) and pointed out the relationship between cerebellum development and the proper control of movements in vertebrates (Eccles, 1969). These experiments were the basis for subsequent mathematical models (Marr, 1969; Albus, 1971) which proposed Purkinje cells as the main elements that would control the deep cerebellar nuclei by a long-term depression, releasing them from a tonic inhibition. Following the theories proposed by Eccles, Marr and Albus, Richard Thompson and collaborators defended the cerebellum as the main structure responsible for generating conditioned eyeblink responses (McCormick et al., 1981, 1984; McCormick and Thompson, 1984a, b; Thompson, 1988). They published many papers proposing a neural circuit necessary and sufficient for eyeblink conditioning involving cerebellar structures, mainly the interpositus nucleus.

But not all authors agree with this view, which moves us to the second theory in which the learning process is not limited to just a single structure. For defenders of this second proposal, it is the contribution of a complex neural network which makes possible the correct learning process (Manto et al., 2012). Perhaps the first review supporting the distributed nature of this ability of the nervous system was made by Lashley at the beginning of the 20th century (Lashley, 1920). He showed different examples of animals with an extensive, or complete, destruction of the cerebrum that still preserve some capability of learning. Later observations showed that rabbits are capable of acquiring classically conditioned nictitating membrane responses in decerebrate-decerebellate conditions (Kelly et al., 1990)

According to this view, it would be possible to find neural activity related with the learning process in many different neural structures. For example, hippocampal

pyramidal cells present patterns of action potentials forming amplitude-time course models of the behavioral conditioned responses (Berger and Thompson, 1978) or encoding information related with the predictive value of the conditioned stimulus (Múnera et al., 2001). Brain stem regions (Desmond and Moore, 1986; Gruart et al., 1994), thalamic nuclei (Meftah and Rispal-Padel, 1994; Halverson and Freeman, 2006; Haight and Flagel, 2014), as well as the trigeminal nucleus (Desmond et al., 1983; Ryan et al., 2014), also participate in this type of learning. Finally, some of these structures also participate in the integration of these simple eyelid responses in more-complex ongoing movements (Wulf and Shea, 2002).

In addition, certain structures (e.g., the red nucleus) considered mere relay centers deserve a special mention since some authors consider them active participants in the learning process. This proposal is in contraposition with the premotor and passive role assigned to the red nucleus (Chapman et al., 1990; Bracha et al., 1993; 2009). Other authors suggest an active participation of this nucleus in the learning process regarding plastic changes observed in magnocellular neurons during the acquisition of skeletal associative learning tasks (Tsukahara et al., 1967, 1981; Ito and Oda, 1994).

In a preceding study (Morcuende et al., 2002), the attenuated rabies virus was injected in the upper eyelid of adult rats. After a waiting period of 3-3.5 days, the dorsolateral part of the contralateral red nucleus appeared labeled, as well as the perirubral area (Morcuende et al., 2002). Moreover, those authors demonstrated that neurons forming the rubro-spinal pathway were concentrated in the main magnocellular division of the nucleus, while those projecting to the facial nucleus, as well as those forming a sort of premotor center, were located mainly in the perirubral zone. The contralateral red nucleus is the target of cerebellar interpositus projecting neurons, which have been related to the formation of classically conditioned responses (Thompson, 2005; Thompson and Steinmetz, 2009). These findings are interesting, because they suggest the existence of a division between skeletal muscles and the specialized (because of their visceral origin) facial muscles (Morcuende et al., 2001). The red nucleus also receives projections from the cerebral motor cortex, as shown in guinea pigs and other mammals (Miller and Gibson, 2009), forming the cortico-rubral pathway. Red nucleus neurons projecting to accessory abducens nucleus motoneurons (i.e., those innervating the retractor bulbi muscle) are also localized laterally in the red nucleus (Robinson et al., 2001). Although less attention has been given until now to studying the involvement of the primary motor cortex in the acquisition of conditioned eyelid responses (Birt et al., 2003), numerous experimental

results suggest that it plays a role in this type of associative learning (Freeman and Steinmetz, 2011; Yang et al., 2015).

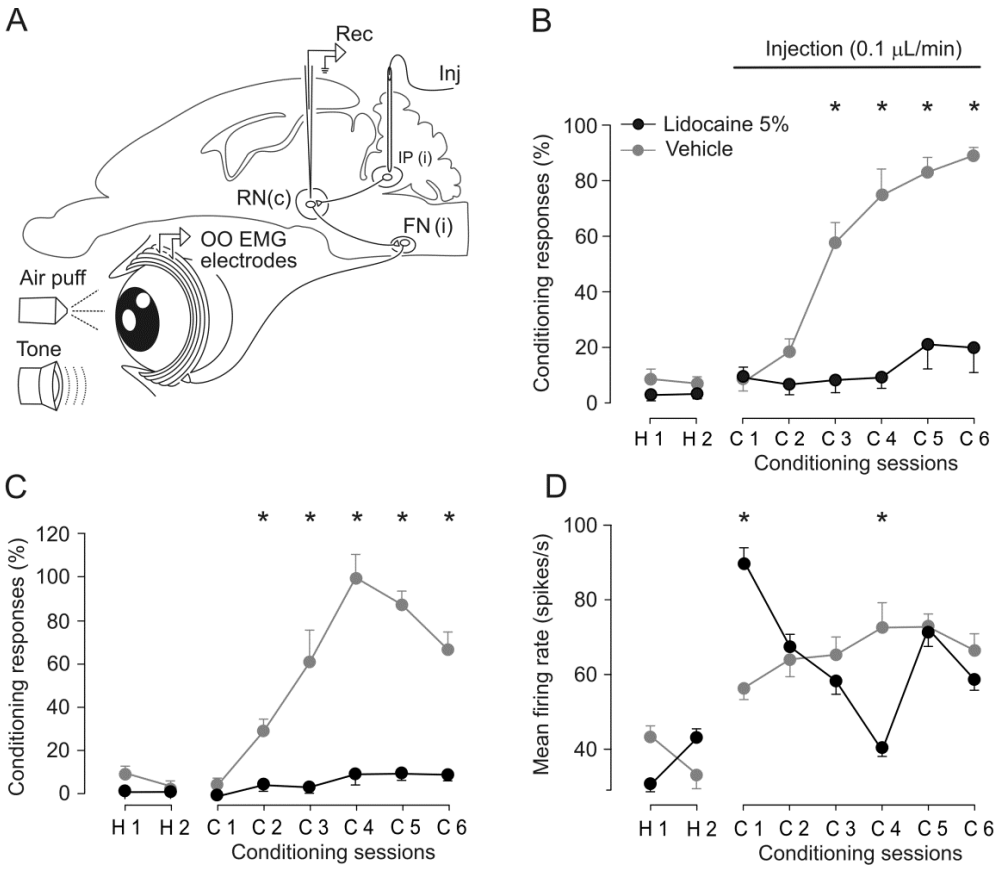

Figure 5. Effects of interpositus nucleus inactivation on learning curves and on the firing rate of red nucleus neurons. A, Experimental design. The contralateral cerebellar interpositus (IP) nucleus was perfused with lidocaine (5% solution at rate of 0.1 µL/min) or vehicle (Inj) during classical eyeblink conditioning and unitary recording (Rec) of red nucleus (RN) neurons. Evolution of the percentage of conditioned responses (**B**), orbicularis oculi (OO) electromyographic (EMG) area (**C**), and mean firing rate (spikes/s) (**D**) for the conditioned responses recorded during the conditioning sessions.

Recently, we have studied the activity of rubral and pararubral neurons in relation to conditioned and unconditioned responses (Pacheco-Calderón et al., 2012). Rubral and pararubral identified neurons increased their firing rates across the successive conditioning sessions, but their discharge rates were related more to the electromyographic activity of the orbicularis oculi muscle than to the learning curves. Reversible inactivation of the interpositus nucleus with lidocaine during conditioning evoked a complete disappearance of both conditioned and unconditioned eyelid responses, and a progressive decrease in conditioned-response-related activity of red nucleus neurons (**Figure 5**). In contrast, motor cortex inactivation evoked a decrease in the acquisition process and an initial dis-facilitation of neuronal firing (which was later recovered), together with the late reappearance of conditioned responses (**Figure 6**). Thus, red nucleus neurons presented learning-dependent changes in activity following

motor cortex inactivation. The direct motor command, for learned responses, arriving at the facial nucleus could thus originate in the red nucleus or in the primary motor cortex (Rosenkranz et al., 2007).

The case of the hippocampal formation is a particular issue in this challenge to define the neural mechanisms underlying learning processes, given that the most accepted statement about the hippocampus is its participation in the learning process of classical conditioning when there is an interval between the conditioned and unconditioned stimuli—for example, in trace eyeblink conditioning (Solomon et al., 1986; Kim et al., 1995; Wu et al., 2014)—whereas it would not be necessary for the acquisition of delay conditioning, where these two stimuli coexist in time. For these reasons hippocampal physiology will be described more extensively below.

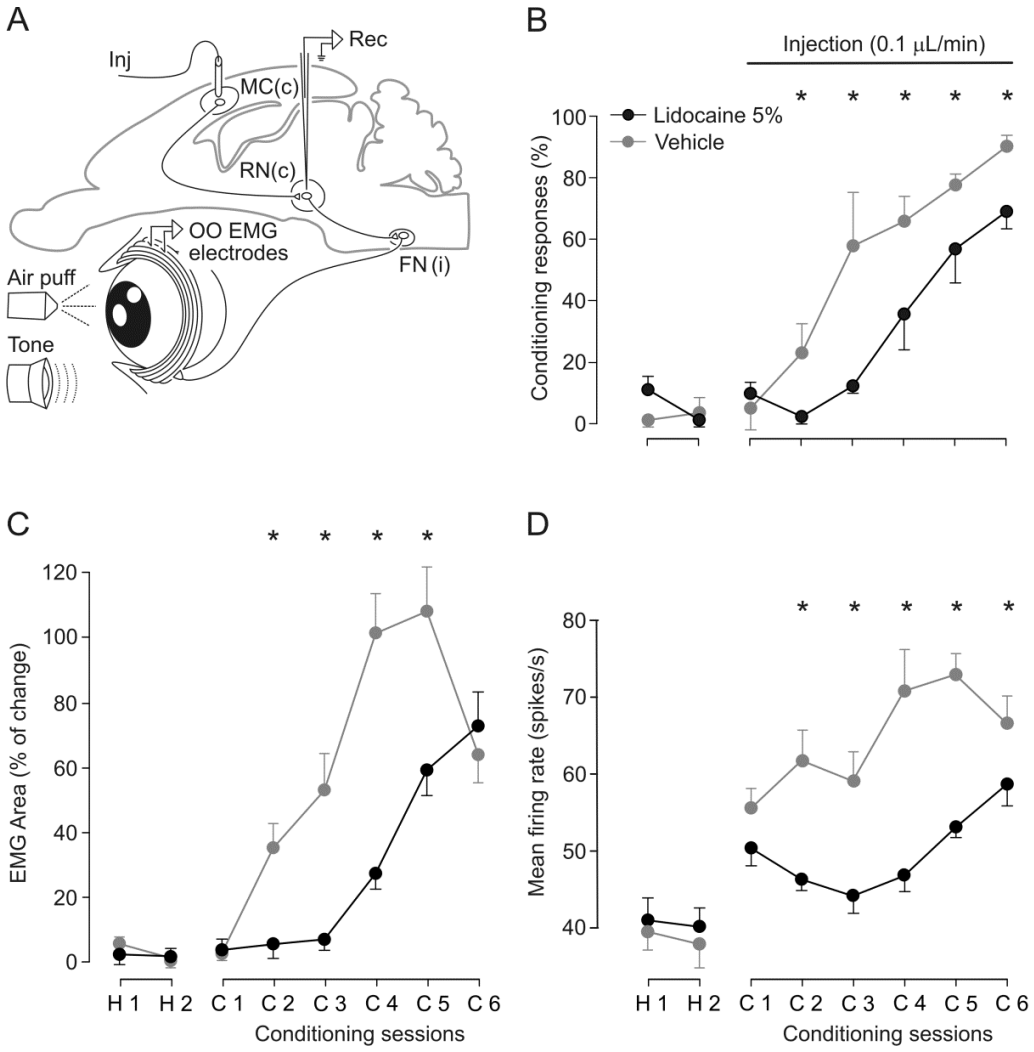

Figure 6. Effects of motor cortex inactivation on learning curves and on the firing rate of red nucleus neurons. A, Experimental design. The ipsilateral motor cortex (MC) was perfused with lidocaine (5% solution at rate of 0.1 µL/min) or vehicle (Inj) during classical eyeblink conditioning and unitary recording (Rec) of red nucleus (RN) neurons. Evolution of the percentage of conditioned responses (**B**), orbicularis oculi electromyographic area (**C**) and mean firing rate (spikes/s) (**D**) for the conditioned responses recorded during the classical conditioning sessions.

Electrophysiological recordings of neural activity across conditioning sessions indicated a significant increase in the amplitude of recorded synaptic field potentials in the hippocampus and related cortical sites (Gruart et al., 2006; Madroñal et al. 2007, 2009), such as motor (Troncoso et al. 2007) and prefrontal cortices (Leal-Campanario et al., 2013; Preston and Eichenbaum, 2013; Chen et al., 2014).

This increase in the amplitude of field potentials evoked in cortical circuits can be interpreted as facilitation (i.e., potentiation) of the synaptic processes underlying associative learning, thereby making possible the generation of acquired conditioned responses following presentations of a conditioned stimulus. Interestingly, the activity-dependent potentiation of synaptic strength in the motor cortex (Troncoso et al., 2007) is significantly larger than that reported at the hippocampal CA3-CA1 synapse during the same type of associative learning (Gruart et al., 2006). Thus, it is highly possible that learning-dependent changes in synaptic strength taking place in cortical networks mainly related to cognitive processes and to the storage of newly acquired abilities (Gruart et al., 2006; Citri and Malenka, 2008; Neves et al., 2008; Dragoi and Tonegawa, 2011) are paralleled by similar changes involving cortical premotor and motor circuits (Troncoso et al., 2007). Therefore, the simple diagram proposed many years ago by Thompson, among other scientists, to explain the neural basis of the classical eyelid conditioning focused on the cerebellar circuit, could become more complex, with the addition of numerous other structures involved in this simple type of learning and increasing the interconnectivity between them (**Figure 4**).

1.3 HIPPOCAMPAL FORMATION

The study of the hippocampal formation received the contribution of relevant and eminent neuroscientists at the end of the 19th century. The importance of the investigations made by Camilo Golgi and the utility of the technique that carries his name are beyond any doubt, but the mention of Golgi necessarily entails recalling Santiago Ramón y Cajal, with whom he shared the 1906 Nobel Prize in recognition of their work on the structure of the nervous system.

However, far from just reproducing the protocols for the Golgi staining method, Ramón y Cajal improved them, and was the first to describe the dendritic spines: ‘‘At first we believed that these protuberances were the result of a tumultuous silver precipitation; but the constancy of their existence [...] inclines us to consider them as normal structures’’ (Cajal, 1888). That statement produced diverse reactions in the scientific community—i.e., there were detractors and defenders; maybe one of the most outstanding within the latter group was Károly Schaffer (Schaffer, 1892), after whom the CA3 to CA1 axonal projection takes its name.

It is quite impressive how the diagrams of Ramón y Cajal (**Figure 7**) included arrows indicating the possible flow of information across the structure. No less surprising is the contribution made by Rafael Lorente de Nó, who used the number of dendritic spines to calculate the relative efficiency of afferents and formulate a special rule about summation of afferent inputs (Lorente de Nó, 1934).

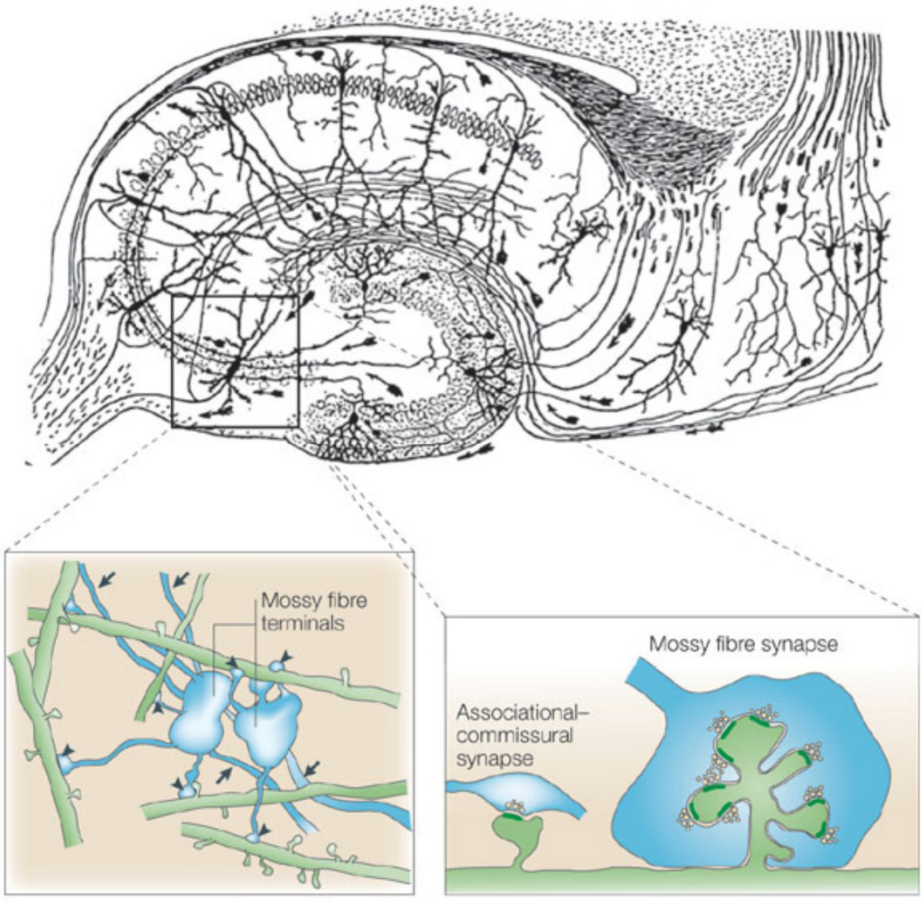

Figure 7. Hippocampal formation slice and hippocampal mossy fiber synapses. Classical drawing of the hippocampal formation by Santiago Ramón y Cajal, using hippocampal slices stained with the Golgi method. Note the arrows indicating the direction of the flux of information, and the precise graphical description of the dendritic arborization of pyramidal cells. Later studies enabled describing more precisely details of these synapses (bottom panels). Reproduced from Nicoll and Schmitz (2005).

As a relevant example, the development of neuroanatomical procedures and new techniques on neural imaging, as well as the use of molecular biology, confocal microscopy, and viral vectors for neuronal labeling, have improved knowledge in this field and the understanding of the elements that compose the massive contacts the main axon of dentate granule cells make on CA· pyramidal neurons, through filopodial extensions from axon terminals (**Figure 7**).

1.3.1 Structure and connectivity

Because the hippocampal formation has been deeply studied in both humans and different animal models, the number of available studies is huge and the data collected is diverse. Here, I will present some general aspects of the hippocampal formation including relevant details needed for the Discussion section. First at all, it is necessary to point out that in the nomenclature used here, "hippocampus" refers only to the region compressed by the CA fields CA1 and CA3 (although further subdivisions can be found in the scientific literature depending on the author). The hippocampal formation would include in addition other areas—that is, the dentate gyrus, subiculum, presubiculum, parasubiculum, and the entorhinal cortex (**Figure 8A**). The reason these six areas should be considered a whole formation is the linking connections that assemble a unidirectional neuronal pathway (**Figure 8B**). In contrast to the neocortex, the projections in this structure are not reciprocal—i.e., the entorhinal cortex projects to the dentate gyrus, but the latter does not send a return projection.

Taking the entorhinal cortex as starting point (for convenience, and considering that most of the cortical input to the hippocampal formation uses this pathway), the next structure is the dentate gyrus (this is in turn the main input to the hippocampal formation and is called the perforant pathway). The entorhinal cortex also projects directly to CA3 and CA1 fields and to the subiculum. The circuit becomes complex because dentate granule cells establish synaptic contacts (by mossy fibers) with CA3 pyramidal cells. In addition, pyramidal cells from the CA3 area send collaterals to the CA1 field (Schaffer collaterals). The outputs of this circuit are the CA1 field and the subiculum. The former establishes synapses with the subiculum and the entorhinal cortex, while the latter sends axon terminals to the pre- and parasubiculum and to the entorhinal cortex (Schultz and Engelhardt, 2014). A brief description of each different subregion is offered below.

1.3.1.1 Entorhinal cortex

The entorhinal cortex (**Figure 8**) delivers sensory information precedent from the primary sensory cortex and other cortical areas to the hippocampal formation via efferent pathways originated in its layers II and III. The major projection sent by the entorhinal cortex to the hippocampal formation is termed the perforant pathway (so named because the fibers pass through the entorhinal cortex and subiculum). The information carried by this projection reaches the dentate gyrus and CA3 (axons originated mainly in layer II) and CA1 and subiculum (axons originated in layer III) (Witter et al., 2000).

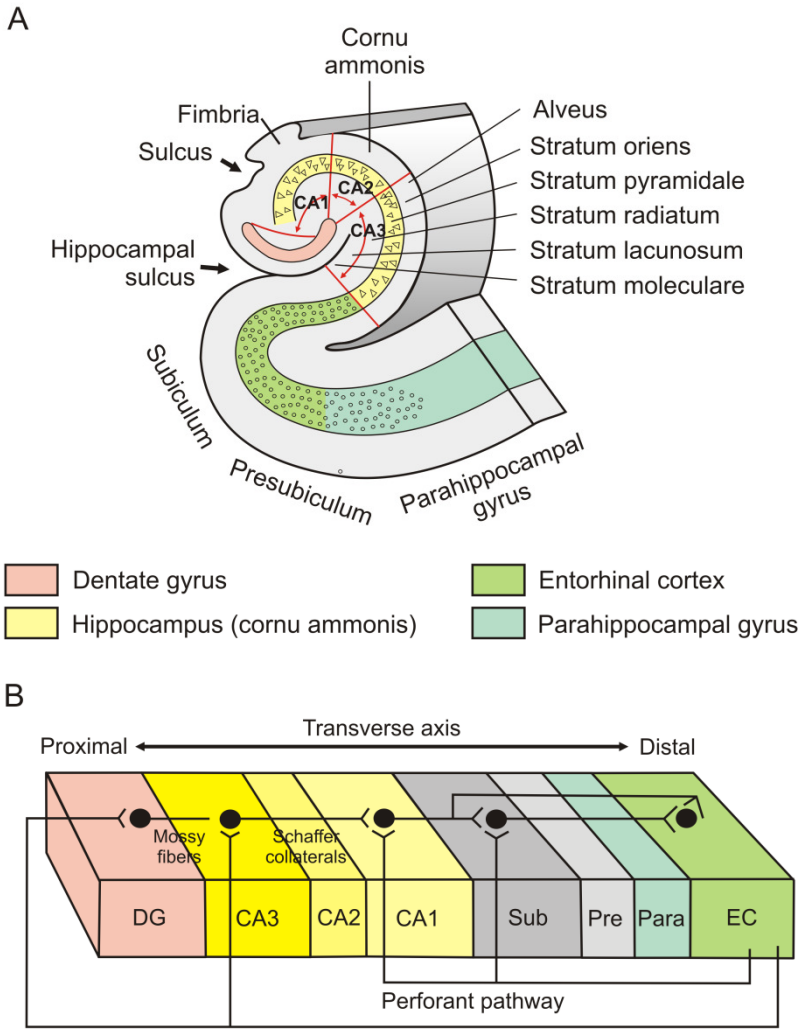

Figure 8. Connectivity in the hippocampal formation. A, Neurons in layer II of the entorhinal cortex (not shown in this diagram) project to the dentate gyrus and the CA3 field of the hippocampus proper via the perforant pathway. Neurons in layer III of the entorhinal cortex project to the CA1 field of the hippocampus and the subiculum via the perforant and alvear pathways. The granule cells of the dentate gyrus project to the CA3 field of the hippocampus via mossy fiber projections. Pyramidal neurons in the CA3 field of the hippocampus project to CA1 via Schaffer collaterals. Pyramidal cells in CA1 project to the subiculum. Both CA1 and the subiculum project back to the deep layers of the entorhinal cortex. **B,** Projections along the transverse axis of the hippocampal formation; the dentate gyrus is located proximally and the entorhinal cortex distally. Taken and modified from http:medicine.academic.ru/Hippocampus (Date: 03/02/2104) and from Amaral and Lavenex (2007).

There is a differentiation in the perforant pathway depending on the topological origin of its fibers. Those projections originated in the lateral entorhinal cortex are commonly known as the lateral perforant pathway, while those originated in the medial entorhinal cortex are known as the medial perforant pathway. These projections differ in the distribution of their synaptic contacts, and in the information that is processed by them (Hargreaves et al., 2005).

1.3.1.2 Dentate gyrus

The perforant pathway terminates in the molecular layer of the dentate gyrus (**Figure 8**); for this reason, some neurons, such as the mossy cells, do not receive a direct input from this projection. In addition to the projection from the entorhinal cortex, the dentate gyrus is reached by fibers arising in presubiculum and parasubiculum (Köhler, 1985). For a better understanding, a brief description of dentate gyrus organization seems useful.

In concordance with other fields of the hippocampal formation, the dentate gyrus is a three-layered structure, with the molecular layer closest to the hippocampal fissure. The principal layer is located under the molecular layer, where the granule cells are confined. These two layers form a U-shaped field that comprises another region, the polymorphic cell layer.

An important aspect of the dentate gyrus is its high connectivity. It has already been mentioned that the main input from the perforant path to the hippocampal formation is via the dentate gyrus, and that the presubiculum also sends projections to the dentate gyrus. It is important to remark here that the presubiculum receives direct input only from the anterior thalamic nucleus. Other important inputs, including the septal nuclei, the supramammillary area, and the brainstem, also reach this hippocampal area.

The septal projection is highly organized and includes two types of fiber: GABAergic fibers that terminate on basket pyramidal cells (mainly on interneurons located in the polymorphic layer) and cholinergic fibers that end on granule cells (in the inner third of the molecular layer). In contrast, the neurotransmitter involved in the hypothalamic afferents to the dentate gyrus is not so clear, but some evidence shows that the primary neurotransmitter could be glutamate (Kiss et al., 2000), and the localization of this input in the dentate gyrus is diffuse.

Finally, the projections coming from the brainstem deserve special mention, starting with the raphe nuclei, whose hippocampal terminals activate type 1a serotonin receptors on interneurons, which suppresses their activity and enhances dentate granular cell responses to perforant path stimulation (Levkovitz and Segal, 1997) from the locus coeruleus (Loy et al., 1980), which is responsible for modulation in long-term potentiation processes in the perforant pathway to dentate gyrus synapse (Harley, 1991; Klukowski and Harley, 1994; Walling et al., 2004) and could be participating in attentional tasks (Rajkowski et al., 2004). Perhaps not so deeply studied, but of increasing interest, is the projection of the ventral tegmental area to the dentate gyrus, whose dopaminergic input to the hippocampal formation could be involved in the

formation of contextual memory (Hamilton et al., 2010; Vivar and van Praag, 2013; Muñoz-López, 2015).

Taking into account the large variety of innervations that the dentate gyrus receives from different brain regions, it seems paradoxical that it projects only to the CA3 field of the hippocampus. Moreover, dentate gyrus efferents are strictly localized in mossy fibers that arise from the granule cells, establishing direct synaptic contacts in a relatively narrow area above the CA3 pyramidal cells (Blackstad et al., 1970; Claiborne et al., 1986). Nevertheless, this feature allows the dentate gyrus to be the main gate for incoming sensorial information into the hippocampal formation.

1.3.1.3 CA3

The pyramidal cells that can be found in the CA3 (**Figure 8**) area are variable in length and inputs. For instance, pyramidal cells located close to the limbs of the dentate gyrus are smaller and their dendritic projections do not reach the stratum lacunosum-moleculare; in consequence, they receive little or no innervation from the entorhinal cortex, but are heavily innervated by dentate mossy fibers (Cherubini and Miles, 2015). A special issue in the organization of the CA3 field is the innervation by mossy fibers. Indeed, this difference in mossy fiber inputs marks another subdivision, not so extended: the CA2 field. This field starts at the precise point where the mossy fibers end their innervations and adjoins the CA1 field. Another important aspect about mossy fiber projections is that each granule cell contacts about 15 CA3 pyramidal cells that can be spread throughout the CA3 field's proximal-distal length. Furthermore, and due to the CA3 pyramidal cell/dentate gyrus granule cell ratio, each CA3 pyramidal cell contacts an average of 72 granule cells (Amaral and Lavenex, 2007).

Projections of CA3 pyramidal cells present a topographic organization; in particular, Schaffer collaterals that are sent by CA3 pyramidal cells close to the dentate gyrus reach mainly the septal levels of the CA1 field, while—in contrast—CA3 cells located close to CA1 project to the temporal level of this area.

The other important projection arising from CA3, the associational projections from CA3 to CA3, is also highly organized, and the proximal portions of the area project to the proximal portions of the contralateral field, while the medial and distal portions send projections through much of the transverse and septotemporal area of the contralateral CA3.

The non-pyramidal cells of the hippocampus are heterogeneous with respect to their morphology, peptide content, physiological properties, and postsynaptic targets. Moreover, the content of peptides (cholecystokinin, somatostatin) and calcium-binding

proteins (parvalbumin and calbindin) of non-pyramidal cells is not related to their characteristic fine structure or synaptic inputs (Danos et al., 1991).

1.3.1.4 CA1

In contrast to the size diversity found in the CA3, pyramidal neurons compressed in the CA1 area keep a strict homogeneity all over the field; however, that fact does not correlate with the differentiated pattern of entorhinal cortex inputs to this hippocampal area (**Figure 8**). The CA1 field is innervated mainly by layer III of the entorhinal cortex and, depending on the relative position of the pyramidal cells, entorhinal projections reach different portions —namely, distal regions of CA1 receive inputs from the lateral entorhinal area, while proximal CA1 pyramidal cells are contacted by fibers arising in the medial entorhinal cortex (Amaral and Lavenex, 2007).

An important extrinsic connection in CA1 is the strong innervation arising from the thalamic reunions nucleus. The reuniens nucleus was assumed to be exclusively of an excitatory nature (Herkenham, 1978; Wouterlood et al., 1990), but some reports have shown recently that the reuniens nucleus is able to drive putative inhibitory interneurons in the strata oriens and radiatum (Dolleman-Van der Weel et al., 1997; Dolleman-Van der Weel and Witter, 2000).

Efferents of the CA1 region end in two intrahippocampal areas: the subiculum and the entorhinal cortex. Axons emerging from CA1 pyramidal cells travel through the stratum oriens and then bend towards the subiculum, where they enter the pyramidal cell layer and ramify. In this case, there is an "inverted" spatial distribution, since distal portions of CA1 innervate proximal portions of subiculum while the distal and medial ones are contacted respectively by proximal and medial pyramidal cells of the CA1 field. Data regarding efferent pathways to the entorhinal cortex will be described together with the subiculum efferents to this same place (Amaral and Lavenex, 2007).

1.3.1.5 Subiculum

It is necessary here to point out that the nomenclature used in the literature to name the different regions of the subicular complex is not well established, and we can find that the term subiculum (**Figure 8**) has been extensively used to refer to a region that can be divided in two: the presubiculum and the subiculum (Ding, 2013). The nomenclature used here is the most simple, which subdivides the subicular complex into three regions.

The subiculum represents the major output of the hippocampal formation (Meibach and Siegel, 1977a,b; Rosene and Van Hoesen, 1977; Swanson and Cowan, 1977) and possibly because of the magnitude of this feature it is considered to

participate in different processes from long-term memories to affective behavior and learning processes (Squire et al., 2004; O'Mara et al., 2009). However, the subiculum should be considered a part of the hippocampal formation, and the functions that this field is able to carry out are possible because it works not alone and isolated, but in consonance with other hippocampal regions.

As is expected for the output of a structure that receives different sensory inputs, the subiculum projects to different brain areas. For instance, there is a great flux of information from the subiculum to cortical regions. Thus, different areas within the restrosplenial cortex (retrosplenial dysgranular cortex, retrosplenial granular cortex a and b) receive dense projections from the septal portion of the subiculum (Wyss and Van Groen, 1992), while the lateral and medial prefrontal cortices are innervated by neurons of the stratum pyramidale and of the temporal and intermediate portions of the subiculum (Verwer et al., 1997). The amygdaloid complex receives a strong projection from the ventral portion of the subiculum, as described in monkeys (Rosene and Van Hoesen, 1977; Aggleton, 1986) and rats (Canteras and Swanson, 1992).

However, the most-prominent projections arising from the subiculum (more specifically, from its entire dorso-ventral and transverse extent) are those sent to septal and accumbens nuclei (Ishizuka, 2001). This innervation is unidirectional in the case of the nucleus accumbens, or the back projection is weak, as in the case of the cholinergic input of the septal nucleus into the subiculum.

Finally, other significant connections of the subiculum are those established with hypothalamic and thalamic structures, such as the inputs to the mammillary nuclei (Aggleton et al., 2005), which are in fact the most important in this structure, and send to the nucleus reuniens from the septal and temporal areas respectively of the subiculum (Varela et al., 2014).

1.3.1.6 Presubiculum

The boundary between the subiculum and presubiculum is clear using a Nissl staining, since the latter has a distinct and densely packed external cell layer consisting of small pyramidal cells, more dense in layer II than in layer III.

The intrinsic and commissural connections of this region are strong. In the case of the layer II, ventrally located neurons send fibers to the more-dorsal portions, while opposite projections arise from deeper layers. Commissural connections are projected to layers I and III of the contralateral presubiculum (Van Groen and Wyss, 1990).

Despite the fact that the presubiculum (**Figure 8**) is part of the hippocampal output structure (the subicular complex and the pre- and parasubiculum are considered a single whole functional region), it is influenced by other structures and sends, in turn,

projections to different brain areas such as thalamic nuclei and other cortical regions. Perhaps, the most important projection from the presubiculum is that sent to the entorhinal cortex (Shipley, 1975), innervating the layer III of the medial entorhinal cortex.

1.3.1.7 Parasubiculum

In contrast with the pyramidal neurons of the presubiculum (**Figure 8**), those of the parasubiculum are large and densely packed in layers II and III. Nevertheless, this region shares some characteristics with the anatomically adjacent presubiculum, such as the associational connections which are distributed dorsally and ventrally from cells of different origins, and the commissural connections that terminate in layers I and III (Amaral and Lavenex, 2007).

In the case of the extrinsic connections, the pattern of innervation of the thalamic nuclei is almost identical to that seen in the presubiculum, but some differences can be found in the case of the entorhinal cortex. Thus, the presubiculum projects to medial and lateral entorhinal areas (instead of only specifically to the medial area) and innervates only the layer II (in the case of presubiculum, the innervated layer is the layer III).

All these important intrinsic, commissural, and extrinsic projections situate the hippocampal formation as a major candidate for participating in learning and memory processes, a point that is discussed in the next section.

1.3.2 Hippocampal formation and classical conditioning

This curved structure located within the medial temporal lobe of the human brain, together with its contralateral half, strongly resembles the horns of a ram, the reason for which members of the Alexandrian school of medicine named it cornu Ammonis. Although this terminology is no longer used, it still survives in the acronyms for the hippocampal subfields CA1, CA2, and CA3. It was a Bolognese anatomist, Giulio Cesare Aranzi (1564), who first coined the term "hippocampus" because of its resemblance to the well-known tropical fish, the seahorse. As can be deduced from the dates of origin of the terms referring to the hippocampus and its subregions, this structure has been a matter of study and discussion since antiquity, and the functions attributed to it have appeared and been modified with the progressive development of neuroanatomical and histological procedures (Amaral and Lavenex, 2007).

Until the 1930s, the hippocampal formation was considered to be a part of the olfactory system, maybe induced by clinical observations of patients presenting olfactory hallucinations preceding and/or during hippocampal epileptic seizures.

However, a key review made by Alf Brodal raised doubts about the role of the hippocampus in olfaction (Brodal, 1947). Another significant hypothesis about the functions of the hippocampus was the so-called Papez circuit, which placed the hippocampal formation as a collector of sensory information inside a set of structures believed to be the anatomical substrate of emotion (Papez, 1937). But again in this case, it was Brodal who showed some skepticism about this circuit, and thought that there was no biological basis for this hypothesis (Brodal, 1981).

The association between hippocampal formation and memory was not raised until the observations made by Brenda Milner and William Scoville in 1957 (Scoville and Milner, 1957) during the study of the famous patient Henry Gustav Molaison (H.M.), who suffered severe epileptic seizures that did not improve with drugs and finally had to be surgically treated with a bilateral resection of the medial temporal lobe. This case, together with those published (Penfield and Milner, 1958) of two other patients who became amnesic after a left temporal lobotomy and additionally showed concomitant electrographic abnormalities in the right medial temporal lobe, strengthened the idea of the involvement of the hippocampal formation for long-term declarative memory, including the acquisition of new semantic knowledge (Gabrieli et al., 1988). From these experiments, many scientists have pointed out the strong link between the hippocampus and learning and memory processes (Barnes, 1988; Vivar and van Praag, 2013; Muñoz-López, 2015).

Previous experiments done in the Division of Neuroscience of the Pablo de Olavide University on the hippocampal role in classical eyeblink conditioning showed that the hippocampus is involved in the abstract analysis of temporal relationships between conditioned and unconditioned stimuli, their associative strength, and, perhaps, the predictive value of conditioned stimulus, but not in the genesis and/or performance of acquired conditioned responses (Múnera et al., 2001). These results are in some contradiction with previous reports on hippocampal activity of rabbits during classical conditioning of the nictitating membrane response (Berger et al., 1983; Thompson, 1988; Moyer et al., 1990, 1996; Thompson and Krupa, 1994; McEchron and Disterhoft, 1997, 1999). However, various authors have also reported significant differences for conditioned-stimulus presentation between rabbits and cats (Patterson et al., 1979) or between hippocampal areas (Suter et al., 2013).

There are some considerations that might bear on the observed differences. Although cats and rabbits are both mammals, they belong to different orders. Since the former are predators and the latter are prey, their cognitive strategies to cope with specific tasks could be different. Moreover, there are noticeable differences in the control of lid movements in cats and rabbits. For example, whereas eye retraction in

rabbits is the key component of the blink (Leal-Campanario et al., 2004), in cats the active closure of the lid by the contraction of the orbicularis oculi muscle is more crucial (Gruart et al., 1995, 2000). This is even more evident for classically conditioned blink responses (Trigo et al., 1999a,b). In addition, there is an anatomical peculiarity of the rabbit's hippocampus that has not been identified in other species (Gloor, 1997)—i.e., a recurrent projection from the subiculum to CA1 and CA2 regions (Berger et al., 1980). These differences in motor and neural control of eyelid movements are not restricted to the facial motor system, because considerable differences have also been reported for the oculomotor system of the two species (Graf and Simpson, 1981).

In this Doctoral Thesis, a delay conditioning paradigm with a 500-ms interstimulus interval has been used. Although a 250-ms interval is more usual, the longer interval has occasionally been used. This strategy was selected to dissect out neuronal responses to the conditioned and unconditioned stimuli within a longer-lasting CS-US time window. In addition, in the present experiments, the trace conditioned stimuli lasted only 20 ms, in contrast with the usual 100–500 ms. This feature made the task more cognitively demanding and allowed a longer time window for both unitary and field potential recordings in the absence of any experimentally evoked sensory stimulus.

The most usual technique for eyeblink conditioning in rabbits involves a restriction of eyelid movements and the recording of the nictitating membrane displacement. However, in the present experiments we allowed free movements of the lids and recorded the position of the upper eyelid using the search coil in a magnetic field technique. As already shown by our group in rabbits (Gruart et al., 2000), there are considerable differences between lid and nictitating membrane kinematics. Mainly, lid responses are the result of the direct action of the orbicularis oculi muscle rather than a passive displacement following eyeball retraction into the orbit. As a consequence, lid displacements have a shorter latency and a less-damped profile. These differences are extremely important for the establishment of quantitative relationships between movement profiles and neural firing rates.

In a previous experiment done in our laboratory, we carried out single-unit recording of hippocampal pyramidal cells with glass micropipettes directed toward the dorsal hippocampus through a recording chamber of 8 mm x 3 mm x 8 mm (Múnera et al., 2001). This chamber afforded an actual recording area of about 18 mm^2, comprising predominantly the CA1 region, and a narrow band of the CA3 region. Isolated units were identified as pyramidal neurons using not only their antidromic activation from the fornix but also the firing profile criteria used by others (Fox and Rank, 1981; Berger et al., 1983; McEchron and Disterhoft, 1997). Previous studies of

hippocampal activity in awake rabbits during classical conditioning of nictitating membrane responses were, in general, based on multiunit activity records obtained using fixed or adjustable arrays of metallic electrodes. Multiunit activity was either processed as a whole or discriminated by means of computer-assisted devices. The latter, however, are prone to mistakes, due to the variability in shape of extracellularly recorded action potentials from pyramidal and non-pyramidal cells. Moreover, the activity of nearby different subtypes of hippocampal interneurons could shadow the activity of actual pyramidal cells (Parra et al., 1998), with the single spike of an identified pyramidal cell being surrounded by electrical activity from nearby cells. Notwithstanding, the computer-based discrimination technique has demonstrated a wider range of response profiles of the hippocampal neurons during the classical conditioning of the nictitating membrane response. Berger et al. (1983), using single-unit recording with tungsten electrodes, reported a population of hippocampal neurons that displayed, as reported here, strong conditioned-stimulus-evoked and weak unconditioned-stimulus-evoked responses. Those neurons were not antidromically or orthodromically activated, but their firing properties were similar to those of the hippocampal pyramidal neurons reported in the paper of Múnera et al. (Múnera et al., 2001). Also, in coincidence with the results of Múnera et al., Berger et al. reported similar changes in the firing rates of CA1 and CA3 pyramidal neurons during conditioning (Berger et al., 1983).

Since hippocampal pyramidal cell firing is characterized by brief bursts, the claim that their firing forms a temporal model of the conditioned responses is difficult to explain. There are only two conditions in which such a model could be generated by a single pyramidal neuron: first, by changing its firing pattern from phasic to tonic; and second, as an averaging artifact if the neuron fires bursts randomly around the time of unconditioned-stimulus presentation. Previous studies on hippocampal pyramidal cell activity during classical conditioning of eyeblink responses did not report any shift in their firing pattern, which rules out the first possibility. Even so, if the second one turns out to be right, it is difficult to accept that such a random firing could have any functional significance for the control of conditioned-response execution.

1. 4 CHANGES IN SYNAPTIC STRENGTH DURING CLASSICAL CONDITIONING

One of the key neuroscientific questions raised in recent years is whether learning processes induce changes in synaptic strength. These changes should be expected, since it is commonly accepted that acquired learning abilities are stored in the form of functional and/or structural changes in synaptic efficiency (Hebb, 1949). The

hippocampal CA3-CA1 synapse is one of the most used to address this issue, mainly in experiments carried out with wild-type and genetically manipulated mice.

One of the most widely used experimental models for studying the neural processes underlying learning is the classical conditioning of the eyelid responses using a trace paradigm. The Division of Neuroscience has developed a precise protocol for the study of neural events accompanying the acquisition of this type of associative learning in mice (**Figure 9A**). For evoking this conditioning task, the experimental animal is presented with a tone as conditioned stimulus and an electrical shock to the trigeminal nerve, 500 ms afterwards, as unconditioned stimulus (Gruart et al., 2006). At the same time, field excitatory postsynaptic potentials evoked in the hippocampal CA1 pyramidal cells by the electrical stimulation of the ipsilateral Schaffer collateral-commissural pathway can be recorded in vivo (**Figure 9B**). This experimental design includes the presentation of a single electrical pulse to Schaffer collaterals, 300 ms after presentation of the conditioned stimulus (i.e., the tone). Thus, changes in field excitatory postsynaptic potentials evoked right after conditioned-stimulus presentation (during habituation, acquisition, extinction, retrieval, and reconditioning sessions) can be analyzed (Gruart et al., 2006; Madroñal et al., 2007).

During classical eyeblink conditioning, mice present a typical learning curve starting from 30% and rising to 80% of conditioned responses by the 10th conditioning session (**Figures 9C and 10**). Mice are very active, and during the habituation sessions present not less than 15% of eyelid responses to tone presentations. In each of the 60 trials per session, a field excitatory postsynaptic potential is evoked by the electrical stimulation of Schaffer collaterals during the conditioned and unconditioned interval. As already indicated, an important question is whether this type of associative learning can modify the synaptic strength of hippocampal CA3-CA1 synapses. Results collected in the Division of Neuroscience show that the slope of evoked field excitatory postsynaptic potentials increases progressively across conditioning, to a maximum of 140% during the 8th and 9th conditioning sessions. For extinction, the field excitatory postsynaptic potential slopes decrease back to baseline values. In general, changes in synaptic efficacy present a linear relationship with the amount of acquired, or extinguished, learning level (Gruart et al., 2006).

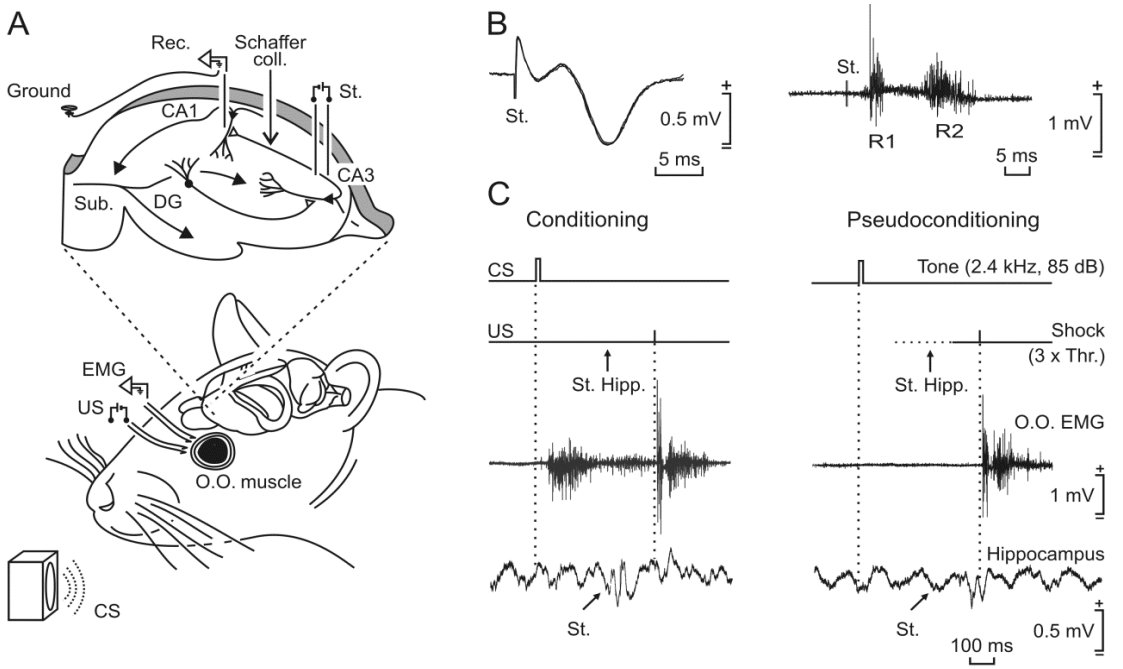

Figure 9. Methodology to study the hippocampal synaptic field potential during classical eyeblink conditioning of behaving mice. A, Placement of chronically implanted electrodes for stimulation and recording. The loudspeaker for the conditioned stimulus was placed in front of the animal. **B,** Three superimposed recordings on the left illustrate the extracellular synaptic field potential recorded in the stratum radiatum of the CA1 area after electrical stimulation (St.) of Schaffer collaterals. On the right, example of a blink reflex recorded from orbicularis oculi muscle electromyography after trigeminal nerve stimulation (St.). **C,** Diagrammatic representation of the classical conditioning paradigm, with examples of muscle electromyography and hippocampal recordings for conditioned (left) and pseudoconditioned (right) mice. (Modified from Gruart et al., 2006).

In contrast, the percentage of conditioned responses or field excitatory postsynaptic potential values collected during pseudoconditioning (i.e., during the unpaired presentations of tones and eyelid shocks) do not show any significant change in slope values (**Figures 9C and 10**). Interestingly, stimuli presented during the experimental sessions, but outside the conditioned and unconditioned interval, evoke field excitatory postsynaptic potential slope values similar to those collected during the conditioned- / unconditioned-stimulus interval, meaning a general increase in synaptic strength during the whole experimental session. The percentage of conditioned responses and the field excitatory postsynaptic potential slope increases are maintained during the retrieval sessions after a week, and are easily recovered—and even exceeded—during reconditioning sessions.

The involvement of hippocampal unitary activity in classical conditioning of nictitating membrane/eyelid responses is very well known (Gruart and Delgado-García, 2007). Using unitary in vivo recordings, it is found that hippocampal pyramidal cell firing to conditioned-stimulus presentations increases several sessions in advance of behavioral conditioning (McEchron and Disterhoft, 1997; Múnera et al., 2001). Although

it seems that the discharge rate of hippocampal CA1 pyramidal neurons does not encode the kinetic peculiarities of conditioned eyelid responses, the CA1 firing is linearly related with the progressive acquisition of the eyelid learned response, with a gain of ~0.035 spikes per second per trial, as determined in behaving cats during trace conditioning (Múnera et al., 2001). The slow building up of hippocampal neuronal responses across conditioning is similar to the small increase in the slope of fEPSPs evoked in the apical dendrites of CA1 pyramidal cells by single pulses applied to Schaffer collaterals during trace conditioning in mice: a 0.03% increase in the fEPSP slope per trial (Gruart et al., 2006).

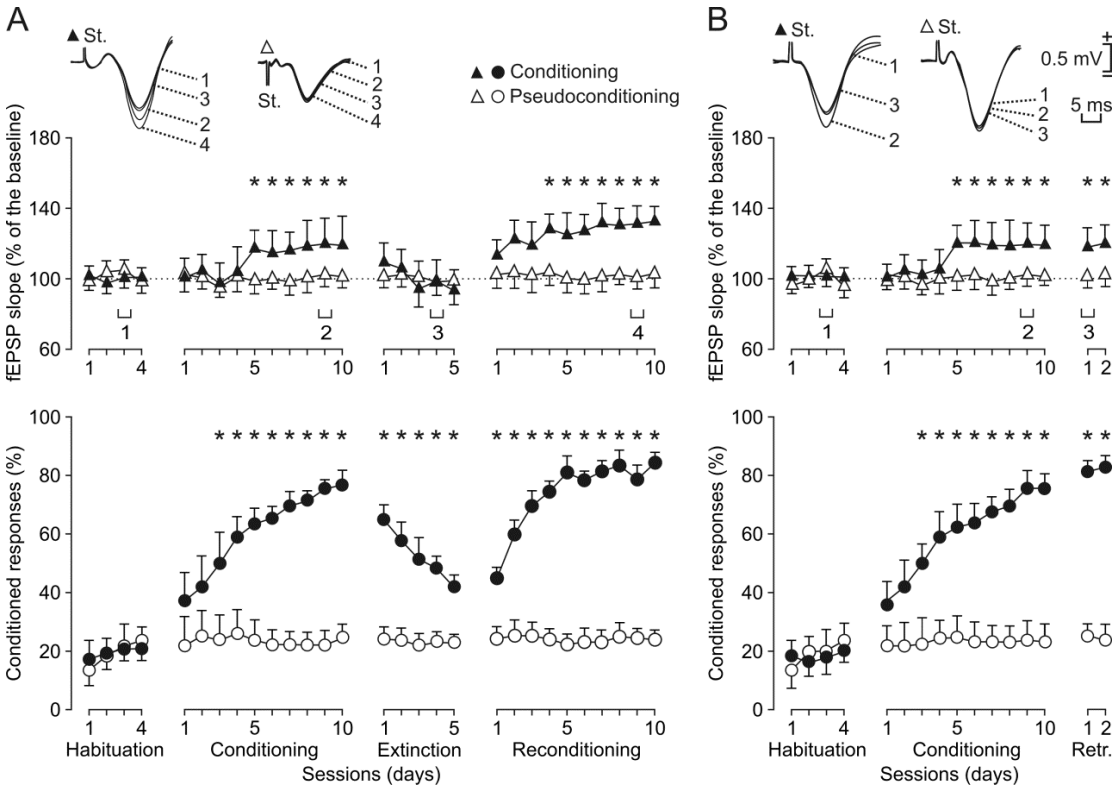

Figure 10. Learning curves and evolution of hippocampal synaptic field potential during classical eyeblink conditioning of behaving mice. A, Synaptic field potentials and learning curves for conditioned (filled symbols) and pseudoconditioned (open symbols) mice during four different learning phases: habituation, conditioning, extinction, and reconditioning. **B,** Synaptic field potentials and learning curve during two retrieval (Retr.) sessions for conditioned (filled symbols) and pseudoconditioned (open symbols) mice. (Modified from Gruart et al., 2006).

The reported modulation in CA3-CA1 synaptic strength during acquisition, extinction, retrieval, and reconditioning is a slow process that seems to be originated by changes in the probability of releasing synaptic vesicles by CA3 terminals and/or by subtle modifications in the number of presynaptic active zones and/or postsynaptic receptor sites. From a functional point of view, the increased (or decreased) responsivity of CA1 pyramidal cells to Schaffer collateral stimulation suggests that,

during the conditioned- / unconditioned-stimulus interval, they are in a facilitated (or disfacilitated) state, evoked by changes in coincident inputs of different (entorhinal, septal) origin (Andersen et al., 2007). It is still possible that several synaptic mechanisms taking place at different neuronal structures are acting in parallel to enhance hippocampal CA3-CA1 synaptic transmission across classical conditioning of the eyelid.

2. HYPOTHESIS AND OBJECTIVES

Learning and memory processes probably require the participation of several different neural circuits. These related neural structures have to change their activities in certain periods across the learning process as well as during memory storage and retrieval. The animal's basal state (previous learning, attention, motivation, pain, etc.), environmental constraints (context, temperature, etc.), or the learning protocol (stimuli, duration of the session, phases of the process, etc...) will certainly have an impact on the activity of different neural interconnected structures. In this sense, and in order to have a general picture from the circuitry interaction to the specific changes taking place at the synaptic contacts, the learning process has to be studied in vivo and using different methodological procedures.

In this Doctoral Thesis, a double aim was proposed to cover each of these two levels of analysis. All the experiments were carried out in alert behaving rabbits, and the learning was quantified as the percentage of conditioned responses evoked during classical eyeblink conditioning paradigms. A multidisciplinary approach was used to answer the proposed questions.

The hypotheses and objectives of this work were as follows:

a) **Hypothesis 1.** The hippocampal formation is part of the neural circuitry needed to generate classically conditioned eyelid responses, and changes in the activity of the different synapses included in this structure will depend on the type of protocol used and on the different contextual constraints.

To test this hypothesis, the following three **Objectives** were experimentally addressed:

a1) To determine whether field excitatory postsynaptic potentials evoked in different synapses of the hippocampal formation change their slope values during different learning situations.

a2) To check whether the putative changes are similar in all the synapses during the different learning phases, or in non-learning paradigms (context or pseudoconditioning).

a3) To establish the possible specific roles of the different subdivisions of the hippocampal formation.

b) **Hypothesis 2.** Some alternative to the generally accepted paradigm of memories being stored in the molecular structure of synaptic dendritic spines seems to be needed, since no consistent data can show a convincing relationship between learning processes and molecular composition.

To test this hypothesis, the following two **Objectives** were experimentally addressed:

b1) To test the capability of reducing the learning rate and the concomitant synaptic activity, by temporarily silencing synaptic contacts between dentate gyrus and CA3 pyramidal cells in alert behaving rabbits.

b2) To determine the degree of recovery of learning levels and of synaptic activities once the above-mentioned inactivation is finished. If memories are stored in the dendritic spines, the experimental inactivation and/or dis-connection of dentate gyrus-CA3 synapses should interfere in memory storage processes.

3. MATERIALS AND METHODS

3.1 ANIMALS

Experiments were carried out in New Zealand male adult rabbits, provided by Isoquimen (Barcelona, Spain), and weighing 2.5-3.0 kg upon their arrival at the Pablo de Olavide Animal House. Animals were housed in individual cages and kept on a 12 h light/dark cycle with constant environmental temperature (21 ± 1 ºC) and humidity (55 ± 5%). Food and water were available ad libitum for them. All the experiments were carried out during the light phase and in accordance with the guidelines of the European Union (2010/63/UE) and Spanish regulation (RD 53/2013) for the use of laboratory animals in chronic studies. In addition, all experimental protocols were approved by the local Ethics Committee of the Pablo de Olavide University.

3.2 ELECTRODES AND GROUND PREPARATION

Tetrodes for the recording of field excitatory postsynaptic potentials (**Figure 11**) were made from 50 µm, Teflon-coated, tungsten wire (Advent Research, Eynsham, UK). The four wires were twisted together and linked with a layer of primer (Loctite® 406) and, 30 min afterwards, a layer of glue (Loctite® 770). Three hours later, these four joined wires were cut at different lengths, and Teflon was removed to 200 µm from each tip. In this way, they formed a step-down electrode where each wire could record at a different point in depth (**Figure 11A**). Stimulating electrodes were made identically, but assembled with 3 wires instead of 4, and with an uncovered tip of 300 µm.

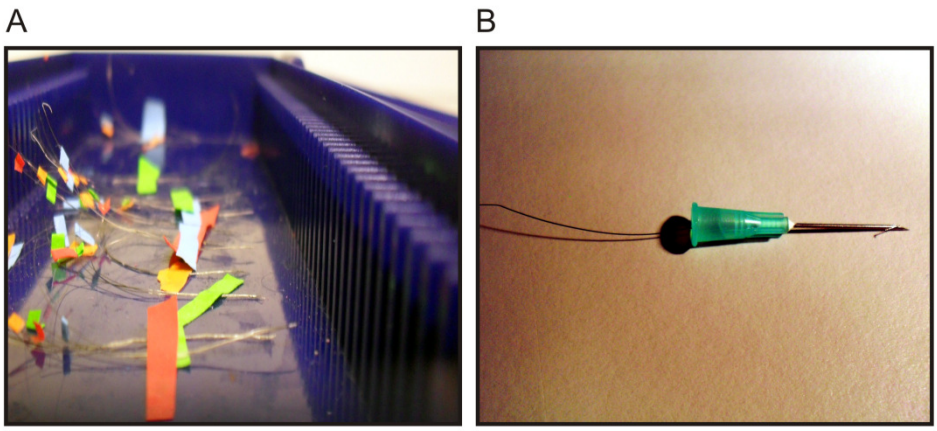

Figure 11. Photographs of the electrodes used for electrophysiological recordings. A, Tetrodes used for field excitatory postsynaptic potential recordings in the hippocampal formation. As can be observed, these electrodes were labeled with colored tape such that each tip of the tetrode could be identified and distinguished from the others. **B,** Seven-stranded, Teflon-coated, stainless steel wire for electromyographic recordings introduced inside a hypodermic needle to facilitate implantation into the orbicularis oculi muscle. The electrode tip to be inserted in the muscle is bent to assist its fixation to the muscle fibers.

A 7-stranded, Teflon-coated, annealed stainless steel wire with an external diameter of 50 μm (793500, A-M systems Inc., WA, USA) was used for electromyographic recordings. In order to facilitate their proper insertion, the wire was placed inside an insulin hypodermic needle (**Figure 11B**). Once the wire was inside the needle, the tip was bared of Teflon and bent to form a hook which prevented the de-insertion of the electrode.

A silver wire (783000, A-M systems Inc., WA USA) soldered with tin to a screw served as ground.

3.3 PRE-SURGERY

A daily handling protocol was started at least one week before the surgery day. During this period, rabbits were habituated to the experimental conditions and to the restraining box. Only rabbits which did not present stressing signals under these conditions were chosen for the following experimental phase.

3.4 SURGERY

3.4.1 Common procedures

Rabbits were pre-anesthetized with a mixture of the hypnotic drug Ketaminol (Imalgene®, 25 mg/kg) and the sedative drug Xylazine (Rompun®, 3 mg/kg) delivered i.m. To prevent secretions, atropine sulfate (0.1 mg/kg) was injected with the same procedure.

When the proper level of anesthesia was reached, the frontal, occipital, and parietal zones of the head were shaved using an electric shaver. The margin of the right ear and a small perimeter of the anterior left leg were also shaved. After shaving, an antiseptic solution (Dermozel®, Schering-Plough S.A., Spain) was applied to the skin to prevent infections.

Animals were then moved to the surgery room, and cannulated in the marginal vein of the right ear using an intravenous catheter of gauge 24G (Abbocath®) connected to an adjustable flow probe. The infusion flow was maintained at 25 mL/h, and consisted of 100 mL of physiological serum with a drug concentration of 10 mg/mL Ketaminol and 3 mg/mL Xylazine.

For the correct monitoring of vital signals (heart rate and oxygen saturation), a sensor connected to a pulsioxymeter (Canl-425SV, MED Associates INC.) was fixed to the shaved leg. In addition, the animal's temperature was constantly monitored and controlled thanks to a temperature control system (TR-200, Fine Science Tools INC.)

coupled to an anal thermometric probe and to a thermal pad beneath the animal. The body temperature of animals was kept within physiological values (39.0 ± 0.5 ºC).

After this initial preparation, the animal was placed in a stereotaxic frame (**Figure 12A**, David Kopf Instruments 1204, Tujunja, CA, USA) and its head was immobilized with the help of a buccal support located under the incisors and two lateral brackets applied to both zygomatic bones. A transparent gel was applied on both corneas (Methocel® 2%, CIBA vision) to prevent ocular damage by desiccation.

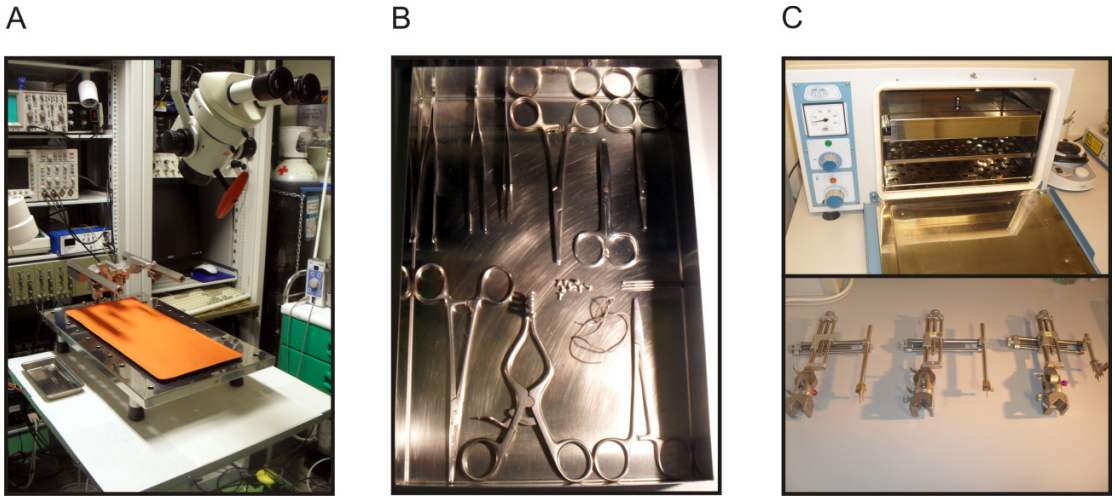

Figure 12. Material prepared for surgery. Once animals were pre-anesthetized, they were i) moved to the surgery room; ii) cannulated in the marginal vein of the right ear; and iii) placed on an electrical blanket extended in a stereotaxic frame (**A**). The head was immobilized to determine the correct system of coordinates. All the material used in the surgery (**B**) was previously sterilized using a cycle of dry heat of 150 ºC for 60 min (top equipment in **C**). The Bregma and Lambda points were located and all coordinates and distances were measured with the help of stereotaxic manipulator arms (bottom equipment in **C**).

All the material for surgery was previously sterilized (**Figure 12B and C**) applying a dry heat cycle at 150 ºC for 60 min in a sterilizer (Dryterm, Cod. 2000787, J.P. Selecta S.A, Barcelona, Spain). As a standard procedure, all surgery was carried out according to the following steps:

a. A medial fronto-occipital incision of the head skin and subcutaneous tissues, a retraction of temporal muscles, and the removal of the periosteum with the help of a scalpel and a palette knife was performed to achieve the correct exposure of cranial bones. The exposed area was cleaned with a Ringer solution at 38 ºC and any bleeding was stopped with bone wax (Ethicon®, Johnson & Johnson Intl., Beerse, Belgium).

b. The correct positioning of the animal's head was needed in order to get an accurate system of coordinates to locate the desired points on the surface of

the skull. Bregma and Lambda positions were determined and then the sagittal plane was adjusted, with the help of a stereotaxic manipulator arm (**Figure 12C**, bottom), until the difference of depth between Bregma and Lambda was equal to 1.5 mm, which is the stereotaxic horizontal position of the rabbit's head (Girgis and Shih-Chang, 1981).

c. With the help of a needle attached to a second stereotaxic manipulator arm, the antero-posterior distance between Bregma and Lambda was verified. This distance should be approximately 18 mm. At this point, a correct system of reference was established and it was possible to mark the places of interest using the needle attached to the micromanipulator.

d. The perforation of cranial bones for the subsequent electrode implantation and insertion of screws (which served as ground and anchoring) were performed with the help of a dental drill (NE 120, NSK Dental-Spain, Madrid, Spain). After implantation, a layer of cyanocrylate (Superglue 3, Loctite®) was applied as initial fastener before dental cement (Duralay®, Dental Mfg. Co., IL, USA) application.

e. Three more screws (25 mm in length and 5 mm in diameter) were attached to the surface of the skull, so the head of the animal could be fixed in position during the conditioning sessions, preventing avoidance of the air puff.

f. Two electrodes for electromyographic recording of the orbicularis oculi muscle activity were implanted in all animals.

g. All wires coming from recording and stimulating electrodes, as well as the ground, were soldered to a nine-pin female connector (DB-9) which was in turn affixed to the skull with dental cement.

h. Once the whole assembly was finished, the rostral and caudal sides of the incision were sutured with a silken thread (2:0, F.S.T, Cat. Nº 18020-30, USA), applying single plain stitches. In addition, eye drops containing gentamicine and dexamethasone (Gentadexa®) was applied to the sutured incision, as well as a topical ointment (Blastoestimulin®) to assist the re-growth of fibroblasts. Finally, to prevent any possible infection, animals were injected with 0.5 mL of penicillin (Penilevel®, Benzylpenicillin sodium 250000 UI/mL, *Laboratorios* ERN SA, Barcelona, Spain) and were taken back to their home cages.

3.4.2 Specific procedures

For each set of experiments, a different assembly of electrodes was implanted in the corresponding groups of animals; in particular, two main specific types of preparative surgery were performed. The first type was applied in the groups to be used for the study of synaptic activities within the hippocampal formation in different experimental situations. In this case, several recording and stimulating electrodes were implanted to extract information of different synapses across the training sessions. The second type of surgical preparation was aimed at assessing the effect of dentate gyrus inhibition in the acquisition, storage, and retrieval of conditioning eyeblink responses.

3.4.2.1 Synaptic state of hippocampal formation

To recruit all the data needed to construct a model of synaptic functional states, various electrodes were implanted in these groups of animals in such a way that a recording of the selected synapses was possible. For all electrodes, the reference of the system on the anterior-posterior axis and laterality was the Bregma point. In the case of the depth coordinate, the surface of the brain was considered 0 or starting point.

a. Perforant pathway - dentate gyrus synapse: a stimulating electrode was implanted in the perforant pathway using the coordinates 8.9 mm anterior-posterior (AP), -6 mm lateral (L), and 5 mm depth (D). A recording electrode was implanted in the dentate gyrus using the coordinates 5.5 mm AP, -5.5 mm L, and 5 mm D.

b. Perforant pathway - CA3 synapse: a stimulating electrode was implanted in the perforant pathway using the coordinates 8.9 mm AP, -6 mm L, and 5 mm D, and a recording electrode was chronically implanted for the CA3 region recording at the coordinates 5.5 mm AP, -8.5 mm L, and 6 mm D.

c. Perforant pathway – CA1 synapse: a stimulating electrode was implanted using the coordinates 8.9 mm AP, -6 mm L, and 5 mm D, and for the CA1 area recordings an electrode was implanted at the coordinates 3.5 mm AP, 2.5 mm L and 4 mm D.

d. Dentate gyrus – CA3 synapse: an electrode for stimulation in the dentate gyrus was implanted using the coordinates 5.5 mm AP, -5.5 mm L, and 5 mm D, and for the recording in the CA3 area, 3 electrodes were implanted: i) number 1, at 3 mm AP, -5.5 mm L, and 4.5 D; ii) number 2, at 4 mm AP, -7 mm L, and 4.5 mm D; and iii) number 3, at 5.5 mm AP, -8.5 mm L, and 6 mm D.

e. CA3 – CA1 synapse: the stimulating electrode in the CA3 area was placed at the final coordinates 5.5 mm AP, -8.5 mm L, and 6 mm D, and the recording electrodes in the ipsilateral CA1 area were located at 4.5 mm AP, -5.5 mm L, and 3.8 mm D, and at 3.5 mm AP, -2.5 mm L, and 4 mm D.

f. CA3 – cCA1 synapse: a stimulating electrode was implanted at the position 5.5 mm AP, -8.5 mm L, and 6 mm D, and the recording electrode in the contralateral CA1 area was finally located at coordinates 4.5 mm AP, 5.5 mm L, and 3.8 mm D, and at 3.5 mm AP, 2.5 mm L, and 4 mm D.

3.4.2.2 Dentate gyrus inhibition

With the aim of achieving a successful and precise inhibition of the dentate gyrus area, an inducible silencing of synaptic transmission (INSIST) system was used, which enables a temporary, induced inhibition of the injected neurons. In this case, two sets of recombinant adeno-associated viruses (rAAVs) were used in the different groups that will be described later.

a. SET-1 included rAAV-human Synapsin 1 (hSYN-tTA) and rAAV- bidirectional tetanus promoter (P_{tet}bi)-tandem dimer Tomato (tdTOM) viruses; the former expresses the regulator rtTA under the expression of the human synapsin promoter, and the latter expresses the fluorescent protein tdTOM under the control of the P_{tet}bi promoter, whose activity is in turn modified by the reverse tetracycline-controlled transactivator (rtTA) regulator when doxycycline is present (**Figure 13**).

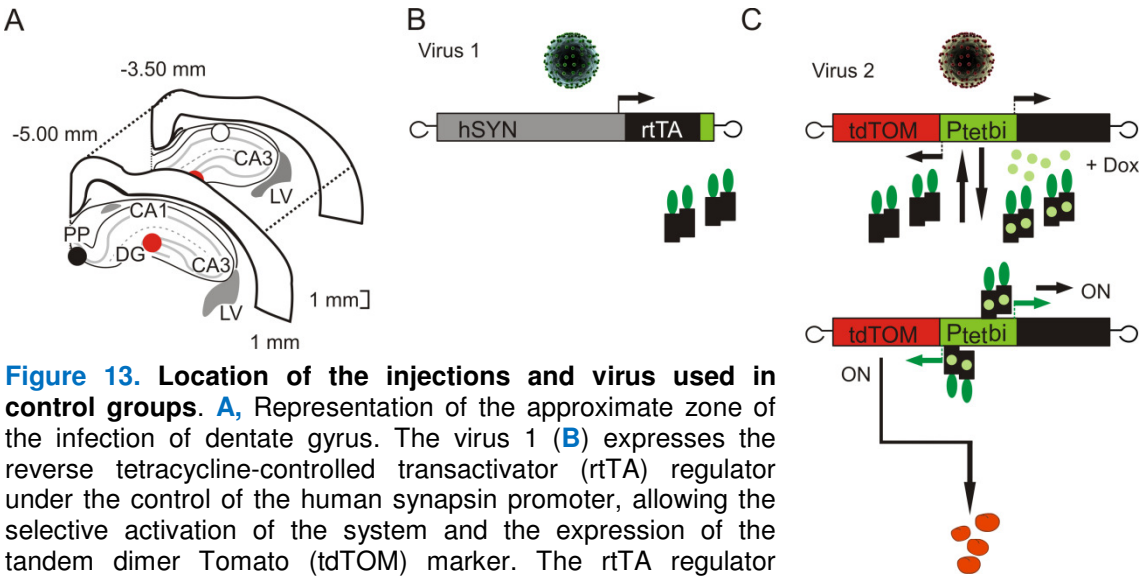

Figure 13. Location of the injections and virus used in control groups. **A,** Representation of the approximate zone of the infection of dentate gyrus. The virus 1 (**B**) expresses the reverse tetracycline-controlled transactivator (rtTA) regulator under the control of the human synapsin promoter, allowing the selective activation of the system and the expression of the tandem dimer Tomato (tdTOM) marker. The rtTA regulator interacts with the bidirectional tetanus (P_{tet}bi) promoter contained in the vector carried by the virus 2 (**C**) and activates the expression of the tdTOM fluorescent protein.

b. SET-2 included recombinant adeno-associated viruses (rAAV)- human Synapsin 1 (hSYN)- tetracycline-controlled transactivator (tTA) and rAAV- bidirectional tetanus promoter (P_{tet}bi)- tetanus toxin light chain (TeTxLC)/ tandem dimer Tomato (tdTOM), which expresses the fluorescence protein td-TOM and a variant of the Tetanus toxin (**Figure 14**).

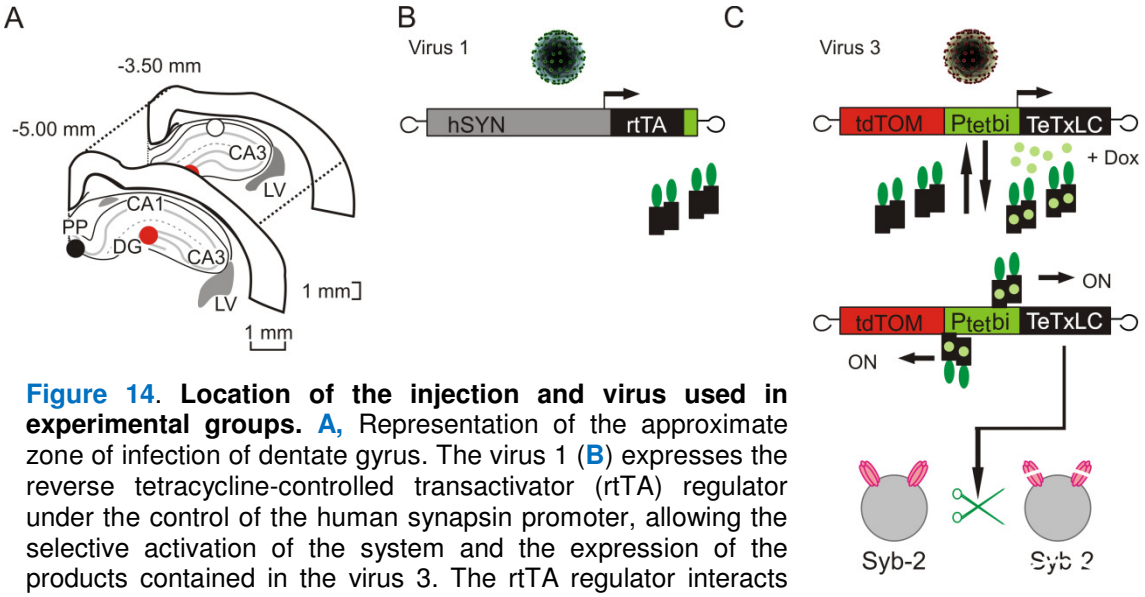

Figure 14. Location of the injection and virus used in experimental groups. A, Representation of the approximate zone of infection of dentate gyrus. The virus 1 (**B**) expresses the reverse tetracycline-controlled transactivator (rtTA) regulator under the control of the human synapsin promoter, allowing the selective activation of the system and the expression of the products contained in the virus 3. The rtTA regulator interacts with the P_{tet}bi promoter contained in the vector carried by the virus 3 (**C**) and activates the expression of the tandem dimer Tomato (tdTOM) fluorescent protein and the tetanus toxin light chain (TeTxLC) product, a modified chain of the tetanus toxin.

The injections for the experimental groups could be unilateral or contralateral. Additionally, mice could be submitted to one of two different classical conditioning protocols: recall or over-conditioning. For the sake of clarity, the different groups, according to the set of viruses injected and the experimental procedure carried out, can be found in **Table 1**.

Table 1. Description of experimental groups in relation to the infection and virus injections, side of the injection, and classical condition protocol.

Group	Procedure	Virus infection
1	Recall	Unilateral
2	Recall	Bilateral
3	Recall	Control
4	Over-conditioning	Bilateral
5	Over-conditioning	Control

To accomplish an acceptable level of infection, 9 sites of the dentate gyrus for unilaterally infected animals, and 18 sites for bilaterally infected animals, were injected with the corresponding set of viruses. For this purpose, the required number of points were drilled in the animal's skull during the surgery, and the viral cocktail was delivered using a glass pipette connected to a plastic tube and, finally, to a 50 mL syringe that was used as an impulsion system (**Figure 15**). About 0.75 µL was injected in each of the selected sites, at a rate of 0.25 µL/min. The stereotaxic coordinates used to spread the infection over the whole dentate gyrus are shown in **Table 2.**

Table 2. Injection coordinates for virus delivery in the three axes: antero-posterior (AP), lateral (L), and depth (D). For control and unilaterally Tet-infected animals the lateral coordinate used was only each negative value. For bilaterally infected animals the lateral coordinates were both negative and positive values to cover both hippocampal sites. The volume of viral cocktail used at each hippocampal site was 0.75 µL, and the injection process was performed slowly to prevent tissue damage.

Injection point	AP coordinate (mm)	L coordinate (mm)	D coordinate (mm)
1	3	±2	4.7
2	3	±3	4.5
3	4	±3	4.5
4	5	±4	4
5	5	±5	4.5
6	6	±5	4.3
7	6	±6.5	4.7
8	7	±6	5.3
9	7	±8.3	6.2

A set of a stimulating electrode (in the perforant pathway) and a recording electrode (in the CA3 area) was implanted in these animals to evaluate the functional state of the dentate gyrus using the coordinates previously described for the perforant path (8.9 mm AP, -6 mm L, 5 mm D) and the CA3 area (5.5 mm AP, -8.5 mm L, 6 mm D, and 4 mm AP, -4.5 mm L, and 4 mm D).

Figure 15. Device to deliver the virus. For its correct delivery the virus was loaded into a glass pipette ending in a very fine tip. The glass pipette was connected to a plastic tube and, finally, to a 50 mL syringe that served as impulsion system. An approximate volume of 0.75 µL was injected per selected site, at a rate of 0.25 µL/min.

3.5 POST-SURGERY

After surgery, rabbits had a recovery period (of about a week) in their home cages. The general state and food intake of the animals were strictly recorded during this period. Once no signs of discomfort were apparent in the animals, they started a preparatory phase with daily handling and habituation to the restraining box (**Figure 16**). Rabbits were also habituated to their transportation to the experimental room and to the recording system attached to the connector fixed on the animal's scalp.

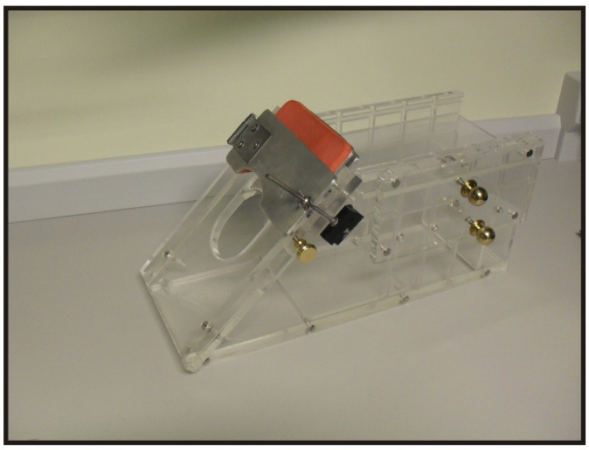

Figure 16. Plexiglas restraining box for rabbits. For transportation of the animal to the recording room and to prevent any motion during the experimental protocol, a restraining box was used. This box allowed adjusting the internal space depending on the size of the animal, and the position of the head could be fixed with a padded clamp. Before each experiment, the animal underwent a period of habituation to this box.

3.6 EXPERIMENTAL PROTOCOLS

At the end of the preparatory phase, the different groups of animals started their corresponding experimental protocol. Two main sets of experiments were performed: the first was aimed at studying the physiology of the hippocampal formation and its synaptic state under different experimental situations; it was termed multisynapse preparations. The second set was designed to study the effect on the learning process and the accessibility of stored information after the inhibition of the dentate gyrus; it was termed synaptic inhibition.

3.6.1 Multisynapse preparations

For this protocol, animals were transported in a restraining box to the recording room, and then prepared for the recording sessions. Depending on the experimental group, they started a different program of training (**Figure 17**): context, pseudoconditioning, trace, or delay conditioning.

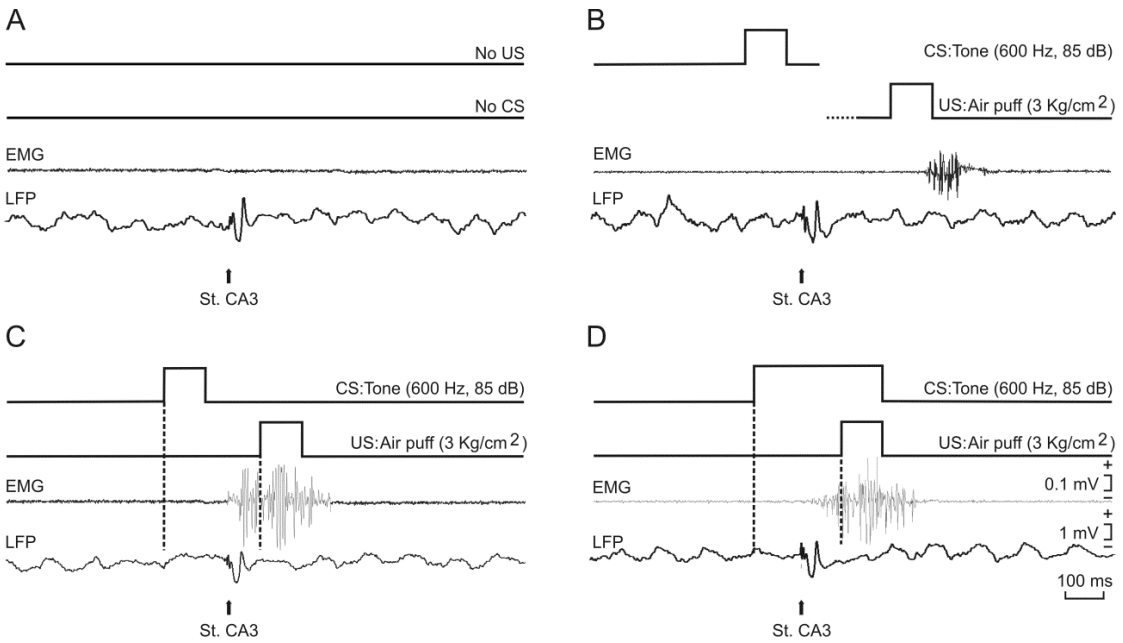

Figure 17. Experimental paradigms. In addition to hippocampal stimulating and recording electrodes, animals were implanted with electromyography (EMG) recording electrodes in the left orbicularis oculi muscle. For classical eyeblink conditioning, the unconditioned stimulus (US) consisted of an air puff presented to the ipsilateral cornea, whilst the conditioned stimulus (CS) consisted of tones presented bi-aurally. Animals were presented with four different training situations: i) controls, placed in the restraining box with no CS or US presentations (**A**); ii) pseudoconditioning (**B**) with non-paired CS and US presentations; iii) a trace conditioning paradigm (**C**); and, iv) a delay conditioning paradigm (**D**). In **A-D** and from top to bottom are illustrated CS and US presentations, the EMG activity of the orbicularis oculi muscle, and the local field potential recorded in the CA1 area, as well as the field excitatory postsynaptic potentials (fEPSPs) evoked by a stimulus presented to the ipsilateral Schaffer collaterals. Calibrations in **D** are also for **A-C**. Note that only trace and delay conditioning evoked conditioned responses.

3.6.1.1 Context situation

The context situation protocol was designed to obtain information about the synaptic changes produced by the experimental procedures and the environment apart from the learning training itself. Animals were placed in a restraining box with dim light in the recording room and they were connected to the recording system (which is shown later). An electrical stimulus was applied (1 stimulus/min) to evoke the field potentials at the selected synapses. Rabbits were trained for a total of 17 sessions, each of which had a duration of ~1 h. A diagram of this protocol is shown in **Figure 17A**.

3.6.1.2 Pseudoconditioning situation

In the pseudoconditioning situation, rabbits were also placed in a restraining box in a dimly light recording room and they were connected to the recording system (which is shown later). During the pseudoconditioning sessions, they received a certain number of unconditioned and conditioned stimuli (an air puff to the cornea and a tone, respectively), but both stimuli were presented at random (with intervals of 50–70 s) for a

total of 66 times. Due to the non-paired presentation, no causal relationship could be established between the two stimuli (**Figure 17B**). In addition, an electrical stimulus was applied 200 ms after the onset of conditioned stimuli (i.e., the tone) to evoke field excitatory postsynaptic potential at the selected recording site. No unconditioned stimulus was presented in the first two pseudoconditioning sessions. In the next ten sessions, both conditioned and unconditioned stimuli were presented randomly, and the protocol ended with five sessions without unconditioned-stimulus presentation. After each pseudoconditioning session, which lasted for ~1 h, animals were returned to their home cages.

3.6.1.3 Trace and delay conditioning

The next two groups (trace and delay conditioning) were the animals submitted to a real learning process. In both protocols, rabbits were placed in a restraining box in a dimly lit recording room and connected to the recording system (which is shown later). Conditioning sessions consisted of 66 trials (6 series of 11 trials each) separated at random by intervals of 50–70 s. Of the 66 test trials, 6 were trials in which the conditioned stimulus was presented alone. A complete conditioning session lasted for ~1 h. The conditioned stimulus was presented alone during habituation and extinction sessions for the same number of blocks/session and trials/block. As criterion, we considered a conditioned response the presence—during the conditioned–stimulus / unconditioned-stimulus interval—of electromyographic activity lasting >10 ms and initiated >50 ms after conditioned-stimulus onset. In addition, the integrated electromyographic activity recorded during the conditioned-stimulus / unconditioned-stimulus interval had to be at least 1.2 times greater than the integrated electromyography recorded immediately before conditioned-stimulus presentation (Porras-García et al., 2010). As a criterion for learning, animals should evoke >70% conditioned responses by the 10th conditioning session (Gruart et al., 2000; Leal-Campanario et al., 2007).

The trace conditioning paradigm (**Figure 17C**) consisted of a 100 ms, 600 Hz, 85 dB tone followed 250 ms after conditioned-stimulus onset by a 100 ms, 3 kg/cm^2 air puff aimed at the left cornea; thus, a trace interval of 150 ms was left between conditioned-stimulus end and unconditioned-stimulus onset.

In the delay paradigm (**Figure 17D**), the conditioned stimulus consisted of a 350 ms, 600 Hz, 85 dB tone. The unconditioned stimulus started 250 ms after conditioned-stimulus onset, and consisted of a 100 ms, 3 kg/cm^2 air puff aimed at the left cornea; in this case, the unconditioned stimulus co-terminated with the conditioned stimulus.

3.6.2 Synaptic inhibition

After the surgery and the viral infection, animals were given a period of 30 days to recover and to start the handling process so that the correct level of viral expression could be achieved. Two main protocols were applied to the different groups of animals. The first was the recall protocol; in this, rabbits were presented with two recall sessions after doxycycline injection. The second set of experiments was an over-conditioning protocol because rabbits were trained once daily after the doxycycline injection until the end of the experiment. In both types of experiment, a trace conditioning paradigm was applied.

3.6.2.1 Recall protocol

Three groups of animals were trained under this protocol: the control group (control); the unilaterally infected group (unilateral tetanus toxin (TeTx)); and, finally, the bilaterally infected group (bilateral tetanus toxin (TeTx)). A diagram of the training sessions is shown in **Figure 18**. Briefly, the protocol started with two sessions of habituation (no unconditioned stimulus was applied) and after six conditioning sessions a single dose of doxycycline (45 µg/g of animal weight) was injected i.p. in these three groups.

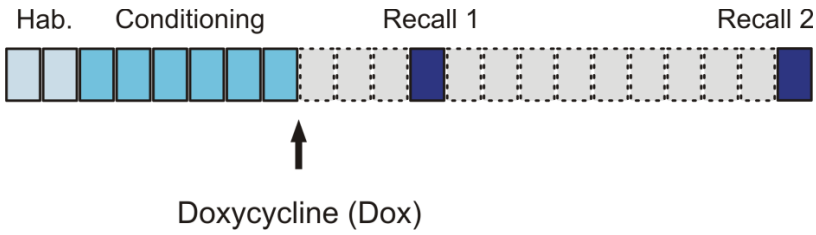

Figure 18. Recall protocol. As is shown in the diagram, this protocol consisted of a total of 22 sessions. The first two were sessions of habituation and were followed by six conditioning days. At the end of the sixth conditioning day, doxycycline (45 µg/g of animal weight) was injected, and animals were not trained for three days. The fourth post-injection day consisted of a recall session, which assessed the effect of the tetanus toxin expression. Finally, after nine days (with no training sessions) a second recall session was applied to evaluate the recovery of the expression of conditioned responses.

To evaluate the level of synaptic inhibition, animals were taken to the recording room, and 10 electrical stimuli were applied to evoke the field excitatory postsynaptic potentials at the dentate gyrus – CA3 synapse. The slope of those field potentials was measured and the level of inhibition was quantified. A maximum inhibition was observed 96 h after doxycycline injection (**Figure 19**). Once the maximum level of inhibition was reached, animals were submitted to a recall session (Recall 1). Similarly, the recovery of

the evoked field excitatory postsynaptic potentials slope was monitored by recording 10 electrical stimuli with their corresponding responses on subsequent days. A second training session (Recall 2), was applied once the normal levels of the evoked field excitatory postsynaptic potentials slope were reached (**Figure 19**).

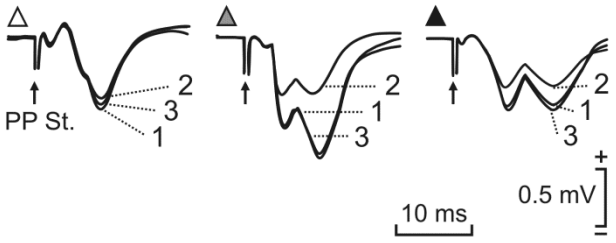

Figure 19. Evolution of the second component of field excitatory postsynaptic potentials evoked in the CA3 area by electrical stimulation of the perforant pathway. Representative examples of field excitatory postsynaptic potentials (fEPSPs, averaged 5 times) evoked in the CA3 area by electrical stimulation of the perforant pathway (PP St.) during the CS-US interval (200 ms after CS presentation). Numbers refer to the session: 1 is the 6th conditioning day, when doxycycline was injected. After this injection, the fEPSPs were recorded, and the next conditioning session (Recall 1) was applied when a decrease in the fEPSP was noticeable in unilateral (gray filled triangles) or bilateral (black filled triangles) groups, which happened at number 2 (Recall 1, the 4th day after doxycycline injection). Finally, the recall 2 session (number 3) was applied when there was a recovery of the fEPSP in unilaterally and bilaterally infected groups. No changes in fEPSP were observed in the control group (white filled triangles) during these days.

3.6.2.2 Over-conditioning protocol

A control group and a bilateral tetanus toxin (TeTx) group were included in this protocol (**Figure 20**). Both groups started with two sessions of habituation followed by six conditioning sessions. At the end of the sixth conditioning session, doxycycline (45 µg/g animal weight) was administered i.p. Animals continued the training protocol the day after doxycycline injection, and were conditioned 1 h per day until the 22nd conditioning day.

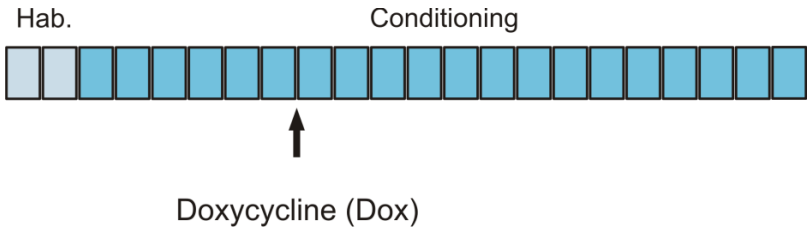

Figure 20. Over-conditioning protocol. As is shown in the diagram, this protocol consisted of a total of 22 sessions. The first two were habituation sessions and were followed by 20 conditioning days. At the end of the sixth conditioning day, doxycycline (45 µg/g of animal weight) was injected, and animals kept on with the training sessions for 14 more days.

3.7 PERFUSION AND HISTOLOGY

At the end of each experimental protocol a histological confirmation of the final position of implanted electrodes was performed and electrodes which did not reach the correct region (< 5%) were excluded from subsequent analysis.

3.7.1 Perfusion

For trans-cardiac perfusion, animals were previously anesthetized with an intravenous injection of a mixture of the muscular relaxant Xylazine (Rompun®, 3 mg/kg of animal weight) and the hypnotic Ketaminol (Imalgene®, 25 mg/kg of animal weight). Once the animals were deeply anesthetized, chloral hydrate (10%. 141975, *Panreac Química* S.A.U. Barcelona, Spain) was injected i.p. The next step included the exposure of the heart by making a U-shaped incision in the thoracic cage of the animal, the separation of pericardial tissue, and then an injection of 0.5 mL of sodium heparin (Sodium Heparin 1000 UI/mL, Chiesi-Spain S.A) in the ventricular cavity.

Finally a cannula was inserted in the right atrium, and with the assistance of a peristaltic pump (Master Flex® L/S®, Thermo Fisher Scientific Cat. Nº 7524-45, USA) 1 L of saline solution cleaned the circulatory system of blood and facilitated the posterior fixation, which was performed with 2 L of paraformaldehyde (4%). To amplify the effect of the fixation solution, the descendent portion of the aorta was clamped.

3.7.2 Nissl staining

At the end of the perfusion process, the brain was carefully extracted and preserved in a cryoprotectant solution (30% saccharose in a phosphate buffer solution) until it was completely sunk into the solution (normally this process needed 4 days).

After this, fixed brains were sliced using a microtome (Leica SM200R, Leica Microsystems, Nusslock GmbH, Germany). The slices (50 µm diameter) were classified into a multi-well dish containing a phosphate-buffered solution (0.2 M).

These slices were inspected using a magnifying glass, and placed on a gelatinized microscope slide if they contained information about the insertion site of an electrode. The tissue was protected to prevent the deposit of any particle on it while it dried (this process usually lasted about 12 h). At this point, the staining protocol could be started.

Nissl staining marks the cell somas of the nervous system with basic colorants such as Toluidine blue. The neuronal branches are not colored by this staining, so the main information obtained with this technique is about the distribution, size, and morphology of cell bodies. The staining protocol consists of various steps, which are described below:

a. Microscope slides with the dried sections of tissue were completely immersed in a cuvette containing Toluidine blue (0.1%) for 30 s.

b. The excess colorant was removed by a quick wash in distilled water, and the surplus liquid was dried using blotting paper.

c. The slices were dehydrated by immersing them in a successive set of solutions with increasing concentration of ethyl alcohol, starting with 50º, then 60º, 95º, and finally 100º. The tissue remained in these solutions for 2 min, except for 100º ethyl alcohol, in which they stayed for 1 min (sometimes more, depending on the quantity of colorant observed in the slices).

d. To improve the degree of dehydration the slices were finally immersed in two consecutive cuvettes with xylene (100%) for 5 min.

e. A drop of Distrene Plasticizer Xylene (DPX) mounting media was applied to the tissue, and after it was completely extended across the slide, a coverslip was carefully placed on the preparation. Any bubble was removed by knocking softly using a plastic stick.

f. After Distrene Plasticizer Xylene (DPX) became solidified, any excess was removed from the edges of the slides and the glass was cleaned using xylene. The histological preparations were now ready for their recording using an optical microscope (Leica DMRE type 020-525-025, Leica Microsystems, Wetzlar GmbH, Germany).

3.7.3 Immunohistochemistry / Confocal microscopy

For confocal analysis, only the best-perfused brains were included: five rabbits infected with the control virus (expressing only TdTOM) and seven rabbits infected with the TeTxLC virus were selected for the analysis of puncta density after the induced activation of the corresponding vectors. After perfusion, brains were cryoprotected using a solution of 30% sucrose in phosphate buffer (PB), and were then sliced in coronal sections with a microtome (Leica SM2000R) and stored in 30% glycerol, 30% ethylene glycol in PB at –20 ºC.

Once all the samples were prepared for immunohistochemistry, all the sections were processed simultaneously, so that differences intrinsic to the protocol could be ruled out. For the analysis of density of the puncta expressing the presynaptic marker "vesicular glutamate transporter 1" (VGLUT1), and those expressing the postsynaptic marker "postsynaptic density 95" (PSD95), a double immunohistochemistry was

performed. In the cases of both pre- and postsynaptic markers, a primary antibody against "CaM-dependent protein kinase II" (CAMKII), a marker of principal neurons (Millipore Iberica S.A.U, Madrid, Spain), was used, and then co-incubated with a primary antibody against VGLUT1 or PSD95, respectively.

The first step was an incubation with 5% normal donkey serum (AbD Serotec, MorphoSys, Kidlington, UK) for 1 h in phosphate-buffered saline (PBS) with 0.2% Triton-X-100 (Sigma-Aldrich, St. Louis, MO, USA), and then samples were incubated overnight at room temperature with mouse monoclonal IgG anti-VGLUT1 (1:1000) and rabbit monoclonal IgG anti-CAMKII (1:700) or mouse monoclonal IgG anti-PSD95 (1:700) and rabbit monoclonal IgG anti-CAMKII (1:700), with PBS containing 0.2% Triton-X-100 and 3% normal donkey serum.

The second day, sections were washed and then incubated for 1 h with anti-mouse Immunoglobulin (IgG) and anti-rabbit IgG secondary antibodies generated in donkey and conjugated with Alexa 488 and Alexa 647 (1:200; Millipore Iberica S.A.U, Madrid Spain) in PBS with 0.2% Triton-X-100 and 3% normal donkey serum. At the end of this procedure, sections were mounted on slides and coverslipped using Prolong Gold antifade reagent fluorescent mounting medium (Millipore Iberica S.A.U, Madrid Spain).

Finally, the analysis of density of puncta expressing VGLUT1 and PSD95 was carried out in the neuropil next to the CAMKII-expressing dendrites in the CA3 sub-region of the hippocampus. All the sections selected belonged to the same rostro-caudal allocation and were examined under a confocal microscope (Leica TCS SPE). Using a sequential scanning mode and further processing with Image J software, Z-series of optical sections (0.5 µm apart) were obtained. The values of acquisition settings were identical for each stack taken from the same level, as well as the time of exposure to the confocal laser.

In order to achieve the correct level of homogeneity, only images from similar Z-position in which the same level of antibody penetrability was observed were chosen, and five randomly selected samples of 16 µm x16 µm were used for the analysis, and background fluorescence was subtracted. Means were determined for each experimental group, and the data were subjected to unpaired Student's *t*-test.

3.8 ACQUISITION AND DATA ANALYSIS

3.8.1 Acquisition

The field excitatory postsynaptic potentials evoked by electrical stimuli at different synaptic sites of the hippocampal formation, the electromyographic activity of orbicularis oculi muscle, and the pulses corresponding to the electrical, conditioned, and

unconditioned stimuli were recorded and acquired online using an analogical-to-digital converter card (**Figure 21A**) with 24 channels (Power 1401 MK II, Cambridge Electronic Design. Cambridge, United Kingdom). In the case of physiological signals (field excitatory postsynaptic potentials and electromyography recordings), a first step of pre-amplification and amplification (**Figure 21B** top, 16 Channel extracellular amplifier with head stage model 3600, A-M systems, U.S.A) was performed, so the original signal was amplified 1000 times.

In the case of electrodes implanted in the hippocampal formation, the reference was set using the ground installed on the skull of the animal, and for electromyography, a differential recording was made using two electrodes inserted in the orbicularis oculi muscle with another ground installed on the skull of the animal as basal reference.

The online monitoring of the conditioning process, physiological signals, and stimuli was performed with the software Spike2 (Spike2 7.02a, Cambridge Electronic Design. Cambridge, UK). The acquisition rate was fixed at 4 kHz for physiological signals and at 1 kHz for stimuli and pulses.

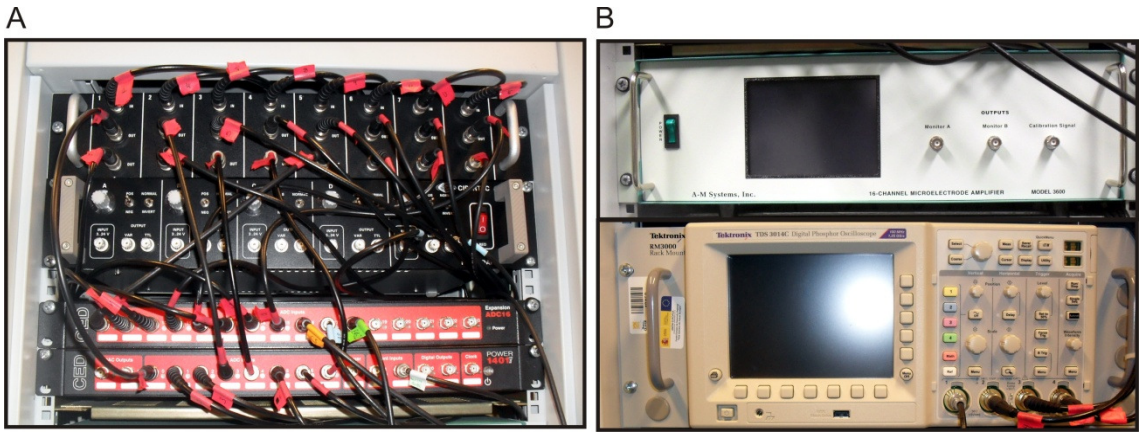

Figure 21. Amplification, acquisition, and monitoring system. The acquisition system is shown in **A,** an analogic-to-digital card converter (Power 1401 MKII with an expansion ADC16 from Cambridge Electronic Design) that appears at the bottom, and a panel at the top which sends the signals previously amplified (amplifier shown in top panel of **B,** A-M systems Inc.) to the analog-to-digital converter card and to an oscilloscope (in the bottom panel of **B,** Tektronix Rm3000) which enables the online observation of the signal.

3.8.2 Field excitatory postsynaptic potential slopes and muscle electromyography measurements

Processing and analysis of the recorded signals was performed with the help of the software Signal (Signal v 3.10, Cambridge Electronic Design, Cambridge, UK). Collected data were divided in temporal windows using the electrical stimuli as reference, choosing a total length of 750 ms and taking 350 pre-stimulus recording. In

this way, the selected frames always included all the important information—that is, the conditioned-stimulus / unconditioned-stimulus interval (when there were conditioned and unconditioned stimuli) and 200 ms of information preceding and following the conditioned-stimulus / unconditioned-stimulus interval.

3.8.2.1 Analysis of field excitatory postsynaptic potentials

Each synapse was carefully identified by its electrophysiological characteristics, latency, duration, and the slopes of evoked field excitatory postsynaptic potentials, generated with the same stimulus intensity and presenting no inflexions in the first 2-3 ms following the stimulus artifact.

The typical latency of hippocampal synapses was 3-4 ms, the point at which the first cursor was placed to start the measurements. Once all the defective frames were discarded (no correct stimulus, interferences due to animal motion, etc.), the field excitatory postsynaptic potential were averaged and the value of the resultant slope for that day was measured. The evolution of the field excitatory postsynaptic potential slopes across the different days of training was represented as a percentage of the basal situation—that is, the mean value of the first two conditioning days.

3.8.2.2 Analysis of the electromyographic activity of the orbicularis oculi muscle

To evaluate the motor learning process it was necessary to quantify the number of learned responses that were generated by the left eyelid of the animal within the conditioned-stimulus / unconditioned-stimulus interval. The electrical signal corresponding to the orbicularis oculi muscle activity was rectified in a new digital channel. A valid conditioned response meant a recorded muscle electromyographic activity generated before the air-puff presentation (unconditioned stimulus) and after the start of and during tone (conditioned stimulus) presentation. In addition, the area of the rectified electromyographic activity had to be at least 20% higher than a rectified area of electromyographic activity with the same length but recorded before the onset of the conditioned stimulus. Finally, the percentage of conditioned responses was calculated for each session, and these data were used to build the learning curve for each animal.

3.8.3 Statistical analysis

Statistical analysis of collected data was performed with the help of Sigma Plot 11.0 (Sigma Plot. CA, USA) using a significance level of $P = 0.05$. Values presented here refer to the arithmetic average accompanied by standard error values. Data of experimental groups were analyzed using one-way analysis of variance (ANOVA) tests

with repeated measures (sessions). When data did not reach the normality or variance homogeneity criteria, a non-parametric test in ranges was applied. For comparisons, the Student-Fisher test was used.

4. RESULTS

4.1 EVOLUTION OF CONDITIONED RESPONSES AND OF FIELD POSTSYNAPTIC POTENTIALS ACROSS CONDITIONING SESSIONS

The evolution of conditioned responses and of the slopes of field excitatory postsynaptic potentials was followed in implanted rabbits for 17 days (see some examples in **Figures 22** and **23**). In the case of trace and delay conditioning paradigms, protocols consisted of 2 habituation, 10 conditioning, and 5 extinction sessions (for details, see Gruart et al., 2000). For conditioning sessions, animals received the paired presentation of conditioned and unconditioned stimulations, whose duration and characteristics were dependent on the conditioning (trace, delay) paradigm. During habituation and extinction sessions, only the conditioned stimulus was presented to the animals. Pseudoconditioning was carried out with the same scheme, but rabbits received the same number of stimuli, although the conditioned and unconditioned stimuli were specifically not paired. In the case of the context group, only the electrical stimulus was applied at the selected hippocampal site to evoke field excitatory postsynaptic potentials. The final placement of the recording and stimulation electrodes was confirmed by subsequent histological analysis. Those electrodes that did not reach the correct position were eliminated from the electrophysiological analysis.

The electromyographic activity of the orbicularis oculi muscle was recorded in parallel with the acquisition of field excitatory postsynaptic potentials with the help of 7-strand stainless steel implanted electrodes. Conditioned responses were easily distinguished from the background noise in the electromyographic recordings. No startle response was recorded in rabbits due to conditioned-stimulus (tone) presentation. With the aim of avoiding any interference with the state of alertness of the animal (Bramham and Srebro, 1989), all the recording sessions lasted for ~60 min and were carried out at the same hour every day until the end of the experimental sessions.

4.1.1 Learning curves

With the exception of the context situation, the percentage of conditioned responses was quantified in each session in order to have a physiological measurement of the learning process (Schneiderman et al., 1962). A learning curve was built for the three trained groups (pseudoconditioned, trace, and delay), using the mean values and standard errors of the percentage of conditioned responses for each group in each learning phase: habituation, conditioning, and extinction (**Figure 22**).

Animals included in the context group did not present any conditioned response and these data were not included in the graph. In coincidence with previous reports (Múnera et al., 2001), pseudoconditioned animals presented a very low percentage (< 10%) of conditioned responses during pseudoconditioning sessions — i.e., at a rate

similar to values presented during habituation and extinction sessions. Obviously, the pseudoconditioned group failed to reach criterion (> 70% of conditioned responses) by the tenth conditioning session (**Figure 22,** black diamonds). Parameters corresponding to the unconditioned (reflex) responses to the air puff directed at the cornea were normal in this group of rabbits. No extinction was observed, since no learning was produced by this paradigm.

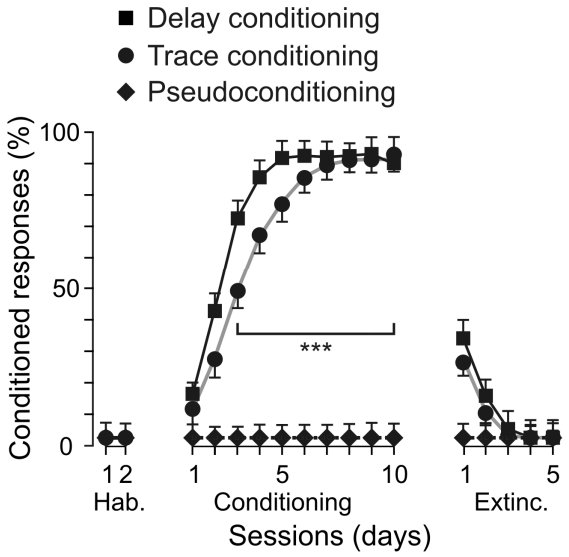

Figure 22. Learning curves. Evolution of the percentage of conditioned responses in the group of rabbits trained with a pseudoconditioning (diamonds), trace (circles), and delay (squares) paradigms are illustrated during the successive habituation (Hab.), conditioning, and extinction (Extinc.) sessions. n = 6 animals/group. *** means $P < 0.001$, and represents the statistically significant differences between the percentage of conditioned responses in the delay and trace conditioning groups with the pseudoconditioning one.

For animals included in the trace group, the percentage of conditioned responses increased rapidly across conditioning, reaching 50% by the 3rd conditioning session and asymptotic values (90%) from the 7th to the 10th conditioning sessions. The percentage of conditioned responses presented by the trace group during the 3rd to 10th conditioning sessions was significantly larger than those collected during habituation from the 3rd to the 10th conditioning sessions [$F_{(10,54)} = 51.352$; $P < 0.001$; **Figure 22**]. Finally, the delay group acquired their conditioning paradigm even faster than the trace group, reaching percentages of conditioned responses significantly different from habituation values from the 2nd to the 10th conditioning sessions [$F_{(10,54)} = 24.677$; $P < 0.001$; **Figure 22**].

As reported previously (Graves and Solomon, 1985), although the percentage of conditioned responses was similar for both (trace and delay) paradigms, the trace group presented a lower rate of learning, although both groups reached the same phase of saturation with a level of conditioned-response expression above 90%. In accordance, even taking into account scientific reports which claim the non-absence of significant differences between trace and delay conditioning if the inter-stimulus interval is equal to

or shorter than 150 ms in the trace paradigm (Moyer et al., 1990), a difference in the acquisition process is still noticeable in these learning curves (**Figure 22**).

The evolution of conditioned responses during the extinction phase was identical for the two groups, with a decay of 60% the 1st day of extinction, and showed no conditioned responses at the end of the 3rd extinction session. This is an important fact, taking into account that, although it was initially proposed that conditioning and extinction processes may share similar underlying mechanisms (Pavlov, 1927; Konorski, 1948; Vianna et al., 2001; Debiec et al., 2002; Li et al., 2003, Lattal et al., 2006), data collected here suggest the presence of different neural activities. It can be predicted that these differences should be observed in the hippocampal functional states evoked by the different (habituation, conditioning, extinction) sessions.

4.1.2 Polynomial fits for field excitatory postsynaptic potentials slope evolution

As mentioned before, in parallel with orbicularis oculi electromyographic recordings, the changes in the slopes of 6 selected synapses were recorded during the conditioning process. Three of the synapses belong to inputs to the hippocampal formation: i) the perforant pathway to the dentate gyrus (PP to DG); ii) the perforant pathway to the CA3 area (PP to CA3); and iii) the perforant pathway to the CA1 area (PP to CA1). The other three studied synapses constitute the intrinsic trisynaptic hippocampal circuit: i) dentate gyrus to the CA3 area (DG to CA3); ii) the CA3 area to the ipsilateral CA1 area (CA3 to CA1); and iii) the CA3 area to the contralateral CA1 area (CA3 to cCA1).

In order to facilitate the interpretation of the collected results, firstly is an explanation of a representative example of changes taking place in one of the hippocampal synapses across the successive training sessions in one of the experimental groups (trace conditioning paradigm). Afterwards, the other five synapses will be described. Specifically, **Figure 23** illustrates changes in synaptic strength taking place at the synapse between the dentate gyrus and the CA3 area (DG-CA3 synapse) in the trace conditioning group.

In accordance with an early study (Weisz et al., 1984), field excitatory postsynaptic potentials evoked by the electrical stimulation of the perforant pathway changed in slope (taking the slope of field excitatory postsynaptic potentials collected during the two habituation sessions as a 100%—i.e., as a baseline value) across conditioning sessions in the trace conditioning group. Moreover, the evoked field potential shows a recognized profile and latency, indicating its monosynaptic nature. However, those changes represented either an increase or a decrease with respect to the baseline values, probably due to the specific position of the electrodes in the target recording area (Whitlock et al., 2006). As has been illustrated in **Figure 23**, field

excitatory postsynaptic potentials recorded at different sites corresponding to the DG-CA3 synapse either increased (left set of recordings) or decreased (right set of recordings) across the training sessions. Each recording block included three different evoked potential responses to an electrical stimulation of the same intensity and duration. A quantitative analysis of the 1st recording site (**Figure 23A**, +Δ electrode, and **Figure 23B**, black triangles) showed field excitatory postsynaptic potentials significantly larger [$F_{(7,127)} = 71.514$; $P < 0.001$] than baseline (habituation) values from the 6th to the 10th conditioning sessions and for the 5 extinction sessions. In turn, the 2nd recording site (**Figure 23A**, −Δ electrode, and **Figure 23B**, white triangles) evoked field excitatory postsynaptic potentials significantly smaller [$F_{(6,111)} = 47.628$; $P < 0.001$] than baseline values from the 5th to the 10th conditioning sessions and for the 5 extinction sessions.

In **Figure 23C** is represented the evolution at 5 recording sites corresponding to the DG-CA3 synapse, presenting field excitatory postsynaptic potentials that increased (+Δ) significantly ($P \leq 0.01$) in slope across the conditioning sessions, and another 5 recording sites presenting field excitatory postsynaptic potentials that decreased (−Δ) significantly ($P \leq 0.01$) in slope across training. Following two previous studies (Whitlock et al., 2006; Fernández-Lamo et al., 2009), those recording sites that did not change significantly in slope across training (i.e., when regression analysis applied to the collected slopes did change < ± 1 SD) were also considered. Using this analytical procedure, it was found that for the DG-CA3 synapse, 40% (6 out of 15) of the recording electrodes showed a significant increase ($P \leq 0.01$) in slope across conditioning sessions, whilst 33.3% (5 out of 15) presented decreasing ($P \leq 0.01$) field excitatory postsynaptic potentials slopes, and 26.7% (4 out of 15) presented no significant changes. The polynomial regressions shown in **Figure 23D** correspond to the algebraic mean [([+Δ] + [−Δ]) / N] of data collected from electrodes (N) presenting significant changes during conditioning sessions.

Since there are two types of trend in these recordings of similar values and opposite directions, analysis including all of them will result in a cancellation of any possible effect. To solve this issue, it was decided to eliminate the sign from the recorded data, and to work with the magnitude of the change as is represented in **Figure 23D**. Therefore, the evolution of the change in field excitatory postsynaptic potential slopes for the particular synapse (in this case, between DG and CA3) was expressed as its absolute value.

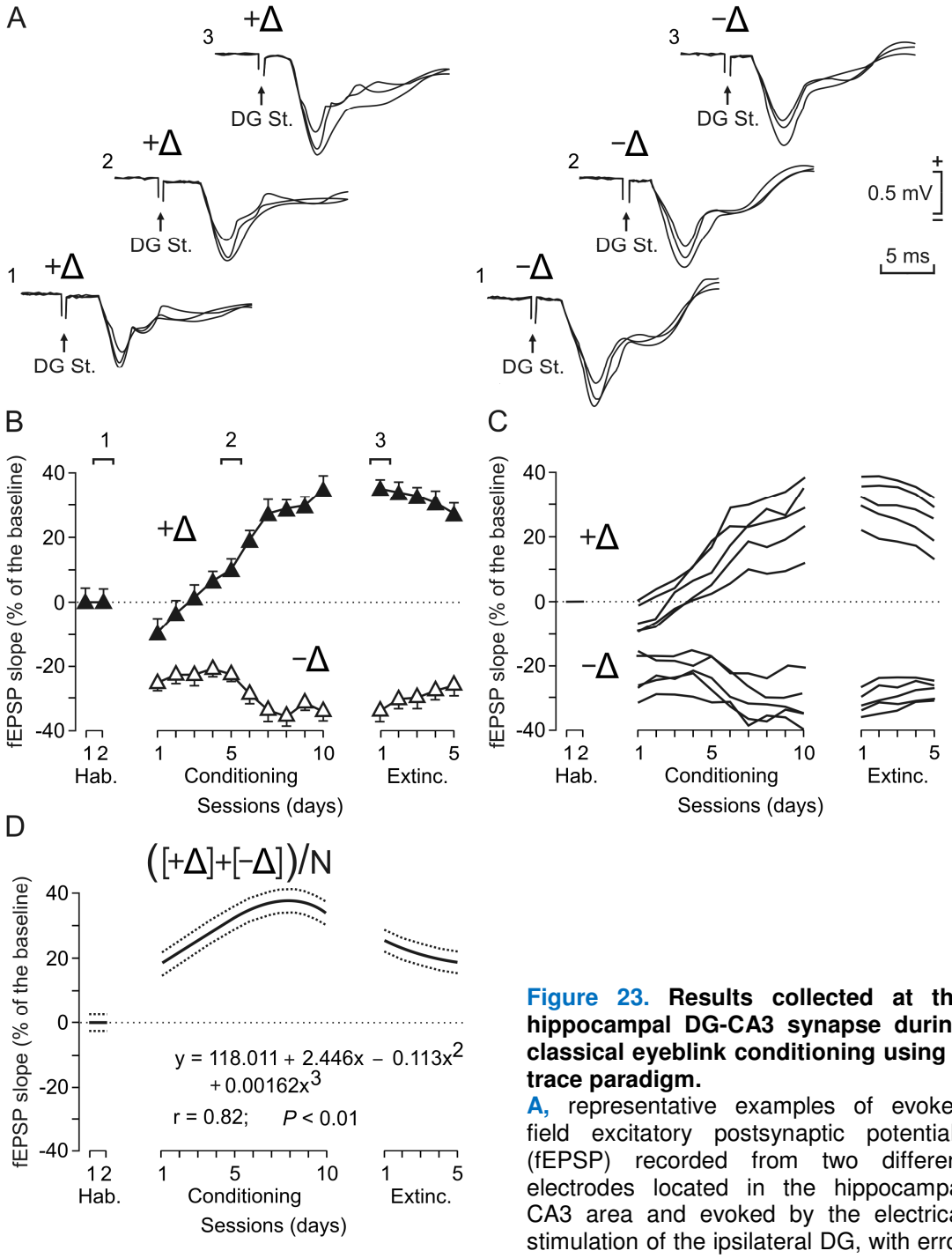

Figure 23. Results collected at the hippocampal DG-CA3 synapse during classical eyeblink conditioning using a trace paradigm.

A, representative examples of evoked field excitatory postsynaptic potentials (fEPSP) recorded from two different electrodes located in the hippocampal CA3 area and evoked by the electrical stimulation of the ipsilateral DG, with error deviation for each electrode.

B, evolution of fEPSP slopes recorded from two different electrodes implanted in the CA3 area and evoked by DG stimulation, across the successive training sessions, habituation (Hab.), conditioning, and extinction (Extinc.). Values are expressed as the means. Representative examples of the recorded fEPSPs at the indicated times (1, 2, 3) are illustrated in A for the two recording sites. **C,** evolution of fEPSP slopes recorded from selected electrodes implanted in the CA3 area. fEPSPs were also evoked by the electrical stimulation of the ipsilateral DG. B-C, Note that fEPSP slopes either increase (+Δ, black triangles, n = 5) or decrease (−Δ, n, open triangles, = 5) in slope across training. **D,** Algebraic mean [([+Δ] + [−Δ]) / N] of fEPSP evolution from electrodes (n = 15) located in the hippocampal CA3 area and activated by DG stimulation. The equation corresponding to the best polynomial fit to data collected during conditioning sessions is indicated, as well as the corresponding regression curve and the simultaneous 95% confidence bands.

Additionally, a polynomial fit to these curves was applied, to obtain a mathematical function that could give us the best estimated physiological value of field excitatory postsynaptic potential slope change at a given time. This is a very important fact since one of the goals in the present work was to represent the synaptic state of different hippocampal formation synapses in a given phase of the learning training. Regression illustrated in **Figure 23D** is, then, an accurate representation of the global changes in synaptic strength taking place in the DG-CA3 synapse during trace conditioning in behaving rabbits.

4.1.3 Context

Although the physiology of the hippocampal formation in spatial memory has been largely studied (Ferbinteanu et al., 2003, Nadel et Hardt, 2004; Oler et al., 2008), there is still some discussion about the specific role of this neural structure in tasks where contextual components are relevant (Mahut and Zola, 1973; Becker et al., 1980; Burgess et al., 2001; Griffin et al., 2007; Watanabe et al., 2013). Moreover, the hippocampal formation includes several intrinsic and extrinsic circuits, containing different synapses that could have particular roles in learning and memory processes. Following this hypothesis, consideration was given to including 6 different synapses in the present study of effects of context effects on the activity of hippocampal circuits.

Any learning protocol involves many different stimuli and situations, apart from the ones strictly related to the learning and memory processes, which could globally be named as the context. The putative changes in the synaptic strength during the context situation should be taken in account at the time of discussing changes in the synaptic strength found during the learning protocols. The experimental situation described as context should not be considered simple, as described in the Material and Methods section, since it includes specific non-recorded information that animals received when being changed from their home cage located in the resting room to the restraining box used for training. Moreover, every training day they were manipulated, introduced into a restraining box, moved to the recording room, and, finally, connected to the stimulation and recording system.

This approach revealed interesting data and different trends for the 6 recorded synapses along the successive recording sessions (**Figure 24**). The synapses between the perforant pathway and dentate gyrus (PP-DG) showed an initial period of increased field excitatory postsynaptic potential slopes that decreased (**Figure 24A**), while the values recorded in the synapses between dentate gyrus and CA3 (DG-CA3) presented minor changes (**Figure 24B**) along the successive recording sessions. In particular,

synapses which act as inputs to the hippocampal formation (that is, PP to DG (**Figure 24A**), PP to CA1 (**Figure 23C**), and PP to CA3 (**Figure 24E**), showed significant increases in synaptic strength of around 120% of the baseline values. These large increases were maintained for longer (12 days at least) periods. Moreover, the synapses comprising part of the trisynaptic hippocampal circuit presented some clear differences.

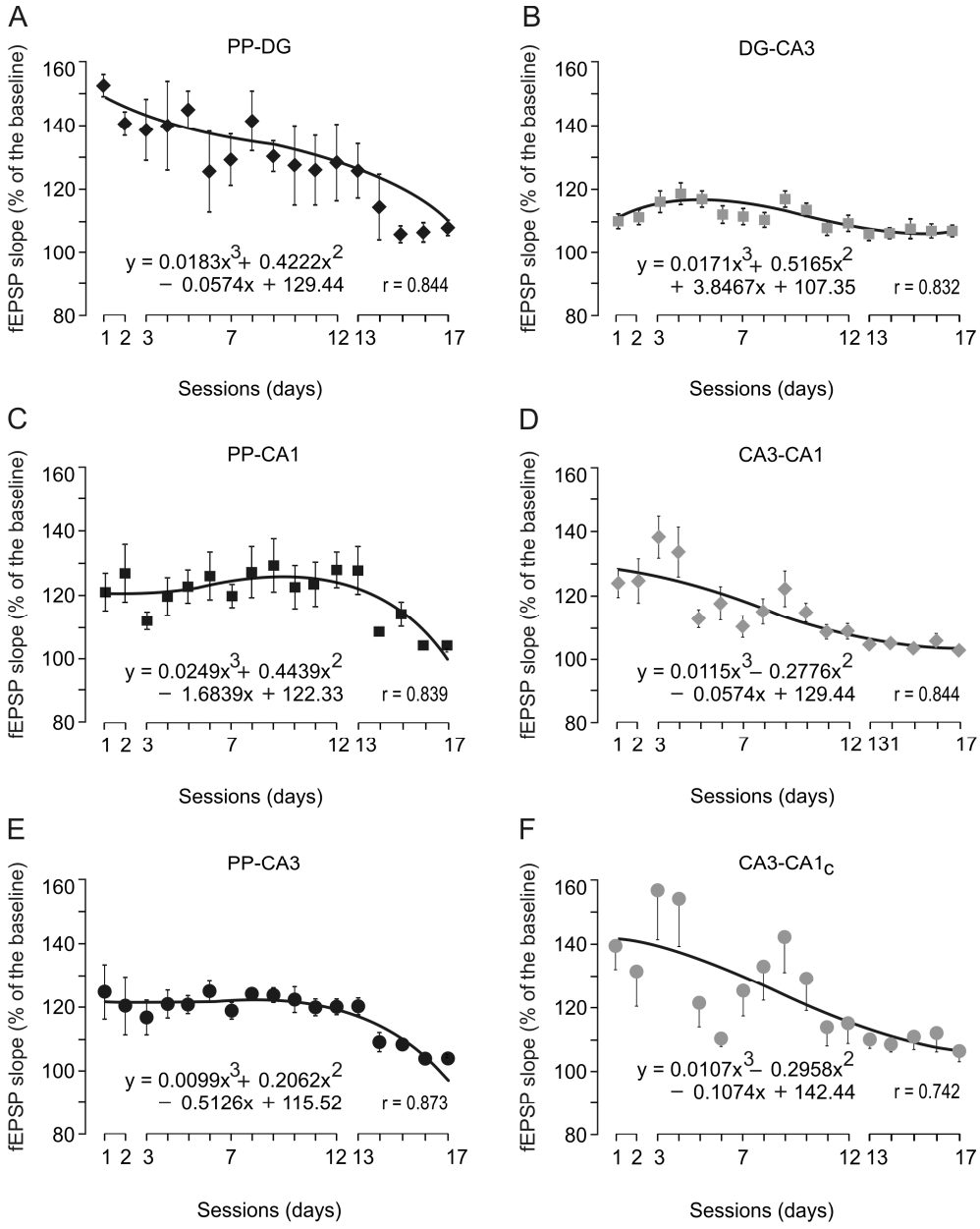

Figure 24. Main changes in synaptic strength evoked in the hippocampal circuit by the context situation. A-F, evolution of the evoked field excitatory postsynaptic potential (fEPSP) slopes at the 6 selected synapses due to the context: PP to DG (**A**), DG to CA3 (**B**), PP to CA1 (**C**), CA3 to CA1 (**D**), PP to CA3 (**E**), and CA3 to cCA1 (contralateral CA1) (**F**). Note that substantial changes are observed for both input (i.e., PP to DG) and intra-hippocampal (i.e., CA3-CA1) synapses, and the main trend is stability, so minor changes were recorded in the last days of the context protocol. For A-F are illustrated the best polynomial fits ($r \geq 0.742$) $P \leq 0.01$) for the fEPSP data collected from the 6 synapses.

The synapse between the dentate gyrus and CA3 area (DG-CA3 synapse) was the most stable, presenting minor changes along the training sessions, mainly concentrated in the first 5 days (**Figure 24B**). The synapses between CA3 and the ipsilateral CA1 area (CA3-CA1 synapse, **Figure 24D**) and the contralateral CA1 area (CA3-cCA1 synapse, **Figure 24F**) presented peaks of variability in the 3rd and 9th sessions, but they showed a strong trend to stability, reaching values close to baseline on the 11th day. The CA3-cCA1 synapse showed more variability across training sessions than any other recorded synapse. The best polynomial fits ($r \geq 0.81$; $P \leq 0.01$) are presented for the evolution of field excitatory postsynaptic potential slopes of the 6 selected synapses.

In general, the successive recording sessions in the context protocol showed a differential evolution in each of the 6 synapses, but all the data tended to reach the baseline values after 10-12 days of recording in experimental sessions where exactly the same procedure was kept to.

4.1.4 Pseudoconditioning

After the confirmation of the proposed hypothesis indicating that context can evoke synaptic changes at the hippocampal formation it was necessary to test the possible significance of the uncoupled presentation of stimuli in the hippocampal circuits. This seems a non-relevant point, since it is well known that the hippocampal formation receives a great variety of sensory information, such as olfactory (Schwerdtfeger et al., 1990), vestibular (O'Mara et al., 1994; Zheng et al., 2001) auditory (Mohedano-Moriano et al., 2007; Muñoz-López et al., 2010), and visual (Suzuki and Amaral, 1994; Murray and Kreutz-Delgado, 2007). The pseudoconditioning test could explain whether the putative changes in the synaptic strength of the different synapses were due to the mere presentation of conditioning stimuli, in a way similar, or otherwise, to that found for the context test. At least it could allow stating how much of the possible changes found during the learning processes could be due to the presentation of the selected stimuli and not to the learning process itself.

As can be observed in **Figure 25**, the evolution of the field excitatory postsynaptic potential slopes recorded in the input synapses tended to reach control values at the end of the recording sessions, as was found for the context situation. However, the results collected through this new protocol presented clear kinetic differences. The best fit function for the data obtained in the synapses between the perforant pathway and the dentate gyrus (PP-DG) presented a parabolic shape ($r = 0.919$) with the peak values in the 8th pseudoconditioning session (**Figure 25A**), and

the first increase observed in the curve coincided with the appearance of the air-puff stimulus to the cornea in the protocol. Consistently, the minimum values of change observed occurred in the phase where this air-puff stimulus was removed. Similar results were obtained in the synapse between the perforant pathway and the CA3 area (PP-CA3). In this case, the highest values in the parabolic-like shape function were recorded in the 7th pseudoconditioning session (**Figure 25E**). Again, the first increase in the curve coincided with the presentation of the air-puff stimulus, and the lowest values with its removal. However, the data recorded at the synapse between the perforant pathway and the CA1 area (PP-CA1) showed an almost constant distribution of values during the first 10 recording sessions, and values started to decrease when the air puff was removed (**Figure 25C**).

The presentation of the air-puff stimulus produced a marked effect at the intrahippocampal synapses (**Figure 25B, D, E**). One of the synapses most affected was that formed between the CA3 and CA1 areas, where a 153 ± 4.2% change in field excitatory postsynaptic potential slope was recorded on the 2nd day of pseudoconditioning and decreased continuously throughout the rest of the sessions (**Figure 25D**). An even more striking decrease in the synaptic strength values was recorded during the extinction phase when the air-puff stimulus was removed. In the case of the synapses between CA3 and the contralateral CA1 area, the curve of the best fit function was similar to that obtained in the ipsilateral side, but with a stronger increase on the 2nd day of pseudoconditioning and lower values during the extinction phase. Importantly, a more irregular distribution was found in this synapse ($r = 0.802$) in the conditioned sessions, when both tones and air puffs were presented in a non-paired way. During the extinction phase, when the air puff was removed, values were lower than in any other phase, and with great homogeneity.

Finally, values collected from the synapse between the dentate gyrus and CA3 (DG-CA3 synapse) showed the most stable profile of the 6 synapses included in this study (**Figure 25B**), with a similar trend to the one found in the context situation, although with lower values (103 ± 1.5% and 119.1 ± 2.2%). These data suggest that this DG-CA3 synapse could have a low specific weight in paradigms where there is not a causal relationship between stimuli, or where contextual cues do not provide information about the air-puff stimulus.

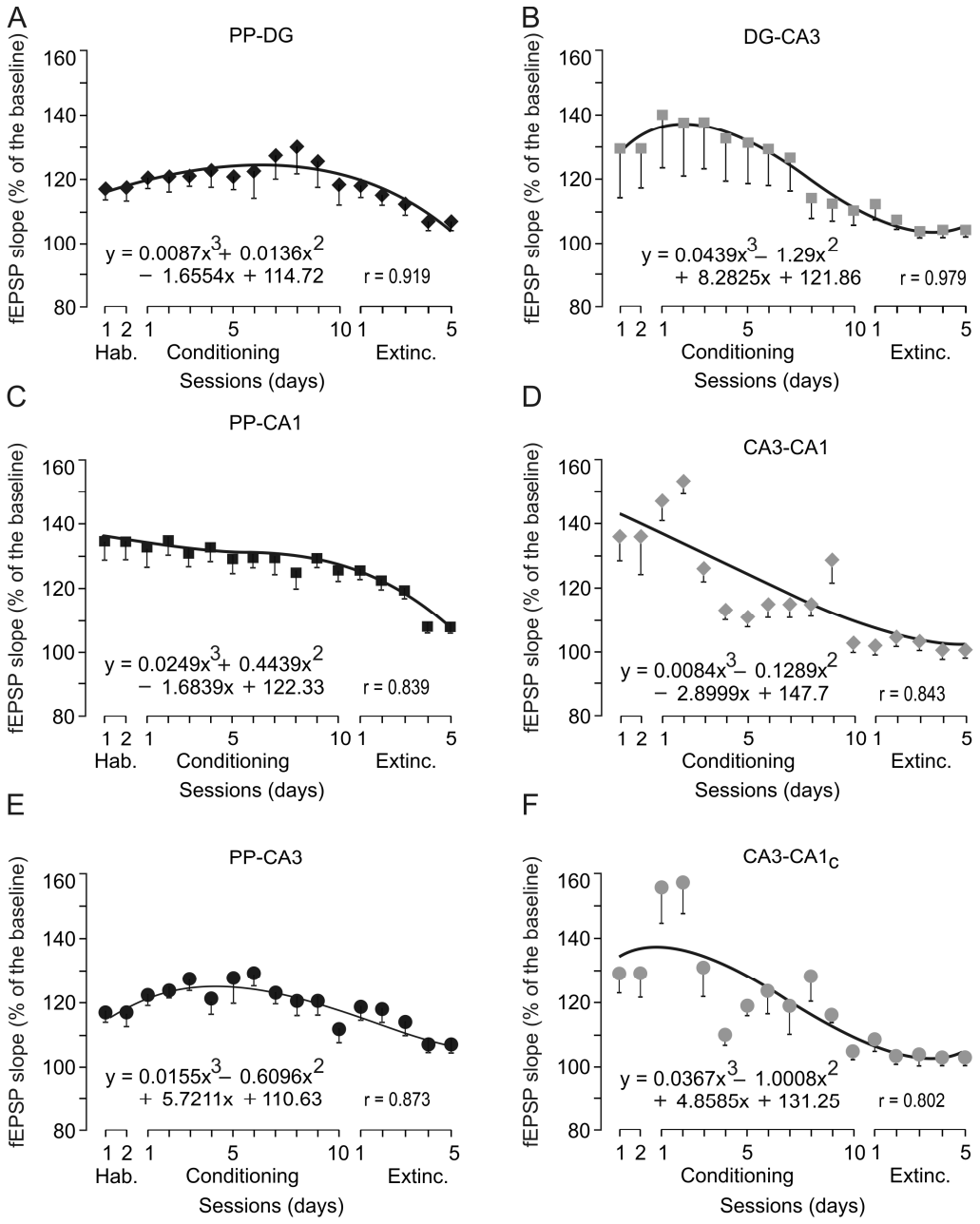

Figure 25. Main changes in synaptic strength evoked in the hippocampal circuit by pseudoconditioning. A-F, evolution of the evoked field excitatory postsynaptic potential (fEPSP) slopes at the 6 selected synapses during pseudoconditioning sessions: PP to DG (**A**), DG to CA3 (**B**), PP to CA1 (**C**), CA3 to CA1 (**D**), PP to CA3 (**E**), and CA3 to cCA1 (contralateral CA1) (**F**). Great changes are observed on the initial days in all synapses, and similarly to the context situation, the mean trend is stability, so minor changes were recorded in the last days of the pseudoconditioning protocol. For A-F are illustrated the best polynomial fits ($r \geq 0.802$; $P \leq 0.01$) for the fEPSP data collected from the 6 synapses.

4.1.5 Trace conditioning

Once the control paradigms were analyzed from the point of view of the percentage of conditioned responses and the changes in the evoked synaptic potentials, a new series of experiments was designed to find any relationship between associative learning and

hippocampal synaptic activity. As is shown in **Figure 22**, animals trained in a trace conditioning paradigm reached a level of conditioned responses higher than that expected from chance (> 50%) by the 4th conditioning session. In consequence, an increase in the slopes of evoked field excitatory postsynaptic potentials could be expected, at least during the conditioning phase. Some differences between the 6 recorded synapses were also predicted.

Recordings carried out in rabbits trained with a trace conditioning paradigm also showed a clear evolution in the synaptic strength in hippocampal input pathways. In particular, synapses between the perforant pathway and the dentate gyrus (PP-DG synapse, **Figure 26A**) and between the perforant pathway and the CA3 area (PP-CA3 synapse, **Figure 26E**) showed a clear increase in the slope of evoked field excitatory postsynaptic potentials. The maximum change took place in the 6th conditioning session in the case of the PP-DG synapse and in the 4th conditioning session for the PP-CA3 synapse. Both synapses maintained a high level of synaptic strength during the whole conditioning phase, and experienced a reduction during the extinction phase. Moreover, and also in these two synapses, the percentage of change in the field excitatory postsynaptic potentials was similar to that found in the 1st conditioning session. A different activity profile was found for the synapses between the perforant pathway and the CA1 area (PP-CA1 synapse). In the PP-CA1 synapse there was a continuous increase in the slope of evoked field excitatory postsynaptic potentials during the conditioning phase, reaching the maximum level for the 9th and 10th conditioning sessions (**Figure 26C**). Interestingly, the slope of evoked potentials during the 1st extinction session was similar to baseline values, but in the successive extinction sessions the values started to increase again. This recovery effect could be attributed to the change in the predictive value of the conditioned stimulus (i.e., the tone), since no unconditioned stimulus (i.e., the air puff) was presented in this phase.

The strength of intra-hippocampal synapses changed dramatically compared with values obtained with context (**Figure 24**) and pseudoconditioning (**Figure 25**) tests. In context and pseudoconditioning tests, the three synapses that were part of the trisynaptic hippocampal circuit started to show an increase of activity at the beginning of the recording sessions and ended up with lower and more-stable values. In contrast, the intra-hippocampal synapses during the trace conditioning paradigm (**Figure 26B, D, F**) showed a continuous change in the slopes of evoked field excitatory postsynaptic potentials, with a maximum value by the 4th conditioning session for synapses between the dentate gyrus and CA3 (DG-CA3 synapse) and between the CA3 and CA1 areas (CA3-CA1 synapse), and between the 8th and 10th sessions for synapses between the CA3 and contralateral CA1 areas (CA3-cCA1 synapse). In addition, DG-CA3 and CA3-

CA1 synapses reached their maximum values in the extinction phase (during the 1st session for DG to CA3 and in the 5th session for CA3 to CA1), when no unconditioned stimulus was presented. In contrast, the slopes of the field excitatory postsynaptic potentials of the CA3 to cCA1 synapses fell to control values during the extinction period.

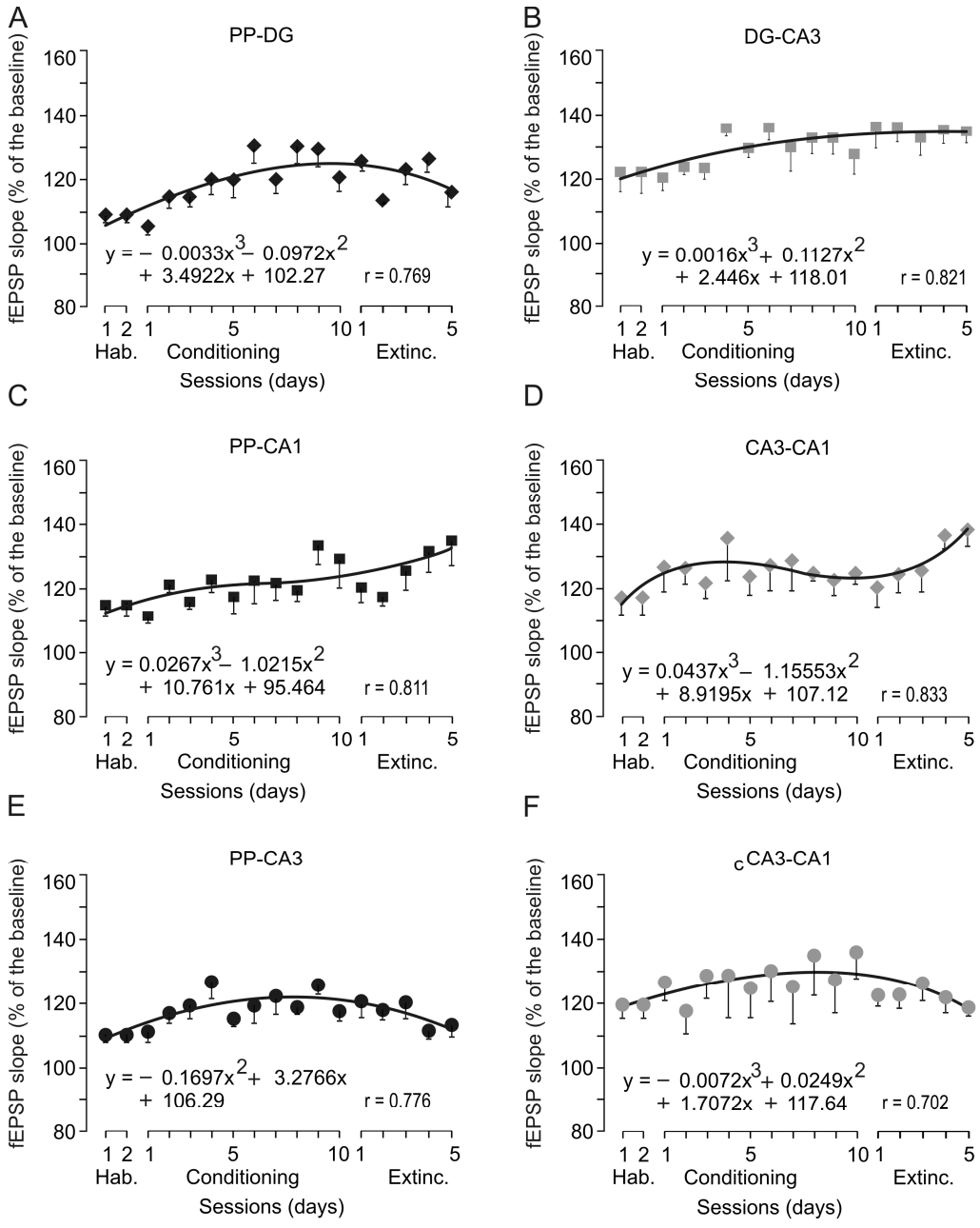

Figure 26. Main changes in synaptic strength evoked in the hippocampal circuit by trace conditioning. A-F, evolution of the evoked field excitatory postsynaptic potential (fEPSP) slopes at the 6 selected synapses during trace conditioning sessions: PP to DG (**A**), DG to CA3 (**B**), PP to CA1 (**C**), CA3 to CA1 (**D**), PP to CA3 (**E**), and CA3 to cCA1 (contralateral CA1) (**F**). In general, a different change of fEPSP slopes is observed across the training days during the trace conditioning paradigm, but the most frequent trend is towards the variation of activity. For **A-F** are illustrated the best polynomial fits ($r \geq 0.702$) $P \leq 0.01$) for the fEPSP data collected from the 6 synapses.

In summary, we obtained very interesting data for hippocampal changes during the trace conditioning paradigm, and most importantly, these data clearly differed from those obtained previously during the context and pseudoconditioning tests.

4.1.6 Delay conditioning

A commonly accepted proposal is that trace conditioning requires a conscious knowledge or an explicit memory of the relevant relationships between the conditioned and the unconditioned stimuli, a condition not required for the acquisition of a delay conditioning (Clark and Squire, 1998; Beylin et al., 2001; Eichenbaum, 2001; Lee and Kim, 2004). However, multiunit recordings in behaving rabbits during the classical conditioning of the nictitating membrane response have shown that pyramidal and other hippocampal cell types fire indistinctly during the CS–US interval for both conditioning paradigms (Berger et al., 1983; McEchron and Disterhoft, 1997). Moreover, hippocampal pyramidal cells located preferentially in the CA3 area, and identified by their antidromic activation from the ipsilateral fornix, fire a similar burst of action potentials in response to CS presentation for both trace and delay conditioning paradigms in alert behaving cats (Múnera et al., 2001). It could also be that the hippocampus is critical for delay conditioning under specific protocols. For example, lesions in the hippocampal formation impair the acquisition of delay conditioning when a relatively soft tone is used (Wu et al., 2009). Faced with all this contradictory information, it was decided to repeat the same protocols used for the trace conditioning paradigm in delay paradigms, where there is an overlapping of conditioned and unconditioned stimuli.

Data obtained in the present experiments revealed some differences with data obtained during trace conditioning paradigms, but, interestingly, the evolution of the field excitatory postsynaptic potential slopes across learning sessions was more similar to that recorded during this trace paradigm than during context and pseudoconditioning tests. Electrophysiological recordings carried out in rabbits trained with a delay conditioning paradigm showed similar evolution in strength for synapses of the input pathways: that is, synapses between the perforant pathway and the dentate gyrus (PP-DG) (**Figure 27A**) and between the perforant pathway and the CA1 (PP-CA1, **Figure 27C**) and CA3 (PP-CA3, **Figure 27E**) areas. For these three different synapses, an increase in strength was found at the beginning of the conditioning sessions that decreased across this training phase. At the end of the conditioning sessions (for the PP-DG synapse) or at the beginning of the extinction sessions (for the PP-CA1 and PP-cCA1 synapses), an inflexion in the curve could be observed, indicating a delayed

increase in strength. After a mild decrease during the extinction session, all three synapses showed an increase in the slopes of field excitatory postsynaptic potentials at the end of the experiment.

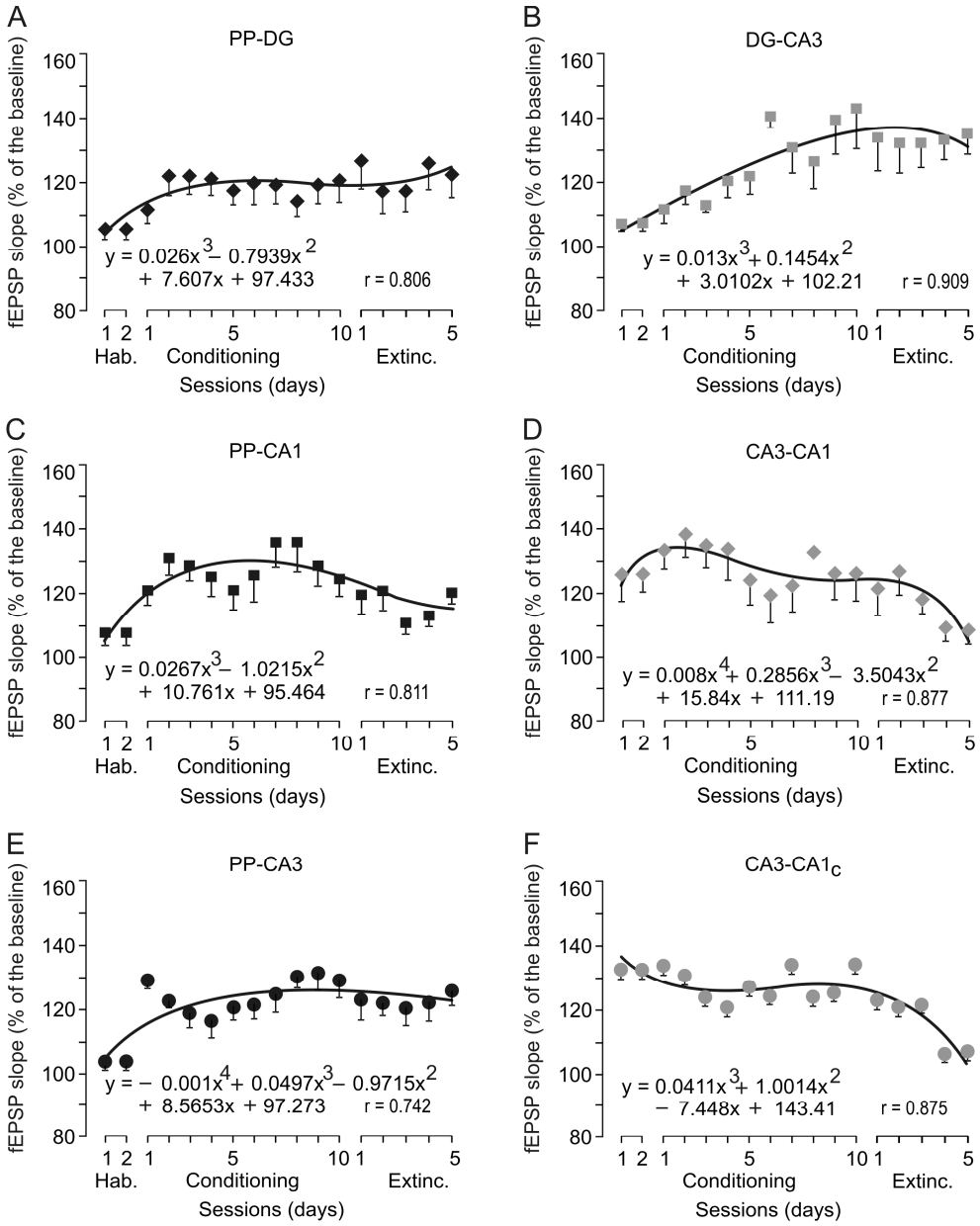

Figure 27. Main changes in synaptic strength evoked in the hippocampal circuit by delay conditioning. A-F, evolution of the evoked field excitatory postsynaptic potential (fEPSP) slopes at the 6 selected synapses during delay conditioning sessions: PP to DG (**A**), DG to CA3 (**B**), PP to CA1 (**C**), CA3 to CA1 (**D**), PP to CA3 (**E**), and CA3 to cCA1 (contralateral CA1) (**F**). Similarly to the results obtained during the trace conditioning paradigm, all the observed synapses did not show the same trend across the training sessions, and there was a greater increase in variability than in context and pseudoconditioning situations. For **A-F** are illustrated the best polynomial fits ($r \geq 0.742$; $P \leq 0.01$) for the fEPSP data collected from the 6 synapses.

The evolution in strength of intra-hippocampal synapses presented clear differences across the conditioning sessions during the delay conditioning paradigm. Synapses between the CA3 and CA1, both ipsilateral (CA3-CA1 synapse, **Figure 27D**)

and contralateral (CA3-cCA1 synapse, **Figure 27F**), showed similar profiles, although there were some differences during the habituation, with higher values for the CA3-CA1 synapse. Surprisingly, for both synapses there was an increase in the slopes of field excitatory postsynaptic potentials at the beginning of conditioning and extinction sessions, followed by a decrease throughout each phase, until they reached the lowest values in the last sessions of the extinction phase. Finally, a completely different profile was observed for the synapses between the dentate gyrus and the CA3 area (DG-CA3 synapses, **Figure 27B**), consisting of a constant increase in synaptic strength during the conditioning sessions and a stabilization of these high values during the five extinction sessions.

In summary, data collected using the delay conditioning paradigm clearly differed from those previously obtained with context and pseudoconditioning protocols, with some important differences in values and trends found during the trace conditioning paradigm.

4.1.7 Functional synaptic states for the different experimental situations

The last step of this experiment was to compare the changes found in the 6 selected synapses during the 17 sessions of the 4 experimental situations. The collected data were also compared with the percentage of conditioned responses generated during the different conditioning protocols. All of the recorded changes in the slope of field excitatory postsynaptic potentials for the 6 hippocampal synapses included in this study and collected during the 4 training protocols (context, pseudoconditioning, and trace and delay conditioning paradigms) were analyzed as already illustrated in **Figure 23** for the DG-CA3 synapse during a trace conditioning paradigm. As shown in **Figure 28**, the increase in the percentage of conditioned responses (**Figure 28A**) and the change $[([+\Delta] + [-\Delta]) / N]$ in synaptic strength at each selected synapse (**Figure 28B**) were transduced into a color code. In the learning curve, the bluish colors correspond to the absence or very low values of conditioned responses; the reddish colors are the maximum percentage of learned responses (to 100%); and the green color represents 50% of conditioned responses. With regard to a change in synaptic strength, the green color signifies zero or absence of change in the synaptic activity, the reddish color an increase in the change of synaptic strength, and the bluish color a decrease in that value. The equation corresponding to the best quadratic fit to data collected during conditioning sessions is indicated, as well as the corresponding regression curve and the simultaneous 95% confidence level.

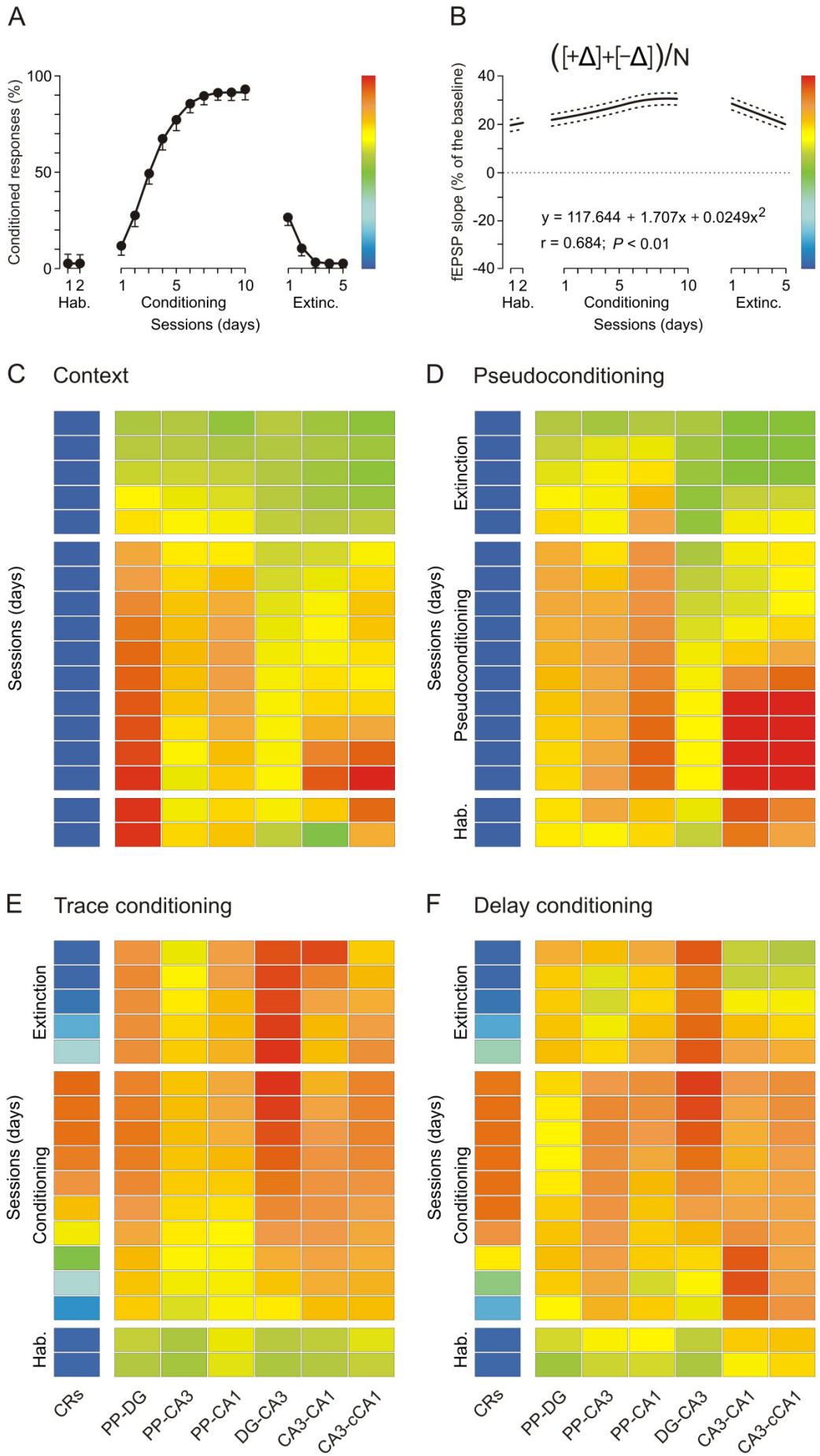
A
Conditioned responses (%)
100
50
0
1 2
Hab.
1
5
10
Conditioning
1
5
Extinc.
Sessions (days)
B
([+Δ]+[−Δ])/N
fEPSP slope (% of the baseline)
40
20
0
-20
-40
y = 117.644 + 1.707x + 0.0249x2
r = 0.684; P < 0.01
1 2
Hab.
1
5
10
Conditioning
1
5
Extinc.
Sessions (days)
C
Context
Sessions (days)
D
Pseudoconditioning
Extinction
Sessions (days)
Pseudoconditioning
Hab.
E
Trace conditioning
Extinction
Sessions (days)
Conditioning
Hab.
CRs
PP-DG
PP-CA3
PP-CA1
DG-CA3
CA3-CA1
CA3-cCA1
F
Delay conditioning
Extinction
Sessions (days)
Conditioning
Hab.
CRs
PP-DG
PP-CA3
PP-CA1
DG-CA3
CA3-CA1
CA3-cCA1

Figure 28. Evolution of the evoked field excitatory postsynaptic potential slopes at six different synapses of the hippocampal intrinsic circuit during the four selected conditioning situations. A-B, evolution of the percentage of conditioned responses (CRs) (**A**) and of field excitatory postsynaptic potential **(**fEPSP) slopes evoked at the CA3-cCA1 synapse (**B**) across conditioning sessions using a trace paradigm (n = 6 animals). Illustrated fEPSP regression curves were averaged [([+Δ] + [−Δ]) / N] from 15 electrodes implanted in the cCA1 area. The equation corresponding to the best polynomial fit to data collected during conditioning sessions is indicated, as well as the corresponding regression curve and the simultaneous 95% confidence bands. Note the color code bars located to the right of **A** and **B** panels. **C-F,** Evolution of CRs (%) and of fEPSP slopes (as % of baseline values, see **B**) collected at six hippocampal synapses across the successive training sessions in four different experimental situations: context (no CS or US presentations, **C**); pseudoconditioning (**D**); and trace (**E**) and delay (**F**) conditioning paradigms. In the case of context (**C**) and pseudoconditioning (**D**), the baseline was the values of fEPSP slopes collected during the last two (14th and 15th) training sessions. In contrast, baseline values for fEPSP slopes in trace (**E**) and delay (**F**) conditioning were collected from the first two (habituation) sessions.

In **Figure 28C-F** are shown the increase in the percentage of conditioned responses (isolated left bar) and the changes in field excitatory postsynaptic potential slopes taking place in the 6 selected synapses (PP-DG, PP-CA3, PP-CA1, DG-CA3, CA3-CA1, and CA3-cCA1) during context (**C**), pseudoconditioning (**D**), and trace (**E**) and delay (**F**) conditioning paradigms. For the sake of clarity, the same fEPSP results collected from the 6 synapses are represented in **Figures 29-32** in the form of best polynomial fit ($r \geq 0.81$; $P \leq 0.01$) for context (**Figure 29A**), pseudoconditioning (**Figure 30A**), and trace (**Figure 31A**) and delay (**Figure 32A**) conditioning. A minimum of 15 recording electrodes/selected synapse presenting absolute changes in strength were included in the illustrated analysis.

Just placing experimental animals in the restraining box for up to 17 sessions (context group) evoked significant ($P \leq 0.007$) changes in field excitatory postsynaptic potential slopes (**Figures 28C and 29A**) at selected synapses and at different times across training, although no eyelid conditioned responses were recorded. The most noticeable increase in activity took place at the synapse between the perforant pathway and dentate gyrus (PP-DG synapse) in the very first sessions of the training. Similar increases in field excitatory postsynaptic potential slopes were also observed in the synapses between the CA3 and CA1 areas, both ipsilaterally (CA3-CA1 synapse) and contralaterally (CA3-cCA1 synapse), but for a short period of time. The most-significant ($P \leq 0.01$) and longest-lasting changes in synaptic strength took place at the three synapses (PP-DG, PP-CA3, PP-CA1) corresponding to the input from the perforant pathway to the hippocampal intrinsic circuit. The equation corresponding to the best quadratic fit to data collected during conditioning sessions was calculated and represented for each studied synapse (**Figure 29A**) during the context situation. An attempt was also made to represent the synaptic changes in activity in the studied hippocampal circuitry in two periods of the recording protocol: that is, the 9th and 15th

days. The diagrammatic representation shows a clearly increasing activity in the dentate gyrus and a more moderate one in the CA3 and CA1 areas nine days after the recording sessions started (**Figure 29B**). In all these areas, the increase of activity was much more moderate 6 days afterwards (at the fifteenth session, **Figure 29C**). It is interesting that the changes in activity were not exactly the same in the pathways between CA3 and CA1, ipsi- and contralaterally; although the differences between them were maintained with time.

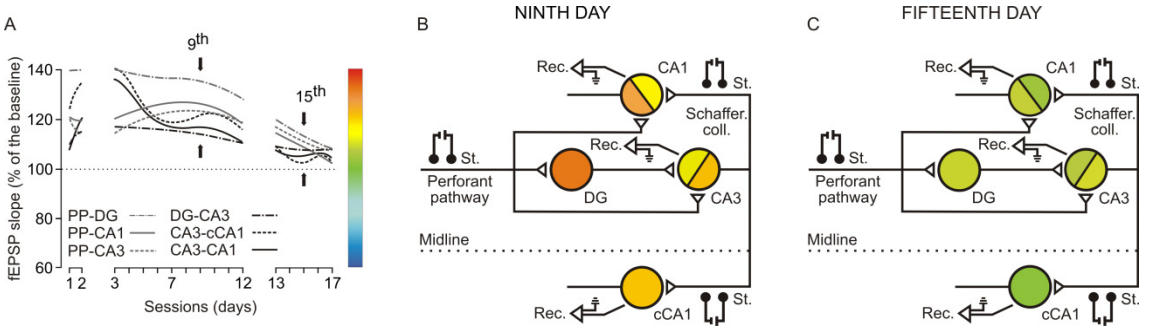

Figure 29. Synaptic state of the hippocampal circuit during context situation. A, evolution of the evoked field excitatory postsynaptic potential (fEPSP) slopes at the 6 selected synapses when any specific protocol was applied. The best polynomial fits ($r \geq 0.742$; $P \leq 0.01$) are illustrated for the data collected at the 6 selected synapses (see line codes in **A**). **B-C,** representation of the synaptic strength corresponding to each recorded synapse during the 9th and 15th (7th conditioning session and 3rd extinction session, respectively; see arrows) recording days. The corresponding color codes are represented to the right of panel **A**. Note that the greatest changes in the 9th training session (**B**) were observed at the PP-DG and—with lower intensity—the PP-CA3 and PP-CA1 synapses, and a stable situation is observed for all the recorded synapses by the 15th day (**C**).

The pseudoconditioning group also presented sustained ($P \leq 0.01$) changes in the three input synapses from the perforant pathway, to the dentate gyrus (PP-DG synapse), and to the CA3 (PP-CA3 synapse) and CA1 (PP-CA1 synapse) areas from the hippocampal intrinsic circuit during the first 10-12 training sessions (**Figures 28D and 30A**). Increases in synaptic strength similar to those in the context group, but of a shorter duration, were also observed in the synapses between the CA3 and CA1 areas, both ipsilaterally (CA3-CA1 synapse) and contralaterally (CA3-cCA1 synapse). The equation corresponding to the best quadratic fit to data collected during conditioning sessions was calculated and represented for each studied synapse during the pseudoconditioning protocol (**Figure 30A**). Similarly to that already indicated for the context group, the slopes of field excitatory postsynaptic potentials evoked at the 6 selected synapses during pseudoconditioning decreased progressively with training, reaching the lowest values during the last two training sessions (**Figure 30B-C**). Moreover, during the extinction phase, without the air puff, profiles of the changes recorded in each of the synapses were more similar to those recorded during the pseudoconditioning sessions.

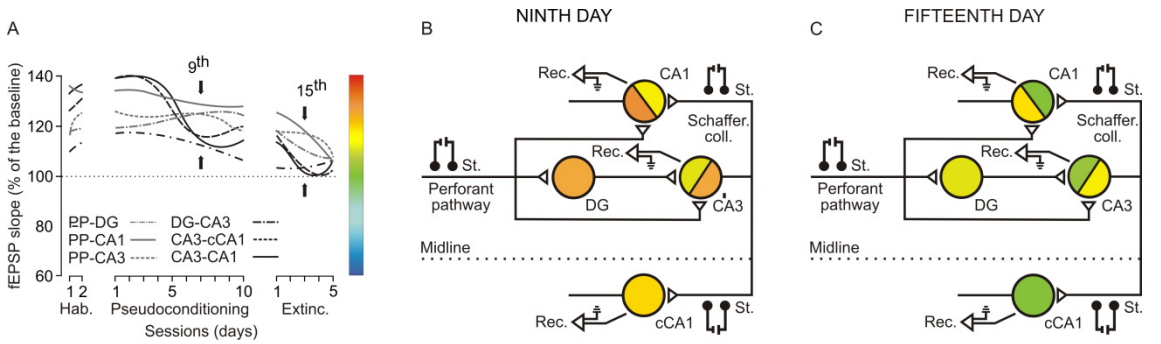

Figure 30. Synaptic state of the hippocampal circuit during pseudoconditioning. A, Evolution of the evoked field excitatory postsynaptic potential (fEPSP) slopes at the 6 selected synapses during pseudoconditioning. The best polynomial fits ($r \geq 0.802$; $P \leq 0.01$) are illustrated for the data collected at the 6 selected synapses (see line codes in **A**). **B-C,** representation of the synaptic strength corresponding to each recorded synapse during the 9th and 15th (7th conditioning session and 3rd extinction session respectively; see arrows) recording days. The corresponding color codes are represented to the right of panel **A**. Note that the greatest changes in the 9th training session (**B**) were observed at the PP-DG and -with lower intensity- the PP-CA3 and PP-CA1 synapses and a stable situation is observed for all the recorded synapses by the 15th day (**C**).

During trace conditioning, animals presented very interesting changes in absolute synaptic strength (**Figures 28E and 31A**). Firstly, major changes took place across the training (i.e., during both conditioning and extinction) sessions. Major significant ($P \leq 0.01$) changes in synaptic strength were observed not only in the synapse between the perforant pathway and the dentate gyrus (PP-DG synapse), but also in some of the synapses included in the hippocampal intrinsic circuit, between the dentate gyrus and the CA3 area (DG-CA3 synapse), the CA3 and CA1 areas, both ipsilateral (CA3-CA1 synapse) and contralateral (CA3-cCA1 synapse). Other synapses (PP-CA3 and PP-CA1) were apparently less involved in the acquisition of this trace conditioning paradigm. Some synapses, such as the one between the perforant pathway and the dentate gyrus (PP-DG synapse), the one between the dentate gyrus and the CA3 area (DG-CA3 synapse), and the one between the CA3 and CA1 areas (CA3-CA1 synapse), were still very active during the last extinction sessions, even more than in the last sessions of the conditioning phase (**Figure 31B-C**). The equation corresponding to the best quadratic fit to data collected during conditioning sessions was calculated and represented for each studied synapses during the trace conditioning protocol (**Figure 31A**).

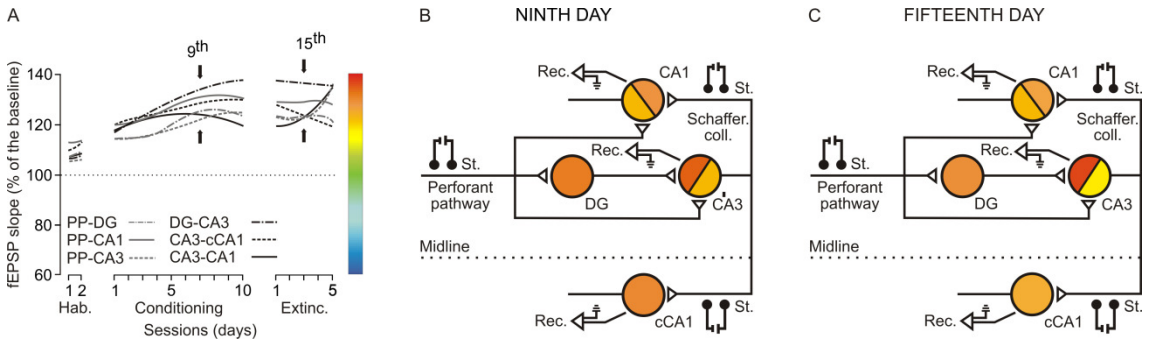

Figure 31. Synaptic state of the hippocampal circuit during trace conditioning. A, Evolution of the evoked field excitatory postsynaptic potential (fEPSP) slopes at the 6 selected synapses during trace conditioning. The best polynomial fits ($r \geq 0.702$; $P \leq 0.01$) are shown for the data collected at the 6 selected synapses (see line codes in **A**). **B-C,** representation of the synaptic strength corresponding to each recorded synapse during the 9th and 15th (7th conditioning session and 3rd extinction session respectively; see arrows) recording days. The corresponding color codes are represented to the right of panel **A**. The general trend of variation for all synapses is remarkable, especially for the intra-hippocampal ones. Moreover, a similar synaptic state in terms of synaptic activity changes can be observed in both the 9th (**B**) and the 15th (**C**) sessions, suggesting a similar process for the two phases of learning: conditioning and extinction.

Finally, during delay conditioning (**Figures 28F and 32**), changes were observed in synaptic strength, though—surprisingly—not exactly equal to those during trace conditioning. For example, in this case, the synapses presenting the highest rate of change ($P \leq 0.01$) were two located in the hippocampal intrinsic circuit, between the dentate gyrus and CA3 area (DG-CA3 synapse) and between the CA3 and CA1 areas (CA3-CA1 synapse), although the changes in the former took place later than those in the latter. Interestingly, some seminal studies (Segal et al., 1972; Segal and Olds, 1972) using a tone-food association test did report changes in the CA3-CA1 synapse not dependent upon those taking place in the dentate gyrus. The equation corresponding to the best quadratic fit to data collected during conditioning sessions was calculated and represented for each studied synapse during the delay conditioning protocol (**Figure 32A**). Finally, smaller changes in strength were also observed in synapses corresponding to hippocampal inputs (PP-CA3) and the hippocampal commissural pathway (CA3-cCA1 synapses).

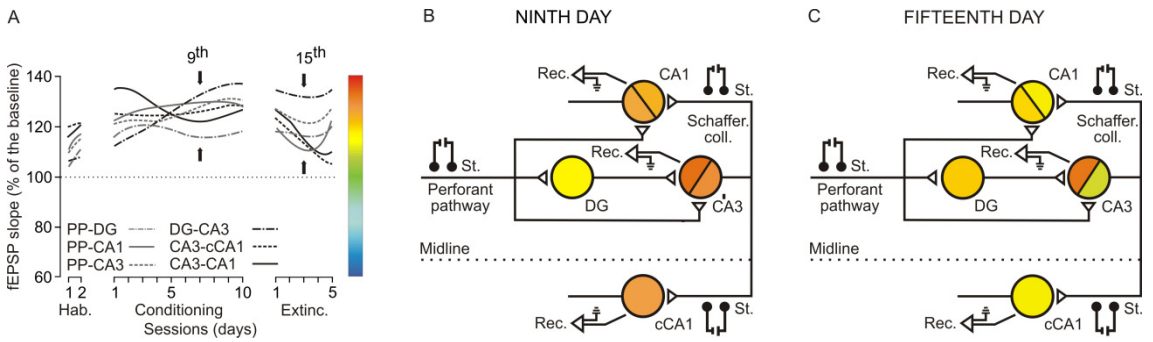

Figure 32. Synaptic state of the hippocampal circuit during delay conditioning. A, Evolution of the evoked field excitatory postsynaptic potential (fEPSP) slopes at the 6 selected synapses during trace conditioning. The best polynomial fits ($r \geq 0.742$; $P \leq 0.01$) are shown for the data collected at the 6 selected synapses (see line codes in **A**). **B-C,** representation of the synaptic strength corresponding to each recorded synapse during the 9th and 15th (7th conditioning session and 3rd extinction session respectively; see arrows) recording days. The corresponding color codes are represented to the right of panel **A**. A situation similar to the one found in trace conditioning can be observed for delay conditioning, although the trend of variation is not so strong in the delay conditioning results. Again, the noteworthy synapses are the intra-hippocampal synapses during extinction. In this case, the synaptic state on the 15th day (**C**) has intermediate values and less variability than that observed during the trace conditioning. However, data obtained during delay conditioning show higher variability than those obtained in context or pseudoconditioning situations.

Figure 33 displays an overview of the synaptic state of the hippocampal synapses included in this study at the same time—i.e., the 9th (purple columns) and the 15th (blue columns) recording days—across the four experimental situations considered here: context, pseudoconditioning, and trace and delay conditionings. Results included in these diagrams illustrate clearly the different functional states in which hippocampal circuits are placed during these 4 experimental situations. For example, in both context and pseudoconditioning, peak changes by the 9th recording day were observed at synapses afferent to hippocampal circuits, mainly between the perforant pathway and the dentate gyrus, and to a lesser degree between the perforant pathway and the CA3 (PP-CA3 synapse) or CA1 (PP-CA1 synapse) areas. In contrast, by the same recording day (corresponding to the 7th conditioning session in conditioned animals), the main changes in synaptic strength taking place during both trace and delay conditioning also involved synapses located in the hippocampal intrinsic circuit (i.e., DG-CA3, CA3-CA1 synapses) or in the commissural pathway (CA3-cCA1 synapse). Differences were even more noticeable during the 15th training day (corresponding to the 3rd extinction session in conditioned animals), because most hippocampal synapses presented the smallest changes in strength in both context and pseudoconditioning groups, whilst considerable changes in strength were still taking place in the hippocampal circuit in both trace (mostly PP-DG, DG-CA3, and CA3-CA1 synapses) and delay (mostly in the DG-CA3 synapse) during this (3rd) extinction session. Similar results were obtained considering the functional status of each selected synapse for a given day and training situation.

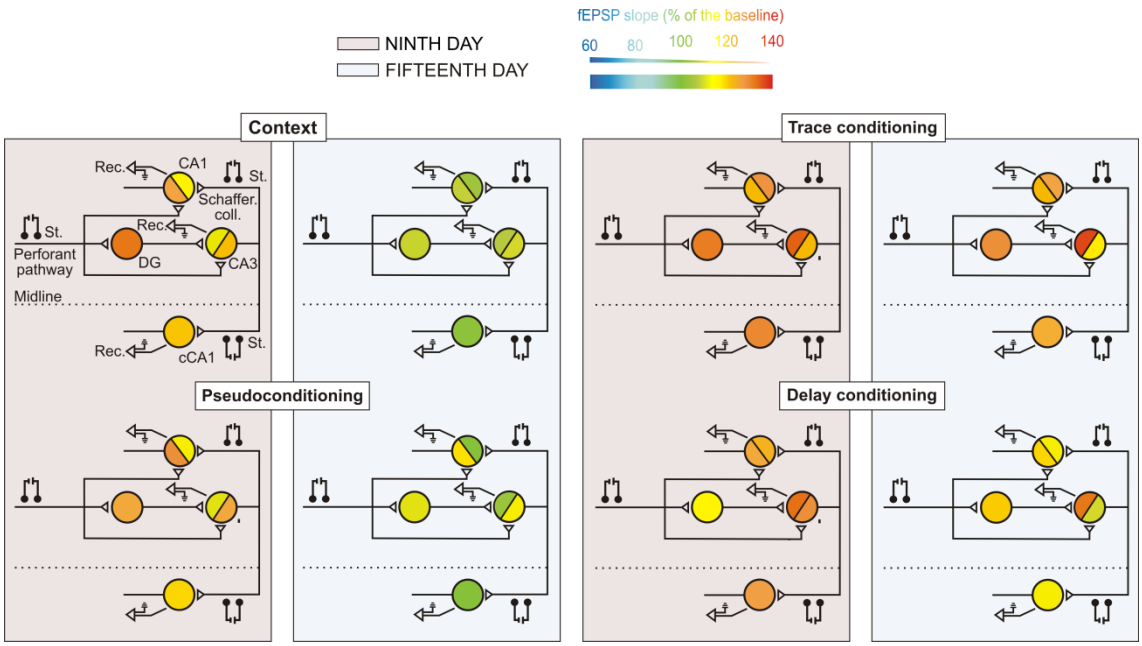

Figure 33. Overview of synaptic state, in terms in changes in the synaptic activity, of the hippocampal circuit in different situations. From left to right and from top to bottom, the synaptic state of the hippocampal formation is represented for context situation, pseudoconditioning, trace conditioning, and delay conditioning. In alternate colored columns the two analyzed sessions (9th session in purple and 15th session in blue) are shown for the four paradigms. The representation shows clear similarities between the situations that do not produce any new behavior (context and pseudoconditioning) and between the ones that do produce it (trace and delay conditioning). The highest variability is found on the hippocampal input pathway (PP to DG, CA1 and CA3) in the context and the pseudoconditioning situations, whereas it is found in the intra-hippocampal synapses (DG to CA3, CA3 to CA1, and CA3 to cCA1) in the trace and delay conditionings. The changes in synaptic activity were more notable during the trace conditioning, perhaps due the greater difficulty in learning this type of paradigm. Regarding extinction (second and fourth columns), similar results were found. In this case, context and pseudoconditioning situations show a stable synaptic view (second column, in blue), lower in the case of pseudoconditioning. This result is consistent with the fact that no unconditioned stimulus is presented in this session. However, in the case of trace and delay conditionings, the synaptic state is similar to the one observed on the 9th day, and the differences of variability between input pathways and intra-hippocampal synapses are even stronger.

4.1.8 Histological confirmation of implanted sites

The final position of the recording (white dots) and the stimulating (black dots) electrodes was established during the surgery with the help of electrophysiological techniques (see Material and Methods section), and at the end of the experiments, those positions were checked in each rabbit. Before the analysis of field excitatory postsynaptic potential slopes, the position of the implanted electrodes was checked using histological protocols. Electrodes that were outside the corresponding area were eliminated from subsequent analysis. The discard rate was very low, and only two recording sites from two different rabbits were not considered. **Figure 34** shows an example of each conditioning or stimulating electrode position. The brain slices were

obtained from different rabbits from the 4 protocols and they were stained using a Nissl protocol with blue Toluidine colorant.

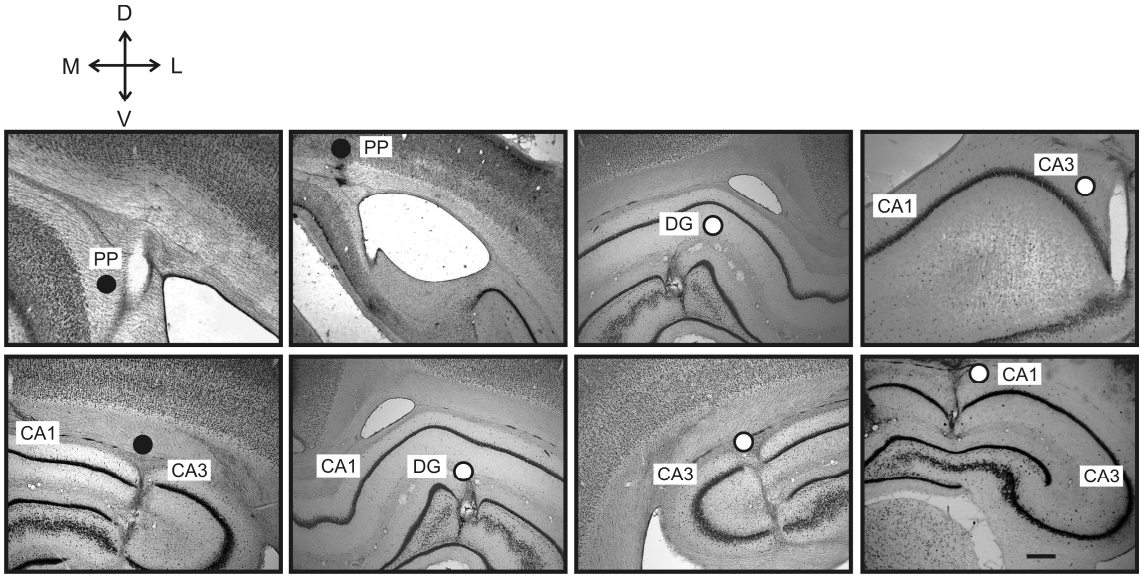

Figure 34. Histological confirmation of electrode positions. Photomicrographs illustrate the final location of the implanted electrodes. The recording electrode track is indicated with closed white circles and the stimulating electrode track with closed black circles. Calibration bar is 1 mm for all the sections. Abbreviations: D, L, M, V, dorsal, lateral, medial, ventral; DG, dentate gyrus; CA1 and CA3, areas 1 and 3 of the cornu Ammonis; LV, lateral ventricle; PP, perforant pathway.

4.2 DENTATE GYRUS INHIBITION

Prior analysis of the synaptic strength state of the hippocampal formation circuit revealed interesting data about which synapses within the hippocampal formation could be most suitable as the physiological substrate for different phases of the associative learning.

In particular, it was proposed that the dentate gyrus could be a crucial region in this type of learning since it showed surprising changes in excitability during the exposure of the animal to contextual paradigms. Moreover, mossy fibers going from the dentate gyrus to the CA3 area (DG-CA3 synapse) showed a substantial change in synaptic activity during trace and delay conditioning paradigms. For these two reasons, in the following set of experiments an attempt was made to temporarily inactivate the dentate gyrus and to check how this experimental interference in the synaptic state could modify the learning process. Finally, it was also proposed to test the recovery capability of both synaptic and learning properties after the dentate gyrus returned to its previous physiological state.

4.2.1 Evoked field excitatory postsynaptic potential slope evolution of PP to CA3 synapse

After animals recovered from electrode implantation, they were divided in two different conditioning situations: i) a double recall protocol (**Figure 35**); and ii) an over-conditioning protocol (**Figure 36**). In addition, different groups of animals were included in each experimental situation. For the double recall experiment, three groups were included: i) a control group, in which a non-tetanus-expressing virus was injected; ii) a unilaterally infected group, with a tetanus-toxin-expressing virus injected in only one hemisphere; and, iii) a bilaterally infected group, with a tetanus-neurotoxin-expressing virus injected in both hemispheres. Similarly, two groups were prepared for the over-conditioning protocol: i) a control group, in which a non-tetanus-expressing virus was injected; and ii) a bilaterally infected group, with a tetanus-toxin-expressing virus injected in both hemispheres. Before virus activation by the doxycycline injection, the evolution of the field excitatory postsynaptic potential slopes was normal in the three groups of the recall experiment (**Figures 35**) and in the two groups of the over-conditioning experiment (**Figure 36**).

4.2.1.1 Recall protocol

The recall protocol (**Figure 35A**) used in the present experiments included 2 habituation sessions, 6 conditioning sessions, and 2 recall sessions. The recall sessions were carried out 4 (Recall 1) and 14 (Recall 2) days after the last conditioning session. Both conditioning and recall sessions followed a trace paradigm. Rabbits were injected with doxycycline just after the last conditioning session.

In the first recall session (day 12, and marked as 2 in **Figure 35B**), it was observed, 4 after days of its administration, that the injection of doxycycline triggered a reduction in the slopes of fEPSPs in unilaterally (gray triangles) and bilaterally (black triangles) tetanus-toxin-infected animals ($P < 0.001$). Importantly, the control virus group (white triangles) did not show any change in the field excitatory postsynaptic potential slopes 4 days after the administration of doxycycline, and no statistically significant differences were found between the increase in synaptic strength on the 6th conditioning day (marked as 1 in **Figure 35B**) and in the 1st recall session (marked as 2 in **Figure 35B**).

The second recall session (day 22, and marked as 3 in **Figure 35B**) also revealed important information, since no significant differences were found between the 3 experimental groups, and all of them showed no statistically significant differences with the field excitatory postsynaptic potential values obtained in the last sessions of conditioning (marked as 1 in **Figure 35B**).

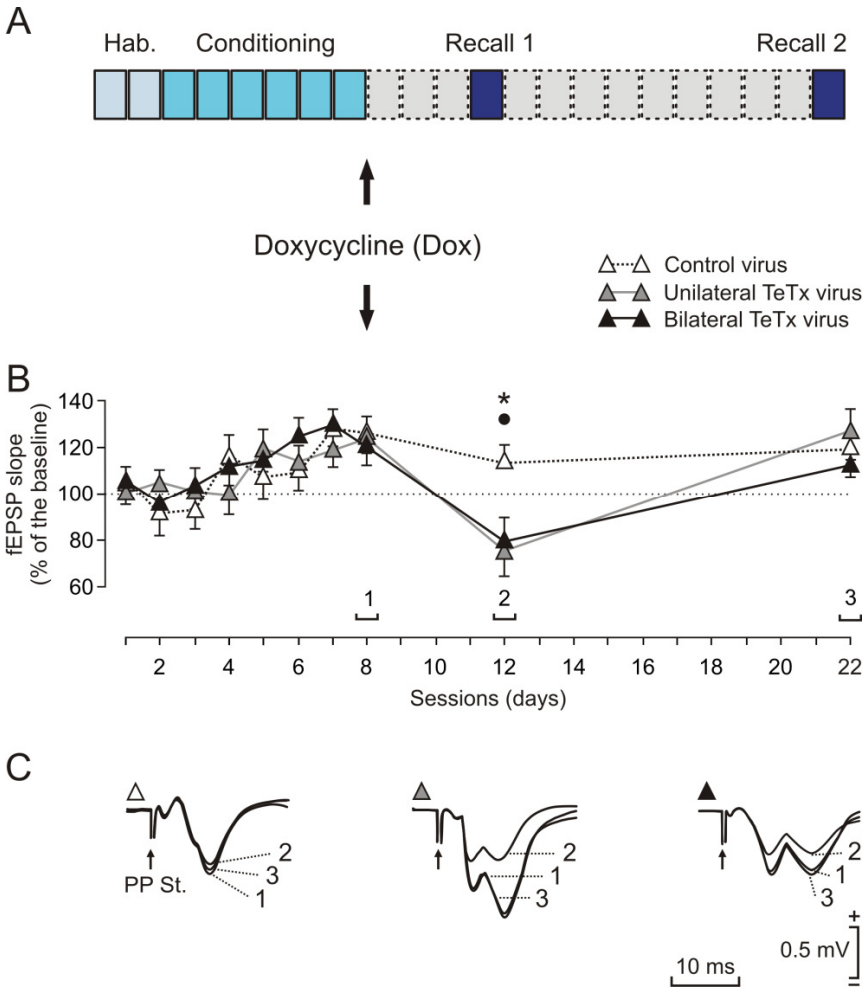

Figure 35. Evoked field excitatory postsynaptic potential slope evolution of PP to CA3 synapse using a recall protocol. A, Diagram of the experimental protocol, which includes 2 sessions of habituation (Hab.), 6 sessions of conditioning, and 2 sessions of recall, 4 (Recall 1) and 14 (Recall 2) days after the last conditioning session, respectively. After the 6th session of conditioning, a single injection of doxycycline (45 µg/g of animal weight) was administered i.p. (1), and only two more sessions were applied to assess the level of conditioned responses: a recall session (2) the 4th and another recall session (3) the 14th day after Dox injection to the 3 experimental groups: i) Control (white triangles); ii) Unilateral TeTx virus (injected with the tetanus toxin in the hippocampus unilaterally, gray triangles); and iii) Bilateral TeTx virus (injected with the tetanus toxin bilaterally in the hippocampus, black triangles). **B,** Changes in the evoked field excitatory postsynaptic potential (fEPSP) slopes along the 22 days that the protocol lasted. Note the clear decrease in the fEPSP slope for both tetanus-toxin-injected groups during the Recall 1 session and the complete synaptic recovery during the Recall 2. **C,** Representative examples of fEPSPs recorded in the hippocampal CA3 area and evoked by the electrical stimulation of the ipsilateral perforant pathway (PP St.). Traces indicated with number 1 correspond to the 6th conditioning day, number 2 to the Recall 1 day, and number 3 to the Recall 2 day, for each experimental group (see **B**). (***, $P < 0.001$).

Although the experiment was aimed at isolating the synaptic deactivation mediated by tetanus-toxin virus injection to only the mossy fibers going to CA3 area (DG-CA3 synapse), this approach was extremely difficult due to the not-totally controlled

diffusion of the virus, and the limited accuracy of the available stereotaxic atlas for rabbits. For this reason, a reduction was observed not only in the 2nd component of the evoked field potentials, but also in the first component of this field at the PP-DG synapse (**Figure 35C**) for the unilaterally and bilaterally infected groups. The control group did not show noteworthy changes in the slope and amplitude of its field excitatory postsynaptic potentials during the 3 days represented in **Figure 35C**.

4.2.1.2 Over-conditioning protocol

The recall protocol used here showed the synaptic and functional disruption when mild interferences are applied to the hippocampal circuit. The next experimental test, using an over-conditioning protocol, enabled assessing not only the accessibility of the information generated in the hippocampal formation, but the capability of restoring it by continuously training the rabbits in the classical conditioning after doxycycline injection. As is shown in **Figure 36A**, after two habituation sessions, rabbits received twenty consecutive classical conditioning sessions; doxycycline was injected after the 6th conditioning session (marked as 1 in **Figure 36B**) to the 2 groups of rabbits: controls (white triangles) and bilaterally injected with the tetanus toxin in the hippocampus (black triangles). Conditioning sessions followed a trace paradigm.

The profile of the field excitatory postsynaptic potential slope evolution (**Figure 36B**) in control and bilaterally infected groups was similar to those obtained during the previous recall protocol. Both groups showed an increase in the field excitatory postsynaptic potential slopes during the first 6 conditioning days, reaching an average value of 116% with respect to baseline measurements. After doxycycline injection, no significant differences were obtained in the slope of evoked field excitatory postsynaptic potentials in the control group (white triangles) along the subsequent conditioning days. In the case of the bilaterally infected rabbits, field excitatory postsynaptic potential slopes (black triangles) decreased, reaching values close to 83% with respect to baseline in the 4 days doxycycline injection. The decrease in the field excitatory postsynaptic potential slope values was statistically significant ($P < 0.001$) in each of these 4 conditioning sessions with respect to the controls. The experimental group reached the same statistically equal values in session 12—that is, 5 days after the doxycycline injection.

The shape of the field excitatory postsynaptic potential slopes recorded in these groups (**Figure 35C**) exactly matched the ones usually recorded at the PP-CA3 synapse. Therefore, a specific reduction of the disynaptic component corresponding to the mossy fibers of the dentate gyrus to CA3 area could be accomplished in the

bilaterally infected group. This component recovered its normal values when the induction of the expression of tetanus toxin ceased.

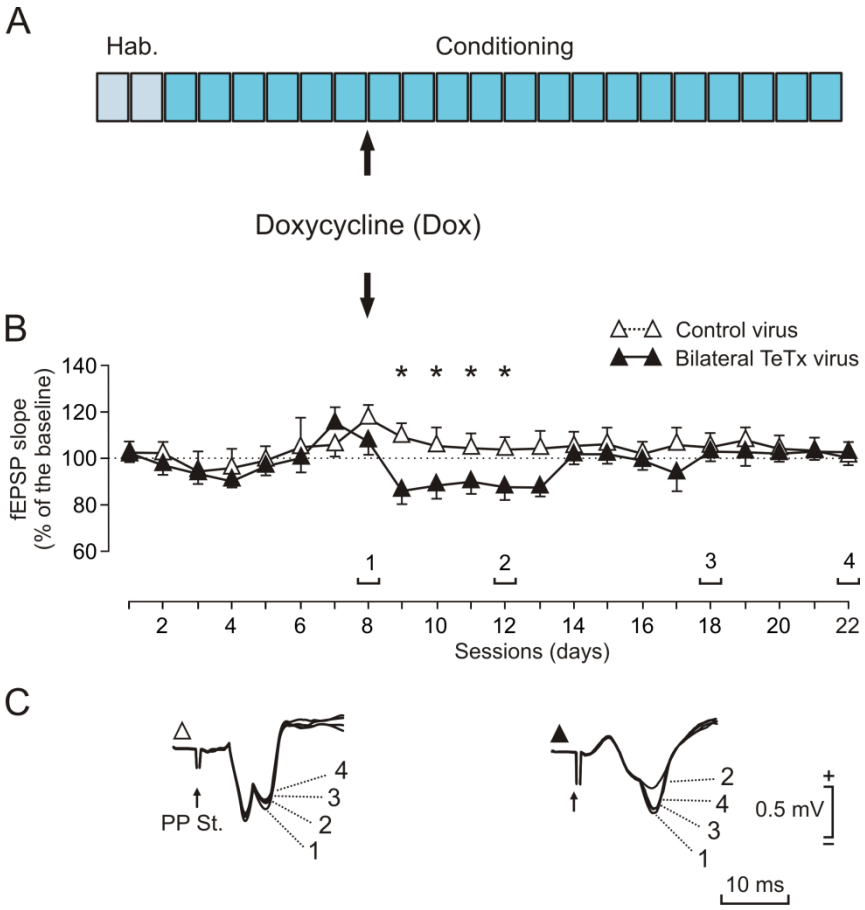

Figure 36. Evoked field excitatory postsynaptic potential slope evolution of PP to CA3 synapse using an over-conditioning protocol. A, Diagram of the experimental protocol, which includes 2 sessions of habituation (Hab.) and 20 consecutive days of conditioning sessions. After 2 habituation days and 6 conditioning sessions, a single injection of doxycycline (45 µg/g animal weight) was administered i.p. to the two experimental groups: i) Control (white triangles); and ii) Bilateral Tet virus (injected with the tetanus toxin bilaterally in the hippocampus, black triangles). **B,** Evolution of the evoked field excitatory postsynaptic potential (fEPSP) slopes along the 22 days that the protocol lasted. Note the clear decrease in the percentage of change in the fEPSP slope for the injected group that recovered 6 days after the Dox injection. **C,** Representative examples of fEPSPs recorded in the hippocampal CA3 area and evoked by the electrical stimulation of the ipsilateral perforant pathway (PP St.). Traces indicated with number 1 correspond to the 6th conditioning day, numbers 2, 3, and 4 correspond to 4, 10, and 14 days, respectively, after doxycycline injection for the 2 groups of mice (see **B**). (***, $P < 0.001$).

4.2.2 Evolution of the percentage of conditioned responses

In addition to field excitatory postsynaptic potential parameters, the experimental approach used here revealed important information after tetanus neurotoxin injection. Interestingly, not only was the rate of acquisition of conditioned responses strongly affected by tetanus toxin activation, but the accessibility to the previously stored information was also disrupted.

4.2.2.1 Recall protocol

The learning rate did not differ between the 3 experimental groups in the first 6 conditioning sessions (**Figure 37**). All of them—control, and animals unilaterally and bilaterally infected with tetanus-toxin virus—reached a level of conditioned responses between 85-89% by the 6th conditioning sessions, and no statistically significant differences were found between them in this initial phase. Doxycycline was injected in all rabbits after the 6th conditioning session, and 2 recall tests were applied, 4 and 14 days after the injection (**Figure 37A**).

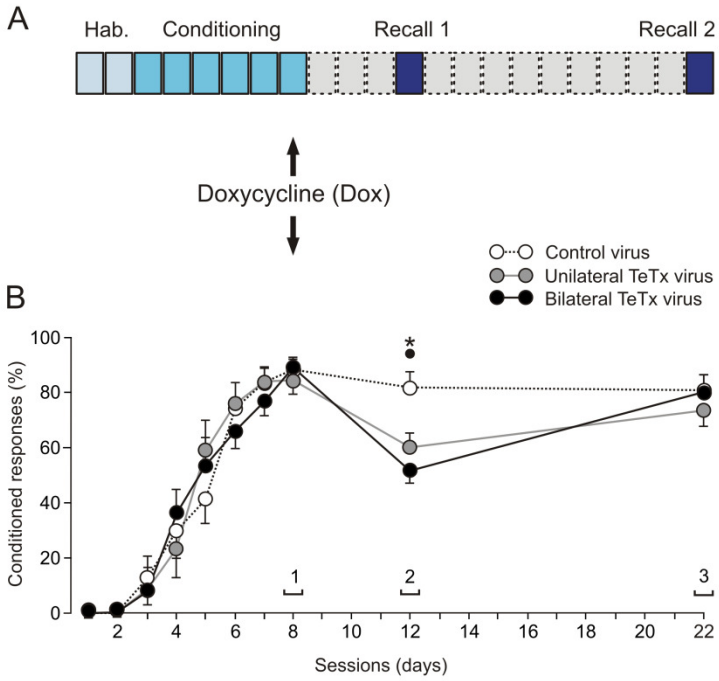

Figure 37 Evolution of the percentage of conditioned responses using a recall protocol. A, Diagram of the experimental protocol, which includes 2 sessions of habituation (Hab.), 6 sessions of conditioning, and 2 sessions of recall 4 (Recall 1) and 14 (Recall 2) days after the last conditioning session. After the 6th conditioning session, a single injection of doxycycline (Dox, 45 µg/g animal weight) was administered i.p. to the three experimental groups: i) Control (white circles); ii) Unilateral TeT virus (injected with the tetanus toxin unilaterally in the hippocampus, gray circles); and iii) Bilateral TeT virus (injected with the tetanus toxin bilaterally in the hippocampus, black circles). **B,** Evolution of the learning curve along the 22 days that the protocol lasted. Note the clear decrease in the percentage of conditioned responses for both tetanus-toxin-injected groups during the Recall 1 session and the complete synaptic recovery during Recall 2. Data shown were collected during the session prior to the Dox injection (1), and to the Recall 1 (2) and Recall 2 (3) sessions. (***, $P < 0.001$).

During the 1st recall session, a significant decrease in the percentage of conditioned responses was recorded for the unilaterally infected group (gray circles), with a reduction of 24%. Even greater was the decrease in the percentage of conditioned responses recorded in the bilaterally infected group (black circles), where the reduction was 37%. In contrast, the control group (white circles) maintained the same level of conditioned responses during recall session 1 as that presented in the last conditioning session. Moreover, the reduction in the percentage of conditioned responses in both infected groups with respect to the control group was statistically significant ($P < 0.05$). Since the control group maintained the level of learning after the

injection, any effect caused by the virus infection, time course, and/or the administration of doxycycline can be ruled out.

Finally, a 2nd recall session was performed 10 days after the 1st recall session to evaluate the level of expression of conditioned responses once the effect of the doxycycline expression was finished and the tetanus neurotoxin was inactivated. In this session, it was found that there were no significant differences between and within groups when comparing the percentage of conditioned responses of the 2nd recall session (marked as 3 in **Figure 37B**) versus the 6th conditioning day (marked as 1 in **Figure 37B**). This result was in agreement with the data previously analyzed from field excitatory postsynaptic potential slopes (**Figure 35**), and it could be concluded that, with the recovery of the field excitatory postsynaptic potential slopes, the previous level of conditioned responses was also recovered, even when a conditioning (recall) session was applied in a disrupted hippocampal system.

4.2.2.2 Over-conditioning protocol

In the over-conditioning protocol (**Figure 38**), after 2 habituation sessions 20 conditioning sessions were applied uninterruptedly to the experimental groups. As already indicated, doxycycline was injected after the 6th conditioning session; before TeTxLC activation, no significant differences were detected between the control (blank circles) and bilaterally (black-filled circles) infected group.

The effect of TeTxLC activation was noticeable in the bilaterally infected group, as was seen with the field excitatory postsynaptic potential slopes in **Figure 36** from the day after doxycycline injection—that is, the 7th conditioning day. On this (7th) conditioning day the level of conditioned responses diminished some 21% with respect to the previous day (6th conditioning day, marked as 1 in **Figure 36**), and this level continued decreasing until it reached a maximum decay of 39% on the 12th conditioning day (marked as 2 in **Figure 36**). Significant differences were found between control and the bilaterally infected group from the 6th conditioning day until the 13th conditioning day ($P < 0.05$), but the conditioned responses of the bilaterally infected group did not reach normal values until the 18th (3 in **Figure 36**) conditioning session, and no differences were found on the 22nd conditioning day, either between or within groups, with respect to the 6th conditioning day (1).

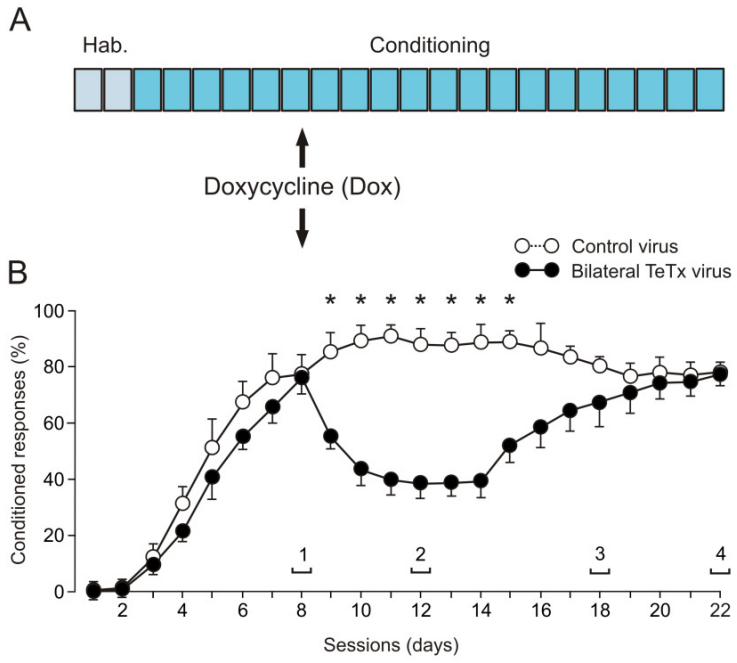

Figure 38. Evolution of the percentage of conditioned responses using an over-conditioning protocol. A, Diagram of the experimental protocol, which includes 2 sessions of habituation (Hab.) and 20 consecutive days of conditioning sessions. After 2 habituation days and 6 conditioning sessions, a single injection of doxycycline (Dox, 45 µg/g animal weight) was administered i.p. to the 2 experimental groups: i) Control (white circles); and ii) Bilateral TeT virus (injected with the tetanus toxin bilaterally in the hippocampus, black circles). **B,** Evolution of the learning curve along the 22 days that the protocol lasted. Note the clear decrease in the percentage of conditioned responses for the injected group that recovered 8 days after the Dox injection. Data shown were collected during the sessions prior to the Dox injection (1), and during the Recall 1 (2) and Recall 2 (3) sessions. (***, $P < 0.001$).

This is a situation similar to that observed with the field excitatory postsynaptic potential slope recordings in **Figure 36,** where there is a period of field excitatory postsynaptic potential slope decrease after doxycycline injection in the bilaterally infected group, and total stability is not observed in this parameter until the 18th conditioning day.

4.2.3 Electromyography recordings of the orbicularis oculi muscle

Examples of orbicularis oculi electromyographic recordings from the animals included in the 2 training protocols (recall and over-conditioning) used here are shown in **Figure 39**. Some traces obtained during the recall protocol are displayed in **Figure 39A**: from top to bottom are represented the control (white circles), the unilaterally infected with tetanus toxin virus (gray circles), and the bilaterally infected with tetanus toxin virus (black circles) groups. Traces marked as 1 were taken from the last session of conditioning (6th session) and before the doxycycline injection, while traces marked as 2 and 3 correspond to the first and second recall sessions, respectively; as is indicated in the upper diagram of **Figure 39A**.

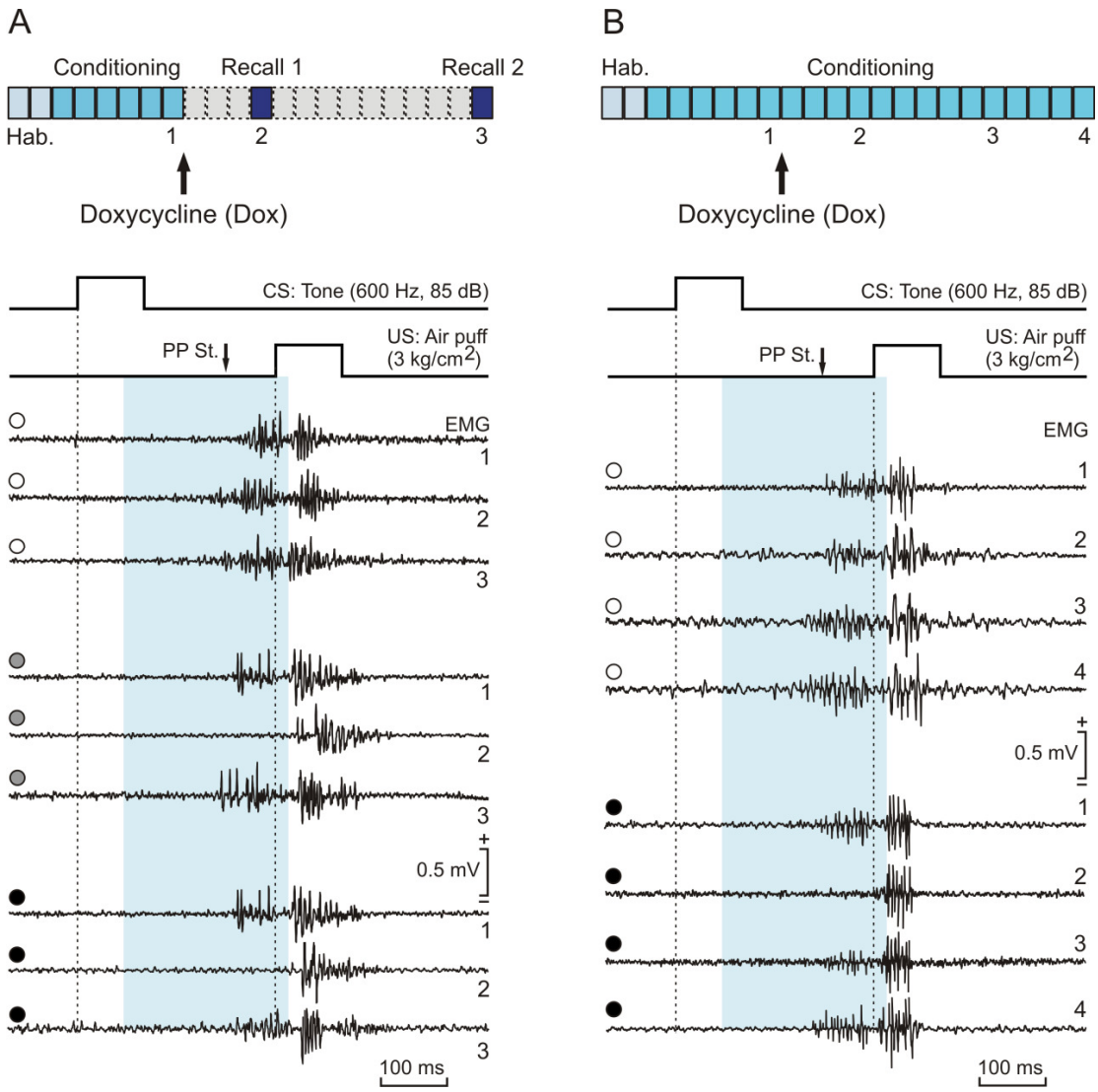

Figure 39. Electromyography recordings of the orbicularis oculi muscle in the different experimental groups. On the left (**A**) are shown the traces of control (white circles), and unilaterally infected (gray circles) and bilaterally infected (black circles) animals that followed the discontinuous protocol. The numbers to the right of these traces indicate the session—that is, 1 is the 6th conditioning session, 2 the 1st Recall session (4 days after doxycycline injection), and 3 the 2nd Recall session. On the right (**B**) are shown traces from animals that received the continuous protocol; briefly, white circles for control animals and black circles for bilaterally infected animals. In this case, the first 2 traces (numbered 1 and 2) of each animal are taken from the 4th session after doxycycline administration, and the second 2 traces (numbered 3 and 4) from the last session, in which no effects of doxycycline can be observed.

Figure 39B illustrates orbicularis oculi electromyographic traces from rabbits participating in the over-conditioning protocol. From top to bottom are displayed the control (white circles) and the bilaterally infected with tetanus toxin virus (black circles) groups. Traces marked as 1 were taken from the last conditioning session (6th session) and before the doxycycline injection; responses marked as 2, 3, and 4 correspond to the conditioning sessions 10, 16, and 20, corresponding to 4, 10, and 14 days, respectively, after the doxycycline injection, as indicated in the upper diagram of **Figure 39B**.

The profile of conditioned responses in the case of the control group was completely normal even after doxycycline injection (**Figure 39A, B**, 2 in the white circles), and the reflex responses were not affected by this inductor. A different situation was found in the case of unilaterally and bilaterally infected groups for recall and over-conditioning protocols (**Figure 39A, B**, 2 in the gray and black circles). In these groups, there was a reduction or even a complete disappearance of the conditioned response following doxycycline injection. Importantly, in all cases the reflex response was preserved.

4.2.4 Pre- and postsynaptic markers

The correct delivery of tdTOM/TeTxLC was assessed via immunohistochemistry and subsequent confocal microscopy, as can be seen in **Figure 40**. The expression of tdTOM/TeTxLC vector reached the expected levels (as shown in A: from left to right, td-tomato labeling infected tissue in CA3 region, a merger of VGLUT1 and CAMKII labeling, synaptic buttons of mossy fibers and their co-localization with PSD95 and CAMKII proteins). We focused on the quantification of proteins in the CA3 region, specifically in the portion in which the mossy fibers that come from the granule cells establish their synaptic connections. The quantification was performed for control animals (**Figure 40E**: from left to right, microphotographs of VGLUT1, td-tomato, and the resulting merge. The results of animals infected with the tetanus-toxin-expressing virus are shown in F, with the same structure as in the control case). An identical procedure was applied in the study of PSD95 in controls (**Figure 40G**) and animals infected with the tetanus-toxin-expressing virus (**Figure 40H**). This approach showed that the presynaptic protein VGLUT1 (**Figure 40I**), and the postsynaptic protein PSD95 (**Figure 40J**) were expressed at a significantly lower level in the Tet group than in the control group ($P < 0.05$).

Figure 40. Immunohistochemical confirmation of tetanus toxin effects. The correct delivery of tetanus toxin and fluorescent markers was assessed by immunohistochemistry and confocal microscopy. Microphotographs of CA3 subregion are displayed in **A,** showing (from left to right) td-tom labeling due to viral infection, a merge with td-tom VGLUT1 and CAMKII labeling, synaptic buttons of mossy fibers and the co-localization of mossy fibers synaptic buttons, PSD95 and CAMKII proteins. Our region of interest was CA3 (**B**), where mossy fibers coming from granule cells (**C,D**) establish their synaptic connections. In this region we quantified the level of the presynaptic protein VGLUT1 in animals infected with the Control Virus (Control, in **E**) and with the virus that expresses the tetanus toxin (Tet, in **F**). A comparison between E and F shows a decrease in VGLUT1 levels (left), with a similar degree of infection (center), and that VGLUT1 levels are lower in the presence of tetanus toxin (right). Similar results were found with the postsynaptic marker PSD95 (**G** and **H**), with lower levels of protein in Tet than in Control (left), reaching similar levels of infection (center) and a smaller co-localization between mossy fibers of Tet group animals with respect to controls. Differences were significant for both markers between the Control and Tet groups, as can be observed in I (VGLUT1) and J (PSD95). *, $P < 0.05$ (Student's *t*-test).

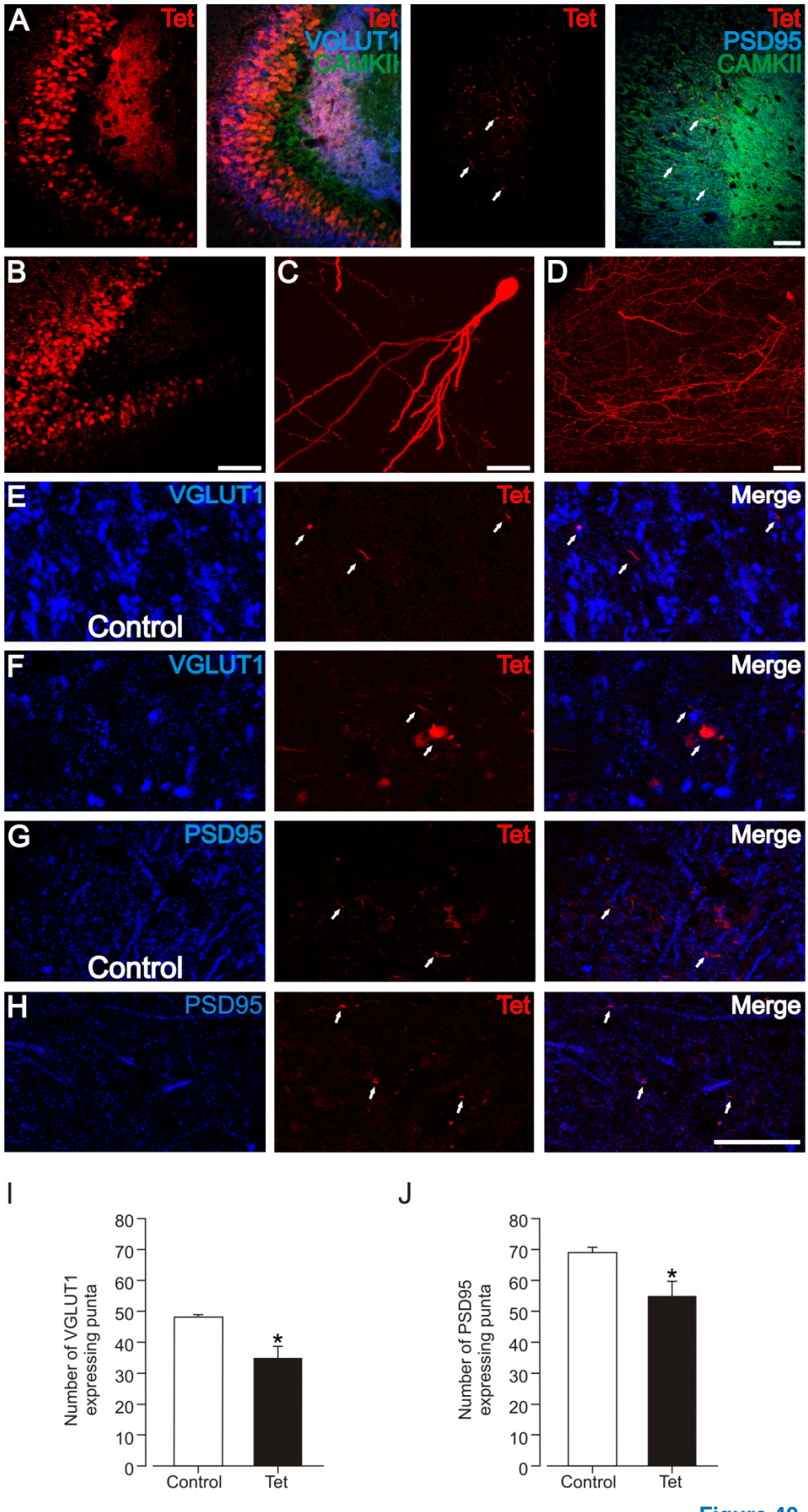
A
Tet
Tet
VGLUT1
CAMKII
Tet
Tet
PSD95
CAMKII
B
C
D
E
VGLUT1
Control
Tet
Merge
F
VGLUT1
Tet
Merge
G
PSD95
Control
Tet
Merge
H
PSD95
Tet
Merge
I
Number of VGLUT1 expressing punta
80
70
60
50
40
30
20
10
0
Control
Tet
*
J
Number of PSD95 expressing punta
80
70
60
50
40
30
20
10
0
Control
Tet
*

Figure 40

4.2.5 Histological confirmation of implanted sites

After the end of the experiments, all animals were perfused and the final position of the electrodes was confirmed. **Figure 41** shows the final position for a stimulating (black-filled circles) electrode in the perforate pathway (left) and for a recording (blank circles) electrode in the CA3 area (right). Electrodes found to be outside the corresponding area were ruled out for subsequent analysis. The obtained brain slices were stained using the Nissl protocol with blue Toluidine colorant.

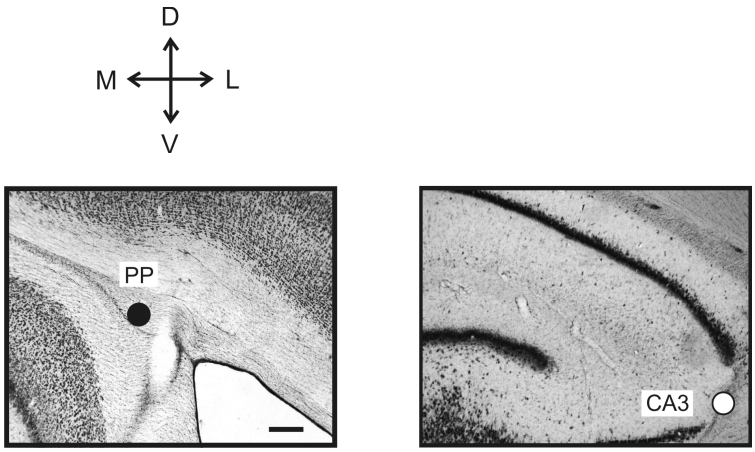

Figure 41. Histological confirmation of electrode positions. Photomicrographs illustrating the final location of implanted electrodes, with indication of recording (white circles) and stimulating (black circles) sites. Calibration bar is 1 mm. Abbreviations: D, L, M, V, dorsal, lateral, medial, ventral; PP, perforant pathway.

5. DISCUSSION

5.1 DIFFERENT PATHWAYS FOR DIFFERENT LEARNING SITUATIONS

Confirming some previous data and contentions (Delgado-García and Gruart, 2002), the present results suggest that a specific functional synaptic state corresponds to each learning protocol and training session. In particular, direct projections from the entorhinal cortex to the three main neuronal elements of the hippocampal intrinsic circuit (i.e., PP-DG, PP-CA3, and, to a lesser degree, PP-CA1 synapses) seem to be mostly involved in general and/or contextual aspects of the training situation, while those synapses integrating the intrinsic circuit (DG-CA3, CA3-CA1, and CA3-cCA1) are preferentially involved in aspects related to the salience or predictive value of the conditioned stimulus and/or associative strength of conditioned and unconditioned stimuli (Rescorla, 1988; Eichenbaum, 1999; Múnera et. al., 2001). **Figure 42** represents in a diagrammatic form these two important functional differences and the specific roles of hippocampal inputs (context and pseudoconditioning, **Figure 42A**) and of the hippocampal intrinsic circuit (trace and delay conditioning, **Figure 42B**).

The separation of functions between entorhinal projections to the hippocampus and hippocampal synapses present in its intrinsic circuit reported in this thesis has already been proposed on both theoretical (Marr, 1971; McNaughton and Morris, 1987; Treves and Rolls, 1994) and experimental (McHugh et al., 2007; McHugh and Tonegawa, 2009; Nakashiba et al., 2012) grounds.

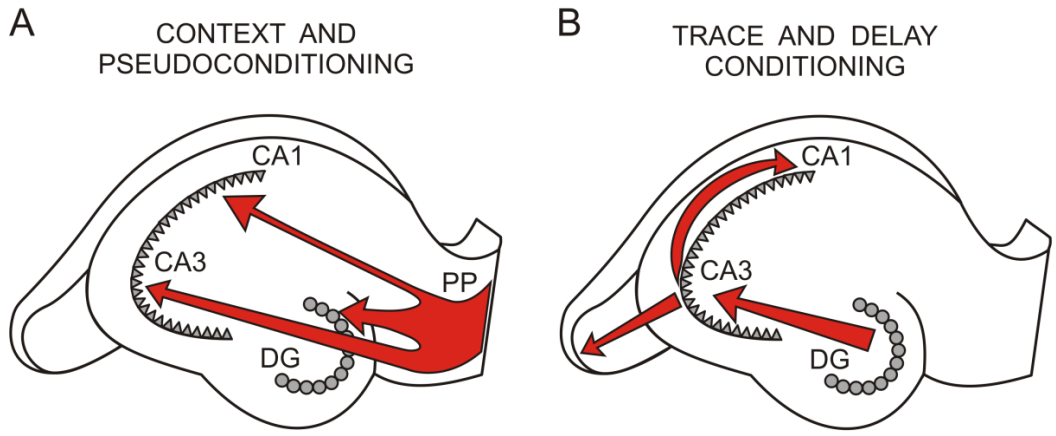

Figure 42. A diagrammatic representation of the major changes in synaptic strength taking place in the hippocampus. It was found that during context and pseudoconditioning (**A**), the biggest variations in the field excitatory postsynaptic potentials were in the perforant pathway (PP) projecting into dentate gyrus (DG), CA3, and CA1. During the trace and delay conditioning (**B**), the greatest changes in synaptic strength were found in the intrinsic circuit. The line thickness is proportional to the size of the modification in synaptic strength.

5.1.1 Perforant pathway and contextual information

In accordance with the present results, direct projections from the entorhinal cortex to dentate granule neurons and to hippocampal CA3 and CA1 pyramidal cells carry memory information related to general environmental aspects, places, and other spatial-temporal details and configurations (**Figure 42A**). Moreover, the weight in the learning and memory role is directly proportional to the amount of fibers in the different sub-pathways. Fibers from the perforant pathway to the dentate gyrus seem to assume a major role in defining the contextual information, while the ones projecting to the CA3 area and, mainly, those going to the CA1 area, have less relevance in this activity. The proportionally large number of dentate granule neurons can allow the proper separation of these sensory-motor and cognitive memories. Those incoming entorhinal patterns of activity not involved in Hebbian association processes (Kornorski, 1948; Hebb, 1949) will be erased and/or blocked at these three (PP-DG, PP-CA3, and PP-CA1) hippocampal synapses. Similar filtering and/or erasing roles have already been proposed for the dentate gyrus (Hsu, 2007; McHugh et al., 2007; Nakashiba et al., 2012) and the hippocampal CA3 (McHugh and Tonegawa, 2009) and CA1 (Izumi and Zorumski, 2008) areas.

Information transmitted through the perforant pathway has been studied with some detail since these fibers, originated at the entorhinal cortex, have been signaled as an essential structure for memory formation. The rat parahippocampal region is a homolog of the primate and human medial temporal lobe and it includes the entorhinal, the perirhinal, and the postrhinal cortices. It seems that its function could be to mediate the cortical input and output of the hippocampus (Furtak et al., 2007). Lesions of the perirhinal or postrhinal cortex severely impair the proper conditioning of the corneal reflex with a trace paradigm, while lateral entorhinal lesions do not (Suter et al., 2013). Those authors concluded that direct projections from the perirhinal cortex to the hippocampus are relevant to the acquisition of trace conditioning paradigms, and that this region could have a role for persistent spiking in time-bridging associations (Suter et al., 2013).

The entorhinal cortex has a crucial role in cortico-hippocampal bidirectional interactions. Nonetheless, substantial differences in the cortical, subcortical, and hippocampal connections of the lateral and medial entorhinal areas indicate that their functions in the processing of information could be different (Hargreaves et al., 2005; Hafting et al., 2005; Kerr et al., 2007). From functional studies, neurons of the medial entorhinal area contribute spatially specific information, whereas neurons of the lateral entorhinal area show considerably less spatial specificity. Such findings are consistent with the anatomy, since the lateral part receives more input from the piriform cortex and

insular regions and less from the visual, posterior parietal. In addition, the lateral entorhinal areas receive a considerable input from the amygdala and olfactory structures (Kerr et al., 2007).These inputs may play a role in providing non-spatial information about context, including its emotional significance. In contrast, the medial entorhinal part receives a much heavier input from visual association, posterior parietal, and cingulate cortices (Kerr et al., 2007). This afferent organization is consistent with studies showing that neurons in this medial entorhinal area encode spatial information (Hargreaves et al., 2005; Hafting et al., 2005). In our experiments in rabbits, we could not differentiate between fibers in the lateral or medial area in the entorhinal cortex, but we did find similar differences in the projections of the perforant pathway axons. A clear relationship with the contextual clues was found in the synapses between the perforant pathway and the dentate gyrus. In contrast, the changes in synaptic strength were not so evident during pseudoconditioning or during classical conditioning using a delay paradigm.

Experiments done in rats have shown that the dentate gyrus combines the medial and lateral perforant pathway inputs to generate a spatial representation (Hunsaker et al., 2007). Moreover, information arriving by the lateral perforant pathway is used to identify the visual objects occupying specific spatial locations. The reported results suggest that the medial and lateral perforant pathway inputs to CA3 are combined to generate a spatial representation of the visual objects together with their spatial locations. In contrast, the same inputs into the CA1 area are not mixed. It seems then that the dentate gyrus and the CA1 and CA3 areas receive information from the medial and the lateral pathways with a different role in learning and memory processes, which can be dissociated using different behavioral tasks (Kesner, 2013). Similar results were found in human subjects using high-resolution functional magnetic resonance imaging (fMRI) during a mnemonic discrimination between object identity or object spatial localization (Reagh and Yassa, 2014). Consistent with results collected from animal models, Reagh and Yassa (2014) have shown the presence of a domain-selective dissociation between lateral and medial entorhinal cortex, and between perirhinal and parahippocampal cortices as a function of information content. In their study they showed that hippocampal dentate gyrus and CA3 area present changes in activity consistent with resolution of mnemonic interference across different domains.

Silencing the dentate gyrus or the CA3 area in mice produced different effects in a contextual fear conditioning, suggesting divergent roles between these two hippocampal areas (Denny et al., 2014). The dentate gyrus seems to be involved in intermediate phases of the learning process, while the CA3 area seems not to be, probably because the memory trace is no longer in the hippocampus. In present results,

the synapses between the perforant pathway and the dentate gyrus showed the largest differences in the slope of field excitatory postsynaptic potentials during the context situation. Mild changes in the same synapses were found during the trace conditioning paradigm, but not during the pseudoconditioning or the delay conditioning paradigm. Interestingly, no significant changes in strength were found in the synapses between the perforant pathway and the CA3 area.

The contextual information was also studied in an experiment carried out with adult mice kept for a month alone, alone in a physically enriched environment, or in groups in the absence or presence of an enriched environment (Madroñal et al., 2010). When trained for eyeblink classical conditioning with a trace paradigm, the four groups of mice presented similar increases in the strength of field excitatory postsynaptic potentials evoked at the hippocampal CA3-CA1 synapse across the conditioning sessions, with no significant differences between groups. These results are in agreement with the idea that the context and environmental cues are mainly analyzed in the perforant pathway, while CA3-CA1 synapses could have a secondary role in this task. The change in synaptic strength of the CA3-CA1 synapse across the conditioning sessions with the trace paradigm in rabbits was smaller than the one recorded in mice (Madroñal et al., 2010; Gruart et al., 2014).

Changes in the hippocampal activity due to context and environmental parameters have been recorded not only in the field excitatory postsynaptic potentials, as in the present Doctoral Thesis, but also in the dominant frequencies observed in local field potentials. Previous experiments allowed concluding that a high level of hippocampal gamma rhythm could indicate a more aroused or attentive state and this could evoke a more efficient learning process (Berry and Thompson, 1978; Nokia et al., 2009; Nokia et al., 2012). However, effects of gamma-triggered training could also depend on the task and on the context where it is developed. Moreover, any distinguishable spontaneously generated (hippocampal) oscillatory state can affect learning by setting the stage for excitatory versus inhibitory responding at the neural and behavioral levels, and perhaps also by serving as an additional cue or context for learning (Nokia and Wikgren, 2014). The patterns traditionally defined as hippocampal gamma may actually comprise separate gamma subtypes with distinct frequencies and unique functions (Colgin, 2015).

5.1.2 Hippocampal trisynaptic circuit and stimuli information

Synapses involved in the hippocampal intrinsic circuit (represented here by the DG-CA3, CA3-CA1, and CA3-cCA1 synapses) could play a discriminating role, reinforcing Hebbian association between relevant environmental stimuli (Vinogradova, 2001; Hsu,

2007), such as, for example, that taking place between the conditioned and unconditioned stimuli presented in a paired form during both trace and delay paradigms. It has been proposed that this selective role of the hippocampal intrinsic synapses will be supported on the dense network of axon collaterals reaching both CA3 and CA1 pyramidal neurons (Lorente de Nó, 1933, 1934; Marr, 1971). Currently, it is assumed that these recurrent connections will probably help to determine the conditioned-stimulus cognitive salience and/or the associative strength between conditioned and unconditioned stimuli. This conceptual approach to hippocampal functions is further supported by data provided in the present Doctoral Thesis (**Figure 42B**).

Some changes in the strength of synaptic activation of dentate granule cells by perforant pathway axons during the acquisition of nictitating membrane - conditioned responses in behaving rabbits had already been suggested some years ago by Weisz et al. (1984). This activity-dependent modulation in synaptic strength was further confirmed for the CA3-CA1 synapse in behaving mice, and extended to the extinction process (Gruart et al., 2006), suggesting that the two phenomena are equally active (Dudai, 2012). It has also been shown that changes in synaptic efficacy evoked in the hippocampal CA3-CA1 synapse present a linear relationship with the amount of acquired, or extinguished, learning (Gruart et al., 2006). The increase in slope of field excitatory postsynaptic potentials during the acquisition process explains the increased firing in hippocampal CA1 areas across conditioning described for both rabbits (McEchron et al., 2003) and cats (Múnera et. al., 2001).

The involvement of hippocampal unitary activity in the classical conditioning of the nictitating membrane/eyelid responses was reported years ago (Berger et al., 1983; Moyer et al., 1990). Hippocampal pyramidal cell firing to conditioned stimulus presentation increases several sessions in advance of behavioral conditioning (McEchron and Disterhoft, 1997). Although it has been shown that the discharge rate of hippocampal CA1 pyramidal neurons does not encode the kinematic peculiarities of conditioned eyelid responses (Múnera et al., 2001; Sánchez-Campusano et al., 2007), discharge rates of CA1 pyramidal cell firing appear linearly related to the progressive acquisition of conditioned responses, with a gain of approximately 0.035 spikes/s/trial, as measured in behaving cats during trace conditioning (Múnera et. al., 2001). It is of note that this slow building up of hippocampal neuronal firing responses across conditioning sessions is similar to the maximum increases in field excitatory postsynaptic potential slopes evoked in the six synapses included in this Doctoral Thesis (i.e., 0.03-0.04% of increase in the slope of field excitatory postsynaptic potential per trial). A similar increase in the slope of the field excitatory postsynaptic potential slopes recorded in the CA3-CA1 synapse during trace (tone-shock) conditioning of

behaving mice has also been reported (Gruart et al., 2006). Taken together, these results suggest that changes in neuronal firing rates across conditioning sessions are more-or-less related to the underlying changes in synaptic efficacy and/or strength.

Although it has been pointed out (Moyer et al., 1990) that 250-ms trace conditioning is not dependent on the hippocampus in the rabbit, results collected in this Doctoral Thesis convincingly show that hippocampal circuits are also modified by this type of associative learning task. Múnera et al. (2001) found in cats that changes in the firing rates of pyramidal neurons in CA1 and CA3 areas along conditioning sessions were independent of the type of conditioned stimulus (tone or mild air puff), of the conditioning paradigm (trace or delay), and of the kinematics of conditioned eyelid responses. In all the combined situations, the firing rate of the recorded neurons increased after conditioned-stimulus presentations and decreased after unconditioned-stimulus presentations, along the ten conditioning sessions. Moreover, the decrease in synaptic strength taking place in different recording sites in both input and intrinsic hippocampal synapses could be related to the recently reported increase in the intrinsic excitability of hippocampal interneurons (McKay et al., 2013).

In a recent review on the neural circuitry underlying delay and trace eyeblink conditioning in mice, Yang et al. (2015) propose that each paradigm are maintained by two different circuits. The structures responsible for the delay paradigm include the brainstem-cerebellar circuit, while the amygdale modulates this path and the medial prefrontal cortex is the main structure of the extra-cerebellar circuit. In the case of the trace eyeblink conditioning, an essential role is played by forebrain regions, whereas the cerebellar cortex seems to be out of the neural circuitry involved. The hippocampal role in both paradigms is to be an interface between the sensory cortex and the medial prefrontal cortex. The general idea proposed in mice is partly supported by data presented in this Doctoral Thesis.

5.2. DIFFERENT SITUATIONS AND DIFFERENT SYNAPTIC STATES

The results presented in this Doctoral Thesis suggest that selected hippocampal synapses in the main afferent inputs and intrinsic circuit are involved in selective processes related not only to the acquisition and extinction of different forms (trace and delay) of classical eyeblink conditioning, but also to more-general aspects of the leaning situation —namely those related to environmental constraints and to the unpaired presentations of conditioned and unconditioned stimuli. The six different hippocampal synapses included in this study underwent a slow algebraic modulation (i.e., increase or decrease) in synaptic strength (Kornorski, 1948; Hebb, 1949) across the different

training situations in parallel with the acquisition and extinction of conditioned eyelid responses and/or the mere repetition of sessions (context and pseudoconditioning).

Interestingly, changes in synaptic weights did not take place simultaneously in the six selected synaptic sites nor were similar absolute changes in strength presented across the successive training sessions. Obviously, this new picture of differential plastic changes taking place in different hippocampal synapses in a given experimental situation and in a precise moment across the training situation would be impossible to observe in only one selected synapse (Weisz et al., 1984; Gruart et al., 2006; Whitlock et al., 2006).

It has already been proposed (Delgado-García and Gruart, 2002) that learning is a precise functional state of the brain, and that we should take a dynamic approach to the study of neural and synaptic activities in ensembles of sensorimotor circuits during actual learning in alert behaving animals. An example has been shown in the present work: the significantly different synaptic weights presented by the six selected hippocampal synapses on the same training days, but in four different conditioning situations (i.e., context, pseudoconditioning, and trace and delay conditioning paradigms). In general, it can be proposed that each environmental and social situation demanding a behavioral response will evoke a corresponding differential state of synaptic weights in hippocampal circuits. Additional neural, synaptic, and motoric information can be collected experimentally and added for a better determination of ongoing functional states. For example, and with regard to classical eyeblink conditioning, it has already been reported that facial motoneurons present two specific functional states corresponding to their firing activities during reflexively evoked blinks and to their discharge rate during acquired (i.e., classically conditioned) eyelid responses (Delgado-García and Gruart, 2006). However, it is important to point out that current information with regard to brain functioning during a given learning situation is greatly constrained by the difficulty of recording a large enough number of kinetic (i.e., firing and synaptic activities of neuronal elements) and kinematic (i.e., biomechanical characteristics of evoked motor responses) parameters in simultaneity with the newly acquired motor and/or cognitive ability (Delgado-García and Gruart, 2002).

To resolve these constraints, it seems necessary to record enough different neural kinetic data at the same time as collecting data from enough kinematic variables. In a previous study, we were able to collect up to 24 kinetic variables (related to neural firing activities in the facial and cerebellar interpositus nuclei) together with 36 kinematic variables (related to eyelid biomechanics and to the electrical activity of the orbicularis oculi muscle) from alert behaving cats during classical eyeblink conditioning (Sánchez-Campusano et al., 2007). Present results further confirm the above contentions, and

allow a dynamic interpretation of the hippocampal role in learning and memory processes underlying the acquisition of new motor and cognitive abilities, as opposed to an excessively localizationist view of hippocampal functions (McHugh et al., 2007).

The hippocampus will have an almost infinite repertoire of functional states corresponding to the enormous possibilities of sensory stimulations and the different needs of behavioral responses. Thus, and depending on the specific and timed activation of its multiple synaptic contacts, the hippocampus would be involved in many different functions, such as object recognition (Clarke et al., 2010), spatial orientation (Moser et al., 2008), and other different forms of memory acquisition, storage, and retrieval (Bliss and Collingridge, 1993; Neves et al., 2008; Wang and Morris, 2010). The different level of neural activity probably has a molecular correlate. For example, forebrain expression of a strong constitutively active cyclic adenosine monophosphate (cAMP) response element-binding protein (VP16-CREB) showed that the enhanced hippocampal long-term potentiation in response to high-frequency stimulation is not necessarily associated with better performance in hippocampal-dependent tasks. During classical conditioning experiments in mice, changes in CREB activity occur during the acquisition process, but the timing and duration of these changes are tightly regulated and deviation of this sequence is able to disrupt the whole learning process (Gruart et al., 2012).

An example of how learning can be manipulated depending on basal activity was provided by Nokia et al. (2010). They found that the rate of conditioned eyeblink responses in rabbits using a trace paradigm was affected by presenting the conditioned stimuli selectively at a moment when the hippocampus was free from subcortical control. This latter state was monitored with the relative absence of theta rhythm oscillations and an appearance of a sharp wave ripple activity. At such moment the hippocampus is most responsive to external stimulation, resulting in a more synchronized theta-band oscillatory response, probably leading to enhanced information flow between learning-related brain structures. Exploratory behavior (i.e., perception) in rodents is characterized by pronounced theta rhythm in the hippocampal formation with embedded gamma oscillations, while consummatory behavior (i.e., memory storage) is related to the appearance of sharp wave ripple activity (Chrobak and Buzsáki, 1996). The role of the CA3 and CA1 areas of the hippocampus as encoding conditioned stimulus predictive value during classical conditioning was also found in cats (Múnera et al., 2001). Transition between these two states of activity can be rather abrupt and it can be timed when a novel situation requires reorientation, such as sudden changes in the environment or in body state requiring changes of attention and behavior. Moreover, some variability found in hippocampal recordings during the same learning protocol

could be due to the final electrode position or to these basal electrophysiological activities.

5.3 SYNAPTIC STATE IMPAIRMENTS AND DG-CA3 SYNAPSE DISCONNECTION

One of the main aims in this Doctoral Thesis was to test the role of the dentate gyrus, since previous experiments provided some interesting data during the classical conditioning of the eyelid responses. In the hippocampus, granule cells of the dentate gyrus project along the mossy fiber pathway to the area 3 of the cornus Ammonis (CA3). As discussed before, the synapse between the dentate gyrus and the CA3 synapse presents marked changes during trace and delay paradigms. Therefore, the silencing of this synapse during learning should evoke a decrease in the level of both learning and the change in synaptic strength. This approach enabled us to test one of our main interests in this work—that is, to check the most generalized paradigm in the neuroscientific field: that memory storage takes place in the form of molecular changes in synaptic dendritic spines.

Many different neuroscientists have long defended the idea that learning results from changes in synaptic strength, a position suggested by Santiago Ramón y Cajal (1894) based upon his anatomical and histological studies. The proposal that the modulation of synaptic connectivity is the basis of learning and memory processes was incorporated into Hebb's synaptic theory (Hebb, 1949). After these foundational studies, many neuroscientists followed the idea that memories are maintained by persistent molecular and cellular alterations in synaptic structures themselves (Bailey and Kandel, 2008; Kandel et al., 2014). However, until now, no well-defined experimental protocol has been carried out to clearly demonstrate that memory is stored in the synapse itself (Delgado-Garcia and Gruart, 2020; Mayford, et al., 2012).

In this Doctoral Thesis, an attempt has been made to test whether the synaptic contacts between cortical cells are used to store memories. Silencing of the dentate gyrus neurons, using the C fragment of the tetanus neurotoxin six days after the start of conditioning, evoked a decrease in the percentage of conditioned eyelid responses and in the concomitant increase of synaptic strength between the dentate gyrus and the CA3 area. This disruption was found during the first recall session (four days after the silencing session), but it was reverted in the second recall session (fourteen days after the silencing session), i.e., when tetanus neurotoxin effects had disappeared. Similar results were found in the over-conditioning protocol, where the conditioning sessions continued after the silencing session. This capability of recovering the learning level after DG-CA3 synapse disconnection and reconnection suggests that memories are

probably not kept in the synaptic structure, since memory and learning processes are not lost as a result of synaptic restructuring (**Figure 43**).

The main conclusion reached from the present results is that in the normal situation, the boutons of the mossy fibers from dentate gyrus cells are connecting the spines from the apical dendrites of the pyramidal neurons in the CA3 area. All the recorded rabbits reached a considerable percentage of conditioned responses by the sixth conditioning session. In parallel, a significant change (increase or decrease) in the synaptic strength of DG-CA3 synapses could be recorded (**Figure 43A**). After the sixth conditioning session, an injection of doxycycline was given to rabbits previously injected with an adenovirus carrying the genetic elements to generate tetanus neurotoxin expression in dentate granule cells. The silencing of this hippocampal structure produced a disconnection of the DG-CA3 synapses from six to ten days following doxycycline injection. In this period, the number of conditioned responses during a recall session or following conditioning sessions was clearly diminished, at the same time that the synaptic strength was also reduced. Our interpretation of these results is that the boutons from the mossy fibers could be retracted and the synapses between the dentate gyrus and the CA3 area temporarily broken (**Figure 43B**). Interestingly, twenty-two days afterwards (and fourteen after the doxycycline injection) the learning level and the synaptic activity are completely recovered, in both protocols (recall and over-conditioning). In consequence, we infer that the boutons are connecting again to the dendritic spines, but we also assume that these connections are not going to be exactly in the same position as before, so that a considerable degree of synaptic redistribution can be expected (**Figure 43B**).

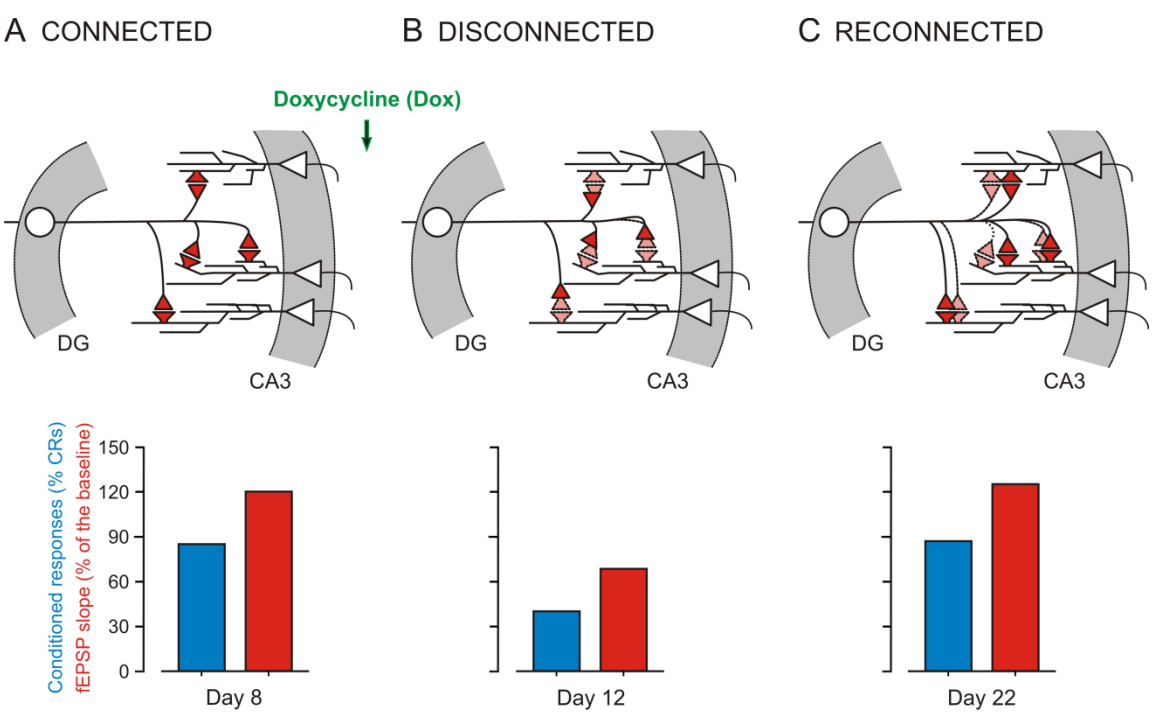

Figure 43. A diagrammatic representation of the changes taking place due to the DG-CA3 synapse disconnection. A, Mossy fiber pathway from granule cells of the dentate gyrus (DG) projects to the dendritic area of the pyramidal cells in the area 3 of the *cornus Ammonis* (CA3). In this connected situation, the percentage of conditioned responses and the percentage of increase in the field excitatory postsynaptic potentials (fEPSPs) on day 8 of training. **B,** After doxycycline injection, the level of learning and the level of change in synaptic strength decrease significantly by day 12 of training. It is assumed that due to the tetanus toxin effect, the boutons from the dentate gyrus pathway could be disconnected from the dendritic spines. **C,** Finally, when the silencing effects of the tetanus toxin end, reconnection can take place. On day 22 of training, the percentages of learning and of changes in synaptic strength resemble the levels obtained before the silencing by tetanus toxin.

The tetanus neurotoxin belongs to the family of clostridial neurotoxins. It can produce a motor tetanus, which is characterized by spastic paralysis due to a tetanus-neurotoxin-mediated blockade of inhibitory circuits in the spinal cord (Caleo and Schiavo, 2012). Interestingly, the tetanus neurotoxin has been used in various experimental approaches. In the peripheral nervous system, it has been used for characterizing the mechanisms of the retrograde transport of tetanus toxin in motoneurons (Lalli et al., 2003; Deinhardt et al., 2006). The ability of this toxin to undergo retrograde transport and transcytosis has also been exploited for tracing neural circuits and drug delivery in experimental settings (Blisland and Schiavo, 2008). High doses of intrahippocampal tetanus neurotoxin provide a chronic model of temporal lobe epilepsy (Ferecskó et al., 2015).

A low or a high dose of tetanus neurotoxin injected in the lateral rectus muscle of the cat caused functional block of (at low dose) inhibitory synapses only or (at high dose) of both inhibitory and excitatory synapses at the same time in abducens neurons (González-Forero et al., 2003). In a following paper, the same authors demonstrate that

the high dose of the tetanus neurotoxin causes the retraction of a significant proportion of presynaptic boutons, a decrease in the number of gephyrin postsynaptic clusters, and the intensification of postsynaptic membrane remodeling evidenced by increased numbers of clathrin-coated vesicles and pits and the appearance of somatic spines (González-Forero et al., 2004). The inhibitory synaptic retraction could be a consequence of the lower activity in the neuron and or a direct effect of the tetanus neurotoxin. A similar explanation could be given for results obtained here; that is, the tetanus neurotoxin expressed in dentate gyrus neurons could evoke the retraction of presynaptic boutons forming DG-CA3 synapses. Consequently, a decrease in the field excitatory postsynaptic potentials in these synapses should be expected.

In a model of chronic epileptic syndrome, unilateral tetanus toxin injections carried out into dorsal hippocampus showed a reduction in the amplitude of postsynaptic evoked responses around 16 weeks after the injection (Jefferys et al., 1992). Moreover, cognitive and other behavioral impairments persisted after the evoked seizures. Interestingly though, no significant loss of pyramidal neurons was found in the CA1 and CA3 areas. In the present model, although no seizures or pathological oscillations in the hippocampal recordings were found, we did observe some molecular changes at the level of synaptic contacts. Nevertheless, it can also be concluded that there were no substantial changes in the number of neurons, as rabbits recovered the same learning capabilities a few days after the inactivation of tetanus toxin effects.

It is widely accepted that specific molecular changes underlie long-term synaptic plasticity and that they play an important role in the plastic changes taking place during memory storage and retrieval (Mayford et al., 2012). However, a strong degree of conservation of memory mechanisms has also been found in different brain regions. Therefore, it is possible that the synaptic changes in efficacy are not sufficient and other types of functional (or structural) change could be expected at different levels of cortical and subcortical circuits.

To compare cells activated during encoding and during expression of memory, Denny et al. (2014) created a transgenic mouse line. They found that mice tested in a fear-conditioning task had a greater percentage of re-activated cells in the dentate gyrus and CA3 area than did mice exposed to a novel context. They also observed that these differences disappeared with time. The experiments carried out with rabbits in the present Doctoral Thesis were designed to record neuronal and behavioral changes during long periods of time, since classical conditioning takes around ten days to be acquired. The classical conditioning of eyelid responses enables a better identification of the different memory phases. Similarly to our approach, Denny et al. (2014) silenced the dentate gyrus or the CA3 cells, although they used optogenetic tools. They found

that this inactivation prevented expression of the corresponding memory. It also seems that the stimulation of a specific population of dentate gyrus cells recruited during memory encoding is sufficient to elicit partial expression of the corresponding memory (Lie et al., 2012).

An interesting finding in the work of Denny et al. (2014) is that of a given collection of activated cells, only a reduced percentage can be devoted to a particular memory trace (e.g., fear conditioning). It could also be that the memory traces have already moved out of the hippocampus. Results from different studies are not conclusive about the period in which the hippocampus can keep memory retrieval and expression (Winocur et al., 2009; Frankland et al., 2006). Results from Denny et al. (2014) suggest that the dentate gyrus and CA3 could have different cell recruitments. The dentate gyrus seems still involved in intermediate phases of the learning, while the CA3 area seems not, probably because the memory trace is no longer in the hippocampus. In the present experiments, only the dentate gyrus was silenced, and it was found that the inactivation could be reverted at the same level as before the silencing period.

A key question still unsolved in this Doctoral Thesis is: what type of morphological or structural changes take place in the synapses during the silencing? The decrease of changes in synaptic strength recorded during the period the tetanus toxin is acting should include some changes in the synaptic structure, which can be reversed once the toxin is removed and has no further effects. Some new insights have come from a study done in the marine mollusk *Aplysia californica* (Chen et al., 2014), using the sensitization of the gill- and siphon-withdrawal reflex—that is a form of learning whose cellular and molecular substrates are particularly well understood (Kandel, 2001; Glanzman, 2010). The main conclusion those authors reached is that the persistence of sensitization-related long-term memory does not require the persistence of the synaptic connections generated during learning (Chen et al., 2014). It seems that the long-term memory appears to be regulated by a homeostatic mechanism that specifies the net synaptic strength according to experience. These ideas are fully in agreement with the results found in the present experiments and with the proposal that learning is a complex process that includes different circuits depending on the animal's state, environmental and context constraints, and task paradigms.

Experiments carried out in *Aplysia* showed that neither reconsolidation blockade nor inhibition of Mx-interacting protein kinase (PKM) caused the varicosity number to drop below the starting value (Chen et al., 2014) or to change the excitatory postsynaptic potential values (Cai et al., 2011, 2012). Probably, the homeostatic mechanism toggles between these two all-or-none states, a facilitated, sensitization-

related state and a non-facilitated one, similarly to the results collected in the mammalian central nervous system (Turrigiano, 2007). However, all of these arguments are in conflict with the findings of scientists studying morphological changes during long-term memory in mice, who found that dendrites chronically imaged in the intact, living brain are modified by experience. Many of these studies showed stability of some dendritic spines for periods of weeks-to-months after training (Xu et al., 2009; Yang et al., 2009; Liston et al., 2013). The spines in the adult mammalian cortex also have little turnover (Grutzendler et al., 2012). For all these arguments, stable spines were proposed as a good physical basis for lifelong maintenance of memories (Bhatt et al., 2009), although other studies of the mouse brain using similar in vivo imaging techniques have reported a high degree of spine instability in the cerebral cortex of adult mammals (Trachtenberg et al., 2002; Holtmaat et al., 2005).

Since chelerythrine disruption of long-term memory in *Aplysia* is blocked by TSA, chelerythrine antimnemonic actions must involve histone deacetylation. Some studies have speculated on how chelerythrine and the zeta inhibitory peptide (ZIP) disrupt memory maintenance in both *Aplysia* and rats, and have focused on the ability of these pharmacological agents to inhibit the phosphorylation of proteins by atypical PKM (Cai et al., 2011; Sacktor, 2011). The failure to re-establish conditioned taste aversion could be because the unconditioned stimulus was too weak to reverse the disruptive effects of ZIP on mechanisms of long-term memory expression, and probably not because this memory was extinguished (Cai et al., 2011; Chen et al., 2014).

The persistent action of the protein kinase Mzeta (PKMζ) could be necessary for the maintenance of synaptic potentiation induced after learning. To test this, ZIP was used during eyeblink conditioned mice. PKMζ inhibition in the hippocampus disrupted both the correct retrieval of conditioned responses and the experience-dependent persistent increase in synaptic strength observed at CA3-CA1 synapses (Madroñal et al., 2010). Moreover, the effects of ZIP in the same associative test were examined when experimentally evoked long-term potentiation was induced at the hippocampal CA3-CA1 synapse before conditioning. PKMζ inhibition reversed tetanic long-term potentiation effects and prevented the expected long-term potentiation of deleterious effects on eyeblink classical conditioning. Therefore, PKMζ inhibition in the CA1 area is able to reverse both the expression of trace eyeblink conditioning memories and the underlying changes in CA3-CA1 synaptic strength, as well as the anterograde effects of the long-term potentiation on associative learning.

The longitudinal visualization of molecular remodeling of the dendritic spines in rat hippocampal organotypic cultures after a long-term potentiation protocol could give some insights about possible changes during actual learning (Bosch et al., 2014). The

authors of that study found that proteins translocated to the spine in four distinct patterns through three sequential phases. In the initial one, the actin cytoskeleton was rapidly remodeled while active cofilin was massively transported to the spine. In the stabilization phase, cofilin formed a stable complex with F-actin, was persistently retained in the spine, and consolidated spine expansion. In contrast, the postsynaptic density was independently remodeled, because postsynaptic density scaffolding proteins did not change in amount and location until a late protein-synthesis-dependent third phase. It is remarkable how the dendritic spine undergoes such a complex spatiotemporal reorganization.

5.3.1 Future prospects

Recent experiments have been designed to elucidate the nature of the synaptic changes during the DG-CA3 synapse disconnection (Hasan et al., 2014). A method called virus-delivered inducible silencing of synaptic transmission (vINSIST) was developed and applied. This method is based on a novel destabilized tetanus toxin light chain variant (dsTeTxLC) with a very short half-life (roughly 3 min for the new variant instead of 6 days for the original one). The steady-state levels of dsTeTxLC are more than 2000-fold lower than the original TeTxLC. Recombinant adeno-associated viruses (rAAVs) were also developed equipped with chemically-controlled genetic switches for inducible and reversible expression of the dsTeTxLC in the dentate gyrus granule cells of rabbits.

Rabbits were trained in a trace eyeblink conditioning consisting of a tone followed by an air puff to the cornea of the eye with a 500 ms temporal interval. This training resulted in robust memory formation for the conditioned eyeblink response to the tone when presented alone. In vivo electrophysiological recordings of field potentials at the DG-CA3 synapse during trace conditioning sessions, lasting several days, showed learning-dependent increases in field excitatory field potential slopes in parallel with the increase in the percentage of conditioned responses. After carrying out classical conditioning with a trace paradigm, we specifically silenced synaptic transmission of the dentate gyrus mossy fiber input onto CA3 neurons.

As expected, conditioned eyeblink responses to a tone were impaired after silencing of synaptic transmission at the dentate gyrus-CA3 synapse, and there were large decreases in the slope of field excitatory postsynaptic potentials. However, after un-silencing the synaptic transmission, we discovered that both field excitatory field potentials and memory retrieval were recovered fully. These results suggest that in spite of prolonged silencing of the synaptic transmission, the previously formed memory trace was not lost. On the contrary, though with a significant decrease in activity for a few

days, the memory trace was fully recovered after un-silencing of the synaptic transmission. Consistent with similar findings in the motor system (González-Forero et al., 2003; 2004), low TeTxLC expression induced a reduction in selected pre- and postsynaptic markers of the DG-CA3 synapse in the hippocampus. Thus, VGlut and PSD95 puncta corresponding to the dentate gyrus mossy fiber boutons and CA3 spines were reduced by more than 30% and 20%, respectively. Preliminary results with long-term imaging of dentate gyrus mossy fiber boutons in organotypic cultures before and after silencing of synaptic transmission show that the distribution of dentate gyrus mossy fiber boutons remains stable throughout a period of several days. Considering the large reduction in VGlut and PSD95 puncta after silencing of synaptic transmission, it is possible that there is a strong reduction in the synaptic machinery. It is thus tempting to speculate that after silencing of synaptic transmission, the memory trace for the conditioned eyeblink response can be re-assessed with a reorganized assembly of synaptic weights. Undoubtedly, this latter statement deserves future experiments.

6. CONCLUSIONS

The present Doctoral Thesis had a double aim: a) to study the role of hippocampal formation circuits in different associative learning situations; and b) to test the generalized proposal that memories are stored as molecular changes taking place in synaptic dendritic spines. For the first aim we used different hippocampal synapses as an experimental model, while for the second aim the synapses between the dentate gyrus and the area 3 of the cornus Ammonis (CA3) were selected because their activity showed significant changes during the learning process using different protocols. To accomplish these two general objectives, different experiments were designed in rabbits, using both electrophysiological and behavioral techniques. The learning test used was the classical eyeblink conditioning. For synaptic silencing we used selective genetic and molecular biology techniques. In order to acquire enough expertise in the use of these techniques, the author of this Doctoral Thesis spent some time in Dr. Hasan's laboratory at Heidelberg (Germany). The main findings of this study are the following:

1. Synapses of the hippocampal formation circuitry (including its main inputs and outputs) have different roles during learning processes depending on the protocol used and on the characteristics of context and stimuli (cues).

2. Direct projections from the entorhinal cortex to dentate granule neurons and to hippocampal CA3 and CA1 pyramidal cells seem to transmit information related to general environmental aspects, places, and other contextual (spatial and temporal) details and configurations.

3. Synapses involved in the hippocampal intrinsic circuit (dentate gyrus-CA3, CA3-CA1, and CA3-cCA1 synapses) could play a discriminating role during associative learning, reinforcing Hebbian association between relevant environmental stimuli.

4. Different functional states (context, stimuli, attention, motivation, pain, etc.) during associative learning would need different neural circuits activated precisely depending on the time and situation.

5. Silencing of the synapses between the dentate gyrus and the CA3 area produced a decrease in the slopes of field excitatory postsynaptic potentials evoked at this synapse, as well as a reduction in the percentage of conditioned

eyelid responses. Interestingly, both parameters were recovered once the inactivation was reverted. Thus, morphological and structural synaptic redistributions seem to have the capability to adapt to new learning constraints.

6. It is possible that memory storage is supported by other morphological and physiological actions apart from changes taking place in cortical synaptic dendritic spines.

7. REFERENCES

Aben, B., Stapert, S. and Blokland, A. (2012). About the distinction between working memory and short-term memory. *Frontiers in Psychology*, *3*, doi: 10.3389/fpsyg.2012.00301.

Aggleton, J.P. (1986). A description of the amygdalo-hippocampal interconnections in the macaque monkey. *Experimental Brain Research, 64*(3), 515-526.

Aggleton, J.P., Vann, S.D. and Saunders, R.C. (2005). Projections from the hippocampal region to the mammillary bodies in macaque monkeys. *European Journal of Neuroscience, 22*(10), 2519-2530.

Albus, J.S. (1971). A theory of cerebellar function. *Mathematical Biosciences, 10*, 25-61.

Amaral, D. and Lavenex, P. (2007). Hippocampal neuroanatomy. In P. Andersen, R. Morris, D. Amaral, T. Bliss and J. O'Keefe. *The Hippocampus Book*. Oxford: University Press.

Andersen, P., Morris, R., Amaral, D., Bliss, T. and O'Keefe, J. (2007). *The Hippocampus Book*. New York (N.Y.): Oxford University Press.

Atkinson, R.C. and Shiffrin, R.M. (1968). Human memory: A proposed system and its control processes. In K.W. Spence and J.T. Spence (Eds.). *The Psychology of Learning and Motivation: Advances in Research and Theory* (Vol. 2). (pp. 89–195 and 742-775). New York (N.Y.): Academic Press.

Baddeley, A.D. and Hitch, G. (1974). Working memory. In G.H. Bower (Ed.), *The Psychology of Learning and Motivation: Advances in Research and Theory* (Vol. 8, pp. 47–89). New York (N.Y.): Academic Press.

Bailey, C.H. and Kandel, E.R. (2008). Synaptic remodeling, synaptic growth and the storage of long-term memory in Aplysia. In W.S. Sossin, J.C. Lacaille, V.F. Castellucci and B. Sylvie (Eds.). *Essence of Memory*. Amsterdam: Elsevier, pp. 179-198.

Barkworth, T. (1891). Some recent experiments in automatic writing. *Proceedings of the Society for Psychical Research, 7*, 23-29.

Barnes, C.A. (1988). Spatial learning and memory processes: the search for their neurobiological mechanisms in the rat. *Trends in Neuroscience, 11*(4), 163-169.

Bhatt, D.H., Zhang, S. and Gan, W.B. (2009). Dendritic spine dynamics. *Annual Review of Physiology, 71*, 261-282.

Becker, J.T., Walker, J.A. and Olton, D.S. (1980). Neuroanatomical bases of spatial memory. *Brain Research, 200*, 307-320.

Berger, T.W., Rinaldi, P., Weisz, D.J. and Thompson, R.F. (1983). Single-unit analysis of different hippocampal cell types during classical conditioning of rabbit nictitating membrane response. *Journal of Neurophysiology*, *50*, 1197-1219.

Berger, T.W., Swanson, G.W., Milnes, T.A., Lynch, G.S., and Thompson, R.F. (1980). Reciprocal anatomical connections between the hippocampus and subiculum in the rabbit: evidence for subicular innervation of region superior. *Brain Research*, *183*, 265–276.

Berger, T.W. and Thompson, R.F. (1978). Identification of pyramidal cells as the critical elements in hippocampal neuronal plasticity during learning. *Proceedings of the National Academy of Sciences (PNAS)-USA*, *75*, 1572-1576.

Berry, S.D. and Thompson, R.F. (1978). Prediction of learning rate from the hippocampal electroencephalogram. *Science, 200*, 1298-1300.

Beylin, A.V., Gandhi, C.C., Wood, G.E., Talk, A.C., Matzel, L.D. and Shors, T.J. (2001). The role of the hippocampus in trace conditioning: temporal discontinuity or task difficulty? *Neurobiology of Learning and Memory, 76*(3), 447-461.

Binet, A. (1890). La perception des longueurs et des nombres chez quelques petites enfants. *Revue Philosophique*, *30*, 68-81.

Birt, D., Aou, S. and Woody, C.D. (2003). Intracellularly recorded responses of neurons of the motor cortex of awake cats to presentations of Pavlovian conditioned and unconditioned stimuli. *Brain Research*, *969*, 205-216.

Blackstad, T.W., Brink, K., Hem, J. and Jeune, B. (1970). Distribution of hippocampal mossy fibers in the rat. An experimental study with silver impregnation methods. *Journal Comparative Neurology, 138*(4), 433-449.

Blázquez, P.M., Fujii, N., Kojima, J. and Graybiel, A.M. (2002). A network representation of response probability in the striatum. *Neuron*, *33*, 973-982.

Blisland, L.G. and Schiavo, G. (2008). Axonal transporter tracers. In L.R. Squire (ed.). *The New Encyclopedia of Neuroscience.* Oxford (UK): Academic Press, pages 1209-1216.

Bliss, T.V.P. and Collingridge, G.L. (1993). A synaptic model of memory: long-term potentiation in the hippocampus. *Nature, 361*, 31-39.

Bongers, P., van den Akker, K., Havermans, R. and Jansen, A. (2015). Emotional eating and Pavlovian learning: Does negative mood facilitate appetitive conditioning? *Appetite, 89*, 226-236.

Bosch, M., Castro, J., Saneyoshi, T., Matsuno, H., Sur, M. and Hayashi, Y. (2014). Structural and molecular remodeling of dendritic spine substructures during long-term potentiation. *Neuron, 82*(2), 444-459.

Bracha, V., Stewart, S.L. and Bloedel, J.R. (1993). The temporary inactivation of the red nucleus affects performance of both conditioned and unconditioned nictitating membrane responses in the rabbit. *Experimental Brain Research, 94*, 225-236.

Bracha, V., Zbarska, S., Parker, K., Carrel, A., Zenitsky, G. and Bloedel, J.R. (2009). The cerebellum and eye-blink conditioning: learning versus network performance hypotheses. *Neuroscience, 162*, 787-796.

Bramham, C.R. and Srebro, B. (1989). Synaptic plasticity in the hippocampus is modulated by behavioral state. *Brain Research, 493*(1), 74-86.

Brodal, A. (1947). The hippocampus and the sense of smell; a review. *Brain, 70*, 179-222.

Brodal, A. (1981). *Neurological Anatomy in Relation to Clinical Medicine*. New York (N.Y.): Oxford University Press.

Burgess, N., Becker, S., King, J.A. and O'Keefe, J. (2001). Memory for events and their spatial context: models and experiments. Philosophical transactions of the *Royal Society of London. Series B, Biological sciences, 356*(1413), 1493-1503.

Cai, D., Pearce, K., Chen, S. and Glanzman, D.L. (2011). Protein kinase M maintains long-term sensitization and long-term facilitation in Aplysia. *The Journal of Neuroscience, 31*, 6421-6431.

Cai, D., Pearce, K., Chen, S. and Glanzman, D.L. (2012). Reconsolidation of long-term memory in Aplysia. *Current Biology, 22,* 1783-1788.

Cajal, S.R. (1888). Estructura de los centros nerviosos de las aves. *Revista Trimestral de Histología Normal y Patológica, 1*, 1-10.

Cajal, S.R. (1894). The Croonian lecture: La fine structure des centres nerveux. *Proceedings of the Royal Society of London, 55*, 444-467.

Caleo, M. and Schiavo, G. (2009). Central effects of tetanus and botulinum neurotoxins. *Toxicon, 54*, 593-599.

Canteras, N.S. and Swanson, L.W. (1992). Projections of the ventral subiculum to the amygdala, septum, and hypothalamus: a PHAL anterograde tract-tracing study in the rat. *Journal of Comparative Neurology, 324*(2), 180-194.

Cardinal, R.N., Parkinson, J.A., Hall, J. and Everitt, B.J. (2002). Emotion and motivation: the role of the amygdala, ventral striatum, and prefrontal cortex. *Neuroscience & Biobehavioral Reviews, 26*(3), 321-352.

Chapman, P.F., Steinmetz, J.E., Sears, L.L. and Thompson, R.F. (1990). Effects of lidocaine injection in the interpositus nucleus and red nucleus on conditioned behavioral and neuronal responses. *Brain Research, 537*, 149–156.

Chen, S., Cai, D., Pearce, K., Sun, P.Y-W., Roberts, A.C. and Glanzman, D.L. (2014). Reinstatement of long-term memory following erasure of its behavioral and synaptic expression in Aplysia. *eLife, 3*, e03896. doi: 10.7554/eLife.03896.

Chen, H., Wang, Y.J., Yang, L., Hu, C., Ke, X.F., Fan, Z.L., Sui, J.F. and Hu, B. (2014). Predictive nature of prefrontal theta oscillation on the performance of trace

conditioned eyeblink responses in guinea pigs. *Behavioral Brain Research, 265*, 121-131.

Cherubini, E. and Miles, R. (2015). The CA3 region of the hippocampus: how is it? What is it for? How does it do it? *Frontiers in Cellular Neuroscience, 9*:19. doi: 10.3389/fncel.2015.00019. eCollection 2015.

Chrobak, J.J. and Buzsáki, G. (1996). High-frequency oscillations in the output networks of the hippocampal-entorhinal axis of the freely behaving rat. *The Journal of Neuroscience, 16*, 3056-3066.

Citri, A. and Malenka, R.C. (2008). Synaptic plasticity: multiple forms, functions, and mechanisms. *Neuropsychopharmacology*, *33*, 18-41.

Claiborne, B.J., Amaral, D.G. and Cowan, W.M. (1986). A light and electron microscopic analysis of the mossy fibers of the rat dentate gyrus. *Journal of Comparative Neurology, 246*(4), 435-458.

Clark, R.E. and Squire, L.R. (1998). Classical conditioning and brain systems: the role of awareness. *Science*, *280*, 77-81.

Cohen, N.J. and Squire, L.R. (1980). Preserved learning and retention of pattern analyzing skill in amnesia: dissociation of knowing how and knowing that. *Science*, *210*, 207–210.

Colgin, L.L. (2015). Do slow and fast gamma rhythms correspond to distinct functional states in the hippocampal network? *Brain Research*, 1621:309-315.

Craik, F.I.M. (1983). On the transfer of information from temporary to permanent memory. *Philosophical Transactions of the Royal Society of London*, *Series B 302*, pp. 341-359.

Curran, H.V., Gardiner, J.M., Java, R. and Allen, D. (1993). Effects of lorazepam upon recollective experience in recognition memory. *Psychopharmacology*, *110*, 374-378.

Danos, P., Frotscher, M. and Freund, T.F. (1991). Non-pyramidal cells in the CA3 region of the rat hippocampus: relationships of fine structure, synaptic input and chemical characteristics. *Brain Research, 546*(2), 195-202.

Debiec, J., LeDoux, J.E. and Nader, K. (2002). Cellular and systems reconsolidation in the hippocampus. *Neuron, 36*, 527-538.

Deinhardt, K., Berninghausen, O., Willison, H.J., Hopkins, C.R. and Schiavo, G. (2006). Tetanus toxin is internalized by a sequential clathrin-dependent mechanisms initiated within lipid microdomains and independent of epsin1. *Journal of Cell Biology, 174*, 459-471.

Delgado-García, J.M. and Gruart, A. (2002). The role of interpositus nucleus in eyelid conditioned responses. *Cerebellum, 1*, 289-308.

Delgado-García, J.M. and Gruart, A. (2006). Building new motor responses: eyelid conditioning revisited. *Trends in Neurosciences*, *29*(6), 330-338.

Denny, C.A., Kheirbek, M.A., Alba, E.L., Tanaka, K.F., Barachman, R.A., Laughman, K.B., Tomm, N.K., Turi, G.F., Losonczy, A. and Hen, R. (2014). Hippocampal memory traces are differentially modulated by experience, time, and adult neurogenesis. *Neuron, 83*, 189-201.

Desmond, J.E. and Moore, J.W. (1986). Dorsolateral pontine tegmentum and the classically conditioned nictitating membrane response: analysis of CR-related single-unit activity. *Experimental Brain Research, 65*(1), 59-74.

Desmond, J.E., Rosenfield, M.E. and Moore, J.W. (1983). An HRP study of the brainstem afferents to the accessory abducens region and dorsolateral pons in rabbit: implications for the conditioned nictitating membrane response. *Brain Research Bulletin, 10*, 747-763.

Ding, S.L. (2013). Comparative anatomy of the prosubiculum, subiculum, presubiculum, postsubiculum, and parasubiculum in human, monkey, and rodent. *Journal of Comparative Neurology, 521*(18), 4145-4162.

Dolleman-Van der Weel, M.J., Lopes da Silva, F.H. and Witter, M.P. (1997). Nucleus reuniens thalami modulates activity in hippocampal field CA1 through excitatory and inhibitory mechanisms. *The Journal of Neuroscience, 17(*14), 5640-5650.

Dolleman-Van der Weel, M.J. and Witter, M.P. (2000). Nucleus reuniens thalami innervates gamma aminobutyric acid positive cells in hippocampal field CA1 of the rat. *Neuroscience Letters, 278*(3), 145-148.

Domingo, J.A., Gruart, A. and Delgado-García, J.M. (1997). Quantal organization of reflex and conditioned eye lid responses. *Journal of Neurophysiology*, *78*, 2518-2530.

Dragoi, G. and Tonegawa S. (2011). Preplay of future place cell sequences by hippocampal cellular assemblies. *Nature*, *469*(7330), 397-401.

Dudai, Y. (2012). The restless engram: consolidations never end. *Annual Review of Neuroscience, 35*, 227-247.

Eccles, J.C. (1967). Circuits in the cerebellar control of movement. *Proceedings of the National Academy of Sciences (PNAS)-USA*, *58*(1), 336-343.

Eccles, J.C. (1969). The development of the cerebellum of vertebrates in relation to the control of movement. *Naturwissenschaften, 56*(11), 525-534.

Eccles, J.C., Ito, M. and Szentágothai, J. (1967). *The Cerebellum as a Neuronal Machine.* New York (N.Y.): Springer-Verlag.

Eichenbaum, H. (1999). Conscious awareness, memory and the hippocampus. *Nature Neurosciences*, *2*, 775–776.

Eichenbaum, H. (2001). The hippocampus and declarative memory: cognitive mechanisms and neural codes. *Behavioral Brain Research, 127*(1-2), 199-207.

Evinger, C. (1995). A brain stem reflex in the blink of an eye. *Neural Information Processing Systems*, *10*, 147-153.

Evinger, C., Manning, K.A. and Sibony, P.A. (1991). Eyelid movements. Mechanisms and normal data. *Investigative Ophthalmology & Visual Science, 32*(2), 387-400.

Evinger, C., Shaw, M.D., Peck, C.K., Manning, K.A. and Baker, R. (1984). Blinking and associated eye movements in humans, guinea pigs, and rabbits. *Journal of Neurophysiology, 52*(2), 323-339.

Ferbinteanu, J., Ray, C. and McDonald, R.J. (2003). Both dorsal and ventral hippocampus contribute to spatial learning in Long-Evans rats. *Neuroscience Letters, 345*(2), 131-135.

Ferecskó, A.S., Jiruska, P., Foss, L., Powell, A.D., Chang, W-C., Sik, A. and Jefferys, J.G.R. (2015). Structural and functional substrates of tetanus toxin in an animal model of temporal lobe epilepsy. *Brain Structure and Function, 220*, 1013-1029.

Fernández-Lamo, I., Montero-Pedrazuela, A., Delgado-García, J.M., Guadaño-Ferraz, A. and Gruart, A. (2009). Effects of thyroid hormone replacement on associative learning and hippocampal synaptic plasticity in adult hypothyroid rats. *European Journal of Neuroscience, 30*(4), 679-692.

Fox, S.E., and J.B. Ranck, Jr. (1981). Electrophysiological characteristics of hippocampal complex-spike and theta cells. *Brain Research, 41*, 399-410.

Frankland, P.W., Ding, H.K., Takahashi, E., Suzuki, A., Kida, S. and Silva, A.J. (2006). Stability of recent and remote contextual fear memory. *Learning & Memory, 13*, 451-457.

Freeman, J.H., Halverson, H.E. and Hubbard, E.M. (2007). Inferior colliculus lesions impair eyeblink conditioning in rats. *Learning & Memory*, *14*, 842-846.

Freeman, J.H. and Steinmetz, A.B. (2011). Neural circuitry and plasticity mechanisms underlying delay eyeblink conditioning. *Learning & Memory, 18*(10), 666-677.

Furtak, S.C., Wei, S.M., Agster, K.L. and Burwell, R.D. (2007). Functional neuroanatomy of the parahippocampal region of the rat: The perirhinal and postrhinal cortices. *Hippocampus, 17*, 709-722.

Gabrieli, J.D., Cohen, N.J. and Corkin, S. (1988). The impaired learning of semantic knowledge following bilateral medial temporal-lobe resection. *Brain Cognition. 7*(2), 157-177.

Gerwig, M., Kolb, F.P. and Timmann, D. (2007). The involvement of the human cerebellum in eyeblink conditioning. *Cerebellum*, *6*, 38-57.

Girgis, M. and Shih-Chang, W.A. (1981). A new sterotaxic atlas of the rabbit brain. St. Louis: W.H. Green.

Gloor, P. (1997). *The Temporal Lobe and Limbic System*. New York: Oxford University Press.

González-Forero, D., de la Cruz, R.R., Delgado-García, J.M., Álvarez, F.J. and Pastor, A.M. (2003). Functional alterations of cat abducens neurons after peripheral tetanus neurotoxin injection. *Journal of Neurophysiology, 89*(4), 1878-1890.

González-Forero, D., Pastor, A.M., Delgado-García, J.M., de la Cruz, R.R. and Álvarez, F.J. (2004). Synaptic structural modification following changes in activity induced by tetanus neurotoxin in cat abducens neurons. *Journal of Comparative Neurology, 47*1(2), 201-218.

Green, J.T. and Arenos, J.D. (2007). Hippocampal and cerebellar single-unit activity during delay and trace eyeblink conditioning in the rat. *Neurobiology of Learning and Memory*, *87*, 269-284.

Griffin, A.L., Eichenbaum, H. and Hasselmo, M.E. (2007). Spatial representations of hippocampal CA1 neurons are modulated by behavioral context in a hippocampus-dependent memory task. *The Journal of Neuroscience, 27*, 2416-2423.

Gormezano, I., Kehoe, E.J. and Marshall, B.S. (1983). Twenty years of classical conditioning research with the rabbit. *Progress in Psychobiology and Physiological Psychology, 10*, 197-275.

Gormezano, I., Schneiderman, N., Deaux, E.G. and Fuentes, I. (1962). Nictitating membrane: classical conditioning and extinction in the albino rabbit. *Science, 138*, 33–34.

Graf, P., Shimamura, A.P. and Squire, L.R. (1985). Priming across modalities and priming across category levels: Extending the domain of preserved function in amnesia. *Journal of Experimental Psychology: Learning, Memory and Cognition, 11*, 386-396.

Graf, W. and Simpson, J.I. (1981). Relations between the semicircular canals, the optic axis, and the extraocular muscles in lateral-eyed and frontal-eyed animals. In A. F. Fuchs and W. Becker (Eds.): *Progress in Oculomotor Research*. Amsterdam: Elsevier/North-Holland, 1981, p. 409–417.

Graves, C.A. and Solomon, P.R. (1985). Age-related disruption of trace but not delay classical conditioning of the rabbit's nictitating membrane response. *Behavioral Neuroscience, 99*(1), 88-96.

Gruart, A., Benito, E., Delgado-García, J.M. and Barco, A. (2012). Enhanced cAMP response element-binding protein activity increases neuronal excitability,

hippocampal long-term potentiation, and classical eyeblink conditioning in alert behaving mice. *The Journal of Neuroscience 32*(48), 17431-17441.

Gruart, A., Blázquez, P. and Delgado-García, J.M. (1994). Kinematic analyses of classically-conditioned eyelid movements in the cat suggest a brain stem site for motor learning. *Neuroscience Letters, 175*(1-2), 81-84.

Gruart, A., Blázquez, P. and Delgado-García, J.M. (1995). Kinematics of spontaneous, reflex and conditioned eyelid movements in the alert cat. *Journal of Neurophysiology*, *74*, 226-248.

Gruart, A. and Delgado-García, J.M. (2007). Activity-dependent changes of the hippocampal CA3-CA1 synapse during the acquisition of associative learning in conscious mice. *Genes, Brain and Behavior*, *6*, 24-31.

Gruart, A., Morcuende, S., Martínez, S. and Delgado-García, J.M. (2000). Involvement of cerebral cortical structures in the classical conditioning of eyelid responses in rabbits. *Neuroscience*, *100*, 719-730.

Gruart, A., Muñoz, M.D. and Delgado-García, J.M. (2006). Involvement of the CA3-CA1 synapse in the acquisition of associative learning in behaving mice. *The Journal of Neuroscience, 26,* 1077-1087.

Gruart, A., Pastor, A.M., Armengol, J.A. and Delgado-García, J.M. (1997). Involvement of cerebellar cortex and nuclei in the genesis and control of unconditioned and conditioned eyelid motor responses. *Progress in Brain Research, 114*, 511-528.

Gruart, A., Sánchez-Campusano, R., Fernández-Guizán, A. and Delgado-García, J.M. (2014). A differential and timed contribution of identified hippocampal synapses to associative learning in mice. *Cerebral Cortex, 2014* Mar 20. PMID: 24654258.

Gruart, A., Schreurs, B.G., del Toro, E.D. and Delgado-García, J.M. (2000). Kinetic and frequency-domain properties of reflex and conditioned eyelid responses in the rabbit. *Journal of Neurophysiology, 83*(2), 836-852.

Grutzendler, J., Kasthuri, N. and Gan, W.B. (2002). Long-term dendritic spine stability in the adult cortex. *Nature, 420*, 812-816.

Hafting, T., Fyhn, M., Molden, S., Moser, M.B. and Moser, E.I. (2005). Microstructure of a spatial map in the entorhinal cortex. *Nature, 436*, 801-806.

Haight, J.L. and Flagel, S.B. (2014). A potential role for the paraventricular nucleus of the thalamus in mediating individual variation in Pavlovian conditioned responses. *Frontiers in Behavioral Neuroscience, 8*, 79. doi: 10.3389/fnbeh.2014.00079.

Halverson, H.E. and Freeman, J.H. (2006). Medial auditory thalamic nuclei are necessary for eyeblink conditioning. *Behavioral Neuroscience, 120*(4), 880-887.

Halverson, H.E., Lee, I. and Freeman, J.H. (2010). Associative plasticity in the medial auditory thalamus and cerebellar interpositus nucleus during eyeblink conditioning. *The Journal of Neuroscience*, *30*, 8787-8796.

Hamilton, T.J., Wheatley, B.M., Sinclair, D.B., Bachmann, M., Larkum, M.E. and Colmers, W.F. (2010). Dopamine modulates synaptic plasticity in dendrites of rat and human dentate granule cells. *Proceedings of the National Academy of Sciences (PNAS)-USA,* 107(42), 18185-18190.

Hargreaves, E.L., Rao, G., Lee, I. and Knierim, J.J. (2005). Major dissociation between medial and lateral entorhinal input to dorsal hippocampus. *Science, 308*(5729), 1792-1794.

Harley, C.W. (1991). Noradrenergic and locus coeruleus modulation of the perforant path evoked potential in rat dentate gyrus supports a role for the locus coeruleus in attentional and memorial processes. *Progress Brain Research, 88*, 307-321.

Hasan, M.T., Carretero-Guillén, A., Gómez-Climent, M.A., Trevino, M., Dogbevia, G., Sprengel, R., Vlochos, A., Gruart, A. and Delgado-García J.M. (2014) Does memory retrieval depend on precise synaptic organization? *Society for Neuroscience Meeting* 264.15,

Hebb, D.O. (1949). *The Organization of Behavior*. New York (NY): Wiley.

Herkenham M. (1978). The connections of the nucleus reuniens thalami: evidence for a direct thalamo-hippocampal pathway in the rat. *Journal of Comparative Neurology, 177*(4), 589-610.

Holmes, G. (1917). The symptoms of acute cerebellar injuries due to gunshot injuries. *Brain, 40*, 461-543.

Holtmaat, A.J., Trachtenberg, J.T., Wilbrecht, L., Shepherd, G.M., Zhang, X., Knott, G.W., Svoboda, K. (2005). Transient and persistent dendritic spines in the neocortex in vivo. *Neuron, 45*, 279-291.

Hsu, D. (2007). The dentate gyrus as a filter or gate: a look back and a look ahead. *Progress in Brain Research, 163*, 601-613.

Hunsaker, M.R., Mooy, G.G., Swift, J.S. and Kesner, R.P. (2007). Dissociations of the medial and lateral perforant path projections into dorsal DG, CA3, and CA1 for spatial and nonspatial (visual object) information processing. *Behavioral Neuroscience, 121*(4), 742-750.

Ishizuka, N. (2001). Laminar organization of the pyramidal cell layer of the subiculum in the rat. *Journal of Comparative Neurology, 435*(1), 89-110.

Ito, M. and Oda, Y. (1994). Electrophysiological evidence for formation of new corticorubral synapses associated with classical conditioning in the cat. *Experimental Brain Research, 99*, 277–288.

Izumi, Y. and Zorumski, C.F. (2008). Direct cortical inputs erase long-term potentiation at Schaffer collateral synapses. The *Journal of Neuroscience, 28*(38), 9557-9563.

Jefferys, J.G., Evans, B.J., Hughes, S.A. and Williams, S.F. (1992). Neuropathology of the chronic epileptic syndrome induced by intrahippocampal tetanus toxin in rat: preservation of pyramidal cells and incidence of dark cells. *Neuropathology and Applied Neurobiology, 18*(1), 53-70.

Jiménez-Díaz, L., Navarro-López, J. de D., Gruart, A. and Delgado-García, J.M. (2004). Role of cerebellar interpositus nucleus in the genesis and control of reflex and conditioned eyelid responses. The *Journal of Neuroscience*, *24*, 9138-9145.

Kandel, E.R. (2001). The molecular biology of memory storage: a dialogue between genes and synapses. *Science, 294*, 1030-1038.

Kandel, E.R. (2009). The biology of memory: a forty-year perspective. *The Journal of Neuroscience*, *29,* 12748-12756.

Kandel, E.R., Dudai, Y. and Mayford, M.R. (2014). The molecular and systems biology of memory. *Cell, 157*, 163-186.

Kandel, E.R., Schwartz, J.H. and Jessell, T.M. (2000). *Principles of Neural Science.* (4th edition). New York (NY): McGraw-Hill.

Kelly, T.M., Zuo, C.C. and Bloedel, J.R. (1990). Classical conditioning of the eyeblink reflex in the decerebrate-decerebellate rabbit. *Behavioral Brain Research*, *38*, 7-18.

Kerr, K.M., Agster, K.L., Furtak, S.C. and Burwell, R.D. (2007). Functional neuroanatomy of the parahippocampal region: the lateral and medial entorhinal areas. *Hippocampus, 17*, 697-708.

Kesner, R. (2013). Neurobiological foundations of an attribute model of memory. *Comparative Cognition & Behavior Reviews, 8*, 29-59.

Kim, J.J., Clark, R.E. and Thompson, R.F. (1995). Hippocampectomy impairs the memory of recently, but not remotely, acquired trace eyeblink conditioned responses. *Behavioral Neuroscience, 109*(2), 195-203.

Kiss, J., Csáki, A., Bokor, H., Shanabrough, M. and Leranth, C. (2000). The supramammillo-hippocampal and supramammillo-septal glutamatergic /aspartatergic projections in the rat: a combined [3H]D-aspartate autoradiographic and immunohistochemical study. *Neuroscience, 97*(4), 657-669.

Klukowski, G. and Harley, C.W. (1994). Locus coeruleus activation induces perforant path-evoked population spike potentiation in the dentate gyrus of awake rat. *Experimental Brain Research, 102*(1), 165-170.

Knuttinen, M.G., Parrish, T.B., Weiss, C., LaBar, K.S., Gitelman, D.R., Power, J.M., Mesulam, M.M. and Disterhoft, J.F. (2002). Electromyography as a recording system for eyeblink conditioning with functional magnetic resonance imaging. *Neuroimage*, *17*, 977-987.

Köhler, C. (1985). Intrinsic projections of the retrohippocampal region in the rat brain. I. The subicular complex. *Journal of Comparative Neurology*, 236, 504–522.

Kornorski, J. (1948). *Conditioned Reflexes and Neuron Organization*. Cambridge (MA): Cambridge University Press.

Lalli, G., Bohnert, S., Deinhardt, K., Verastegui, C. and Schiavo, G. (2003). The journey of tetanus and botulinum neurotoxins in neurons. *Trends in Microbiology, 11*, 431-437.

Lashley, K.S. (1920). Studies of cerebral function in learning. *Psychobiology, 2*, 55-135.

Lattal, K.M., Radulovic, J. and Lukowiak, K. (2006). Extinction: does it or doesn't it? The requirement of altered gene activity and new protein synthesis. *Biological Psychiatry, 60*, 344-351.

Lee, T. and Kim, J.J. (2004). Differential effects of cerebellar, amygdalar, and hippocampal lesions on classical eyeblink conditioning in rats. *The Journal of Neuroscience, 24*(13), 3242-3250.

Leal-Campanario, R., Barradas-Bribiescas, J.A., Delgado-García, J.M. and Gruart, A. (2004). Relative contributions of eyelid and eye-retraction motor systems to reflex and classically conditioned blink responses in the rabbit. *Journal of Applied Physiology, 96*(4), 1541-1554.

Leal-Campanario, R., Delgado-García, J.M. and Gruart, A. (2006). Microstimulation of the somatosensory cortex can substitute for vibrissa stimulation during Pavlovian conditioning. *Proceedings of the National Academy of Sciences (PNAS)-USA, 103*, 10052-10057.

Leal-Campanario, R., Fairén, A., Delgado-García, J.M. and Gruart, A. (2007). Electrical stimulation of the rostral medial prefrontal cortex in rabbits inhibits the expression of conditioned eyelid responses but not their acquisition. *Proceedings of the National Academy of Sciences (PNAS)-USA*, *104*, 11459-11464.

Leal-Campanario, R., Delgado-García, J.M. and Gruart, A. (2013). The rostral medial prefrontal cortex regulates the expression of conditioned eyelid responses in behaving rabbits. *The Journal of Neuroscience*, *33*(10), 4378-4386.

Levkovitz, Y. and Segal, M. (1997). Serotonin 5-HT1A receptors modulate hippocampal reactivity to afferent stimulation. *The Journal of Neuroscience, 17*(14), 5591-5598.

Li, C-H., Yeh, S-H, Lu, H-Y. and Gean P-W. (2003). The similarities and diversities of signal pathways leading to consolidation of conditioning and consolidation of extinction of fear memory. *The Journal of Neuroscience, 23*(23), 8310-8317.

Liston, C., Cichon, J.M., Jeanneteau, F., Jia, Z., Chao, M.V. and Gan, W.B. (2013). Circadian glucocorticoid oscillations promote learning-dependent synapse formation and maintenance. *Nature Neuroscience, 16*, 698-705.

Liu, X., Ramírez, S., Pang, P.T., Puryear, C.B., Govindarajan, A., Deisseroth, K. and Tonegawa, S. (2012). Optogenetic stimulation of a hippocampal engram activates fear memory recall. *Nature, 484*, 381-385.

Lorente de Nó, R. (1933). Studies on the structure of the cerebral cortex. I. The area entorhinalis. *Journal of Psychology and Neurology (Leipzig), 45*, 381–438.

Lorente de Nó, R. (1934). Studies on the structure of the cerebral cortex. II. Continuation of the study of the ammonic system. *Journal of Psychology and Neurology (Leipzig), 46*, 113-117.

Loy, R., Koziell, D.A., Lindsey, J.D. and Moore, R.Y. (1980). Noradrenergic innervation of the adult rat hippocampal formation. *Journal of Comparative Neurology, 189*, 699-710.

Madroñal, N., Delgado-García, J.M. and Gruart, A. (2007). Differential effects of long-term potentiation evoked at the CA3-CA1 synapse before, during, and after the acquisition of classical eyeblink conditioning in behaving mice. *The Journal of Neuroscience, 27*, 12139-12146.

Madroñal, N., Gruart, A. and Delgado-García, J.M. (2009). Differing presynaptic contributions to LTP and associative learning in behaving mice. *Frontiers in Behavioral of Neuroscience*. *3*,7. PMID: 19636387.

Madroñal, N., Gruart, A., Sacktor, T.C. and Delgado-García, J.M. (2009). PKMζ inhibition reverses learning-induced increases in hippocampal synaptic strength and memory during trace eyeblink conditioning. *PLoS One, 5*(4): e10400.

Madroñal, N., López-Aracil, C., Rangel, A., del Río, J.A., Delgado-García, J.M. and Gruart, A. (2010). Effects of enriched physical and social environments on motor performance, associative learning, and hippocampal neurogenesis in mice. *PLoS One*, *5*(6):e11130.

Mahut, H. and Zola, S.M. (1973). A non-modality specific impairment in spatial learning after fornix lesions in monkeys. *Neuropsychologia, 11*(3), 255-269.

Manto, M., Bower, J.M., Conforto, A.B., Delgado-García, J.M., da Guarda, S.N., Gerwig, M., Habas, C., Hagura, N., Ivry, R.B., Mariën, P., Molinari, M., Naito, E., Nowak, D.A., Oulad Ben Taib, N., Pelisson, D., Tesche, C.D., Tilikete, C. and Timmann, D. (2012). Consensus paper: roles of the cerebellum in motor control--the

diversity of ideas on cerebellar involvement in movement. *Cerebellum, 11*(2), 457-487.

Marr, D. (1969). A theory of cerebellar cortex. *Journal of Physiology (London), 202*, 437-470.

Marr, D. (1971). Simple memory: A theory for archicortex. *Philosophical Transactions of the Royal Society of London*. *Series B, Biological Sciences, 262*(841), 23-81.

Martens, S. and Wyble, B. (2010). The attentional blink: past, present, and future of a blind spot in perceptual awareness. *Neuroscience Biobehavioral Reviews*, *34*, 947-957.

Mayford, M., Siegelbaum, S.A. and Kandel, E.R. (2012). Synapses and memory storage. *Cold Spring Harbor Perspectives in Biology, 4*: a005751.

McCormick, D.A., Lavond, D.G., Clark, G.A., Kettner, R.E., Rising, C.E. and Thompson, R.F. (1981). The engram found? Role of the cerebellum in classical conditioning of nictitating membrane and eyelid responses. *Bulletin of the Psychonomic Society, 18*, 103-105.

McCormick, D.A. and Thompson, R.F. (1984a). Cerebellum: essential involvement in the classically conditioned eyelid response. *Science, 223*, 296-299.

McCormick, D.A. and Thompson, R.F. (1984b). Neuronal responses of the rabbit cerebellum during acquisition and performance of a classically conditioned nictitating membrane-eyelid response. *The Journal of Neuroscience, 4*(11), 2811-2822.

McEchron, M.D. and Disterhoft, J.F. (1997). Sequence of single neuron changes in CA1 hippocampus of rabbits during acquisition of trace eyeblink conditioned responses. *Journal of Neurophysiology, 78*(2), 1030-1044.

McEchron, M.D. and Disterhoft, J.F. (1999). Hippocampal encoding of non-spatial trace conditioning. *Hippocampus 9*, 385-396.

McEchron, M.D., Tseng, W. and Disterhoft, J.F. (2003). Single neurons in CA1 hippocampus encode trace interval duration during trace heart rate (fear) conditioning in rabbit. *Journal of Neuroscience, 23*, 1535-1547.

McHugh, T.J., Jones, M.W., Quinn, J.J., Balthasar, N., Coppari, R., Elmquist, J.K., Lowell, B.B., Fanselow, M.S., Wilson, M.A. and Tonegawa, S. (2007). Dentate gyrus NMDA receptors mediate rapid pattern separation in the hippocampal network. *Science, 317*(5834), 94-99.

McHugh, T.J. and Tonegawa, S. (2009). CA3 NMDA receptors are required for the rapid formation of a salient contextual representation. *Hippocampus, 19*, 1153-1158.

McKay, B.M., Oh. M.M. and Disterhoft, J.F. (2013). Learning increases intrinsic excitability of hippocampal interneurons. *Journal of Neuroscience, 33*, 5499-5506.

McNaughton, B. L., and Morris, R. G. M. (1987). Hippocampal synaptic enhancement and information storage within a distributed memory system. *Trends in Neurosciences, 10*, 408-415.

Meftah, E.M. and Rispal-Padel, L. (1994). Synaptic plasticity in the thalamo-cortical pathway as one of the neurobiological correlates of forelimb flexion conditioning: electrophysiological investigation in the cat. *Journal of Neurophysiology, 72*(6), 2631-2647.

Meibach, R.C. and Siegel, A. (1977a). Subicular projections to the posterior cingulate cortex in rats. *Experimental Neurology, 57*(1), 264-274.

Meibach, R.C. and Siegel, A. (1977b). Efferent connections of the hippocampal formation in the rat. *Brain Research, 124*(2), 197-224.

Miller, L.E. and Gibson, A.R. (2009). In Encyclopedia of Neuroscience, Red Nucleus. In L.R. Squire (Ed.). Vol 8, pp 55–62. Oxford: Academic.

Mohedano-Moriano, A., Pró-Sistiaga, P., Arroyo-Jimenez, M.M., Artacho-Pérula, E., Insausti, A.M., Marcos, P., Cebada-Sánchez, S., Martínez-Ruiz, J., Muñoz, M., Blaizot, X., Martinez-Marcos, A., Amaral, D.G. and Insausti, R. (2007). Topographical and laminar distribution of cortical input to the monkey entorhinal cortex. *Journal of Anatomy, 211*(2), 250-260.

Moore, J.W. and Gormezano, I. (1961). Yoked comparisons of instrumental and classical eyelid conditioning. *Journal of Experimental Psychology, 62*, 552-559.

Morcuende, S., Delgado-García, J.M. and Ugolini, G. (2002). Neuronal premotor networks involved in eyelid responses: retrograde transneuronal tracing with rabies virus from the orbicularis oculi muscle in the rat. *The Journal of Neuroscience, 22*, 8808-8818.

Morcuende, S., Trigo, J.A., Delgado-García, J.M. and Gruart, A. (2001). Harmaline induces different motor effects on facial vs. skeletal-motor systems in alert cats. *Neurotoxicity Research*, *3*, 527-535.

Moser, E.I., Kropff, E. and Moser, M.B. (2008). Place cells, grid cells, and the brain´s spatial representation system. *Reviews in Neuroscience, 31*, 69-89.

Moyer, J.R. Jr., Deyo, R.A. and Disterhoft, J.F. (1990). Hippocampectomy disrupts trace eye-blink conditioning in rabbits. *Behavioral Neuroscience, 104*, 243-252.

Moyer, J.R. Jr., Thompson, L.T. and Disterhoft J.F. (1996). Trace eyeblink conditioning increases CA1 excitability in a transient and learning-specific manner. The Journal of Neuroscience*, 16*, 5536-5546.

Múnera, A., Gruart, A., Muñoz, M.D., Fernández-Mas, R. and Delgado-García, J.M. (2001). Hippocampal pyramidal cell activity encodes conditioned stimulus predictive value during classical conditioning in alert cats. *Journal of Neurophysiology, 86*, 2571-2582.

Muñoz-López, M. (2015). Past, present, and future in hippocampal formation and memory research. *Hippocampus*, doi: 10.1002/hipo.22452.

Muñoz-López, M.M., Mohedano-Moriano, A. and Insausti, R. (2010). Anatomical pathways for auditory memory in primates. *Frontiers in Neuroanatomy, 4*, 129. doi: 10.3389/fnana.2010.00129. eCollection 2010.

Murray, J.F. and Kreutz-Delgado, K. (2007). Visual recognition and inference using dynamic overcomplete sparse learning. *Neural Computation, 19*(9), 2301-2352.

Nadel, L. and Hardt, O. (2004). The spatial brain. *Neuropsychology, 18*(3), 473-476.

Nakashiba, T., Cushman, J.D., Pelkey, K.A., Renaudineau, S., Buhl, D.L., McHugh, T.J., Rodriguez Barrera, V., Chittajallu, R., Iwamoto, K.S., McBain, C.J., Fanselow, M.S. and Tonegawa, S. (2012). Young dentate granule cells mediate pattern separation, whereas old granule cells facilitate pattern completion. *Cell 149*, 188-201.

Neves, G., Cooke, S.F. and Bliss, T.V. (2008). Synaptic plasticity, memory and the hippocampus: a neural network approach to causality. *Nature Reviews. Neuroscience*, *9*, 65-75.

Nicoll, R.A. and Schmitz, D. (2005). Synaptic plasticity at hippocampal mossy fibre synapses. *Nature Reviews. Neuroscience*, *6*, 863-876.

Nokia, M.S., Penttonen, M. Karhonen, T. and Wikgren, J. (2009). Hippocampal gamma-band activity and trace eyeblink and trace eyeblink conditioning in rabbits. *Behavioral Neuroscience, 123*, 631-640.

Nokia, M.S., Penttonen, M. Karhonen, T. and Wikgren, J. (2010). Hippocampal ripple-contingent training accelerates trace eyeblink conditioning and retards extinction in rabbits. *The Journal of Neuroscience, 2010*, *30*(34), 11486-11492.

Nokia, M.S., Sisti, H.M., Choksi, M.R. and Shors, T.J. (2012). Learning to learn: gamma oscillations predict new learning, which enhances related learning and neurogenesis. *PLoS One, 7*: e31375.

Nokia, M.S. and Wikgren, J. (2014). Effects of hippocampal state-contingent trial presentation on hippocampus-dependent nonspatial classical conditioning and extinction. *The Journal of Neuroscience, 34*(17), 6003-6010.

Oler, J.A., Penley, S.C., Sava, S. and Markus, E.J. (2008). Does the dorsal hippocampus process navigational routes or behavioral context? A single-unit analysis. *European Journal of Neuroscience, 28*(4), 802-812.

O'Mara, S.M., Rolls, E.T., Berthoz, A. and Kesner, R.P. (1994). Neurons responding to whole-body motion in the primate hippocampus. *The Journal of Neuroscience, 14*(11 Pt 1), 6511-6523.

O'Mara, S.M., Sánchez-Vives, M.V., Brotons-Mas, J.R. and O'Hare, E. (2009). Roles for the subiculum in spatial information processing, memory, motivation and the temporal control of behaviour. *Progress in Neuro-Psychopharmacology & Biological Psychiatry, 33*(5), 782-790.

Pacheco-Calderón, R., Carretero-Guillén, A., Delgado-García, J.M. and Gruart, A. (2012). Red nucleus neurons actively contribute to the acquisition of classically conditioned eyelid responses in rabbits. *The Journal of Neuroscience, 32*(35), 12129-12143.

Papez, J.W. (1937). A proposed mechanism of emotion. *Archives of Neurology & Psychiatry, 38*(4), 725-743.

Parra, P., Gulyas, A.I. and Miles, R. (1998). How many subtypes of inhibitory cells in the hippocampus? *Neuron, 20*, 983-993.

Patterson, M.A., Berger, T.W. and Thompson, R.F. (1979). Neuronal plasticity recorded from cat hippocampus during classical conditioning. *Brain Research, 163*, 339-343.

Pavlov, I. (1927). *Conditioned Reflexes: An Investigation of the Physiological Activity of the Cerebral Cortex*. Translated and edited by G. V. Anrep. London: Oxford University Press.

Penfield, W. and Milner, B. (1958). Memory deficit produced by bilateral lesions in the hippocampal zone. *Archives of Neurology & Psychiatry, 79*(5), 475-497.

Porras-García, E., Sánchez-Campusano, R., Martínez-Vargas, D., Domínguez-del-Toro, E., Cendelín, J., Vozeh, F. and Delgado-García, J.M. (2010). Behavioral characteristics, associative learning capabilities, and dynamic association mapping in an animal model of cerebellar degeneration. *Journal of Neurophysiology, 104*(1), 346-365.

Preston, A.R. and Eichenbaum, H. (2013). Interplay of hippocampus and prefrontal cortex in memory. *Current Biology, 23*(17), R764-73.

Prince, M. (1914). *The Unconscious*. New York (NY): Macmillan.

Rajkowski, J., Majczynski, H., Clayton, E. and Aston-Jones, G. (2004). Activation of monkey locus coeruleus neurons varies with difficulty and performance in a target detection task. *The Journal of Neurophysiology, 92*(1), 361-371.

Reagh, Z.M. and Yassa, A. (2014). Object and spatial mnemonic interference differentially engage lateral and medial entorhinal cortex in humans. *Proceedings*

of the National Academy of Sciences of the United States of America (PNAS), 111(40), 4264-4273.

Rescorla, R.A. (1988). Pavlovian conditioning. It's not what you think it is. *American Psychologist, 43*(3), 151-160.

Robinson, F.R., Rice, P.M., Holleman, J.R. and Berger, T.W. (2001). Projection of the magnocellular red nucleus to the region of the accessory abducens nucleus in the rabbit. *Neurobiology of Learning and Memory, 76*, 358–374.

Rorick-Kehn, L.M. and Steinmetz, J.E. (2005). Amygdalar unit activity during three learning tasks: eyeblink classical conditioning, Pavlovian fear conditioning, and signalled avoidance conditioning. *Behavioral Neuroscience*, *119*, 1254-1276.

Rosene, D.L. and Van Hoesen, GW. (1977). Hippocampal efferents reach widespread areas of cerebral cortex and amygdala in the rhesus monkey. *Science, 198*(4314), 315-317.

Rosenkranz, K., Kacar, A. and Rothwell, J.C. (2007). Differential modulation of motor cortical plasticity and excitability in early and late phases of human motor learning. The Journal of Neuroscience, *27*, 12058-12066.

Ryan, M., Kaminer, J., Enmore, P. and Evinger, C. (2014). Trigeminal high-frequency stimulation produces short- and long-term modification of reflex blink gain. *Journal of Neurophysiology, 111*(4), 888-895.

Sacktor, T.C. (2011). How does PKMzeta maintain long-term memory? *Nature Reviews. Neuroscience, 12*, 9-15.

Sánchez-Campusano, R. (2007). *Métodos analíticos y experimentales optimizados para el control neuromuscular de las respuestas motoras aprendidas: el sistema motor palpebral*. Universidad Pablo de Olavide, Seville, Spain: Doctoral Thesis.

Sánchez-Campusano, R., Gruart, A. and Delgado-García, J.M. (2007). The cerebellar interpositus nucleus and the dynamic control of learned motor responses. *The Journal of Neuroscience*, *20*, 6620-6632.

Sánchez-Campusano, R., Gruart, A. and Delgado-García, J.M. (2009). Dynamic associations in the cerebellar-motoneuron network during motor learning. *The Journal of Neuroscience, 29*, 10750-10763.

Sánchez-Campusano, R., Gruart, A. and Delgado-García, J.M. (2011). Dynamic changes in the cerebellar-interpositus/red-nucleus-motoneuron pathway during motor learning. *Cerebellum*, *10*(4), 702-710.

Schacter, D.L. (1987). Implicit memory: history and current status. *Journal of Experimental Psychology, 13*(3), 501-518.

Schaffer, K. (1892). Beitrag zur histologie der ammonshornf. *Arch. Microsk. Anat., 39*, 611-632.

Schneiderman, N., Fuentes, I. and Gormezano, I. (1962). Acquisition and extinction of the classically conditioned eyelid response in the albino rabbit. *Science*, *136*, 650–652.

Schultz, C. and Engelhardt, M. (2014). Anatomy of the hippocampal formation. *Frontiers of Neurology and Neuroscience, 34*, 6-17. doi: 10.1159/000360925.

Schwerdtfeger, W. K., Buhl, E. H. and Germroth, P. (1990). Disynaptic olfactory input to the hippocampus mediated by stellate cells in the entorhinal cortex. *Journal of Comparative Neurology, 292*, 163-177.

Scoville, W.B. and Milner, B. (1957). Loss of recent memory after bilateral hippocampal lesions. *Journal of Neurology, Neurosurgery & Psychiatry, 20*(1), 11-21.

Segal, M., Disterhoft, J.F. and Olds, J. (1972). Hippocampal unit activity during classical aversive and appetitive conditioning. *Science, 175*(4023), 792-794.

Segal, M. and Olds, J. (1972). Behavior of units in hippocampal circuit of the rat during learning. *Journal of Neurophysiology, 35*(5), 680-690.

Shipley, M.T. (1975). The topographical and laminar organization of the presubiculum's projection to the ipsi- and contralateral entorhinal cortex in the guinea pig. *Journal of Comparative Neurology, 160*(1), 127-145.

Solomon, P.R., Vander Schaaf, E.R., Thompson, R.F. and Weisz, D.J. (1986). Hippocampus and trace conditioning of the rabbit's classically conditioned nictitating membrane response. *Behavioral Neuroscience, 100*(5), 729-744.

Song, D., Cahn, R.H., Marmarelis, V.Z., Hampson, R.E., Deadwyler, S.A. and Berger, T.W. (2007). Nonlinear dynamic modeling of spike train transformations for hippocampal-cortical prostheses. *IEEE Transactions on Biomedical Engineering, 54*, 1053-1066.

Squire, L.R. (1987). *Memory and Brain*. New York (NY): Oxford University Press.

Squire, L.R., Stark, C.E. and Clark, R.E. (2004). The medial temporal lobe. *Annual Review of Neuroscience, 27*, 279-306.

Suter, E.E., Weiss, C. and Disterhoft, J.F. (2013). Perirhinal and postrhinal, but not lateral entorhinal, cortices are essential for acquisition of trace eyeblink conditioning. *Learning & Memory, 20*(2), 80-84.

Suzuki, W.A. and Amaral, D.G. (1994). Perirhinal and parahippocampal cortices of the macaque monkey: cortical afferents. *Journal of Comparative Neurology, 350*(4), 497-533.

Svensson, P., Bengtsson, F. and Hesslow, G. (2006). Cerebellar inhibition of inferior olivary transmission in the decerebrate ferret. *Experimental Brain Research*, *168*, 241-253.

Swanson, L.W. and Cowan, W.M. (1977). An autoradiographic study of the organization of the efferent connections of the hippocampal formation in the rat. *Journal of Comparative Neurology, 172*(1), 49-84.

Thompson, R.F. (1988). The neural basis of basic associative learning of discrete behavioral responses. *Trends in Neuroscience, 11*, 152–155.

Thompson, R.F. (2005). In search of memory traces. *Annual Review Psychology*, *56*, 1-23.

Thompson, R.F. and Krupa, D.J. (1994). Organization of memory traces in the mammalian brain. *Annual Review of Neuroscience*, *17*, 519-549.

Thompson, R.F. and Steinmetz, J.E. (2009). The role of the cerebellum in classical conditioning of discrete behavioral responses. *Neuroscience*, *162*, 732-755.

Trachtenberg, J.T., Chen, B.E., Knott, G.W., Feng, G., Sanes, J.R., Welker, E. and Svoboda, K. (2002). Long-term in vivo imaging of experience-dependent synaptic plasticity in adult cortex. *Nature, 420*, 788-794.

Treves, A., and Rolls, E.T. (1994). A computational analysis of the role of the hippocampus in memory. *Hippocampus, 4*, 374-392.

Trigo, J.A., Gruart, A. and Delgado-García, J.M. (1999a). Discharge profiles of abducens, accessory abducens, and orbicularis oculi motoneurons during reflex and conditioned blinks in alert cats. *Journal of Neurophysiology*, *81*, 1666-1684.

Trigo, J.A., Gruart, A. and Delgado-Garcia, J.M. (1999b). Role of proprioception in the control of lid position during reflex and conditioned blink responses in the alert behaving cat. *Neuroscience, 90*(4), 1515-1528.

Trigo, J.A., Roa, L., Gruart, A. and Delgado-García, J.M. (2003). A kinetic study of blinking responses in cats. *The Journal of Physiology, 549*(Pt 1), 195-205.

Troncoso, J., Múnera, A. and Delgado-García, J.M. (2007). Learning-dependent potentiation in the vibrissal motor cortex is closely related to the acquisition of conditioned whisker responses in behaving mice. *Learning & Memory*, *14*, 84-93.

Tsukahara, N. (1981). Synaptic plasticity in the mammalian central nervous system. *Annual Review of Neuroscience, 4*, 351-379.

Tsukahara, N., Toyama, K. and Kosaka, K. (1967). Electrical activity of red nucleus neurones investigated with intracellular microelectrodes. *Experimental Brain Research, 4*, 18-33.

Tulving, E. (1985). How many memory systems are there? *American Psychologist, 40*(4), 385-398.

Turrigiano, G. (2007). Homeostatic signalling: the positive side of negative feedback. *Current Opinion in Neurobiology, 17,* 318-324.

Van Groen, T. and Wyss, J.M. (1990). The connections of presubiculum and parasubiculum in the rat. *Brain Research, 518*(1-2), 227-243.

Varela, C., Kumar, S., Yang, J.Y. and Wilson, M.A. (2014). Anatomical substrates for direct interactions between hippocampus, medial prefrontal cortex, and the thalamic nucleus reuniens. *Brain Structure and Function, 219*(3), 911-929.

Verwer, R.W., Meijer, R.J., Van Uum, H.F. and Witter, M.P. (1997). Collateral projections from the rat hippocampal formation to the lateral and medial prefrontal cortex. *Hippocampus, 7*, 397-402.

Vianna, M.R., Szapiro, G., McGaugh, J.L., Medina, J.H. and Izquierdo, I. (2001). Retrieval of memory for fear-motivated training initiates extinction requiring protein synthesis in the rat hippocampus. *Proceedings of the National Academy of Sciences (PNAS)*-USA*, 98,* 12251-12254.

Vinogradova, O.S. (2001). Hippocampus as comparator: Role of the two input and two output systems of the hippocampus in selection and registration of information. *Hippocampus, 11*, 578-598.

Vivar, C. and van Praag, H. (2013). Functional circuits of new neurons in the dentate gyrus. *Frontiers in Neural Circuits, 7*, 15. doi: 10.3389/fncir.2013.00015. eCollection 2013.

Walling, S.G., Nutt, D.J., Lalies, M.D. and Harley, C.W. (2004). Orexin-A infusion in the locus coeruleus triggers norepinephrine (NE) release and NE-induced long-term potentiation in the dentate gyrus. *The Journal of Neuroscience, 24*(34), 7421-7426.

Wang, S.H. and Morris, R.G. (2010). Hippocampal-neocortical interactions in memory formation, consolidation, and reconsolidation. *Annual Review of Psychology, 61*, 49-79.

Watanabe, S., Rost, B.R., Camacho-Pérez, M., Davis, M.W., Söhl-Kielczynski, B., Rosenmund, C. and Jorgensen, E.M. (2013). Ultrafast endocytosis at mouse hippocampal synapses. *Nature, 504*(7479), 242-247.

Weisz, D.J., Clark, G.A. and Thompson, R.F. (1984). Increased responsivity of dentate granule cells during nictitating membrane response conditioning in rabbit. *Behavioral Brain Research*, *12*, 145-154.

Welsh, J.P. (1992). Changes in the motor pattern of learned and unlearned responses following cerebellar lesions: a kinematic analysis of the nictitating membrane reflex. *Neuroscience, 47*(1), 1-19.

Welsh, J.P. and Harvey, J.A. (1991). Pavlovian conditioning in the rabbit during inactivation of the interpositus nucleus. *The Journal of Physiology, 444*, 459-480.

Whitlock, J.R., Heynen, A.J., Shuler, M.G. and Bear, M.F. (2006). Learning induces long-term potentiation in the hippocampus. *Science*, *313*, 1093-1097.

Willingham, D.B., Salidis, J. and Gabrieli, J.D. (2002). Direct comparison of neural systems mediating conscious and unconscious skill learning. *Journal of Neurophysiology, 88*, 1451-1460.

Winocur, G., Frankland, P.W., Sekeres, M., Fogel, S. and Moscovitch, M. (2009). Changes in context-specificity during memory reconsolidation: selective effects of hippocampal lesions. *Learning & Memory, 16*, 722-729.

Witter, M.P., Naber, P.A., van Haeften, T., Machielsen, W.C., Rombouts, S.A., Barkhof, F., Scheltens, P. and Lopes da Silva, F.H. (2000). Cortico-hippocampal communication by way of parallel parahippocampal-subicular pathways. *Hippocampus, 10*(4), 398-410.

Woody, C.D., Wang, X.F., Gruen, E. and Landeira-Fernandez, J. (1992). Unit activity to click CS changes in dorsal cochlear nucleus after conditioning. *NeuroReport. 3*(5), 385-388.

Wouterlood, F.G., Saldana, E. and Witter, M.P. (1990). Projection from the nucleus reuniens thalami to the hippocampal region: light and electron microscopic tracing study in the rat with the anterograde tracer *Phaseolus vulgaris-leucoagglutinin*. *Journal of Comparative Neurology, 296*(2), 179-203.

Wu, G.Y., Yao, J., Hu, B., Zhang, H.M., Li, Y.D., Li, X., Li, Q. and Sui, J.F. (2013). Reevaluating the role of the hippocampus in delay eyeblink conditioning. *PLoS One, 8*(8):e71249. doi: 10.1371/journal.pone.0071249. eCollection 2013.

Wulf, G. and Shea, C.H. (2002). Principles derived from the study of simple skills do not generalize to complex skill learning. *Psychonomic Bulletin & Review, 9*(2), 185-211.

Wyss, J.M. and Van Groen, T. (1992). Connections between the retrosplenial cortex and the hippocampal formation in the rat: A review. *Hippocampus, 2*(1), 1-12.

Xu, T., Yu, X, Perlik, A.J., Tobin, W.F., Zweig, J.A., Tennant, K., Jones, T. and Zuo, Y. (2009). Rapid formation and selective stabilization of synapses for enduring motor memories. *Nature, 462,* 915-919.

Yang, Y., Lei, C., Feng, H. and Sui, J.F. (2015). The neural circuitry and molecular mechanisms underlying delay and trace eyeblink conditioning in mice. *Behavioral Brain Research, 278*, 307-314.

Yang, G., Pan, F. and Gan, W.B. (2009). Stably maintained dendritic spines are associated with lifelong memories. *Nature, 462*, 920-924.

Zheng, Y., Horii, A., Appleton, I., Darlington, C.L. and Smith, P.F. (2001). Damage to the vestibular inner ear causes long-term changes in neuronal nitric oxide synthase expression in the rat hippocampus. *Neuroscience, 105*(1), 1-5.

Zola-Morgan, S. and Squire, L.R. (1993). Neuroanatomy of memory. *Annual Review of Neuroscience*, *16*, 547-563.

Zotova, E., Woody, C.D. and Gruen, E. (2000). Multiple representations of information in the primary auditory cortex of cats. II. Stability and change in early (<32 ms), rapid components of activity alter conditioning with a click conditioned stimulus. *Brain Research*, *868*, 66-78.

8. ANNEXES

8.1 PAPER DIRECTLY RELATED TO THE DOCTORAL THESIS

Cerebral Cortex Advance Access published November 14, 2013

Cerebral Cortex
doi:10.1093/cercor/bht321

Involvement of Hippocampal Inputs and Intrinsic Circuit in the Acquisition of Context and Cues During Classical Conditioning in Behaving Rabbits

Alejandro Carretero-Guillén, Renny Pacheco-Calderón, José M. Delgado-García and Agnès Gruart

Division of Neurosciences, Pablo de Olavide University, E-41013 Seville, Spain

Address correspondence to Prof. Agnès Gruart, Division of Neurosciences, Pablo de Olavide University, Carretera de Utrera, Km. 1, Seville-41013, Spain. Email: agrumas@upo.es

Learning-related changes in strength in selected hippocampal synapses have been described recently. However, information is scarce regarding the spatial-temporal sequence of changes in synaptic weights taking place during the acquisition of a classical conditioning task and the contribution of both context (environmental details) and cues (conditioned and unconditioned stimuli: CS, US) to those activity-dependent changes. We recorded in rabbits the monosynaptic field excitatory postsynaptic potentials (fEPSPs) evoked at 6 different hippocampal synapses during the acquisition and extinction of a classical eyeblink conditioning using trace or delay paradigms, as well as during pseudoconditioning and in the absence of CS and US presentations (context). Context and pseudoconditioning training evoked early, lasting changes in synaptic strength in perforant pathway synapses in dentate gyrus (PP-DG), and hippocampal CA3 (PP-CA3) and CA1 (PP-CA1) areas. Pseudoconditioning also evoked early, nonlasting changes in strength within the intrinsic hippocampal circuit (CA3-CA1 and CA3-cCA1 synapses). In contrast, during both trace and delay training sessions, synaptic changes in strength were mostly noticed within the intrinsic hippocampal circuit (DG-CA3, CA3-CA1, CA3-cCA1). The response of hippocampal synapses to afferent impulses seems to be modulated by both context and cues during associative learning in behaving rabbits.

Keywords: associative learning, behaving rabbits, changes in synaptic strength, hippocamapal synapses, neuronal plasticity

Introduction

One of the more basic tenets of current neuroscience is that newly acquired motor and/or cognitive abilities are stored in the form of functional and structural changes in synaptic efficiency (Ramón y Cajal 1909–1911; Konorski 1948; Hebb 1949). In this regard, convincing relationships have been shown between acquired learning abilities in experimental animals and the underlying changes in synaptic activity, determined by genetic, molecular, and *in vitro* electrophysiological studies (Bliss and Collingridge 1993; Kandel 2001; Neves et al. 2008; Wang and Morris 2010). Nevertheless, functional changes evoked by learning should be susceptible to being detected at synapses relevant to the learning process. For example, activity-dependent changes in synaptic strength have been reported in behaving mammals during the very moment of the acquisition process (Gruart et al. 2006; Whitlock et al. 2006). However, 2 important questions remain to be addressed: Are all synapses of large cortical circuits behaving in the same way during the acquisition and extinction processes? And, are activity-dependent changes in synaptic strength involved only in the relevant association cues or is the context also relevant in the learning process?

Of the cerebral cortical structures, the hippocampus has been one of the most studied, being implicated in a wide variety of learning and memory experimental paradigms, including object recognition (Clarke et al. 2010), spatial orientation (Moser et al. 2008; Wang and Morris 2010), and classical conditioning of eyelid responses (Berger et al. 1983; McEchron and Disterhoft 1997; Múnera et al. 2001). Indeed, firing activities of identified hippocampal CA3 and CA1 pyramidal neurons recorded in behaving cats are related to the acquisition of classical conditioning of eyelid responses, using both trace and delay paradigms (Múnera et al. 2001). But, here again, there is no complete information on the global activity of hippocampal circuits during the same type of associative learning.

In order to address these issues, we decided to determine in behaving rabbits the changes in synaptic strength of selected hippocampal synapses taking place during different classical conditioning protocols. Following the earlier demonstration with regard to perforant pathway projections in dentate gyrus (PP-DG; Weisz et al. 1984) and CA3-CA1 (Gruart et al. 2006) synapses, we studied here whether the acquisition of a classical conditioning task modifies the synaptic weights in 4 additional hippocampal synapses: PP-CA3, PP-CA1, DG-CA3, and CA3-cCA1). For this, we trained rabbits for a classical conditioning of eyelid responses, with both trace and delay paradigms, presenting a tone as CS and an air puff aimed at the cornea as US. Animals were also trained for pseudoconditioning and just to the context situation (i.e., in the absence of CS and/or US presentations). Conditioned responses (CRs) were determined from the electromyographic (EMG) activity of the orbicularis oculi muscle. We recorded field excitatory postsynaptic potentials (fEPSPs) evoked at the 6 hippocampal synapses during the 4 experimental situations. For this, animals were chronically implanted with multiple recording and stimulating electrodes in the selected intra- and extrahippocampal sites. Present results provide substantial evidence of the intrinsic relationships between activity-dependent synaptic changes in strength in the hippocampal circuits and context and cues present in associative learning tasks in mammals.

Materials and Methods

Experimental Animals

Experiments were carried out on adult male rabbits (New Zealand white albino) weighing 2.6–3.1 kg on arrival, obtained from an authorized supplier (Isoquimen, S.L., Barcelona, Spain). Animals were housed in individual cages for the whole experiment, and kept on a 12/12 h light/dark cycle with constant ambient temperature (21 ± 1 °C) and humidity (50 ± 7%). Food and water were available *ad libitum*. All experimental procedures were carried out in accordance with the guidelines of the European Union Council (2003/65/CE) and Spanish (BOE 252/34367-91, 2005) regulations for the use of laboratory animals in chronic experiments. Experimental protocols were also approved by the local University Ethics Committee.

Surgery

Animals were anesthetized with a ketamine-xylazine cocktail (ketaminol, 50 mg/mL; rompun, 20 mg/mL; and atropine sulfate, 0.5 mg/kg). Animals were prepared for the chronic recording of fEPSPs evoked at selected sites within the dorsal hippocampus (Fig. 1*A*). For this, animals were implanted with bipolar stimulating electrodes in the perforant pathway, the dentate gyrus, or the hippocampal CA3 area, and with recording electrodes aimed at the dentate gyrus, and/or the hippocampal CA3 and CA1 areas (see location and coordinates in Fig. 1*B*, *C*,*E*; Girgis and Shih-Chang 1981). Each animal was implanted with

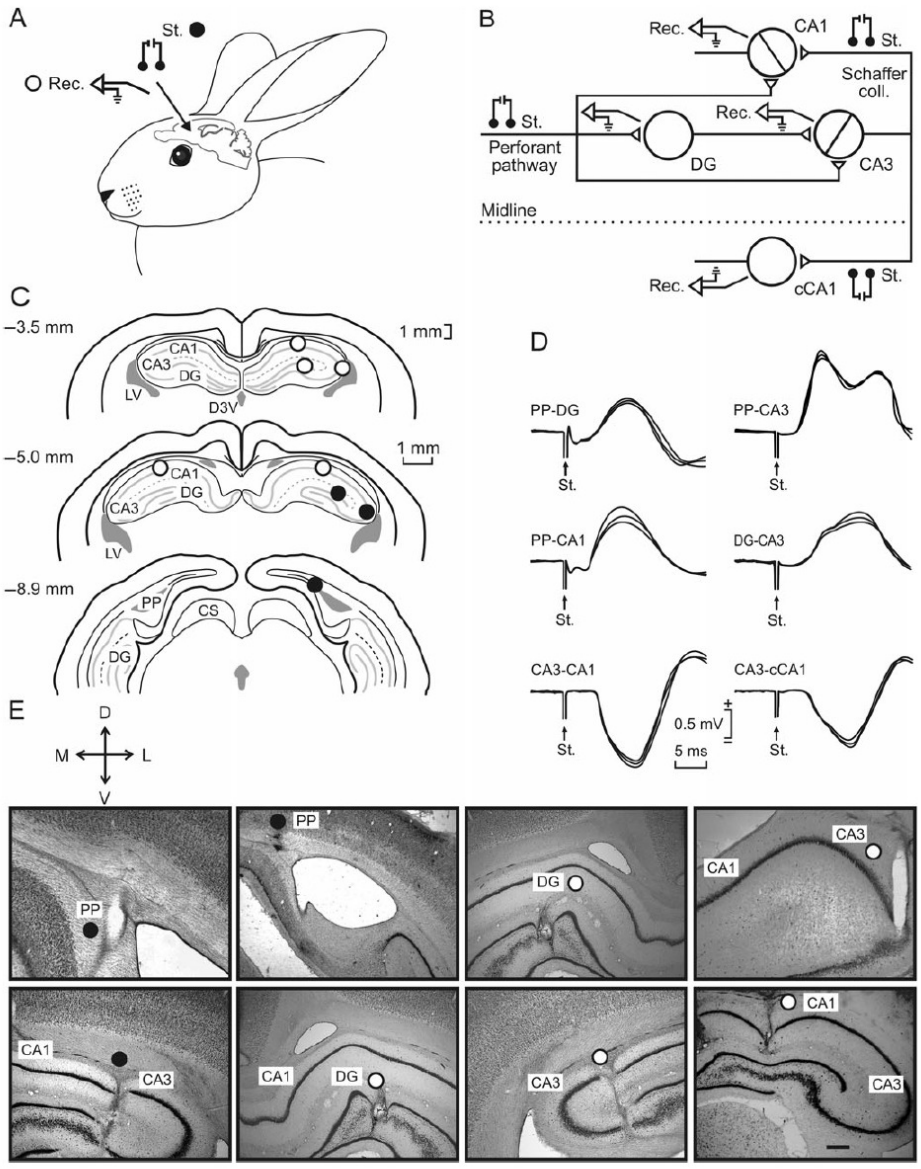

Figure 1. Experimental design. (*A*,*B*) For the classical conditioning of eyelid responses, rabbits were chronically implanted with recording (Rec.) electrodes in the right dentate gyrus (DG) and hippocampal CA1 and CA3 areas, as well as in the contralateral CA1 (cCA1) area. Animals were also implanted with stimulating (St.) electrodes in the perforant pathway and in the ipsi- and contralateral Schaffer collateral/commissural pathway. (*C*) Schematic diagrams in stereotaxic coordinates from rabbit brain (modified from Girgis and Shih-Chang 1981) with indication of selected recording (white circles) and stimulating (black circles) sites. (*D*) Representative records collected from the 6 (PP-DG, PP-CA3, PP-CA1, DG-CA3, CA3-CA1, and CA3-cCA1) synapses included in this study. Calibration at the bottom is for all records. (*E*) Different photomicrographs illustrating the final location of stimulating (black circles) and recording (white circles) electrodes. Calibration bar is 1 mm. D, L, M, V, dorsal, lateral, medial, ventral; CS, superior colliculus; D3 V, dorsal part of the third ventricle; LV, lateral ventricle; PP, perforant pathway.

several (up to 3) stimulating and (up to 16) recording electrodes. Stimulating (bipolar) and recording (tetrode) electrodes were made from 50 µm, Teflon-coated tungsten wire (Advent Research Materials Ltd., Eynsham, England). Tetrode diameter was ≈ 110 µm. The impedance of recording electrodes was always >1 MΩ. The final position of hippocampal stimulating and recording electrodes was determined under recording procedures until a reliable monosynaptic field EPSP was identified (Fig. 1*D*; see Gruart et al. 2006 for details). All the animals were also implanted with recording bipolar hook electrodes in the left orbicularis oculi muscle to record its EMG activity (Fig. 2*A*). These electrodes were made from Teflon-coated stainless steel wire (A-M Systems, Sequim, WA, USA) with an external diameter of 50 µm. A silver electrode (1 mm in diameter) was attached to the skull (occipital bone) as a ground. Terminals of hippocampal stimulating and recording, EMG, and ground electrodes were soldered to three 9-pin sockets. All wire connections were covered with cyanoacrylate glue, and the whole system was attached to the skull with the aid of 3 small screws fastened and cemented with an acrylic resin to the bone (for details see Leal-Campanario et al. 2007).

Recording and Stimulation Procedures

Recording sessions began 2 weeks after surgery. The animal was placed in a Perspex box specially designed for limiting the subject's movements (Gruart et al. 2000). The box was placed on the recording table and covered by a black cloth. The recording room was kept softly illuminated, and a 60-dB background white noise was switched on during the experiments. Animals were divided in 4 experimental groups: context, pseudoconditioning, and trace and delay conditioning.

The EMG activity of the selected muscle was recorded using Grass P511 differential amplifiers with a bandwidth of 0.1 Hz to 10 kHz (Grass-Telefactor, West Warwick, RI, USA). FEPSPs were recorded with a 16-channel extracellular differential AC amplifier (Model 3500, A-M Systems) provided with a head-stage interface adapter.

Air puffs aimed at the left cornea were applied through the opening of a plastic pipette (3 mm in diameter) attached to a metal holder fixed to the animal's 9-pin socket (Dual-channel air-puff device, Biomedical Engineering, Co.). Tones were applied from a loudspeaker located 80 cm below the animal's head. Electrical stimulation of the selected sites was achieved with a CS-220 stimulator across an ISU-220 isolation unit

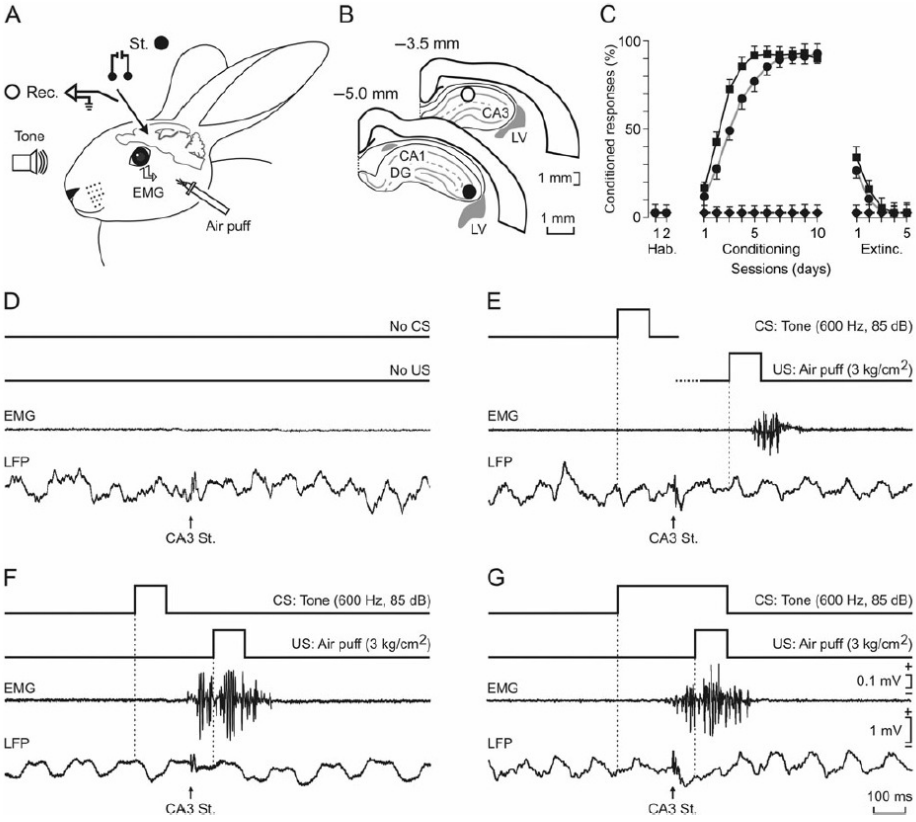

Figure 2. Classical conditioning paradigms. (*A*) In addition to hippocampal stimulating and recording electrodes (Fig. 1), animals were implanted with EMG recording electrodes in the left orbicularis oculi muscle. For classical eyeblink conditioning, the US consisted of an air puff presented to the ipsilateral cornea, while the CS consisted of tones presented biaurally. (*B–G*) Animals were presented with 4 different training situations: 1) placed in the restraining box with no CS or US presentations (*D*); 2) pseudoconditioning (*E*) with non-paired CS and US presentations; 3) a trace conditioning paradigm (*F*); and, 4) a delay conditioning paradigm (*G*). In *D–G* and from top to bottom are illustrated CS and US presentations, the EMG activity of the orbicularis oculi muscle, and the local field potential recorded in the CA1 area (white circle in *B*), as well as the fEPSP evoked by a stimulus presented to the ipsilateral Schaffer collaterals (black circle in *B*). Calibrations in *G* are also for (*D–F*). Note that only trace and delay conditioning evoked CRs. The corresponding learning curves evoked by pseudoconditioning (black diamonds), and trace (black circles) and delay (black squares) paradigms are illustrated in (*C*), during the successive habituation (Hab.), conditioning, and extinction (Extinc.) sessions.

(Cibertec, Madrid, Spain). Single (cathodal, square, 50 μs, <1 mA pulses) or paired (40 of interpulse interval) stimuli were programmed.

Classical Eyeblink Conditioning

Conditioning consisted of 2 habituation, 10 conditioning, and 5 extinction sessions. The trace conditioning paradigm consisted of a 100 ms, 600 Hz, 85 dB tone followed 250 ms after CS onset by a 100 ms, 3 kg/cm^2 air puff aimed at the left cornea; thus, a trace interval of 150 ms was left between CS end and US onset. In the delay paradigm, the CS consisted of a 350 ms, 600 Hz, 85 dB tone. The US started 250 ms after CS onset, and consisted of a 100 ms, 3 kg/cm^2 air puff aimed at the left cornea; in this case, the US co-terminated with the CS. Conditioning sessions consisted of 66 trials (6 series of 11 trials each) separated at random by intervals of 50–70 s. Of the 66 test trials, 6 were trials in which the CS was presented alone. A complete conditioning session lasted for ~ 1 h. The CS was presented alone during habituation and extinction sessions for the same number of blocks/session and trials/block. As criterion, we considered a "CR" the presence—during the CS-US interval—of EMG activity lasting >10 ms and initiated >50 ms after CS onset. In addition, the integrated EMG activity recorded during the CS–US interval had to be at least 1.2 times greater than the integrated EMG recorded immediately before CS presentation (Porras-García et al. 2010). As a criterion for learning, animals should evoke >70% CRs by the 10th conditioning session (Gruart et al. 2000; Leal-Campanario et al. 2007).

For context sessions, the animal was set in the restraining box for 1 h during a total of 17 sessions. No CS or US were presented during context sessions. For pseudoconditioning, unpaired CS and US were presented for 10 sessions (66 times/session) preceded by 2 and followed by 5 sessions during which the CS was presented alone. Pseudoconditioned animals also received 2 habituation and 5 extinction sessions as indicated above.

For trace and delay conditioning, as well as for pseudoconditioning, animals were stimulated in the selected brain sites at 200-ms following CS presentation. In the context group, animals were stimulated at random by intervals of 50–70 s for a total of 66 times.

Histology

At the end of the experiments, animals were deeply anesthetized with sodium pentobarbital (50 mg/kg, i.p.), and perfused transcardially with saline and 4% paraformaldehyde. In order to determine the final location of recording and stimulation sites, the brain was removed and cut into slices (50 μm), and the relevant brain areas were processed for Nissl (toluidine blue) staining (Fig. 1*E*).

Data Collection and Analysis

fEPSPs, the unrectified EMG activity of the recorded muscles, and 1-V rectangular pulses corresponding to CS, US, and electrical stimuli presented during the different experimental situations, were acquired on-line through an 8-channel analog-to-digital converter (CED 1401-plus, CED, Cambridge, UK), and transferred to a computer for quantitative offline analysis. Data were sampled at 8000 Hz (for fEPSP recordings) or 4000 Hz (for EMG recordings), with an amplitude resolution of 12 bits. Computer programs (Spike2 and SIGAVG from CED) were used to analyze field potentials and EMG activities. These programs allowed the quantification, with the aid of cursors, of the onset latency and area (mV × s) of the rectified EMG activity of the orbicularis oculi muscle. Field synaptic potentials (in mV) collected from the same session ($n = 66$) and animal were averaged, and the mean value of the slope (in mV/s) was determined for the rise time period (i.e., the period of the slope between the initial 10% and the final 10% of the evoked field potential).

Statistical analyses were performed using the Sigma Plot 11.0 package (Sigma Plot, San Jose, CA, USA), for a statistical significance level of $P = 0.05$. Unless otherwise indicated, mean values were calculated from ≥15 electrodes, collected from 6 animals. Mean values are followed by their standard error. Nonlinear regression analysis was used to study the evolution of fEPSP slopes across conditioning sessions (Fig. 3*E*) for the 4 experimental conditions. Collected data were analyzed using the one-way or two-way ANOVA test, with time or session as repeated measure, coupled with contrast and/or nonparametric analysis when appropriate. Repeated-measures ANOVA allowed checking the statistical differences of the same group across sessions. The Student *t*-test was used when necessary.

Results

Experimental Design and Identification of Stimulation and Recording Sites

As illustrated in Figure 1*A*, animals were prepared for the chronic recording of fEPSPs evoked in the neuronal components of the hippocampal intrinsic circuit by the electrical stimulation of the main afferent input to the hippocampus (i.e., the perforant pathway) or of some defined axonal projections inside the intrinsic circuit. In accordance with data collected from some preliminary experiments, we selected the following 6 synapses (Fig. 1*B*): the PP-DG and the hippocampal CA3 (PP-CA3) and CA1 (PP-CA1) areas, the dentate gyrus projection to the CA3 area (DG-CA3), the Schaffer collateral projection to CA1 pyramidal cells (CA3-CA1), and CA3 projections to contralateral CA1 neurons (CA3-cCA1). Stimulating and recording electrodes were implanted in the dorsal hippocampus at the sites illustrated in Figure 1*C*. Selected stereotaxic coordinates were collected from the atlas of Girgis and Shih-Chang (1981) and adjusted to obtain well-defined fEPSPs with minimum intensities (<1 mA). Figure 1*D* illustrates a set of representative fEPSPs evoked at the 6 selected synapses. In most of the cases, recorded fEPSPs presented latencies <6 ms —i.e., well in the range of or slightly shorter than those in classical reports of recordings of the same monosynaptic fEPSPs carried out in anesthetized rabbits (Andersen et al. 1966a,b; Lømo 1971a,b). Recorded fEPSPs presented positive or negative components depending on the location of the recording electrode with respect to the soma or dendrites of the postsynaptic element (Andersen et al. 1966a,b; Lømo 1971a,b; Bliss and Lømo 1973). Characteristically, fEPSPs evoked at the PP-CA3 synapse presented a second positive (or negative) component, indicating the secondary activation of pyramidal CA3 cells by DG afferents to them (Fig. 1*D*, top-right recordings). Finally, Figure 1*E* illustrates the proper location of stimulating and recording electrodes.

Context, Pseudoconditioning, and Trace and Delay Conditioning Paradigm Groups

For animal training, animals were additionally implanted with bipolar EMG recording electrodes in the left orbicularis oculi muscle—i.e., in the side contralateral to the hippocampal electrodes (Fig. 2*A*,*B*). Rabbits ($n = 6$ per group) were presented with the following paradigms: 1) Context situation: Animals were placed in the restraining box for 1 h/day for a total of 17 sessions; no CS or US were presented to them (Fig. 2*D*). 2) Pseudoconditioning: Animals were placed in the restraining box for 2 habituation, 10 pseudoconditioning, and 5 extinction sessions (Fig. 2*E*). iii) Trace paradigm: Animals were trained with the trace paradigm described in Materials and Methods (Fig. 2*F*). And, iv) Delay paradigm: These animals were trained with the delay paradigm described in Materials and Methods (Fig. 2*G*).

In all cases, sessions lasted for 1 h and a total of 66 paired (or unpaired) CS and US stimuli were presented during the

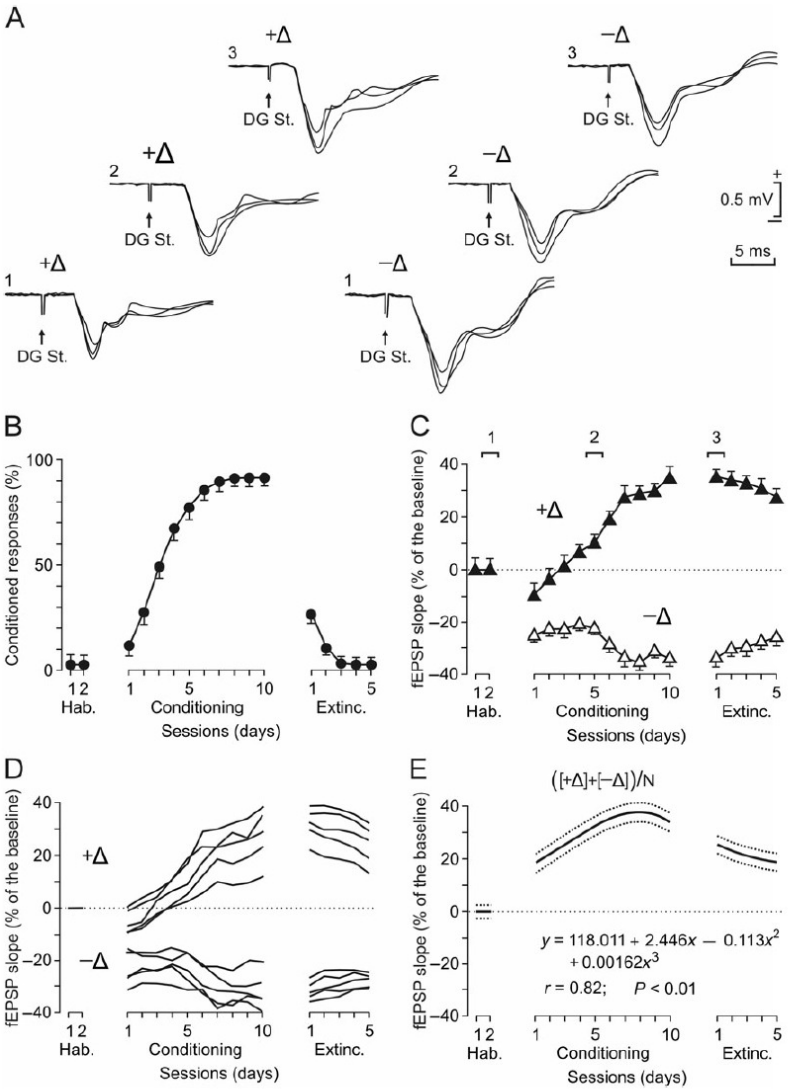

Figure 3. Results collected at the hippocampal DG-CA3 synapse during classical eyeblink conditioning using a trace paradigm. (*A*) Representative examples of fEPSPs recorded from 2 different electrodes located in the hippocampal CA3 area and evoked by the electrical stimulation of the ipsilateral DG. (*B*) Evolution of CRs in the group of rabbits ($n = 6$) trained with a trace paradigm. (*C*) Evolution of fEPSP slopes, recorded from two different electrodes implanted in the CA3 area, across the successive training sessions illustrated in (*B*). Representative examples of the recorded fEPSPs at the indicated times (1, 2, 3) are illustrated in A for the 2 recording sites. (*D*) Evolution of fEPSP slopes recorded from selected electrodes implanted in the CA3 area. fEPSPs were evoked by the electrical stimulation of the ipsilateral DG. Note that fEPSPs either increase (+Δ, $n = 5$) or decrease (−Δ, $n = 5$) in slope across training. (*E*) Algebraic mean [([+Δ] + [−Δ])/*N*] of fEPSP evolution from electrodes ($n = 15$) located in the hippocampal CA3 area and activated by DG stimulation. The equation corresponding to the best polynomial fit to data collected during conditioning sessions is indicated, as well as the corresponding regression curve and the simultaneous 95% confidence bands.

session. As illustrated in Figure 2*B,D–G*, animals of the 4 groups were stimulated at a minimum of 1, or a maximum of 3, hippocampal synapses included in this study. Although the stimuli presented to selected sites disrupted for 100–200 ms, the regular theta rhythm identified in the recorded local field potentials, the rhythm reappeared in phase afterward (Gruart et al. 2006).

Animals included in the context group did not present any CR (Fig. 2*D*). Pseudoconditioned animals presented a low number (<10%) of CRs during the pseudoconditioning sessions—i.e., at a rate similar to values presented during habituation and extinction sessions. Obviously, the pseudoconditioned group failed to reach criterion (>70% of CRs) by the 10th conditioning session (Fig. 2*C,E*). For the animals included in the

trace group, the percentage of CRs increased rapidly across conditioning, reaching 50% by the third conditioning session and asymptotic values (90%) from the 7th to the 10th conditioning sessions. The trace group presented CR values significantly larger than those collected during habituation from the 3rd to the 10th conditioning sessions [$F_{10,54} = 51.352$; $P < 0.001$; Fig. 2*C,F*]. Finally, the delay group acquired their conditioning paradigm even faster than the trace group, reaching percentages of CRs significantly different from habituation values from the 2nd to the 10th conditioning sessions [$F_{10,54} = 24.677$; $P < 0.001$; Fig. 2*C,G*].

Analysis of the Evolution of Evoked Fepsp Across Training Sessions

In order to facilitate the interpretation of the collected results, we will explain here a representative example of the changes taking place at the 6 selected hippocampal synapses across the successive training sessions in the 4 experimental groups. Specifically, in Figure 3 are illustrated the changes in synaptic strength taking place at the DG-CA3 synapse in the trace conditioning group.

In accordance with an early study (Weisz et al. 1984), fEPSPs evoked by the electrical stimulation of the perforant pathway changed in slope in the trace conditioning group (taking the slope of fEPSPs collected during the 2 habituation sessions as 100%) across conditioning sessions. However, those changes could represent either an increase or a decrease with respect to baseline values. As illustrated in Figure 3*A*, fEPSPs recorded at different sites corresponding to the DG-CA3 synapse either increase (left set of recordings) or decrease (right set of recordings) across the training. A quantitative analysis of the first recording site (Fig. 3*A*, +Δ electrode, and Fig. 3*C*, black triangles) showed fEPSPs significantly larger [$F_{7,127} = 71.514$; $P < 0.001$] than baseline (habituation) values from the 6th to the 10th conditioning sessions and for the 5 extinction sessions. Similarly, the second recording site (Fig. 3*A*, −Δ electrode, and Fig. 3*C*, white triangles) evoked fEPSPs significantly smaller [$F_{6,111} = 47.628$; $P < 0.001$] than baseline values from the 5th to the 10th conditioning sessions and for the 5 extinction sessions. In Figure 3*D* is represented the evolution at 5 recording sites corresponding to the DG-CA3 synapse, presenting fEPSPs that increased (+Δ) significantly ($P \leq 0.01$) in slope across conditioning, and another 5 recording sites presenting fEPSPs that decreased (−Δ) significantly ($P \leq 0.01$) in slope across training. Following 2 previous studies (Whitlock et al. 2006; Fernández-Lamo et al. 2009), we also considered those recording sites that did not change significantly in slope across training (i.e., when regression analysis applied to the collected slopes did change <±1 SD). Using this analytical procedure, we found that for the DG-CA3 synapse, 40% (6 of 15) of the recording electrodes showed a significant increase ($P \leq 0.01$) in slope across conditioning sessions, while 33.3% (5 of 15) presented decreasing ($P \leq 0.01$) fEPSP slopes, and 26.7% (4 of 15) presented no significant changes. The polynomial regressions shown in Figure 3*E* correspond to the algebraic mean [([+Δ] + [−Δ])/*N*] of data collected from electrodes (*N*) presenting significant changes during conditioning sessions. The regression illustrated in Figure 3*E* is a good representation of changes in synaptic strength taking place in the DG-CA3 synapse during trace conditioning in behaving rabbits.

Changes in Synaptic Strength Taking Place in the 6 Selected Synapses During the 4 Experimental Procedures

All of the recorded changes in fEPSP slopes for the 6 hippocampal synapses included in this study and collected during the 4 training protocols (context, pseudoconditioning, and trace and delay conditioning paradigms) were analyzed as already illustrated in Figure 3 for the DG-CA3 synapse during a trace conditioning paradigm. As shown in Figure 4, the increase in the percentage of CRs (Fig. 4*A*) and the change [([+Δ] + [−Δ])/*N*] in synaptic strength taking place at each selected synapse (Fig. 4*B*) were transduced into a color code. Thus, in Figure 4*C–F*, we show the increase in the percentage of CRs (isolated left bar in *C-F*) and the changes in fEPSP slopes taking place in the 6 selected synapses (PP-DG, PP-CA3, PP-CA1, DG-CA3, CA3-CA1, and CA3-cCA1) during context (*C*), pseudoconditioning (*D*), and trace (*E*) and delay (*F*) conditioning paradigms. For the sake of clarity, the same fEPSP results collected from the 6 synapses are represented in Figure 5 in the form of best polynomial fit ($r \geq 0.81$; $P \leq 0.01$) for context (*A*1), pseudoconditioning (*B*1), and trace (*C*1) and delay (*D*1) conditioning. A minimum of 15 recording electrodes/selected synapse presenting absolute changes in strength were included in the analysis illustrated in Figures 4 and 5.

Just placing experimental animals in the restraining box for up to 17 sessions (context group) evoked significant ($P \leq 0.007$) changes in fEPSP slopes (Fig. 4*C*) at selected synapses and at different times across training. The most noticeable increase in activity took place at the PP-DG synapse in the very first sessions of the training. Similar increases in fEPSP slopes were also observed in the CA3-CA1 and CA3-cCA1 synapse, but for a short period of time. The most-significant ($P \leq 0.01$) and longest lasting changes in synaptic strength took place at the 3 input synapses (PP-DG, PP-CA3, PP-CA1) representing an input to the hippocampal intrinsic circuit. It should be pointed out that the increased activity observed in hippocampal synapses during the first training sessions decreased with time (Figs 4*C* and 5*A*1).

The pseudoconditioning group also presented sustained ($P \leq 0.01$) changes in the 3 input synapses (PP-DG, PP-CA3, PP-CA1) to the hippocampal intrinsic circuit during the first 10–12 training sessions (Fig. 4*D*). Similar increases in synaptic strength, but of a shorter duration, were also observed in the CA3-CA1 and CA3-cCA1 synapses (Fig. 4*D*). As already indicated for the context group, the slopes of fEPSPs evoked at the 6 selected synapses during pseudoconditioning decreased progressively with training, reaching the lowest values during the last 2 training sessions (Figs 4*D* and 5*B*1).

During trace conditioning, animals presented very interesting changes in absolute synaptic strength (Fig. 4*E*). First, major changes took place across the training (i.e., during both conditioning and extinction) sessions. Major significant ($P \leq 0.01$) changes in synaptic strength were observed not only in the PP-DG synapse, but also in some of the synapses included in the hippocampal intrinsic circuit (DG-CA3, CA3-CA1, and CA3-CA1c). Other synapses (PP-CA3 and PP-CA1) were apparently less involved in the acquisition of this trace conditioning paradigm. Some synapses (PP-DG, DG-CA3, and CA3-CA1) were still very active during the last extinction sessions (Fig. 4*E*).

Finally, during delay conditioning (Fig. 4*F*), we observed changes in synaptic strength not exactly equal to those noticed during trace conditioning. For example, in this case, the synapses presenting the highest rate of change ($P \leq 0.01$) were 2

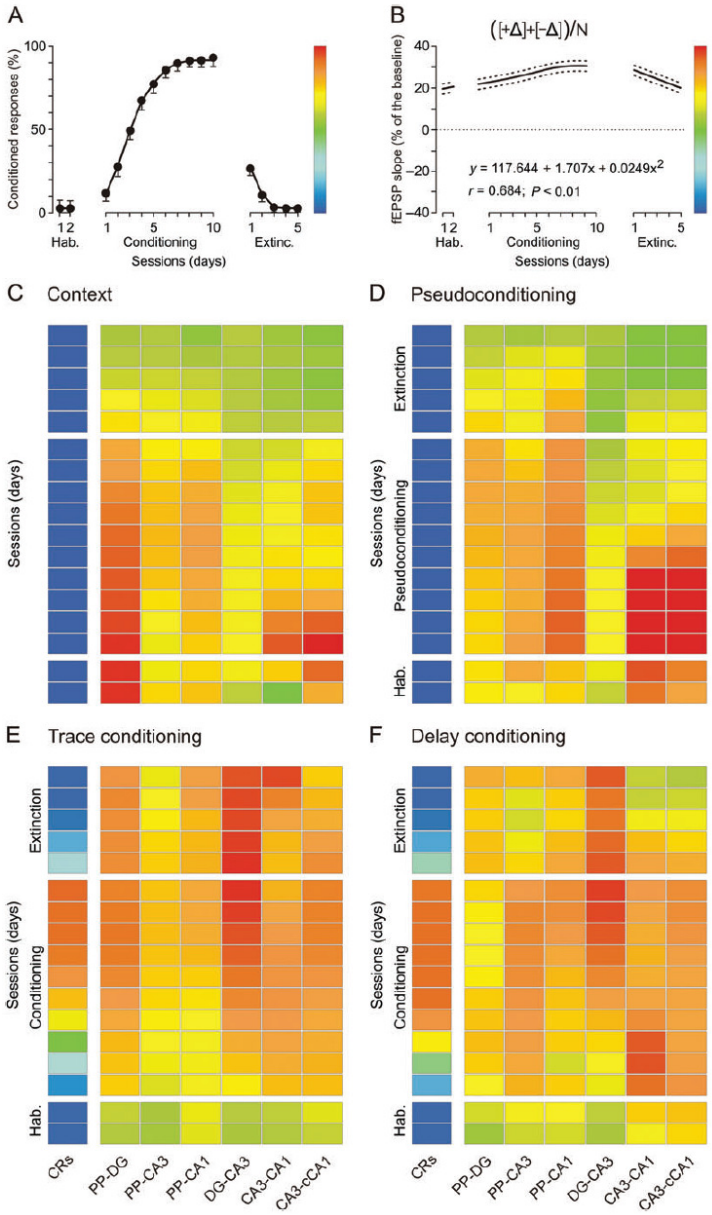

Figure 4. Evolution of fEPSP slopes at 6 different synapses of the hippocampal intrinsic circuit during the 4 selected conditioning situations. (*A,B*) Evolution of CRs (*A*) and of fEPSP slopes evoked at the CA3-cCA1 synapse (*B*) across conditioning sessions using a trace paradigm ($n = 6$ animals). Illustrated fEPSP regression curves were averaged $[([+\Delta] + [-\Delta])/N]$ from 15 electrodes implanted in the cCA1 area. The equation corresponding to the best polynomial fit to data collected during conditioning sessions is indicated, as well as the corresponding regression curve and the simultaneous 95% confidence bands. Note the color code bars located to the right of (*A*) and (*B*) panels. (*C–F*) Evolution of CRs (%) and of fEPSP slopes (as % of baseline values, see (*B*) collected at 6 hippocampal synapses across the successive training sessions in 4 different experimental situations: context (no CS or US presentations, (*C*), pseudoconditioning (*D*), and trace (*E*) and delay (*F*) conditioning paradigms. In the case of context (*C*) and pseudoconditioning (*D*), we took as baseline the values of fEPSP slopes collected during the last 2 (14th and 15th) training sessions. In contrast, baseline values for fEPSP slopes in trace (*E*) and delay (*F*) conditioning were collected from the first two (habituation) sessions.

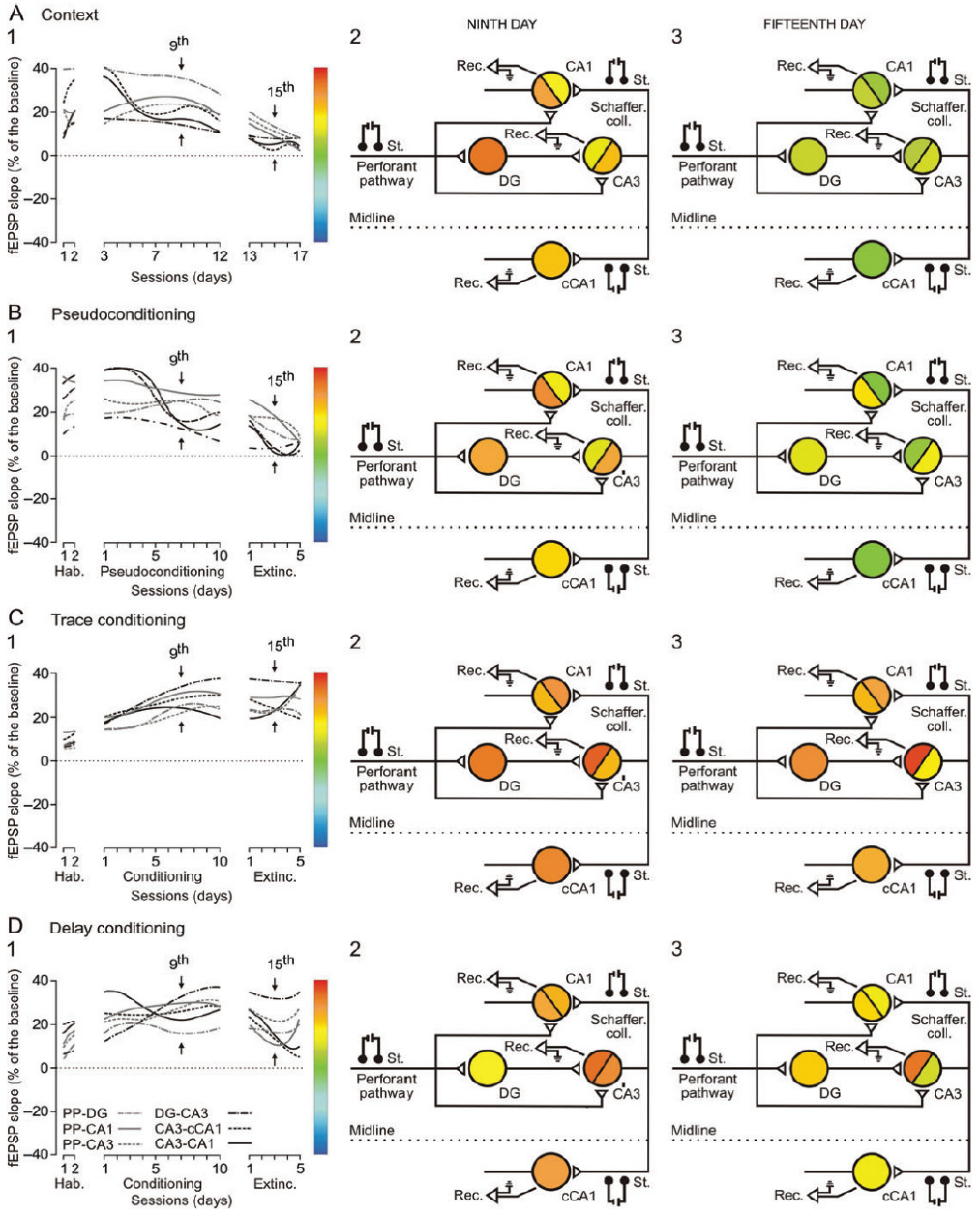

Figure 5. Main changes in synaptic strength evoked in the hippocampal circuit by context and cues present during classical eyeblink conditioning tasks. (*A–D*) Evolution of fEPSP slopes at the 6 selected synapses during context (*A*), pseudoconditioning (*B*), and trace (*C*) and delay (*D*) conditioning. For (*A–D*) in ***1*** are illustrated the best polynomial fits ($r \geq 0.81$; $P \leq 0.01$) for the fEPSP data collected from the 6 selected synapses (see line codes in ***D1***), while in ***2–3*** are represented the synaptic strength corresponding to each synapse and collected during the 9th (corresponding to the 7th conditioning or pseudoconditioning session; see arrows) and 15th (corresponding to the third extinction session; see arrows) recording days. The corresponding color codes are represented to the right of panels ***1*** (for *A–D*). Note that for context, the major changes in the 9th training session were observed at the PP-DG and—with lower intensity—the PP-CA3 and PP-CA1 synapses. Similar results were collected in the 9th training session from pseudoconditioned rabbits. In contrast, during the equivalent training session for trace conditioning, major changes in synaptic strength were observed not only in the input synapses to the hippocampus (PP-DG, PP-CA3, and PP-CA1), but also in the intrinsic circuit (DG-CA3, and to a lower degree in CA3-CA1 and CA3-cCA1 synapses). Similar results were collected during delay conditioning.

located in the hippocampal intrinsic circuit—DG-CA3 and CA3-CA1—although the changes in the former took place later than those in the latter. Interestingly enough, some seminal studies (Segal and Olds 1972; Segal et al. 1972) did report changes in the CA3-CA1 synapse not dependent upon those taking place in the DG, using a tone-food association test. Finally, smaller changes in strength were also observed in synapses corresponding to hippocampal inputs (PP-CA3) and the hippocampal commissural pathway (CA3-cCA1).

Functional State of Hippocampal Circuits at a Given Moment Across Training

Figure 6 represents an attempt to display the functional state of the hippocampal circuits included in this study at a similar moment (i.e., the 9th and the 15th recording days) across training in the 4 experimental situations considered here: context (Fig. 5*A*2,3), pseudoconditioning (Fig. 5*B*2,3), and trace (Fig. 5*C*2,3), and delay (Fig. 5*D*2,3) conditionings. Results included in these diagrams illustrate clearly the different functional states in which hippocampal circuits are placed during these 4 experimental situations. For example, in both context and pseudoconditioning, peak changes by the 9th recording day were observed at synapses afferent to hippocampal circuits (mainly PP-DG, and to a lesser degree PP-CA3 and PP-CA1). In contrast, by the same recording day (corresponding to the 7th conditioning session in conditioned animals), the main changes in synaptic strength taking place during both trace and delay conditioning also involved synapses located in the hippocampal intrinsic circuit (i.e., DG-CA3, CA3-CA1) or in the commissural pathway (CA3-cCA1). Differences were even more noticeable during the 15th training day (corresponding to the third extinction session in conditioned animals), because most hippocampal synapses presented the lowest changes in strength in both context and pseudoconditioning groups, while considerable changes in strength were still taking place in the hippocampal circuit in both trace (mostly PP-DG, DG-CA3, and CA3-CA1 synapses) and delay (mostly in the DG-CA3 synapse) during this (third) extinction session. Similar results are obtained considering the functional status of each selected synapse for a given day and training situation (see Fig. 4*C*–*F*). Thus, the hippocampus seems to present a different functional state for each experimental situation and even for each day, across the successive training sessions.

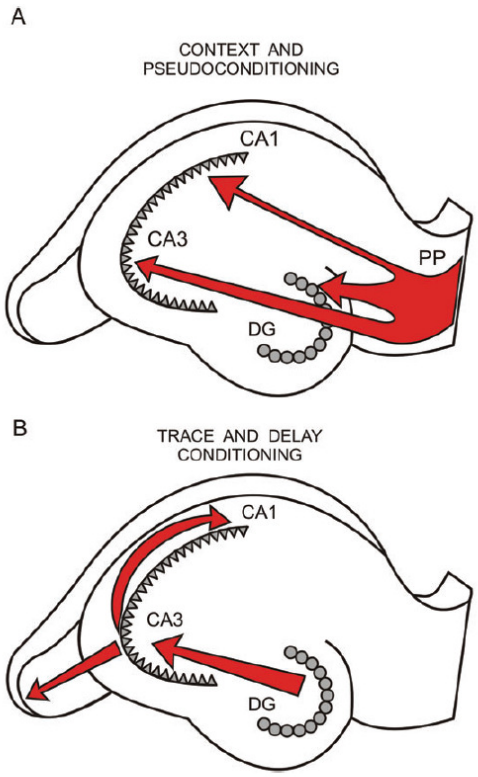

Figure 6. A diagrammatic representation of the major changes in synaptic strength taking place in hippocampal inputs and intrinsic circuit during context and pseudoconditioning (*A*) and during trace and delay conditioning (*B*).

Discussion

General Remarks

We have shown here that hippocampal synapses included in the main afferent inputs and intrinsic circuit are involved in selective processes related not only to the acquisition and extinction of different forms (trace and delay) of classical eyeblink conditioning, but also in more general aspects of the learning situation—namely those related to environmental settings and to the unpaired presentations of CS and US. The 6 different hippocampal synapses included in this study underwent a slow algebraic modulation (i.e., increase or decrease) in synaptic strength (Konorski 1948; Hebb 1949) across the different training situations in parallel (as shown by nonlinear regression analyses) with the acquisition and extinction of conditioned eyelid responses and/or the mere repetition of sessions (context and pseudoconditioning). Interestingly, changes in synaptic weights did not take place simultaneously in the 6 selected synaptic sites nor presented similar absolute changes in strength across the successive training sessions. Obviously, this new picture of differential plastic changes taking place in different hippocampal synapses in a given experimental situation and in a precise moment across the training situation was not possible to observe if only one synapse was observed (Weisz et al. 1984; Gruart et al. 2006; Whitlock et al. 2006). In addition, present results convincingly suggest that a specific functional synaptic state corresponds to each learning paradigm and training session (Fig. 5). In particular, direct projections from the entorhinal cortex to the 3 main neuronal elements of the hippocampal intrinsic circuit (i.e., PP-DG, PP-CA3, and, to a lesser degree, PP-CA1 synapses) seemed to be mostly involved in general and/or contextual aspects of the training situation, while those synapses integrating the intrinsic circuit (DG-CA3, CA3-CA1, and CA3-cCA1) were preferentially involved in aspects related to CS predictive value and/or CS-US associative strength (see Fig. 6; Rescorla 1988; Eichenbaum 1999; Múnera et al. 2001).

Separate Roles of Hippocampal Inputs and Intrinsic Circuit

The separation of functions between entorhinal projections to the hippocampus and hippocampal synapses involved in its

intrinsic circuit reported here has already been proposed on both theoretical (Marr 1971; McNaughton and Morris 1987; Treves and Rolls 1994) and experimental (McHugh et al. 2007; McHugh and Tonegawa 2009; Nakashiba et al. 2012) grounds. In short, direct projections from the entorhinal cortex to the dentate granule neurons and to hippocampal CA3 and CA1 pyramidal cells will carry memory information related to general environmental aspects, places, and other spatial-temporal details and configurations. The proportionally large number of dentate granule neurons will allow the proper separation of these sensory-motor and cognitive memories. As shown here, those incoming entorhinal patterns of activity not involved in Hebbian association processes (Konorski 1948; Hebb 1949) will be erased and/or blocked at these 3 (PP-DG, PP-CA3, and PP-CA1) hippocampal synapses. Similar filtering and/or erasing roles have already been proposed for the dentate gyrus (Hsu 2007; McHugh et al. 2007; Nakashiba et al. 2012), and the hippocampal CA3 (McHugh and Tonegawa 2009) and CA1 (Izumi and Zorumski 2008) areas. In contrast, synapses involved in the hippocampal intrinsic circuit (represented here by the DG-CA3, CA3-CA1, and CA3-cCA1 synapses) will play a discriminant role, reinforcing Hebbian association between relevant environmental stimuli (Vinogradova 2001; Hsu 2007), such as, for example, that taking place between CS and US presented in a paired form during both trace and delay paradigms. It has been proposed that this selective role of the hippocampal intrinsic synapses will be supported on the dense network of axon collaterals reaching both CA3 and CA1 pyramidal neurons (Lorente de Nó 1933, 1934; Marr 1971; Amaral 1993). Currently, it is assumed that these recurrent connections will probably help to determine the CS cognitive salience and/or the CS-US associative strength. This conceptual approach to hippocampal functions is further support by data provide here (see Figs 4 and 5). In addition, Figure 6 attempts to represent in a diagrammatic form these important functional differences and specific roles of hippocampal inputs and that of its intrinsic circuit.

Involvement of the Hippocampus in the Acquisition of Classical Conditioning of Eyelid Responses

In an early, seminal study, Weisz et al. (1984) demonstrated a change in the strength of synaptic activation of dentate granule cells by perforant pathway axons during the acquisition of nictitating membrane CRs in behaving rabbits. This activity-dependent modulation in synaptic strength was further confirmed for the CA3-CA1 synapse of behaving mice, and extended to the extinction process (Gruart et al. 2006), suggesting that the 2 phenomena are equally active (Dudai 2012). Moreover, it has also been shown that the changes in synaptic efficacy evoked in the hippocampal CA3-CA1 synapse present a linear relationship with the amount of acquired, or extinguished, learning (Gruart et al. 2006). The increase in fEPSP slope during the acquisition process explains the increased firing in hippocampal CA1 areas across conditioning, described for both rabbits (McEchron et al. 2003) and cats (Múnera et al. 2001).

The involvement of hippocampal unitary activity in classical conditioning of the nictitating membrane/eyelid responses was reported years ago (Berger et al. 1983; Moyer et al. 1990). Hippocampal pyramidal cell firing to CS presentation increases several sessions in advance of behavioral conditioning (McEchron and Disterhoft 1997). Although it has been shown that the discharge rate of hippocampal CA1 pyramidal neurons does not encode the kinematic peculiarities of conditioned eyelid responses (Múnera et al. 2001; Sánchez-Campusano et al. 2007), discharge rates of CA1 pyramidal cell firing appear linearly related to the progressive acquisition of CRs, with a gain of ≈ 0.035 spikes/s/trial, as measured in behaving cats during trace conditioning (Múnera et al. 2001). It is of note that this slow building up of hippocampal neuronal firing responses across conditioning sessions is similar to the maximum increases in fEPSP slopes evoked at the 6 synapses included in this study (i.e., ≈0.03–0.04% increase in fEPSP slope/trial). A similar increase in the slope of fEPSPs recorded in the CA3-CA1 synapse during trace (tone-shock) conditioning of behaving mice has also been reported (Gruart et al. 2006). Taken together, these results suggest that changes in neuronal firing rates across conditioning sessions are more-or-less related to the underlying changes in synaptic efficacy.

Although it has been pointed out (Moyer et al. 1990) that 250-ms trace conditioning is not dependent of the hippocampus in the rabbit, results collected here (Figs 4 and 5) convincingly shown that hippocampal circuits are also modified by this type of associative learning task.

The decrease in synaptic strength taking place in different recording sites in both input and intrinsic hippocampal synapses could be related to the recently reported increase in intrinsic excitability on hippocampal interneurons (McKay et al. 2013).

Functional Synaptic States Underlying Hippocampal Roles in Associative Learning

It has already been proposed (Delgado-García and Gruart 2002) that learning is a precise functional state of the brain, and that we should take a dynamic approach to the study of neural and synaptic activities in ensembles of sensorimotor circuits during actual learning in alert behaving animals. The color diagrams included in Figure 5*A–D* are a good illustration of the above contention, showing the significantly different synaptic weights presented by the 6 selected hippocampal synapses on the same training days, but in 4 different conditioning situations (i.e., context, pseudoconditioning, and trace and delay conditioning paradigms). In general, it can be proposed that each environmental and social situation demanding a behavioral response will evoke a corresponding differential state of synaptic weights in hippocampal circuits. Obviously, additional neural, synaptic, and motoric information can be collected experimentally and added to the better determination of ongoing functional states. For example, and with regard to classical eyeblink conditioning, it has already been reported that facial motoneurons present 2 specific functional states corresponding to their firing activities during reflexively evoked blinks and to their discharge rate during acquired (i.e., classically conditioned) eyelid responses (Delgado-García and Gruart 2006). However, it is important to point out that our information with regard to brain functioning during a given learning situation is greatly constrained by the difficulty of recording a large enough number of kinetic (i.e., firing and synaptic activities of neuronal elements) and kinematic (i.e., biomechanical characteristics of evoked motor responses) parameters in simultaneity with the newly acquired ability (Delgado-García and Gruart 2002). To solve these constraints, it seems necessary to record enough different neural kinetic data at the same time as

collecting data from enough kinematic variables. In a previous study, we were able to collect up to 24 kinetic variables (related to neural firing activities in the facial and cerebellar interpositus nuclei) together with 36 kinematic variables (related to eyelid biomechanics and to the electrical activity of the orbicularis oculi muscle) from alert behaving cats during classical eyeblink conditioning (Sánchez-Campusano et al. 2007). Present results further confirm the above contentions, and allow a dynamic interpretation of the hippocampal role in learning and memory processes underlying the acquisition of new motor and cognitive abilities, as opposed to an excessive localizationist view of hippocampal functions (McHugh et al. 2007). The hippocampus will have an almost infinite repertoire of functional states corresponding to the enormous possibilities of sensory stimulations and the different needs of behavioral responses. Thus, and depending on the specific and timed activation of its multiple synaptic contacts, the hippocampus would be involved in many different functions, such as object recognition (Clarke et al. 2010), spatial orientation (Moser et al. 2008), and other different forms of memory acquisition, storage, and retrieval (Bliss and Collingridge 1993; Neves et al. 2008; Wang and Morris 2010).

Funding

This study was supported by grants from the Spanish Ministry of Economy and Competitiveness (BFU2011-29089 and BFU2011-29286) and Junta de Andalucía (BIO122, CVI 2487, and P07-CVI-02686) to A.G. and J.M.D.-G.

Notes

The authors thank Dr Raudel Sánchez-Campusano for his help in the analysis of the data and Mr Roger Churchill for his help in manuscript editing. *Conflict of Interest*: None declared.

References

Amaral DG. 1993. Emerging principles of intrinsic hippocampal organization. Curr Opin Neurobiol. 3:225–229.

Andersen P, Blackstad TW, Lømo T. 1966a. Location and identification of excitatory synapses on hippocampal pyramidal cells. Exp Brain Res. 1:236–248.

Andersen P, Holmqvist B, Voorhoeve PE. 1966b. Entorhinal activation of dentate granule cells. Acta Physiol Scand. 66:448–460.

Berger TW, Rinaldi P, Weisz DJ, Thompson RF. 1983. Single-unit analysis of different hippocampal cell types during classical conditioning of rabbit nictitating membrane response. J Neurophysiol. 50:1197–1219.

Bliss TVP, Collingridge GL. 1993. A synaptic model of memory: long-term potentiation in the hippocampus. Nature. 361:31–39.

Bliss TVP, Lømo T. 1973. Long-lasting potentiation of synaptic transmission in the dentate area of the anesthetized rabbit following stimulation of the perforant path. J Physiol (Lond). 232:331–356.

Clarke JR, Cammarota M, Gruart A, Izquierdo I, Delgado-García JM. 2010. Plastic modifications induced by object recognition memory processing. Proc Natl Acad Sci USA. 107:2652–2657.

Delgado-García JM, Gruart A. 2006. Building new motor responses: eyelid conditioning revisited. Trends Neurosci. 29:330–338.

Delgado-García JM, Gruart A. 2002. The role of interpositus nucleus in eyelid conditioned responses. Cerebellum. 1:289–308.

Dudai Y. 2012. The restless engram: consolidations never end. Annu Rev Neurosci. 35:227–247.

Eichenbaum H. 1999. Conscious awareness, memory and the hippocampus. Nat Neurosci. 2:775–776.

Fernández-Lamo I, Montero-Pedrazuela A, Delgado-García JM, Guadaño-Ferraz A, Gruart A. 2009. Effects of thyroid hormone replacement on associative learning and hippocampal synaptic plasticity in adult hypothyroid rats. Eur J Neurosci. 30:679–692.

Girgis M, Shih-Chang W. 1981. A new stereotaxic atlas of the rabbit brain. St. Louis, MO: Warren H. Green.

Gruart A, Muñoz MD, Delgado-García JM. 2006. Involvement of the CA3-CA1 synapse in the acquisition of associative learning in behaving mice. J Neurosci. 26:1077–1087.

Gruart A, Schreurs BG, Domínguez del Toro ED, Delgado-García JM. 2000. Kinetic and frequency-domain properties of reflex and conditioned eyelid responses in the rabbit. J Neurophysiol. 83:836–852.

Hebb DO. 1949. The organization of behavior. New York (NY): Wiley.

Hsu D. 2007. The dentate gyrus as a filter or gate: a look back and a look ahead. Prog Brain Res. 163:601–613.

Izumi Y, Zorumski CF. 2008. Direct cortical inputs erase long-term potentiation at Schaffer collateral synapses. J Neurosci. 28:9557–9563.

Kandel ER. 2001. The molecular biology of memory storage: a dialogue between genes and synapses. Science. 294:1030–1038.

Konorski J. 1948. Conditioned reflexes and neuron organization. Cambridge (MA): Cambridge University Press.

Leal-Campanario R, Fairén A, Delgado-García JM, Gruart A. 2007. Electrical stimulation of the rostral medial prefrontal cortex in rabbits inhibits the expression of conditioned eyelid responses but not their acquisition. Proc Natl Acad Sci USA. 104:11459–11464.

Lømo T. 1971a. Patterns of activation in the monosynaptic cortical pathway: the perforant path input to the dentate area of the hippocampal formation. Exp Brain Res. 12:18–45.

Lømo T. 1971b. Potentiation of monosynaptic EPSPs in the perforant path-dentate granule cell synapse. Exp Brain Res. 12:46–63.

Lorente de Nó R. 1933. Studies on the structure of the cerebral cortex. I. The area entorhinalis. J Psychol Neurol (Lpz). 45:381–438.

Lorente de Nó R. 1934. Studies on the structure of the cerebral cortex. II. Continuation of the study of the ammonic system. J Psychol Neurol (Lpz). 46:113–177.

Marr D. 1971. Simple memory: a theory for archicortex. Philos Trans R Soc Lond B Biol Sci. 262:23–81.

McEchron MD, Disterhoft JF. 1997. Sequence of single neuron changes in CA1 hippocampus of rabbits during acquisition of trace eyeblink conditioned responses. J Neurophysiol. 78:1030–1044.

McEchron MD, Tseng W, Disterhoft JF. 2003. Single neurons in CA1 hippocampus encode trace interval duration during trace heart rate (fear) conditioning in rabbit. J Neurosci. 23:1535–1547.

McHugh TJ, Jones MW, Quinn JJ, Balthasar N, Coppari R, Elmquist JK, Lowell BB, Fanselow MS, Wilson MA, Tonegawa S. 2007. Dentate gyrus NMDA receptors mediate rapid pattern separation in the hippocampal network. Science. 317:94–99.

McHugh TJ, Tonegawa S. 2009. CA3 NMDA Receptors are required for the rapid formation of a salient contextual representation. Hippocampus. 19:1153–1158.

McKay BM, Oh MM, Disterhoft JF. 2013. Learning increases intrinsic excitability of hippocampal interneurons. J Neurosci. 33:5499–5506.

McNaughton BL, Morris RGM. 1987. Hippocampal synaptic enhancement and information storage within a distributed memory system. Trends Neurosci. 10:408–415.

Moser EI, Kropff E, Moser MB. 2008. Place cells, grid cells, and the brain's spatial representation system. Rev Neurosci. 31:69–89.

Moyer JR Jr, Deyo RA, Disterhoft JF. 1990. Hippocampectomy disrupts trace eye-blink conditioning in rabbits. Behav Neurosci. 104:243–252.

Múnera A, Gruart A, Muñoz MD, Fernández-Más R, Delgado-García JM. 2001. Discharge properties of identified CA1 and CA3 hippocampus neurons during unconditioned and conditioned eyelid responses in cats. J Neurophysiol. 86:2571–2582.

Nakashiba T, Cushman JD, Pelkey KA, Renaudineau S, Buhl DL, McHugh TJ, Rodriguez-Barrera V, Chittajallu R, Iwamoto KS, McBain CJ et al. 2012. Young dentate granule cells mediate pattern separation, whereas old granule cells facilitate pattern completion. Cell. 149:188–201.

Neves G, Cooke SF, Bliss TV. 2008. Synaptic plasticity, memory and the hippocampus: a neural network approach to causality. Nat Rev Neurosci. 9:65–75.

Porras-García E, Sánchez-Campusano R, Martínez-Vargas D, Domínguez-del-Toro E, Cendelín J, Vožeh F, Delgado-García JM. 2010. Behavioral characteristics, associative learning capabilities, and dynamic association mapping in an animal model of cerebellar degeneration. J Neurophysiol. 104:346–365.
Ramón y Cajal S. 1909–1911. Histologie du système nerveux de l'homme et des vertébrés. Paris, France: Malonie.
Rescorla RA. 1988. Behavioral studies of Pavlovian conditioning. Annu Rev Neurosci. 11:329–352.
Sánchez-Campusano R, Gruart A, Delgado-García JM. 2007. The cerebellar interpositus nucleus and the dynamic control of learned motor responses. J Neurosci. 27:6620–6632.
Segal M, Disterhoft JF, Olds J. 1972. Hippocampal unit activity during classical aversive and appetitive conditioning. Science. 175:792–794.
Segal M, Olds J. 1972. Behavior of units in hippocampal circuit of the rat during learning. J Neurophysiol. 35:680–690.
Treves A, Rolls ET. 1994. Computational analysis of the role of the hippocampus in memory. Hippocampus. 4:374–391.
Vinogradova OS. 2001. Hippocampus as comparator: role of the two input and two output systems of the hippocampus in selection and registration of information. Hippocampus. 11:578–598.
Wang SH, Morris RG. 2010. Hippocampal-neocortical interactions in memory formation, consolidation, and reconsolidation. Annu Rev Psychol. 61:49–79.
Weisz DJ, Clark GA, Thompson RF. 1984. Increased responsivity of dentate granule cells during nictitating membrane response conditioning in rabbit. Behav Brain Res. 12:145–154.
Whitlock JR, Heynen AJ, Shuler MG, Bear MF. 2006. Learning induces long-term potentiation in the hippocampus. Science. 313:1093–1097.

The Journal of Neuroscience, August 29, 2012 • 32(35):12129–12143 • 12129

Behavioral/Systems/Cognitive

Red Nucleus Neurons Actively Contribute to the Acquisition of Classically Conditioned Eyelid Responses in Rabbits

Renny Pacheco-Calderón, Alejandro Carretero-Guillén, José M. Delgado-García, and Agnès Gruart
Division of Neurosciences, Pablo de Olavide University, Seville-41013, Spain

The red nucleus (RN) is a midbrain premotor center that has been suggested as being involved in the acquisition and/or performance of classically conditioned nictitating membrane/eyelid responses. We recorded in rabbits the activity of RN and pararubral neurons during classical eyeblink conditioning using a delay paradigm. Neurons were identified by their antidromic activation from contralateral facial and accessory abducens nuclei and by their synaptic activation from the ipsilateral motor cortex (MC) and the contralateral cerebellar interpositus (IP) nucleus. For conditioning, we used a tone as a conditioned stimulus (CS) followed 250 ms later by a 100 ms air puff as an unconditioned stimulus (US) coterminating with it. Conditioned responses (CRs) were determined from the evoked changes in the electromyographic activity of the orbicularis oculi (OO) muscle. Recorded neurons were classified by their antidromic activation and by their changes in firing rate during the CS–US interval. Identified neurons increased their firing rates in relation to the successive conditioning sessions, but their discharge rates were related more to the EMG activity of the OO muscle than to the learning curves. Reversible inactivation of the IP nucleus with lidocaine during conditioning evoked a complete disappearance of both conditioned and unconditioned eyelid responses, and a progressive decrease in CR-related activity of RN neurons. In contrast, MC inactivation evoked a decrease in the acquisition process and an initial disfacilitation of neuronal firing (which was later recovered), together with the late appearance of CRs. Thus, RN neurons presented learning-dependent changes in activity following MC inactivation.

Introduction

The RN is a mesencephalic premotor center related to the generation and control of locomotion and of other more specific motor behaviors, including facial motor responses. The red nucleus (RN) receives substantial inputs from both the sensorimotor cortex and cerebellar nuclei (Miller and Gibson, 2009; Gruber and Gould, 2010). In this regard, the RN participates in the neuronal network connecting the cerebellar interpositus (IP) nucleus and the facial and accessory abducens nuclei, a neuronal circuit assumed to be involved in the acquisition and storage of classical eyeblink conditioning (Krupa et al., 1993). In this circuit, the RN is considered a mere relay center, while the learning-dependent changes in synaptic strength underlying the learning process take place in the IP nucleus, or in the overlying cerebellar cortex (Bracha et al., 2009; Freeman and Steinmetz, 2011). These contentions have been supported mainly in transient or permanent lesion studies (Chapman et al., 1990; Clark and Lavond, 1993), because there are only a few studies that have recorded and analyzed the firing activities of putative RN neurons during the acquisition and performance of classically conditioned nictitating membrane (Desmond and Moore, 1991) or eyelid (Porras-García et al., 2010) responses.

It was initially assumed that rubral projections to the facial muscles were collateral to descending rubrospinal axons originated at the magnocellular division of the RN (Courville, 1966). However, the use of more specific neuroanatomical tracing techniques has disproved such a contention, confirming that rubral projections to the facial and the accessory abducens nucleus originate in a specific dorsolateral subdivision of the parvocellular RN, including the pararubral area (Ruigrok and Cella, 1995; Morcuende et al., 2002). This information imposes the need for the proper identification of recorded RN units to precisely determine their contribution to the learning process. In addition, the RN appears to be a junction center (Pong et al., 2008) under the hierarchical control of both the cerebral and cerebellar cortices with a more than passive role in motor control. The selective transient inactivation of these two RN afferent pathways could give a more complete picture of the specific roles of RN neurons in associative learning.

To settle these questions, rabbits were prepared for the chronic recording of the EMG activity of the orbicularis oculi (OO) muscle and of the unitary activity of antidromic- and synaptically identified right RN and pararubral neurons during classical eyeblink conditioning using a delay paradigm. For conditioning, we used a 350 ms tone as a conditioned stimulus (CS) followed by 250 ms from its beginning by a 100 ms air puff directed at the contralateral cornea. Appropriate sites of the ipsilateral motor cortex (MC) and contralateral IP nucleus were subjected to electrical microstimulation and/or microinfusion of lidocaine. Collected results suggest that RN and pararubral neu-

Received April 12, 2012; revised July 6, 2012; accepted July 14, 2012.

Author contributions: J.M.D.-G. and A.G. designed research; R.P.-C., A.C.-G., J.M.D.-G., and A.G. performed research; R.P.-C., A.C.-G., J.M.D.-G., and A.G. analyzed data; R.P.-C., J.M.D.-G., and A.G. wrote the paper.

This study was supported by grants from the Spanish MINECO (BFU2011-29089 and BFU2011-29286) and Junta de Andalucía (BIO122, CVI 2487, and P07-CVI-02686). R.P.-C. is a visiting researcher from the Department of Biology, Faculty of Science and Technology, University of Carabobo, Venezuela. We thank Leopoldo Pérez-Rosendo for animal handling and care and Roger Churchill for his help in manuscript editing.

Correspondence should be addressed to Professor Agnès Gruart, División de Neurociencias, Universidad Pablo de Olavide, Ctra. de Utrera, Km. 1, 41013-Sevilla, Spain. E-mail: agrumas@upo.es.

DOI:10.1523/JNEUROSCI.1782-12.2012

 0270-6474/12/3212129-15$15.00/0

rons are involved more in the proper performance of eyelid conditioned responses (CRs) than in the acquisition process. In addition, the reversible inactivation of the MC and of the IP nucleus produced differential effects on conditioned and/or unconditioned eyelid responses. Interestingly, RN and pararubral neurons seemed to partially substitute the learning deficits evoked by MC, but not by IP nucleus, inactivation.

Materials and Methods

Experimental subjects. Experimental procedures were performed on adult male rabbits (New Zealand White albino; Isoquimen) weighing 2.3–3.1 kg on arrival. Before and after surgery, animals were maintained in the same room, but placed in independent cages. Animals were kept on a 12 h light/dark cycle, with a continuous control of humidity (55 ± 5%) and temperature (21 ± 1°C). Experiments were performed in accordance with European Union guidelines (2003/65/CE) and following Spanish regulations (RD 1201/2005) for the use of laboratory animals in chronic electrophysiological and behavioral studies. Experiments were also approved by the local Ethics Committee of the Pablo de Olavide University (Seville, Spain).

Surgical procedures. Animals were anesthetized with a ketamine–xylazine mixture (Ketaminol, 50 mg/ml; Rompun, 20 mg/ml; and atropine sulfate, 0.5 mg/kg) at an initial dosage of 0.85 ml/kg. Anesthesia was maintained by intravenous perfusion at a flow rate of 10 mg/kg/h.

As illustrated in Figures 1*A* and 2*A*, animals were prepared for the chronic recording of unitary activity in the RN area during classical eyeblink conditioning. For this, under aseptic conditions, a window (6 mm × 6 mm) was drilled through the occipital bone centered on the right RN [anteroposterior (AP) = −8.5 mm;, lateral (L) = 1 mm; Girgis and Shih-Chang, 1981]. The dura mater was removed and the cortical surface was protected with an inert plastic cover. A recording chamber was built with acrylic cement around the window. The recording chamber was covered with sterile gauze and a plastic cap during nonrecording sessions. A silver electrode (1 mm in diameter) in contact with the dura mater was attached to the left parietal bone (AP = −10 mm, L = 6 mm) as a ground for local field potential recordings. Animals were also implanted with stimulating electrodes aimed at the contralateral facial (AP = −18 mm, L = 3.5 mm; dorsal (D) = 10 mm from cerebellum surface) or at the accessory abducens (AP = −15.5 mm, L = 1.2 mm; D = 18 mm from cerebellum surface) nuclei. When necessary, the targeted stimulating sites were approached at AP angles. The final position of these stimulating electrodes was determined by the eyelid or eye retraction movements evoked by a pair of square (50 μs) pulses (1 ms interpulse interval and 0.5–2 mA) applied to the corresponding electrode.

In addition, selected animals were implanted with stimulating electrodes or with guide cannulae in the ipsilateral MC (AP = 2 mm, L = 2 mm; D = 1 mm from brain surface), the contralateral cerebellar IP nucleus (AP = −19 mm, L = 3 mm; D = 6 mm from cerebellum surface), or the ipsilateral RN (AP = 8.5 mm, L = 1.5 mm, D = 10 mm). Guide cannulae were implanted to a depth of up to 1 mm above the selected site. Stimulating electrodes were made from 200 μm enamel-coated silver wire. Guide cannulae consisted of a 21 gauge stainless steel needle protected by a removable 25 gauge stainless steel rod during nonrecording periods.

All the animals were prepared for the classical conditioning of eyelid responses (see Fig. 3*A*,*B*). For this, animals were implanted with recording bipolar hook electrodes in the left OO muscle. These electrodes were made from multistranded, Teflon-coated stainless-steel wire (A-M Systems) with a total external diameter of 230 μm and bared ~1 mm at the tip. A head-holding system, consisting of three bolts cemented to the skull perpendicular to the horizontal stereotaxic plane, was also implanted. All stimulating and recording electrodes were connected to a 9-pin socket attached to the holding system.

Recording and stimulating procedures. Recording sessions began 1 week after surgery. The experimental animal was placed in a Perspex restrainer designed for limiting its movements (Gruart et al., 2000). The restraining box was placed on the recording table and was surrounded by a black cloth. The recording room was kept softly illuminated, and a 50 dB background white noise was switched on during the experiments. For all the subjects, the first two recording sessions consisted of adapting the rabbit to the restrainer and to the experimental conditions; no stimulus was presented during these two sessions.

The EMG activity of the OO muscle was recorded with Grass P511 differential amplifiers with a bandwidth of 0.1 Hz to 10 kHz (Grass-Telefactor). Neuronal electrical activity was recorded in the RN area with a NEX-1 preamplifier (Biomedical Engineering). These recordings were performed with glass micropipettes filled with 2 M NaCl (3–5 MΩ resistance) and filtered in a bandwidth of 1 Hz to 10 kHz. Field potentials were recorded with low-resistance electrodes (1–3 MΩ) or lowpass filtered (>100 Hz) from unitary recordings. The recording area was approached with the help of stereotaxic coordinates (Girgis and Shih-Chang, 1981), and of the antidromic and synaptic field potentials evoked by single or double (1 ms interpulse interval) pulses presented to the implanted stimulating electrodes (Fig. 1*B–G*). Electrical stimulation was achieved across an ISU-220 isolation unit attached to a programmable CS-220 stimulator (Cibertec). Criteria to determine whether the recorded and the activated neuron were the same, and to discriminate somatic versus axonic recordings, were systematically followed (Múnera et al., 2001). The recording micropipette was always removed at the end of each recording session and the recording chamber sterilized and closed.

Tones were applied from a loudspeaker located 80 cm below the animal's head. Air puffs were applied through the opening of a plastic pipette (3 mm in diameter) attached to a metal holder fixed to the animal-holding system (dual-channel air-puff device; Biomedical Engineering).

Classical eyeblink conditioning. Conditioning consisted of two habituation and six conditioning sessions. A delay (tone/air puff) conditioning paradigm was used. The CS consisted of a 350 ms, 600 Hz, 85 dB tone. The US started 250 ms after CS onset, and consisted of a 100 ms, 3 kg/cm^2 air puff directed at the left cornea. The unconditioned stimulus (US) coterminated with the CS. Conditioning sessions consisted of 66 trials (6 series of 11 trials each) separated at random by intervals of 50–70 s. Of the 66 trials, 10% were test trials in which the CS was presented alone. A complete conditioning session lasted for ~1 h. The CS was presented alone during habituation sessions for the same number of blocks/session and trials/block. As criteria, we considered a "CR" the presence, during the CS–US interval, of electromyographic (EMG) activity lasting >10 ms and initiated >50 ms after CS onset. In addition, the integrated EMG activity recorded during the CS–US interval had to be at least 1.2 times greater than the integrated EMG recorded immediately before CS presentation (Gruart et al., 2000; Leal-Campanario et al., 2007).

Neural activity was recorded in the RN area during habituation and conditioning sessions (see Figs. 3–6). Neuron isolation and identification procedures were performed during the time intervals in which the pair of CS–US stimuli was not presented (Múnera et al., 2001). Usually, a range of 2–7 RN neurons were antidromically identified and recorded per conditioning session.

Drug microinjection. A 5% solution of lidocaine (Sigma-Aldrich) was injected by means of a calibrated injection tube (30G), coupled to a 10 μl Hamilton syringe, which was advanced through the guide tube. Drug solutions were constantly injected from 5 min before until the end of the conditioning session at a rate of 0.1 μl/min with the help of a microinfusion pump (310; KD Scientific). Two additional animals were injected in the IP nucleus with 2 μl of a 1 mg/ml solution of muscimol (Sigma-Aldrich), dissolved in artificial CSF, pH 7.4 (Jiménez-Díaz et al., 2004), and at a rate of 0.1 μl/min.

Histology. At the end of the experiments, animals were deeply anesthetized with sodium pentobarbital (50 mg/kg, i.p.), and perfused transcardially with saline and 4% paraformaldehyde (PFA). The proper location of eyelid EMG electrodes was checked. To determine the final location of recording sites, stimulating electrodes, and injection cannulae, the brain was removed and cut into slices (50 μm), and the relevant brain areas were processed for Nissl (toluidine blue) staining (see Fig. 2*B–G*).

In accordance with previous descriptions (Mendez and Hong, 1997), the retrograde fluorescent tracer Fluorogold (2% dissolved in saline; H22845, Invitrogen) was used to localize RN neurons projecting to the facial nucleus (FN; Fig. 2*I–K*). Injections were performed in the FN of

three additional animals with the help of a Hamilton microsyringe (2 μl in 10 min). The injection site was approached previously by antidromic field potentials evoked in the FN by electrical stimulation of the ipsilateral facial nerve. After 1 week of survival time, animals were intracardially perfused with 4% PFA in PB buffer, 0.12 M. Frozen 50 μm sections were coverslipped with Citifluor (Citifluor). Injection sites in the FN and retrograde-labeled cells in the RN were photographed, using a fluorescent microscope with the help of a filter of 365 nm excitation (Observer.Z1; Carl Zeiss MicroImaging).

Data collection and analysis. The unitary activity recorded in the RN area, the unrectified EMG activity of the recorded muscles, and 1-V rectangular pulses corresponding to CS, US, and electrical stimuli presented during the different experimental situations, were acquired online through an 8-channel analog-to-digital converter (CED 1401-plus; CED), and transferred to a computer for quantitative off-line analysis. Data were sampled at 25,000 Hz (for unitary recordings) or 5000 Hz (for EMG recordings), with an amplitude resolution of 12 bits. Computer programs (Spike2 and SIGAVG; CED) were used to display unitary and EMG activities. These programs allowed the quantification, with the aid of cursors, of the onset latency and area (mV × s) of the rectified EMG activity of the OO muscle and the latency, peristimulus time histograms (PSTHs), and instantaneous firing rate of unitary recordings. The programs also allowed the representation of PSTHs and/or the firing rate of the recorded neurons (Múnera et al., 2001; Leal-Campanario et al., 2007). When necessary, PSTHs were converted to firing rate following this equation (Rieke et al., 1997): firing rate (spikes/s) = (No. of spikes per bin/No. of repetitions) × (1000/bin size, in ms).

Statistical analyses were performed using the Sigma Plot 11.0 package (Sigma Plot) for a statistical significance level of $p = 0.05$. Mean values are followed by their SEM. Collected data were analyzed using the one-way or two-way ANOVA test, with time or session as repeated measure, coupled with contrast and/or nonparametric analysis when appropriate. Repeated-measures ANOVA allowed checking the statistical differences of the same group across sessions. The Student-Fisher t test was used when necessary.

Results

Identification of recorded RN and pararubral neurons

As illustrated in Figure 1*A*, the RN was approached using a transcortical approach and following available stereotaxic coordinates (Girgis and Shih-Chang, 1981). Recorded neurons were identified by their antidromic activation from their projection sites (Robinson et al., 2001; Miller and Gibson, 2009): the contralateral facial (Fig. 1*B*) or the accessory abducens nuclei (Fig. 1*C*), and with the additional help of the collision test. Mean activation latencies were 0.92 ± 0.03 ms (mean ± SEM; $n = 109$) from the FN and 1.01 ± 0.04 ($n = 35$) from the accessory abducens nucleus, with no significant differences ($p = 0.09$, Student's t test). Additional support for the antidromic nature of spike activation is that it followed stimulation frequencies of up to 500 Hz.

Identified RN neurons were easily activated (50 μs square, 1 ms of interval paired pulses, 0.5–2 mA) from the ipsilateral MC at 5 ± 0.32 ms of latency (Fig. 1*D*) and from the contralateral cerebellar IP nucleus at a shorter time (1.82 ± 0.06 ms; Fig. 1*E*). Interestingly, the electrical stimulation of the MC also evoked late, variable activations of RN neurons, indicating the presence of local reverberating circuits (Horn et al., 2002). The implanted MC sites were clearly related with eyelid movements, because their stimulation evoked the short-latency (9.4 ± 0.2 ms) activation of the EMG activity of the contralateral OO muscle, while the stimulation of the RN (50 μs single, square pulses, 0.2–2 mA) evoked responses of slightly shorter latencies (7.5 ± 0.2 ms), indicating its disynaptic nature (Fig. 1*F*). Muscle activation from the IP nucleus (by a pair of pulses, 1 ms interval) took 10.1 ± 0.3 ms (data not shown). For comparison, OO muscle activation from the FN took place in 2.5 ms (Fig. 1*F*). The latency of spike-triggered averaged activities of FN and OO muscle further confirmed that RN neurons recorded and analyzed here project to the FN and have a disynaptic activation effect (7.5 ± 0.2 ms) on this muscle (Fig. 1*G*).

Representative photomicrographs with the location of stimulating electrodes are illustrated in Figure 2*A–E*. Small electrolytic lesion marks made with tungsten electrodes at the end of the recording sessions indicated that RN neurons related to eyelid reflex and conditioned responses occupied a dorsolateral position in the rostral part of the nucleus (Fig. 2*F,G*). With the help of these electrolytic marks and collected information regarding stereotaxic coordinates, we made a precise reconstruction of the location of recorded and identified RN neurons ($n = 144$). Figure 2*H* indicates that recorded neurons (types A and B; see below) also formed a cell column over the dorsolateral part of the RN (Desmond and Moore, 1991). To further confirm that these pararubral neurons were also involved in eyelid motor responses, we injected the retrograde tracer Fluorogold in the FN of two animals. As already reported in rats (Ruigrok and Cella, 1995; Morcuende et al., 2002) and cats (Pong et al., 2008), retrograde-labeled neurons were concentrated in the lateral aspect of the contralateral RN and in the dorsally adjoining pararubral area (Fig. 2*I–K*). Probably, those labeled neurons occupying more ventral positions in the RN correspond to type C and E neurons (see below).

Neuronal response types

Apart from some preliminary recording sessions in the absence of conditioning stimuli, performed to adapt the recording system to the experimental needs, red and pararubral nucleus neurons were recorded during the two habituation and the six conditioning sessions presented here to all of the conditioned animals. In Figure 3 the experimental procedures for unitary recording and for classical eyeblink conditioning are illustrated. For analysis, the raw EMG recordings (Fig. 3*B*) were rectified and averaged (Fig. 3*C,D*), while unitary firing data (Fig. 3*B*) were passed across a discrimination window and accumulated (bin size = 10 ms) for (usually) 10 successive trials (Fig. 3*D*).

Recorded neurons were classified in five different groups (A–E) depending on their antidromic activation from the facial or the accessory abducens nucleus, their spontaneous firing, and their firing during the CS–US interval (Fig. 4).

Type A neurons (Figs. 3, 4*A*) were activated antidromically from the FN and presented an irregular spontaneous firing rate, with mean values ranging from 10 to 30 spikes/s ($n = 55$). Type A neurons fired a burst of action potentials preceding (≈10–40 ms) the EMG activation of the OO muscle during the CS–US interval, i.e., during the generation of the CR. In the presence of CRs, type A neurons showed peak firing reaching 500 spikes/s (Fig. 4*A*, right histogram). Characteristically, type A neurons decreased their firing rate immediately after the paired CS–US presentation (Fig. 3*B,C*). Type B neurons (Fig. 4*B*) were activated antidromically from the facial ($n = 29$) or the accessory abducens nucleus ($n = 17$). They showed a higher (40–60 spikes/s) and more stable spontaneous firing rate than type A cells, but were equally activated in the presence of CRs, reaching high peak firing rates during the CS–US interval (Fig. 4*B*, right histogram). In addition, type A and B neurons were easily activated by different types of stimulus, such as air puffs directed at the face, tones, and flashes of light, indicating that they received not only motor commands, but also information of different sensory modalities (Padel et al., 1988). Because of their firing properties, type A and B neurons

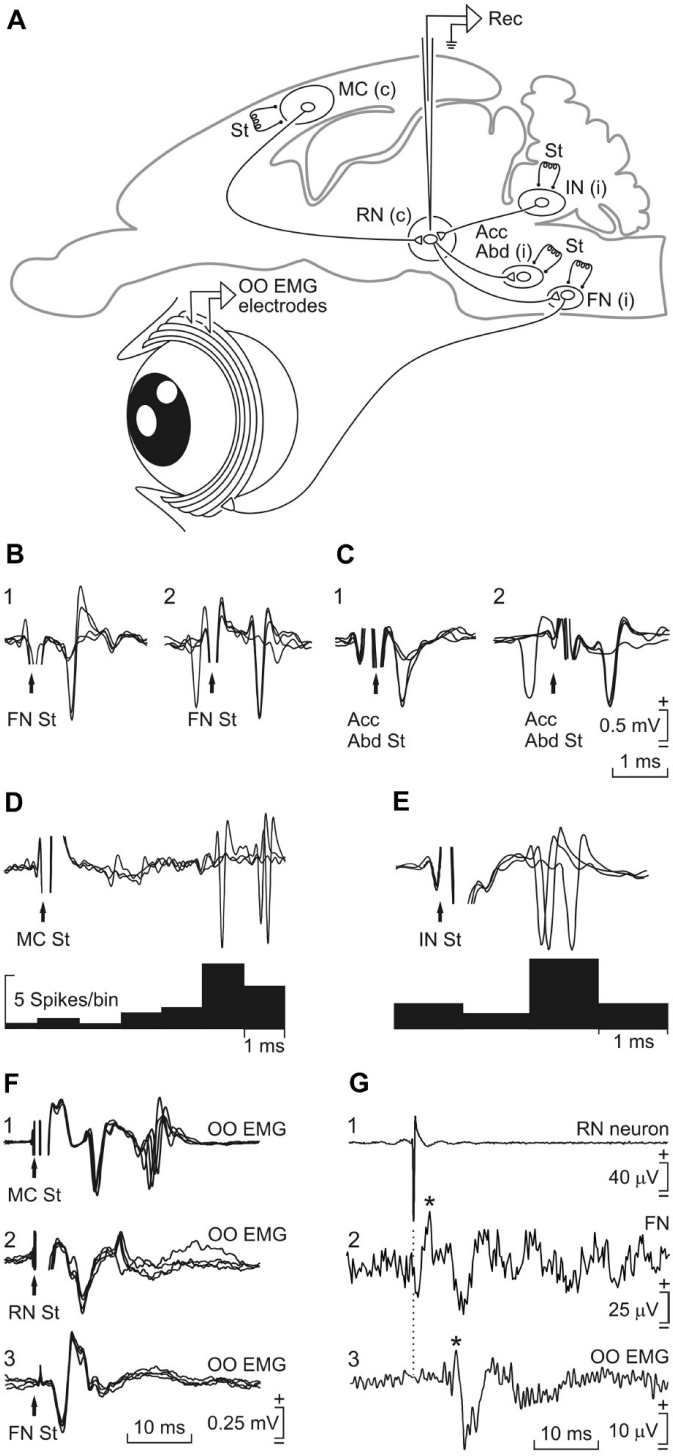

Figure 1. Experimental design and identification of recorded RN neurons. ***A***, Diagrammatic representation of the experimental design. RN neurons contralateral [RN (c)] to the left eye were recorded using a transcranial cortex approach (Rec). Stimulating (St) electrodes were implanted in the ipsilateral facial [FN (i)], accessory abducens [Acc Abd (i)], and cerebellar interpositus [IN (i)] nuclei, and in the contralateral eyelid area of the MC (c). The EMG activity of the OO muscle was also recorded. ***B***, ***C***, Antidromic activation of RN neurons from the FN (***B***,1) or the Acc Abd nucleus (***C***, 1) at threshold straddling intensities. The arrows indicate the stimulus artifacts. Representative examples of the collision test for RN neurons activated from the FN (***B***, 2) and the Acc Abd nucleus (***C***, 2) are also shown. ***D***, ***E***, Synaptic activation of RN neurons from the MC (***D***) and the IN nucleus (***E***). The bottom histograms illustrate PSTHs ($n = 5$ times; bin size = 1 ms). ***F***, From top to bottom are illustrated the EMG activity evoked in the OO muscle by double (1 ms interval) pulses applied to the MC (1) and to the RN (2), and of single pulses presented to the FN (3). ***G***, Spike-triggered extracellular activity (asterisks) recorded in the FN (2) and in the OO muscle (3). The triggering action potential corresponded to an antidromically identified RN neuron (1). Average was repeated 1000 times. Calibrations in ***C*** are also for ***B***, and the one in ***D*** is also for ***E***.

were considered to be directly involved in the acquisition of classically conditioned eyelid responses, and were processed for further quantitative analysis.

Type C neurons were activated antidromically only from the FN ($n = 25$). Like type B neurons, they presented a high-frequency (30–60 spikes/s) tonic firing rate, but, in contrast, they decreased ($-25.6 \pm 3.8\%$ on average) their firing during the CS–US interval in simultaneity with the presence of CRs (Fig. 4*C*). For the following reasons, we assumed that these RN neurons were probably projecting to masticator muscles: (1) they were exclusively activated from the FN; (2) the firing rate of type C neurons did not change (i.e., increase or decrease) across the successive conditioning sessions; and (3) they were inhibited when type A and B neurons increased their firing rate, suggesting that type C neurons were involved in the already described antagonist activities between the zygomatic and buccal branches of the facial nerve (Pauletti et al., 1993; Godefroy et al., 1998; Gruart et al., 2003). Type D neurons ($n = 18$) were activated antidromically only from the accessory abducens nucleus. They presented a high spontaneous firing rate that was increased during CS–US presentations, but without a definite temporal relationship (Fig. 4*D*). In fact, their discharge rates look like a particular case of type B neurons. Finally, type E neurons ($n = 25$) were recorded in the same red and pararubral areas as the other four types, but they could not be activated antidromically and did not modify their firing rates during reflex or conditioned eyeblinks. Most of these neurons responded to neck and/or body movements of the recorded animal, suggesting that they were in fact rubrospinal neurons involved in the activation of skeletal muscles (Eccles et

←

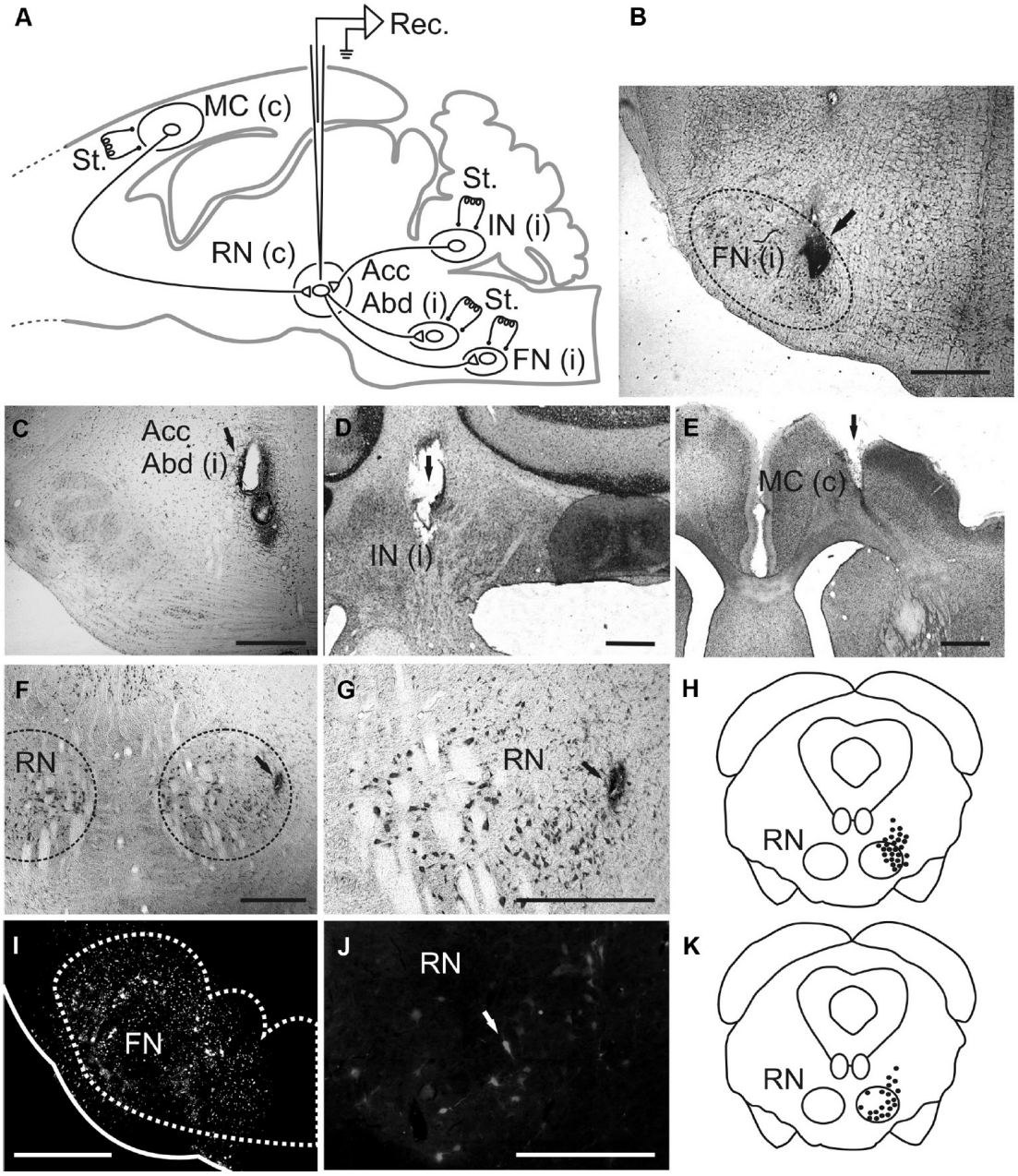

Figure 2. Location of recording and stimulating electrodes. ***A***, Diagram illustrating the different stimulating and recording sites. Abbreviations are as defined in the legend to Figure 1. ***B–E***, Photomicrographs of different brain coronal sections illustrating electrolytic marks (arrows) made with stimulating electrodes implanted in the FN (***B***), the Acc Abd (***C***) and the IN (***D***) nuclei, and the MC (***E***). ***F***, ***G***, Photomicrographs of coronal sections through the midbrain illustrating Nissl-stained RN neurons and a small electrolytic mark corresponding to the recording area. ***I***, A photomicrograph of Fluorogold injection site in the FN. ***J***, A photomicrograph illustrating labeled neurons located in the RN following Fluorogold injection in the contralateral FN. ***H***, Reconstruction of the location of recording RN neurons. Each black circle represents five recorded neurons. ***K***, Map reconstruction of RN and pararubral neurons (black circles) projecting to the FN as indicated by their Fluorogold labeling. Each black circle represents five labeled neurons. Abbreviations: c, i, contra- and ipsilateral. Calibration bars: 1 mm.

al., 1975; Huisman et al., 1981, 1982). Because of their lack of specificity in relation to the evolution and profiles of CRs, RN neurons classified as C–E were not included in the subsequent analysis.

Changes in the activity of RN and pararubral neurons during the acquisition of conditioned eyeblink responses

The top graph of Figure 5*A* illustrates the learning curve of classically conditioned rabbits. As already reported for the same species using similar training paradigms (Gruart et al., 2000; Leal-Campanario et al., 2007), conditioned animals started to increase their percentage of conditioned responses significantly ($F_{(7,14)} = 6.83$; $p < 0.001$) by the third conditioning session (48.2 ± 15.5%), reaching asymptotic values (86.7 ± 5.5%) by the fifth conditioning session. The rectified area (mV × s) of the EMG activity generated by the OO muscle during the CS–US interval (Fig. 5*A*, middle graph) also increased across training, reaching significantly ($p < 0.001$; $\chi^2 = 38.56$) larger values from the second to the sixth conditioning sessions. The increase was 36.7 ± 4.2% with respect to baseline (habituation) values by the second conditioning session. Interestingly, peak values were reached in the fourth and fifth sessions (≈80%), but those values decreased for the sixth session (59.9 ± 6.7%). Changes in neuronal firing across training paralleled those observed for the integrated EMG activity of the OO muscle (Fig. 5*A*, bottom graph): the mean firing activity of recorded type A and B neurons ($n = 75$; $n \leq 10$ per session) showed a significant ($p < 0.001$; $\chi^2 = 422.37$) increase in rate with respect to baseline values by the second session and reached peak values by the fourth. As in the case of the EMG area, the mean firing activity of identified RN and pararubral neurons started to decrease by the fifth conditioning session.

An attempt was made to determine the linear relationships between those three variables included in Figure 5*A*; namely, the percentage of CRs, the EMG area during the CS–US interval, and the mean firing rate during the same period of time (Fig. 2*B*). As illustrated in Figure 5*C*, although the three variables were linearly related, the best linear fit ($r = 0.92$; $p < 0.01$) found was for the relationships between the mean firing rate of type A and B neurons and the rectified EMG area, while the lowest value was for the relationship between the percentage of CRs and the mean firing rate ($r = 0.7$; $p < 0.05$). Finally, the linear relationships between the percentage of CRs and the rectified EMG area had intermediate values ($r = 0.81$; $p < 0.05$).Together, these results suggest that the firing of RN neurons is related more to changes in eyelid motor performance during the training than to the precise evolution of the acquisition process (i.e., the learning curve).

Effects of acute inactivation of the MC on the acquisition of classical eyeblink conditioning and on the firing properties of related RN neurons

It is known that the RN receives a significant collateral projection from descending pathways originated in the ipsilateral facial MC (Tsukahara et al., 1967; Pong et al., 2008; Miller and Gibson, 2009). As shown here, the electrical stimulation of the facial area of the MC evokes a short-latency, potent activation of RN neurons related to eyelid responses (Fig. 1*D*). In a first series of experiments, we studied the effects on MC inactivation (by a local injection of lidocaine) on the acquisition of eyelid CRs (Fig. 6*A*) in controls and injected animals ($n = 3$ per group). As shown in Figure 6*B*, lidocaine infusion into the MC during the fourth and fifth conditioning sessions reduced the percentage of CRs by ~50% ($F_{(7,14)} = 1.606$; $p = 0.006$).

In a subsequent experiment, we decided to study the effects of MC inactivation across all conditioning sessions at the same time we recorded the evoked changes in the discharge rate of identified RN and pararubral type A and B neurons. In Figure 6*C* the rectified and averaged ($n = 66$) EMG activity of the OO muscle corresponding to representative vehicle-injected (left set of records) and lidocaine-injected (right set of records) rabbits across the sixth conditioning sessions are illustrated. It should be noticed that lidocaine injection greatly reduced the expression of CRs, with a minor effect on the performance of the unconditioned responses. In fact, CRs in lidocaine-injected animals only started to appear by the fourth conditioning session, well after their appearance in the control animal.

A quantitative analysis of the evolution of CRs, of the rectified EMG area, and of the mean firing rate during the CS–US interval, is illustrated in Figure 6*D*. As shown, lidocaine infusion into the MC during the six conditioning sessions significantly reduced the percentage of CRs ($F_{(7,14)} = 16.05$; $p < 0.05$), as well as the area of the EMG activity of the OO muscle ($F_{(7,35)} = 4.12$; $p < 0.05$). In fact, in lidocaine-injected rabbits ($n = 3$) the two variables only started to reach a >20% increase over habituation values by the fourth conditioning session. The mean firing rate of RN neurons evoked in lidocaine-injected animals was significantly lower than

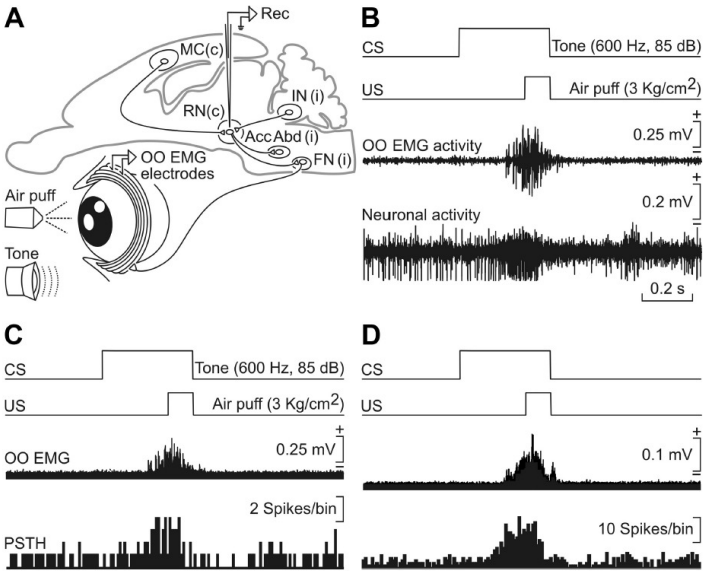

Figure 3. Firing activities of RN neurons during classical eyeblink conditioning using a delay conditioning paradigm. ***A***, The delay conditioning consisted of a tone (350 ms, 600 Hz, 85 dB) presented as a CS that started 250 ms before and coterminated with an air puff (100 ms, 3 kg/cm^2) as a US. ***B***, From top to bottom are CS and US presentations, the EMG activity of the OO muscle, and the firing activity of an RN neuron recorded during the third conditioning session and classified as type A. ***C***, Shows the EMG-rectified activity and the PSTH ($n = 1$ trial; bin size = 10 ms) of the same neuron during the recordings in ***B***. ***D***, Rectified and averaged EMG activity and cumulative records (averaged for 10 trials) of the same neuron during the third conditioning session. Time base in ***B*** is also for ***C*** and ***D***, and labeling in ***C*** is also for ***D***.

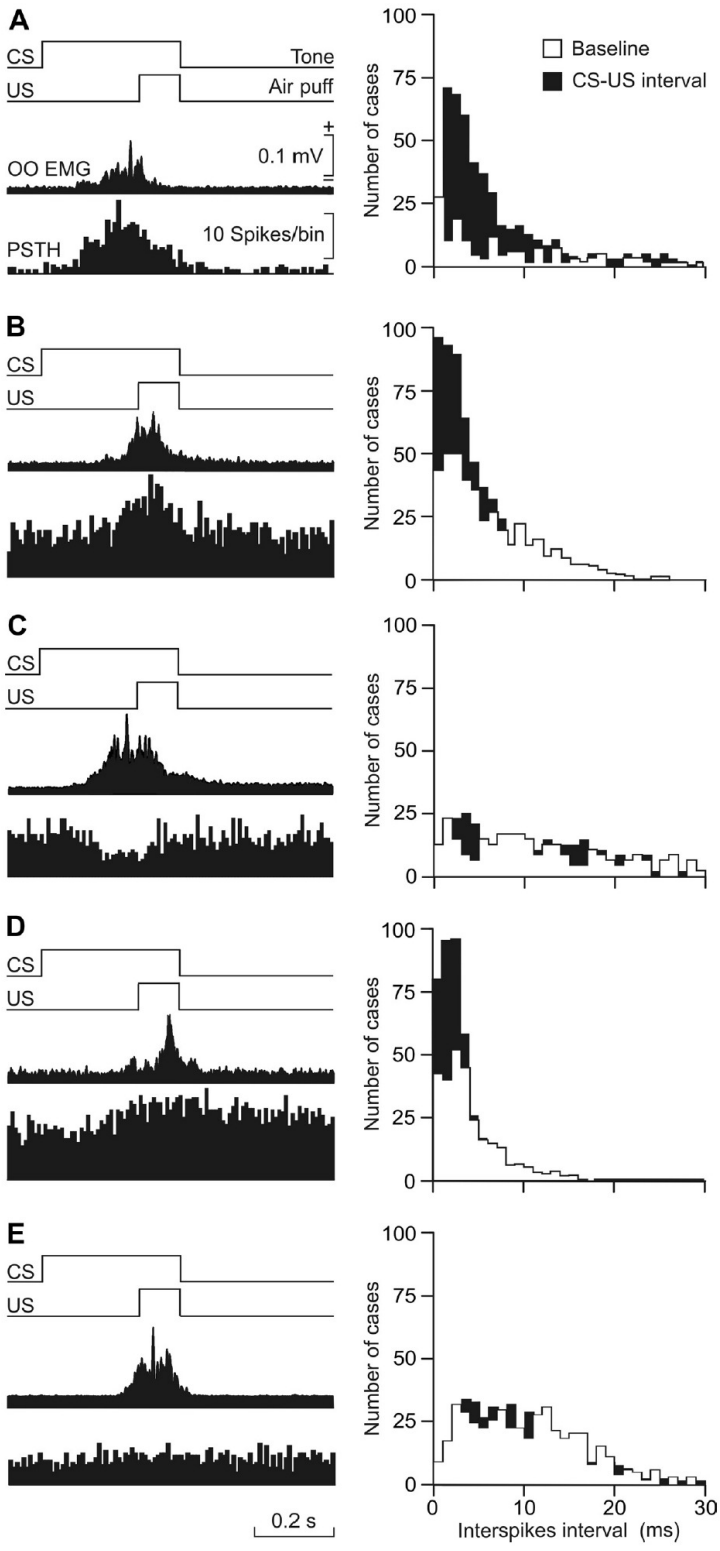

Figure 4. Representative examples of the different types of identified RN neuron recorded during classical conditioning of eyelid responses. All recordings were performed during the fourth conditioning session and were averaged from 10 successive trials. ***A***, Left, Rectified and averaged EMG activity of the OO muscle and the PSTH ($n = 10$ times; bin size = 10 ms) of the firing activity of a type A neuron. Right, The interspike-interval distribution of the same neuron during spontaneous activity (baseline) and during the CS–US interval. ***B–E***, Same as in ***A***, for neurons type ***B–E***.

control values ($p < 0.001$; $\chi^2 = 161.653$). Interestingly, the firing rate of RN neurons recorded in lidocaine-injected rabbits presented a U shape (Fig. 6*D*, bottom graph), because it decreased from the first to the third conditioning sessions (as opposed to the increase in firing rate taking place in control rabbits), but it increased from the fourth to the sixth conditioning sessions, in parallel with the increase observed in the rectified EMG area.

On the whole, these results indicate that the MC plays an important role in the proper and timed generation of CRs in behaving rabbits, with a minor effect on unconditioned eyelid responses. In addition, the delayed initiation of CRs in lidocaine-injected animals could be the result of learning-dependent changes in neuronal firing activities taking place in the ipsilateral RN.

It is generally accepted that delay conditioning can be acquired by decerebrated and decorticated animals (Oakley and Russell, 1972; Ivkovich and Thompson, 1997; Case et al., 2002; Kotani et al., 2002). Indeed, those chronic lesions will allow the activation of hierarchically lower centers, as the RN and the pararubral areas. In opposition to this experimental approach, we performed here an acute inactivation of the MC with functional effects restricted to the conditioning session. In this regard, there are early reports indicating a reversible effect on the expression of CRs by the transient inactivation of cortical circuits (Megirian and Bures, 1970). Thus, transient and short-term inactivation of cortical motor centers will prevent the activation of other brain centers with learning capabilities. But, and as explained below (see Fig. 8*B*), the RN and the pararubral areas showed learning-related changes in firing activities if cortical inactivation is performed in successive conditioning sessions.

Effects of acute inactivation of the cerebellar IP nucleus on the acquisition of classical eyeblink conditioning and on the firing properties of related RN neurons

As reported years ago (Tsukahara et al., 1967; Eccles et al., 1975; Canedo and Lamas, 1989) and further confirmed in Figure 1*E*, the electrical stimulation of the

←

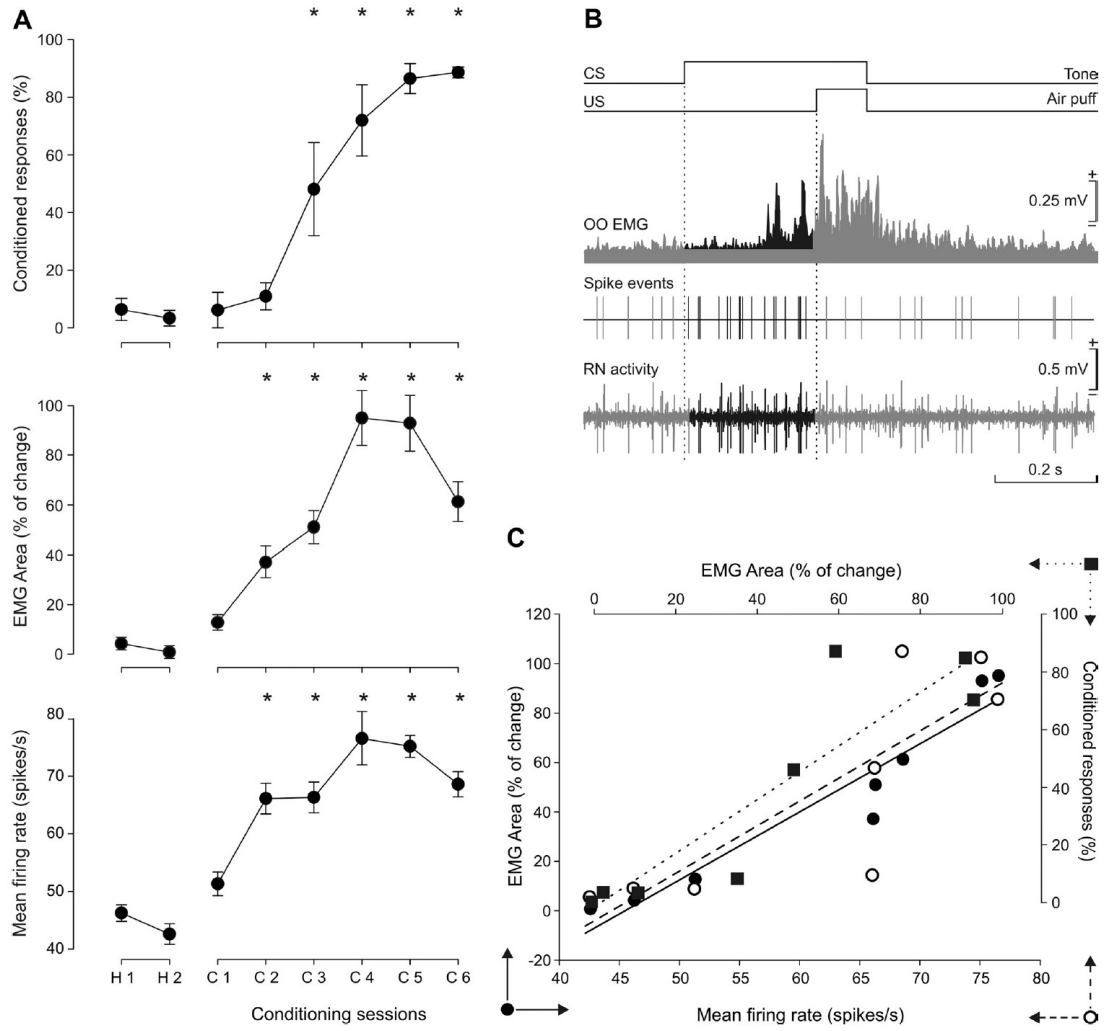

Figure 5. Learning curves and changes in the firing rate of RN neurons. ***A***, The three graphs show the evolution of the percentage (%) of CRs (top graph), of the OO EMG area (mV × s, in % of change, middle graph), and of the mean firing rate (in spikes/s) of identified RN neurons recorded during the indicated sessions (bottom graph). Data were collected from four animals and for 75 identified neurons ($n \leq 10$ per session). *$p < 0.001$, one-way ANOVA. ***B***, Selection of data corresponding to the increase in EMG area and in neuronal firing taking place during the CS–US interval. The selected changes in activity are indicated in black. ***C***, Linear relationships between mean firing rate of type A and B RN neurons and the EMG area of the OO muscle (black circles and continuous line; $r = 0.92$; $p < 0.01$), EMG area and the percentage of CRs (black squares and dotted line; $r = 0.81$; $p < 0.01$), and mean firing rate and CRs (white circles and dashed line; $r = 0.7$; $p < 0.05$).

contralateral cerebellar IP nucleus evokes a monosynaptic activation of RN neurons related to eyelid responses. In consequence, we also studied the effects of lidocaine infusion into the IP nucleus during classical conditioning of eyelid responses and simultaneously with recording the firing activities of RN neurons related to eyelid movements (Fig. 7*A*). Interestingly, lidocaine infusion into the IP nucleus evoked a rapid (<200 s) increase in the spontaneous firing rate of RN neurons (Fig. 7*B*), an effect not observed during lidocaine infusion into the MC. Since this enhanced neuronal firing could be ascribed to an unwanted effect of lidocaine on terminal axons of Purkinje cells, two additional animals were infused with muscimol (a potent agonist of $GABA_A$ receptors). In the two cases, the local microinjection of muscimol evoked a similar unspecific increase in RN firing rates.

In Figure 7*C* the rectified and averaged ($n = 66$) EMG activity of the OO muscle corresponding to representative vehicle-injected (left) and lidocaine-injected (right) rabbits across the six conditioning sessions are illustrated. In contrast to results collected during lidocaine injections in the MC (Fig. 6*C*), lidocaine infusion into the IP nucleus almost completely canceled out the expression of both conditioned and unconditioned eyelid responses (Fig. 7*C*). In fact, CRs in lidocaine-injected animals did not reach significant values for the six conditioning sessions. As already reported in behaving cats (Jiménez-Díaz et al., 2004) muscimol injections in the IP nucleus also significantly decreased ($p < 0.001$) the expression of both conditioned (≥35%) and unconditioned (≥35%) eyelid responses.

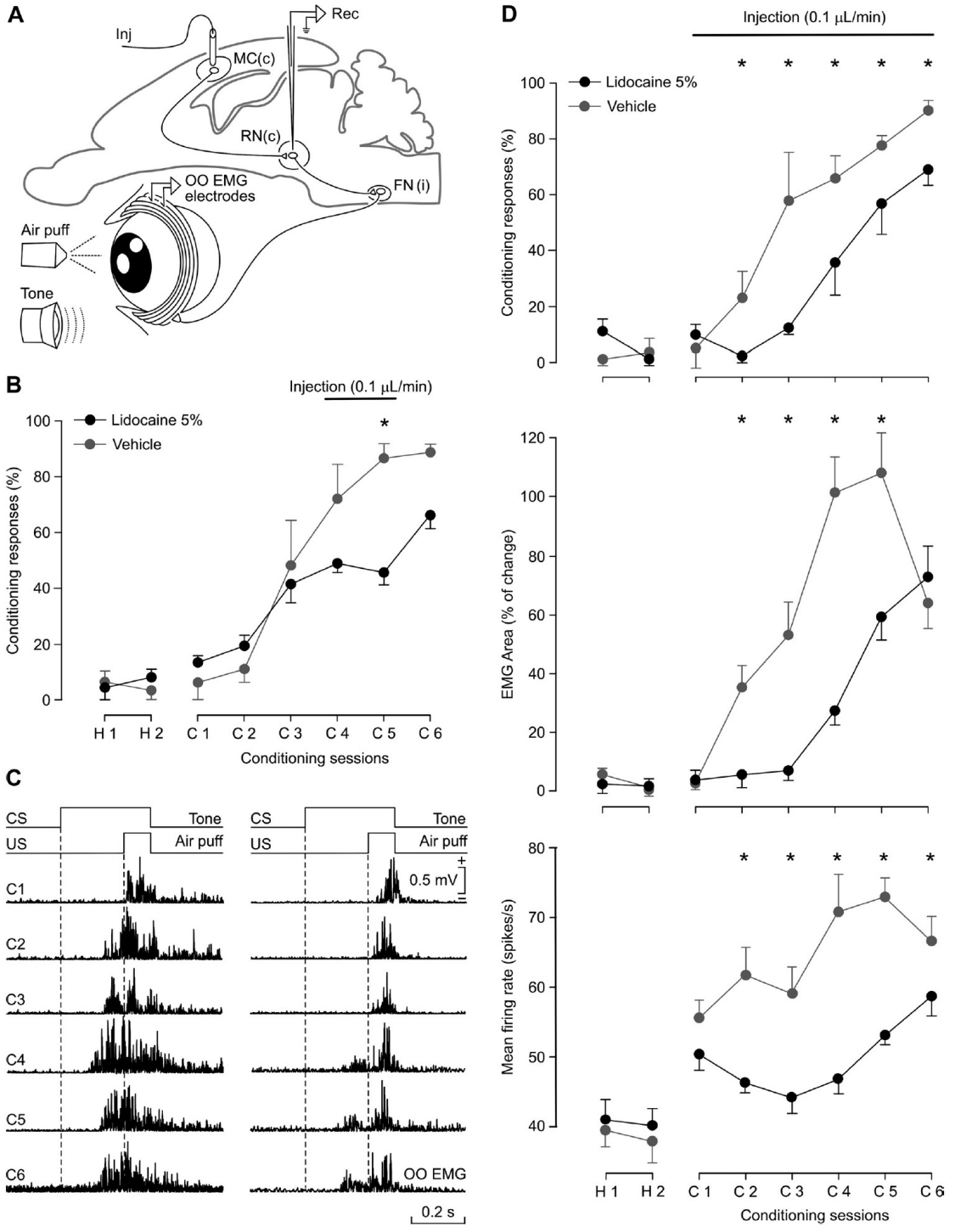

Figure 6. Effects of MC inactivation on learning curves and on the firing rate of RN neurons. ***A***, Experimental design. The ipsilateral MC was perfused with lidocaine (5% solution at a rate of 0.1 μl/min) or vehicle (Inj) during classical eyeblink conditioning and unitary recordings (Rec) of RN neurons. ***B***, Quantitative analysis of data collected from three vehicle-injected (gray circles and lines) and three lidocaine-injected (black circles and lines) animals (mean ± SEM). In this case, lidocaine was injected only during sessions 4 and 5. Note the significant decrease in the percentage of CRs ($p < 0.005$; two-way ANOVA), ***C***, Evolution of the rectified EMG activity of the OO muscle across conditioning sessions in representative animals injected with vehicle (*Figure legend continues.*)

A quantitative analysis of the evolution of CRs, of the rectified EMG area, and of the mean firing rate during the CS–US interval was also performed in rabbits injected with lidocaine in the IP nucleus (Fig. 7*D*). In this case, lidocaine infusion into the IP nucleus during the six conditioning sessions almost completely prevented the appearance of CRs ($F_{(7,14)} = 182.22$; $p < 0.005$), as well as reducing the area of the EMG activity of the OO muscle ($F_{(7,35)} = 13.32$; $p < 0.01$). In fact, in lidocaine-injected rabbits ($n = 3$) the two variables never reached a >20% increase over habituation values across the whole conditioning. Although no significant changes were observed in the mean firing rate presented by the two groups, the mean firing rate of RN neurons evoked in lidocaine-injected animals showed a significant ($p < 0.05$) increase during the first conditioning session (Fig. 7*D*, bottom graphs). The firing rate of RN neurons of lidocaine-injected animals decreased progressively until reaching a minimum during the fourth training session. For the fifth and sixth conditioning sessions, the RN neurons of lidocaine-injected animals presented values similar to those of control rabbits.

We also checked the rate of recovery of CRs during the two conditioning sessions following lidocaine inactivation of the IP nucleus (Fig. 8*C*). The aim was to determine whether the inactivation of the IP nucleus prevented the expression of already acquired CRs. As illustrated in Figure 8*C*, the learning curve after the six lidocaine sessions seemed to start from baseline values suggesting the absence of nonexpressed CRs generated in circuits presynaptic to the IP nucleus. In fact, the percentage of CRs collected during the seventh and eighth sessions from the control group were significantly ($F_{(9,18)} = 268.9$; $p < 0.05$) larger than those reached by the experimental group.

To sum up, lidocaine infusion into the IP nucleus greatly affected the expression of both conditioned and unconditioned eyelid responses for the whole training. The initial inactivation of the IP nucleus evoked a large increase in the spontaneous firing of RN neurons, an effect that decreased, but was still present during successive local injections of lidocaine. Nevertheless, these changes in firing rate could not be related to the acquisition process (see below; Fig. 8*B*,*C*).

The decrease in the amplitude of unconditioned responses following lidocaine or muscimol injections in the IP nucleus deserved a further comment. Indeed, some reported effects in rabbits are different from those reported here in the same species (Poulos et al., 2009). Nevertheless, we have collected similar findings in cats (Jiménez-Díaz et al., 2004) during classical conditioning of eyelid responses. In addition, there are early reports in rabbits indicating a decrease in the amplitude of unconditioned responses following the lesion and/or the inactivation of the IP nucleus (Welsh and Harvey, 1989; Chapman et al., 1990; Welsh, 1992; Wikgren and Korhonen, 2001). It has also been shown that the activation of IP neurons with GABA antagonists also facilitates unconditioned responses (Chen and Evinger, 2006). A possible explanation for this discrepancy is that most lesion studies performed in rabbits refer to a rostral location of IP neurons related to eyelid responses, a fact not confirmed in many other species (mice, rats, cats, monkeys; Sánchez-Campusano et al., 2011). In all of these species eyelid-related neurons are located in more caudal aspects of the IP nucleus as performed here. This anatomical discrepancy could explain the different effects produced by lidocaine injections in deep cerebellar nuclei. In addition, bolus injection of lidocaine has a rather transient effect compared with the continuous perfusion carried put here (see Discussion).

←

(*Figure legend continued.*) (left set of records) or with lidocaine (right set of records) in the MC during the six sessions. Note the decrease in EMG area corresponding to conditioned and unconditioned responses following lidocaine administration. ***D***, From top to bottom are illustrated the evolution of CRs (%), EMG area (% of change), and mean firing rate (spikes/s) for the experiment illustrated in ***C*** ($n = 3$ animals/group). Note the decrease in the percentage of CRs, EMG area, and neuronal firing rate following lidocaine injection in the MC (*$p \leq 0.05$, two-way ANOVA).

Comparative analysis of the effects of lidocaine injection in the MC and in the IP nucleus on increases in firing rates of RN neurons during the CS–US interval

The inactivation of the cerebellar IP nucleus (Fig. 7*D*, bottom graph) produced an initial activation of the spontaneous firing of RN and pararubral type A and B neurons less noticeable than during MC inactivation (Fig. 6*D*, bottom graph). Since this activation was rather unspecific and not related to the learning situation (Fig. 7*B*), we performed a further analysis of unitary data collected during the CS–US interval. In this case, and to consider exclusively the increase in firing rate evoked by the paired CS–US presentation, we removed the spontaneous firing presented by the recorded neuron (Fig. 8*A*). For this, we subtracted from the firing rate computed during the CS–US interval the value of the mean firing rate collected immediately (250 ms) before CS presentation. In this situation, values from control animals (Fig. 8*B*) presented an inverted-U profile similar to the values already illustrated in the bottom graph of Figure 5*A*. In contrast, firing rates collected from RN neurons in animals injected with lidocaine in the MC best fit a linear regression line, with a positive slope ($y = 10.46 + 1.06x$; $r = 0.88$; $p = 0.022$; Fig. 8*B*), while firing rates collected from neurons recorded during lidocaine injections in the IP nucleus better fitted a decreasing linear regression line ($y = 11.48 - 1.09x$; $r = 0.9$; $p = 0.015$; Fig. 8*B*). These results further confirm the proposal of an active involvement of RN neurons in the learning process following the inactivation of the MC but not of the cerebellar IP nucleus.

Comparative analysis of the effects of lidocaine injection in the MC and in the IP nucleus on unconditioned eyelid responses

As shown in Figures 6*C* and 7*C*, the performance of unconditioned responses was differentially affected by the inactivation of the MC and the cerebellar IP nucleus. Indeed, the inactivation of the MC evoked only a minor decrease in the performance of unconditioned responses (Fig. 6*C*), while the inactivation of the IP nucleus almost canceled out its expression (Fig. 7*C*). Figure 9 illustrates the evolution of unconditioned responses across the successive conditioning sessions. For this, we quantified the rectified EMG area (in mV × s) of the OO activation evoked by the US (Fig. 9*A*). As seen in Figure 9*B*, the rectified EMG area in control animals was significantly larger ($p < 0.001$) than in animals injected with lidocaine in the MC and in the cerebellar IP nucleus. In addition, unconditioned eyelid responses evoked in MC animals injected with lidocaine were significantly larger ($p < 0.05$) than values collected from animals injected with lidocaine in the IP nucleus. In accordance, the inactivation of cerebellar output has more-deleterious effects on corneal reflex circuits than does MC inactivation.

Discussion

Principal findings of the present study

We have reported here the firing activities of antidromically identified RN and pararubral neurons related to conditioned and

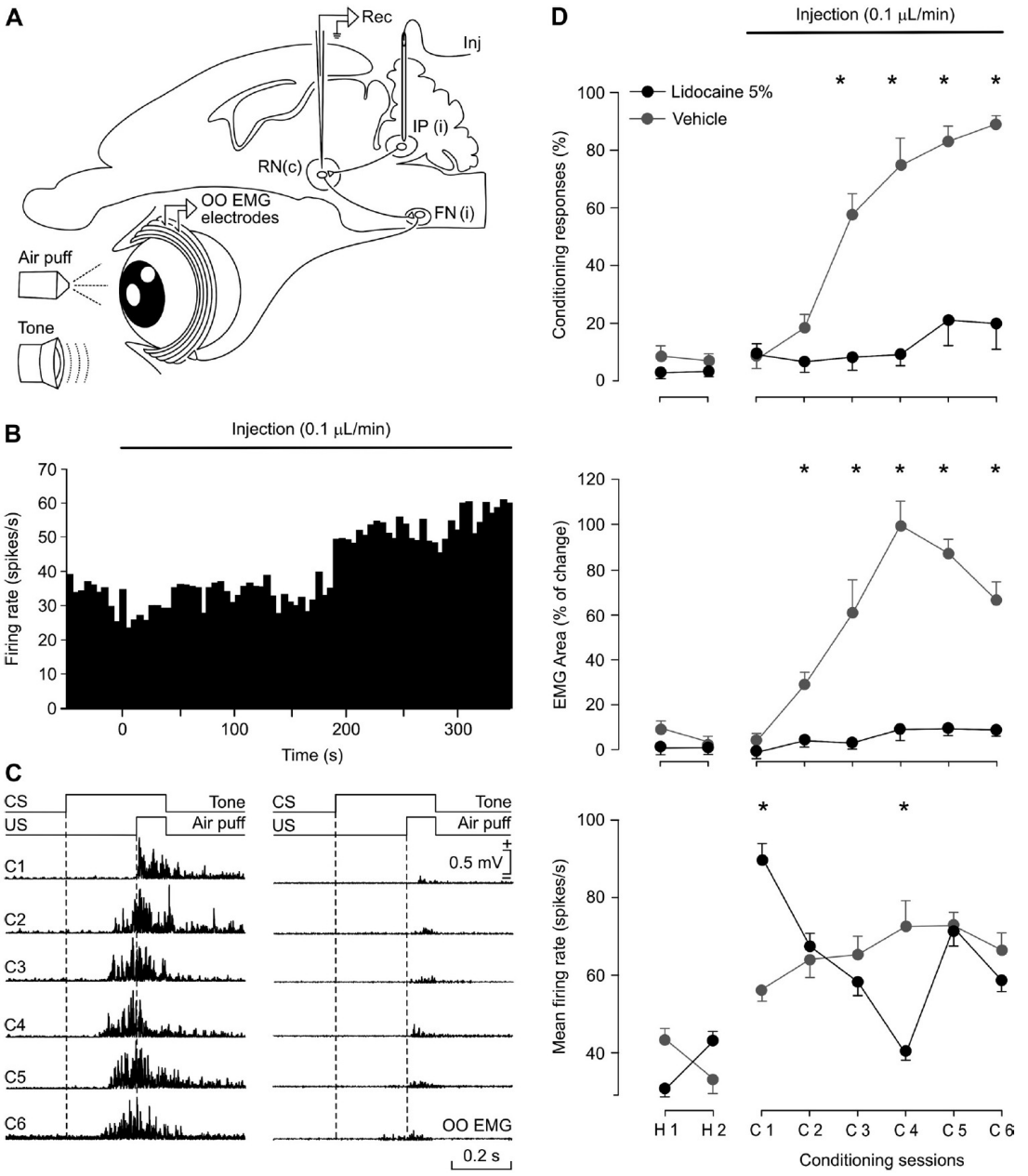

Figure 7. Effects of IP nucleus inactivation on learning curves and on the firing rate of RN neurons. ***A***, Experimental design. The contralateral cerebellar IP nucleus was perfused with lidocaine (5% solution at a rate of 0.1 μl/min) or vehicle (Inj) during classical eyeblink conditioning and unitary recordings (Rec) of RN neurons. ***B***, Increase in the spontaneous firing of identified RN neurons following lidocaine injection in the IP nucleus. ***C***, Evolution of the rectified EMG activity of the OO muscle across conditioning sessions in representative animals injected with vehicle (left set of records) or with lidocaine (right set of records) in the IP nucleus. Note the decrease in EMG area corresponding to conditioned and unconditioned responses following lidocaine administration. ***D***, From top to bottom are illustrated the evolution of CRs (%), EMG area (% of change), and mean firing rate (spikes/s) for the experiment illustrated in ***C*** ($n = 3$ animals/group). Note the decrease in the percentage of CRs and EMG area, and the changes in neuronal firing rate following lidocaine injection in the IP nucleus (*$p \leq 0.01$, two-way ANOVA).

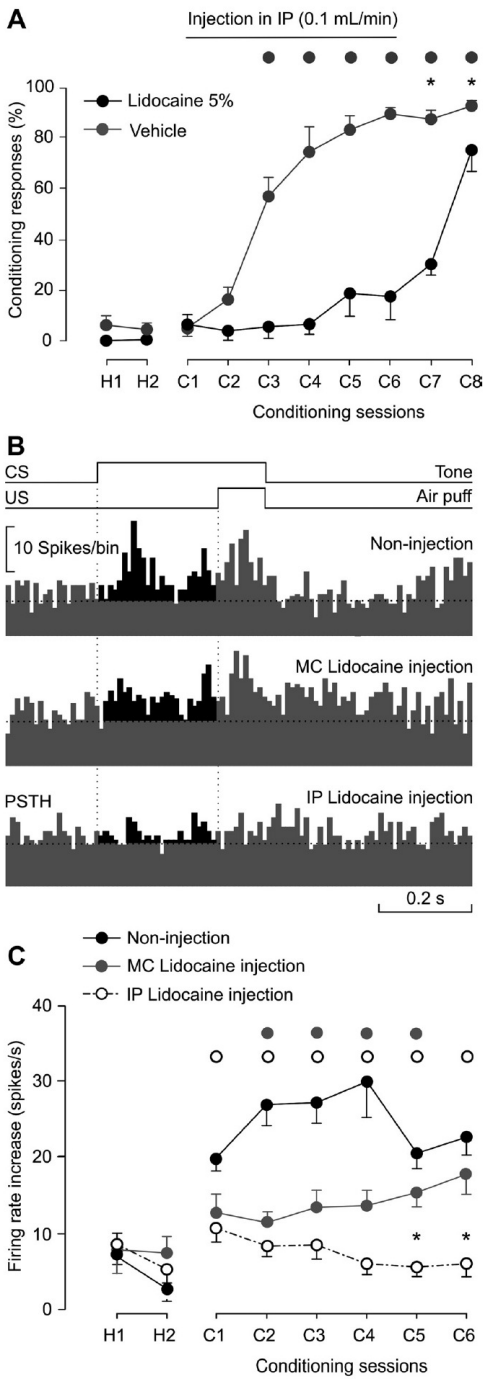

Figure 8. Quantitative analysis of changes evoked, during the CS–US interval, in the firing rate of identified RN neurons by lidocaine injections in the MC or in the cerebellar IP nucleus. The recovery of CRs after lidocaine injections in the IP nucleus is also illustrated. ***A***, Effects of lidocaine injection in the IP during the first six conditioning sessions (top bar) on the acquisition of CRs ($n = 3$; black circles and lines) compared with control (vehicle-injected animals, $n = 3$; gray circles and lines) values. Note the slow increase in the percentage of CRs after the end of lidocaine injections. Gray dots and asterisks at the top indicate significant ($p \leq 0.05$, two-way ANOVA) differences with habituation values for the control and lidocaine-injected groups. ***B***, From top to bottom are illustrated the conditioning paradigm and the PSTH of representative RN neurons collected from noninjected, and MC- and IP-injected rabbits. Illustrated recordings were collected from the third conditioning session. In black are indicated the time windows (CS–US interval) from which the corresponding increases in firing rate were computed. ***C***, Evolution of the increase in mean firing rates during the CS–US interval collected from noninjected (black circles and continuous line), and MC-injected (gray circles and lines) and IP-injected (white circles and dashed line) rabbits ($n = 3$ per group) during habituation and conditioning sessions. Gray and white circles at the top indicate significant ($p \leq 0.01$, two-way ANOVA) differences of the noninjected group with MC- and IP-injected rabbits, and asterisks indicate significant ($p \leq 0.05$, two-way ANOVA) differences observed between the two injected groups.

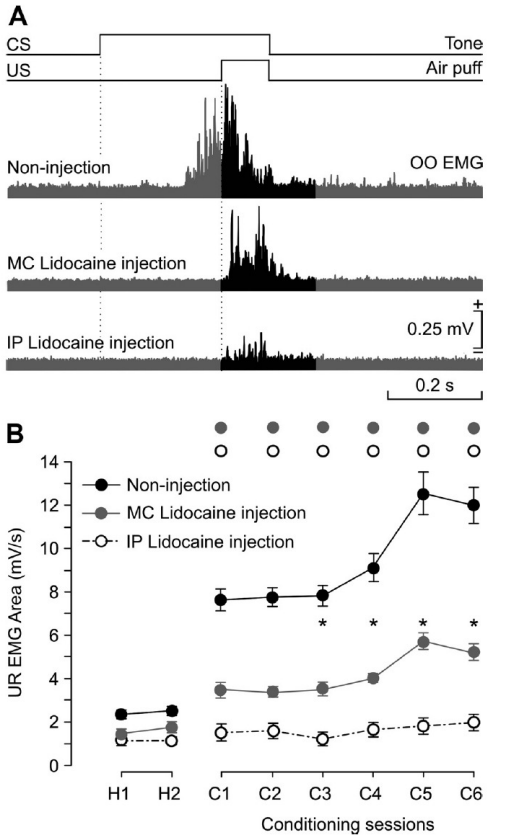

Figure 9. Quantitative analysis of changes evoked in unconditioned eyelid responses by lidocaine injections in the MC or in the cerebellar IP nucleus. ***A***, From top to bottom are illustrated the conditioning paradigm and rectified EMG profiles of the OO muscle collected from representative noninjected, and MC- and IP-injected rabbits. Illustrated recordings were collected from the third conditioning session. In black is indicated the EMG area corresponding to the unconditioned response. ***B***, Evolution of unconditioned response EMG areas (in mV × s) collected from noninjected (black circles and continuous line), and MC-injected (gray circles and lines) and IP-injected (white circles and dashed line) rabbits ($n = 3$ per group) during habituation and conditioning sessions. Gray and white circles at the top indicate significant ($p \leq 0.01$, two-way ANOVA) differences of the noninjected group with MC- and IP-injected rabbits. *$p \leq 0.05$ for differences between the two injected groups.

unconditioned eyelid responses. These neurons seemed to project to the contralateral facial and/or the accessory abducens nuclei and were activated synaptically from the ipsilateral MC and from the contralateral IP nucleus. Interestingly, stimulation of the MC evoked long-latency responses, indicating the presence of local intrinsic circuits. At the same time, RN and pararubral neurons were activated by stimulations of different sensory modalities, suggesting that they could be capable of integrating sensory information with motor commands. Firing rates of these RN and pararubral neurons, during the CS–US interval, seemed to correlate better with the EMG activity of the OO muscle than with the learning curve, suggesting that they were more directly involved in the performance of CRs than in the acquisition process (Desmond and Moore, 1991; Porras-García et al., 2010). The reversible inactivation of the MC during conditioning sessions evoked a significant and lasting reduction in the percentage of CRs and in the firing rates of recorded neurons, with a minor effect on unconditioned responses. However, the firing rate of RN neurons started to recover from the fourth session on, in parallel with the increase in CRs and in the amplitude of the rectified EMG activity of the OO muscle. In contrast, inactivation of the IP nucleus evoked the almost complete disappearance of both conditioned and unconditioned responses for the six conditioning sessions, with a rebound increase of the spontaneous firing of RN neurons. As illustrated in Figure 8, this increase in firing rate of RN neurons during IP inactivation was not related to the learning process, while, as is also illustrated in Figure 8, the recovery of CRs and muscle activity during MC inactivation was probably due to the specific increase in firing rate of RN neurons during the CS–US interval. In general, the RN and its pararubral area seem capable of learning-dependent changes in synaptic strength, which become particularly evident in the absence of MC outputs.

Different roles ascribed to red nucleus neurons

The presence of a definite RN and of a rubrospinal tract seems to be related to the presence of limbs or limb-like structures, as in the case of many terrestrial vertebrates and of certain rays, respectively (ten Donkelaar, 1988). In relation to this widely accepted evolutionary trend, RN axonal projections to facial and accessory abducens nuclei—containing motoneurons innervating OO and eye retractor bulbi muscles, respectively—have usually been considered to be collaterals of magnocellular RN neurons projecting to the spinal cord (Courville, 1966; Mizuno and Nakamura, 1971; Hinrichsen and Watson, 1983). However, recent experiments performed with retrograde tracers and/or using rabies virus immunolabeling have convincingly shown that RN neurons projecting to the FN belong to a specific population located in the parvocellular part of the RN and occupying a dorsolateral position, as well as extending to the dorsally adjoining pararubral area (Ruigrok and Cella, 1995; Morcuende et al., 2002; Pong et al., 2008). As shown here, the stereotaxic reconstruction of recorded neurons belonging to types A and B presented a similar location within the nucleus. From a functional point of view, this finding makes sense, since facial motor functions cannot readily be associated with the control exerted by rubral neurons projecting to spinal cord motor centers related to limb displacements and/or to manipulative behaviors (Horn et al., 2002; Miller and Gibson, 2009).

With respect to the classical conditioning of eyelid responses, the RN has usually been considered an important component of the circuit originated in the cerebellar cortex and/or IP nucleus, having in this regard a mere relay and premotor function. In a seminal study, Chapman et al. (1990) performed multiunitary recordings of putative RN neurons and the reversible lidocaine inactivation of both red and IP nuclei during classical conditioning of behaving rabbits, concluding that the RN acts as a relay nucleus for motor commands generated at cerebellar circuits. In this regard, it has been reported that RN inactivation produced no effect on the acquisition process (Grant and Horcholle-Bossavit, 1986; Clark and Lavond, 1993; Krupa et al., 1993; Robleto and Thompson, 2008), a point of view still accepted by many groups (Bracha et al., 2009; Freeman and Steinmetz, 2011). In dissension, early (Kennedy and Humphrey, 1987; Schmied et al., 1988; Cartford et al., 1997) and recent studies (Miller and Gibson, 2009) proposed that the RN plays a more active role in motor learning processes. According to the present results, the RN seems to occupy a strategic position, receiving descending, and different, motor control commands from the cerebral and cerebellar circuits, which regulate its functioning. However, the putative active role in the acquisition of new motor abilities is noticed only when those afferent inputs are transiently removed during the acquisition process. In this regard, it is very important to mention that lidocaine inactivation has a short-lasting ($\approx$20 min) effect when injected in a single bolus (Martin and Ghez, 1999). For this very reason, we decided to inject lidocaine in a continuous manner during the whole conditioning session. This precise experimental approach could explain the different results reported here with regard to the inactivation of both MC and IP nucleus.

Learning-dependent changes in the neuronal activity of RN and pararubral neurons during classical eyeblink conditioning

In clear opposition to the proposal that the RN is a mere relay premotor center conveying motor commands emanating from the cerebellum—the latter being the proper neuronal site where the acquisition and storage of newly acquired eyelid conditioned responses take place (Chapman et al., 1990; Bracha et al., 1993, 2009; Krupa et al., 1993; Freeman and Steinmetz, 2011)—the RN was one of the first places where activity-dependent changes in synaptic strength was supposed to occur (Tsukahara, 1981). In a series of seminal experiments, Tsukahara et al. (1981) and Murakami et al. (1987, 1988), as well as additional groups (Ito and Oda, 1994; Pananceau et al., 1996), suggested that RN magnocellular neurons could be capable of synaptic plastic changes during the acquisition of different types of skeletal associative learning tasks. These changes in synaptic strength could take place at the distal dendrites of magnocellular neurons, the preferential place of innervation of cortical sensorimotor neurons projecting to the RN (Tsukahara et al., 1967; Pizzini et al., 1975; Eccles, 1986). The present results reopen the possibility of the presence of learning-dependent mechanisms present in RN and pararubral neurons, which can easily be noticed in the absence of the proper activity of MC circuits, but not after the reversible inactivation of cerebellar outputs, and merit a detailed account.

There are early reports indicating that rabbits are capable of acquiring classically conditioned nictitating membrane responses in decerebrate-decerebellate conditions (Kelly et al., 1990), suggesting the presence of additional neural centers with a (limited) capacity for associative learning. More recently, it has been shown in behaving mice that the occlusion of hippocampal circuits by the experimental induction of long-term potentiation still allows the expression of a low rate ($<$40%) of eyelid CRs (Gruart et al., 2006). Indeed, the RN and the pararubral area are suitable for this role, because, in addition to the considerable inputs reaching it from cerebral cortex and cerebellar pathways,

they also receive afferent activation from different sensory modalities (Padel et al., 1988) and, as recently shown, there are intrinsic circuits and synaptic activations within the RN and the pararubral area (Horn et al., 2002), including GABAergic and non-GABAergic neurons (Haley et al., 1988). The different effects produced on classical eyeblink conditioning by the transient inactivation of the cerebral cortex and the cerebellar IP nucleus could be explained by their different innervation of RN neurons. Cerebral cortical axonal projections seem to synapse on distal dendrites activating NMDA and non-NMDA glutamate receptors (Davies et al., 1994), while IP axons seem to terminate on non-NMDA receptors located preferentially on the soma and proximal dendrites of rubral neurons (Billard et al., 1991). Thus, and as originally proposed by Tsukahara et al. (1981), the presence of NMDA receptors could explain the delayed changes in synaptic strength taking place in rubral circuits after the inactivation of the sensorimotor cortex. It is still possible that the compensating learning mechanisms observed in rubral neurons after cerebral cortex inactivation could be the result of a delayed activation of the rubro-olivary-cerebellar circuit (Kennedy and Humphrey, 1987). However, the problem with proposing the rubro-olivary-cerebellar pathway as the one involved in the acquisition process is that this pathway seems to have no ready access to the NMDA receptors located on the membrane of rubral neurons, and that IP nucleus effects on the acquisition process seem to affect conditioned and unconditioned responses equally, their being related more with CR performance, and not with the acquisition process. In fact, and as shown here, the loss of IP neuron responses prevents the proper activity of rubral and pararubral neurons (Figs. 7, 8) and its precise contribution to the acquisition process.

In relation with the above contentions, the RN could have a role in the appropriated timing of CRs. These timing activities could be generated by feedback circuits involving RN, cerebellar IP, and sensory inputs (Houk, 1991; Cartford et al., 1997). The acute disappearance of facilitatory inputs from IP neurons could block these reverberant activities and prevent the learning-depending evolution of rubral activities related to the generation and performance of eyelid CRs. In addition, a reinforcing role of the IP nucleus for the expression of both conditioned and unconditioned eyelid responses has been already shown in recording and/or transient inactivation studies performed in behaving cats (Jiménez-Díaz et al., 2004) and mice (Porras-García et al., 2010). These two phenomena could explain why its inactivation has such a deleterious effects on both conditioned and unconditioned eyelid responses.

The disfacilitatory effects of IP inactivation cannot only be mediated by IP projections to the RN, but also by larger projections to motor and premotor cerebral cortical circuits. These functional changes could also help to explain why acute removal of cerebellar facilitatory outputs has such a deleterious effect on RN functions.

In contrast to the learning-dependent effects activated by the transient inactivation of the MC, the inactivation of the IP nucleus should produce a strong disfacilitation of RN and pararubral neuron firing, because of the strategic location of their axonal terminal boutons in somatic and proximal dendrite sites. The significant increase in the spontaneous firing of rubral neurons following IP nucleus inactivation can tentatively be explained by the disfacilitation of GABAergic neurons (Haley et al., 1988) present in RN intrinsic circuits. In this regard, Nieoullon et al. (1988) proposed that the inactivation of the cerebellum could be compensated by an unspecific increase of corticorubral projections together with a decrease in the activity of rubral GABAergic interneurons. These two separate activities could help to explain the increase in basal activity observed in RN neurons during the inactivation of the IP nucleus.

References

Billard JM, Daniel H, Pumain R (1991) Sensitivity of rubrospinal neurons to excitatory amino acids in the rat red nucleus in vivo. Neurosci Lett 134:49–52.

Bracha V, Stewart SL, Bloedel JR (1993) The temporary inactivation of the red nucleus affects performance of both conditioned and unconditioned nictitating membrane responses in the rabbit. Exp Brain Res 94:225–236.

Bracha V, Zbarska S, Parker K, Carrel A, Zenitsky G, Bloedel JR (2009) The cerebellum and eye-blink conditioning: learning versus network performance hypotheses. Neuroscience 162:787–796.

Canedo A, Lamas JA (1989) Rubrospinal tract of the cat: superposition of antidromic responses and changes in axonal excitability following orthodromic activity. Brain Res 502:28–38.

Cartford MC, Gohl EB, Singson M, Lavond DG (1997) The effects of reversible inactivation of the red nucleus on learning-related and auditory-evoked unit activity in the pontine nuclei of classically conditioned rabbits. Learn Mem 3:519–531.

Case GR, Lavond DG, Thompson RF (2002) Cortical spreading depression and involvement of the motor cortex, auditory cortex, and cerebellum in eyeblink classical conditioning of the rabbit. Neurobiol Learn Mem 78:234–245.

Chapman PF, Steinmetz JE, Sears LL, Thompson RF (1990) Effects of lidocaine injection in the interpositus nucleus and red nucleus on conditioned behavioral and neuronal responses. Brain Res 537:149–156.

Chen FP, Evinger C (2006) Cerebellar modulation of trigeminal reflex blinks: interpositus neurons. J Neurosci 26:10569–10576.

Clark RE, Lavond DG (1993) Reversible lesions of the red nucleus during acquisition and retention of a classically conditioned behavior in rabbits. Behav Neurosci 107:264–270.

Courville J (1966) Rubrobulbar fibres to the facial nucleus and the lateral reticular nucleus (nucleus of the lateral funiculus). An experimental study in the cat with silver impregnation methods. Brain Res 1:317–337.

Davies J, Qume M, Harris NC (1994) Pharmacological characterisation of excitatory synaptic transmission in the cat red nucleus in vivo. Brain Res 649:43–52.

Desmond JE, Moore JW (1991) Single-unit activity in red nucleus during the classically conditioned rabbit nictitating membrane response. Neurosci Res 10:260–279.

Eccles JC (1986) The investigations of N. Tsukahara on relocation of synapses on red nucleus neurones. Neurosci Res 3:476–486.

Eccles JC, Scheid P, Táboríková H (1975) Responses of red nucleus neurons to antidromic and synaptic activation. J Neurophysiol 38:947–964.

Freeman JH, Steinmetz AB (2011) Neural circuitry and plasticity mechanisms underlying delay eyeblink conditioning. Learn Mem 18:666–677.

Girgis M, Shih-Chang W (1981) A new stereotaxic atlas of the rabbit brain. St. Louis: Warren H. Green.

Godefroy JN, Thiesson D, Pollin B, Rokyta R, Azerad J (1998) Reciprocal connections between the red nucleus and the trigeminal nuclei: a retrograde and anterograde tracing study. Physiol Res 47:489–500.

Grant K, Horcholle-Bossavit G (1986) Red nucleus inputs to retractor bulbi motoneurones in the cat. J Physiol 371:317–327.

Gruart A, Schreurs BG, del Toro ED, Delgado-García JM (2000) Kinetic and frequency-domain properties of reflex and conditioned eyelid responses in the rabbit. J Neurophysiol 83:836–852.

Gruart A, Streppel M, Guntinas-Lichius O, Angelov DN, Neiss WF, Delgado-García JM (2003) Motoneuron adaptability to new motor tasks following two types of facial-facial anastomosis in cats. Brain 126:115–133.

Gruart A, Muñoz MD, Delgado-García JM (2006) Involvement of the CA3-CA1 synapse in the acquisition of associative learning in behaving mice. J Neurosci 26:1077–1087.

Gruber P, Gould DJ (2010) The red nucleus: past, present, and future. Neuroanatomy 9:1–3.

Haley DA, Thompson RF, Madden J 4th (1988) Pharmacological analysis of the magnocellular red nucleus during classical conditioning of the rabbit nictitating membrane response. Brain Res 454:131–139.

Hinrichsen CF, Watson CD (1983) Brain stem projections to the facial nucleus of the rat. Brain Behav Evol 22:153–163.

Horn KM, Pong M, Batni SR, Levy SM, Gibson AR (2002) Functional specialization within the cat red nucleus. J Neurophysiol 87:469–477.
Houk JC (1991) Red nucleus: role in motor control. Curr Opin Neurobiol 1:610–615.
Huisman AM, Kuypers HG, Verburgh CA (1981) Quantitative differences in collateralization of the descending spinal pathways from red nucleus and other brain stem cell groups in rat as demonstrated with the multiple fluorescent retrograde tracer technique. Brain Res 209:271–286.
Huisman AM, Kuypers HG, Verburgh CA (1982) Differences in collateralization of the descending spinal pathways from red nucleus and other brain stem cell groups in cat and monkey. Prog Brain Res 57:185–217.
Ito M, Oda Y (1994) Electrophysiological evidence for formation of new corticorubral synapses associated with classical conditioning in the cat. Exp Brain Res 99:277–288.
Ivkovich D, Thompson RF (1997) Motor cortex lesions do not affect learning or performance of the eyeblink response in rabbits. Behav Neurosci 111:727–738.
Jiménez-Díaz L, Navarro-López Jde D, Gruart A, Delgado-García JM (2004) Role of cerebellar interpositus nucleus in the genesis and control of reflex and conditioned eyelid responses. J Neurosci 24:9138–9145.
Kelly TM, Zuo CC, Bloedel JR (1990) Classical conditioning of the eyeblink reflex in the decerebrate-decerebellate rabbit. Behav Brain Res 38:7–18.
Kennedy PR, Humphrey DR (1987) The compensatory role of the parvocellular division of the red nucleus in operantly conditioned rats. Neurosci Res 5:39–62.
Kotani S, Kawahara S, Kirino Y (2002) Classical eyeblink conditioning in decerebrate guinea pigs. Eur J Neurosci 15:1267–1270.
Krupa DJ, Thompson JK, Thompson RF (1993) Localization of a memory trace in the mammalian brain. Science 260:989–991.
Leal-Campanario R, Fairén A, Delgado-García JM, Gruart A (2007) Electrical stimulation of the rostral medial prefrontal cortex in rabbits inhibits the expression of conditioned eyelid responses but not their acquisition. Proc Natl Acad Sci U S A 104:11459–11464.
Martin JH, Ghez C (1999) Phamacological inactivation in the analysis of the central control of movement. J Neurosci Methods 86:145–159.
Megirian D, Bures J (1970) Unilateral cortical spreading depression and conditioned eyeblink responses in the rabbit. Exp Neurol 27:34–45.
Mendez I, Hong M (1997) Reconstruction of the striato-nigro-striatal circuitry by simultaneous double dopaminergic grafts: a tracer study using fluorogold and horseradish peroxidase. Brain Res 778:194–205.
Miller LE, Gibson AR (2009) Red nucleus. In: Encyclopedia of neuroscience, Vol 8 (Squire LR ed), pp 55–62. Oxford: Academic.
Mizuno N, Nakamura Y (1971) Rubral fibers to the facial nucleus in the rabbit. Brain Res 28:545–549.
Morcuende S, Delgado-García JM, Ugolini G (2002) Neuronal premotor networks involved in eyelid responses: retrograde transneuronal tracing with rabies virus from the orbicularis oculi muscle in the rat. J Neurosci 22:8808–8818.
Múnera A, Gruart A, Muñoz MD, Fernández-Mas R, Delgado-García JM (2001) Hippocampal pyramidal cell activity encodes conditioned stimulus predictive value during classical conditioning in alert cats. J Neurophysiol 86:2571–2582.
Murakami F, Higashi S, Katsumaru H, Oda Y (1987) Formation of new corticorubral synapses as a mechanism for classical conditioning in the cat. Brain Res 437:379–382.
Murakami F, Oda Y, Tsukahara N (1988) Synaptic plasticity in the red nucleus and learning. Behav Brain Res 28:175–179.
Nieoullon A, Vuillon-Cacciuttolo G, Dusticier N, Kerkérian L, André D, Bosler O (1988) Putative neurotransmitters in the red nucleus and their involvement in postlesion adaptive mechanisms. Behav Brain Res 28:163–174.
Oakley DA, Russell IS (1972) Neocortical lesions and Pavlovian conditioning. Physiol Behav 8:915–926.
Padel Y, Sybirska E, Bourbonnais D, Vinay L (1988) Electrophysiological identification of a somaesthetic pathway to the red nucleus. Behav Brain Res 28:139–151.
Pananceau M, Rispal-Padel L, Meftah EM (1996) Synaptic plasticity of the interpositorubral pathway functionally related to forelimb flexion movements. J Neurophysiol 75:2542–2561.
Pauletti G, Berardelli A, Cruccu G, Agostino R, Manfredi M (1993) Blink reflex and the masseter inhibitory reflex in patients with dystonia. Mov Disord 8:495–500.
Pizzini G, Tredici G, Miani A (1975) Corticorubral projection in the cat. An experimental electronmicroscopic study. J Submicr Cytol 7:231–238.
Pong M, Horn KM, Gibson AR (2008) Pathways for control of face and neck musculature by the basal ganglia and cerebellum. Brain Res Rev 58:249–264.
Porras-García E, Sánchez-Campusano R, Martínez-Vargas D, Domínguez-del-Toro E, Cendelín J, Vozeh F, Delgado-García JM (2010) Behavioral characteristics, associative learning capabilities, and dynamic association mapping in an animal model of cerebellar degeneration. J Neurophysiol 104:346–365.
Poulos AM, Nobuta H, Thompson RF (2009) Disruption of cerebellar cortical inhibition in the absence of learning promotes sensory-evoked eyeblink responses. Behav Neurosci 123:694–700.
Rieke F, Warland D, van Steveninck RdR, Bialek W (1997) Spikes. Exploring the neural code. Cambridge, MA: MIT.
Robinson FR, Rice PM, Holleman JR, Berger TW (2001) Projection of the magnocellular red nucleus to the region of the accessory abducens nucleus in the rabbit. Neurobiol Learn Mem 76:358–374.
Robleto K, Thompson RF (2008) Extinction of a classically conditioned response: red nucleus and interpositus. J Neurosci 28:2651–2658.
Ruigrok TJH, Cella F (1995) Precerebellar nuclei and red nucleus. In: The rat nervous system (Paxinos G, ed), pp 277–308. San Diego: Academic.
Sánchez-Campusano R, Gruart A, Delgado-García JM (2011) Dynamic changes in the cerebellar-interpositus/red-nucleus-motoneuron pathway during motor learning. Cerebellum 10:702–710.
Schmied A, Amalric M, Dormont JF, Condé H, Farin D (1988) Participation of the red nucleus in motor initiation: unit recording and cooling in cats. Behav Brain Res 28:207–216.
ten Donkelaar HJ (1988) Evolution of the red nucleus and rubrospinal tract. Behav Brain Res 28:9–20.
Tsukahara N (1981) Synaptic plasticity in the mammalian central nervous system. Annu Rev Neurosci 4:351–379.
Tsukahara N, Toyama K, Kosaka K (1967) Electrical activity of red nucleus neurones investigated with intracellular microelectrodes. Exp Brain Res 4:18–33.
Tsukahara N, Oda Y, Notsu T (1981) Classical conditioning mediated by the red nucleus in the cat. J Neurosci 1:72–79.
Welsh JP (1992) Changes in the motor pattern of learned and unlearned responses following cerebellar lesions: a kinematic analysis of the nictitating membrane reflex. Neuroscience 47:1–19.
Welsh JP, Harvey JA (1989) Cerebellar lesions and the nictitating membrane reflex: performance deficits of the conditioned and unconditioned response. J Neurosci 9:299–311.
Wikgren J, Korhonen T (2001) Interpositus nucleus inactivation reduces unconditioned response amplitude after paired but not explicitly unpaired treatment in rabbit eyeblink conditioning. Neurosci Lett 308:181–184.